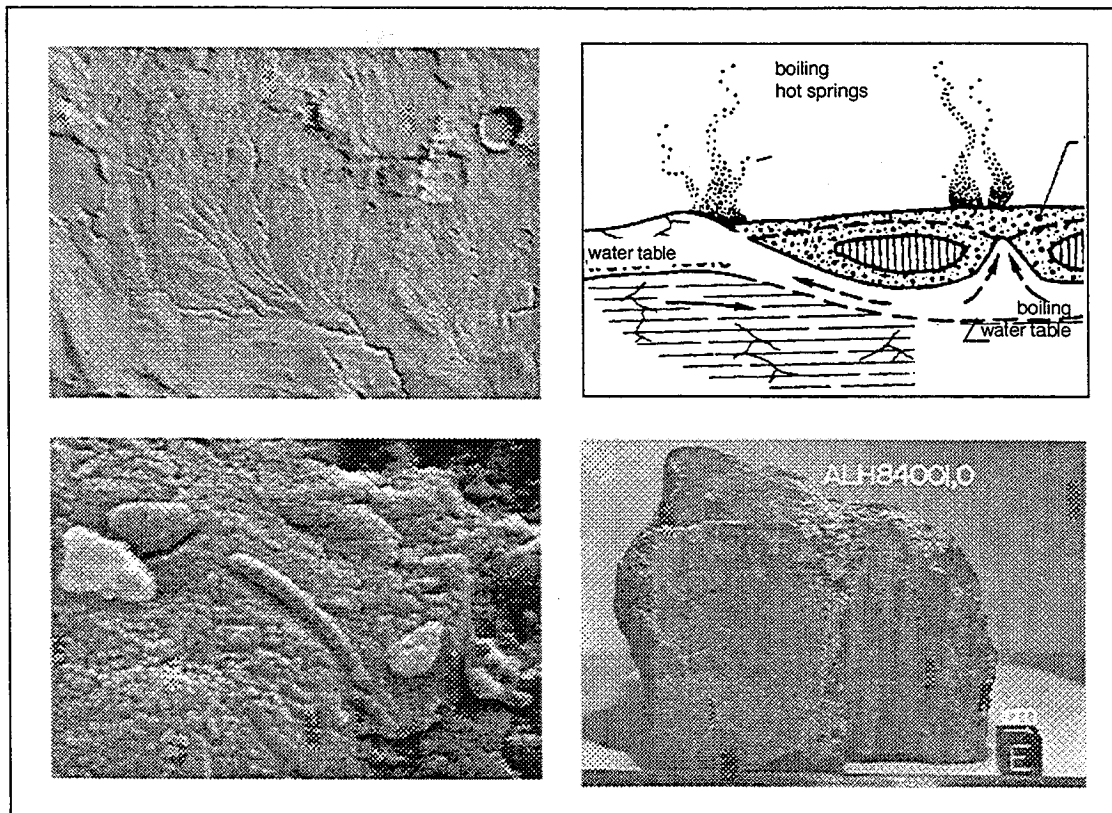


NASW-4574  
IN-91-CR  
025560

# CONFERENCE ON EARLY MARS: GEOLOGIC AND HYDROLOGIC EVOLUTION, PHYSICAL AND CHEMICAL ENVIRONMENTS, AND THE IMPLICATIONS FOR LIFE



April 24–27, 1997  
Houston, Texas





**CONFERENCE ON EARLY MARS:  
GEOLOGIC AND HYDROLOGIC EVOLUTION, PHYSICAL AND  
CHEMICAL ENVIRONMENTS, AND THE IMPLICATIONS FOR LIFE**

Edited by

S. M. Clifford, A. H. Treiman, H. E. Newsom, and J. D. Farmer

Held at  
Houston, Texas

April 24–27, 1997

Sponsored by  
Lunar and Planetary Institute  
National Aeronautics and Space Administration

Lunar and Planetary Institute 3600 Bay Area Boulevard Houston TX 77058-1113

LPI Contribution Number 916

Compiled in 1997 by  
LUNAR AND PLANETARY INSTITUTE

The Institute is operated by the Universities Space Research Association under Contract No. NASW-4574 with the National Aeronautics and Space Administration.

Material in this volume may be copied without restraint for library, abstract service, education, or personal research purposes; however, republication of any paper or portion thereof requires the written permission of the authors as well as the appropriate acknowledgment of this publication.

This report may be cited as

Clifford S. M., Treiman A. H., Newsom H. E., and Farmer J. D., eds. (1997) *Conference on Early Mars: Geologic and Hydrologic Evolution, Physical and Chemical Environments, and the Implications for Life*. LPI Contribution No. 916, Lunar and Planetary Institute, Houston. 87 pp.

This report is distributed by

ORDER DEPARTMENT  
Lunar and Planetary Institute  
3600 Bay Area Boulevard  
Houston TX 77058-1113

*Mail order requestors will be invoiced for the cost of shipping and handling.*



*"Each of us is a tiny being, permitted to ride on the outermost skin of one of the smaller planets for a few dozen trips around the local star . . . We are fleeting, transitional creatures, snowflakes fallen on the hearth fire. That we understand even a little of our origins is one of the great triumphs of human insight and courage."*

— from *Shadows of Forgotten Ancestors*

*In Memory of Carl Sagan  
(1934–1996)*

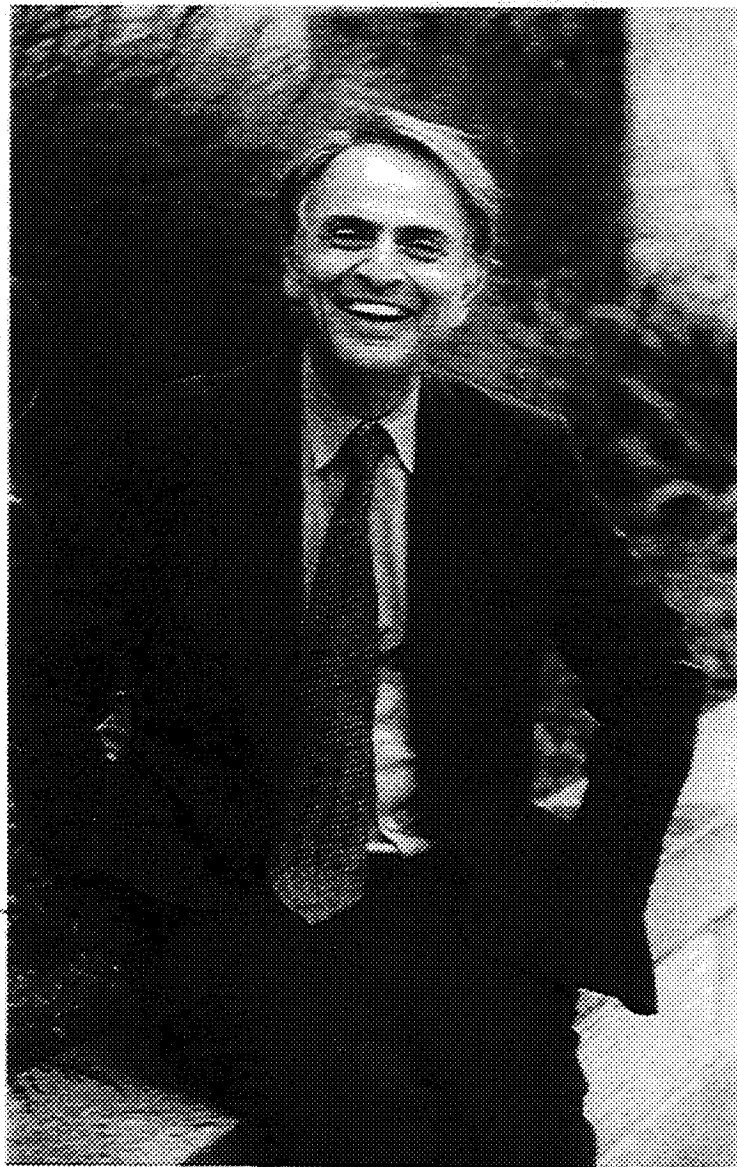


Photo by Michael Okoniewski. Copyright © 1994.



## Preface

---

This volume contains abstracts that have been accepted for presentation at the Conference on Early Mars: Geologic and Hydrologic Evolution, Physical and Chemical Environments, and the Implications for Life, April 24–27, 1997, in Houston, Texas. The conveners for the conference were Stephen Clifford (*Lunar and Planetary Institute*), Allan Treiman (*Lunar and Planetary Institute*), Horton Newsom (*University of New Mexico*), and Jack Farmer (*NASA Ames Research Center*).

Members of the Scientific Organizing Committee included Michael Carr (*U.S. Geological Survey*), Benton Clark (*Lockheed Martin*), Roger Clark (*U.S. Geological Survey*), Michael Drake (*University of Arizona*), Fraser Fanale (*University of Hawai'i*), Matthew Golombek (*Jet Propulsion Laboratory*), James Gooding (*NASA Johnson Space Center*), Virginia Gulick (*NASA Ames Research Center*), Bob Haberle (*NASA Ames Research Center*), Alan Howard (*University of Virginia*), Bruce Jakosky (*University of Colorado*), James Kasting (*Pennsylvania State University*), Ted Maxwell (*National Air & Space Museum*), George McGill (*University of Massachusetts*), Christopher McKay (*NASA Ames Research Center*), David McKay (*NASA Johnson Space Center*), Richard Morris (*NASA Johnson Space Center*), Susan Postawko (*University of Oklahoma*), Carl Sagan (*Cornell University*), Peter Schultz (*Brown University*), Everett Shock (*Washington University*), Steven Squyres (*Cornell University*), Carol Stoker (*NASA Ames Research Center*), and Kenneth Tanaka (*U.S. Geological Survey*).

Logistics and administrative and publications support were provided by the Publications and Program Services Department staff at the Lunar and Planetary Institute.



# Contents

---

Mössbauer Spectroscopy of Thermal Springs Iron Deposits as Martian Analogs <i>D. G. Agresti, T. J. Wdowiak, M. L. Wade, and L. P. Armendarez</i> .....	1
Geologic Alteration and Life in an Extreme Environment: Pu'u Waiau, Mauna Kea, Hawai'i <i>C. C. Allen, R. V. Morris, D. C. Golden, and C. S. Upchurch</i> .....	2
The Early Martian Climate Was Episodically Warm and Wet <i>V. R. Baker</i> .....	3
Developing a Chemical Code to Identify Magnetic Biominerals (Biomagnetite and Biogreigite) in Mars Soil and Rocks <i>A. Banin and R. L. Mancinelli</i> .....	4
Effect of Impacts on Early Martian Geologic Evolution <i>N. G. Barlow</i> .....	5
Biomarkers for Analysis of Martian Samples <i>L. Becker, G. D. McDonald, and J. L. Bada</i> .....	6
Application of the CHEMIN XRD/XRF Instrument in Analyzing Diagnostic Mineralogies: Quantitative XRD Analysis of Aragonite and Basalt <i>D. Bish, D. Vaniman, P. Sarrazin, D. Blake, S. Chipera, S. A. Collins, and T. Elliott</i> .....	8
Spectroscopic Identification of Minerals in Hematite-bearing Soils and Sediments: Implications for Chemistry and Mineralogy of the Martian Surface <i>J. L. Bishop, J. Friedl, and U. Schwertmann</i> .....	9
$^{39}\text{Ar}$ - $^{40}\text{Ar}$ Age of Allan Hills 84001 <i>D. D. Bogard and D. H. Garrison</i> .....	10
Scientific Issues Addressed by the Mars Surveyor 2001 Gamma-Ray/Neutron Spectrometer (GRS/NS) <i>W. V. Boynton, W. C. Feldman, S. W. Squyres, J. I. Trombka, J. R. Arnold, P. A. J. Englert, A. E. Metzger, R. C. Reedy, H. Wänke, S. H. Bailey, J. Brückner, L. G. Evans, H. Y. McSween, and R. Starr</i> .....	12
Experimental Studies of Mars-Analog Brines <i>M. A. Bullock, J. M. Moore, and M. T. Mellon</i> .....	13
Hydrogeology and Exobiology Significance of Martian Large Crater Lakes <i>N. A. Cabrol and E. A. Grin</i> .....	14

Microbial Diversity in Hyperthermophilic Biofilms: Implications for Recognizing Biogenicity in Hydrothermal Deposits <i>S. L. Cady, C. E. Blank, D. J. Des Marais, M. R. Walter, and J. D. Farmer</i> .....	15
The Highlands Crust of Mars and the Pathfinder Mission: A Prospective View from Mariner 6 Infrared Spectroscopy <i>W. M. Calvin, A. H. Treiman, and L. Kirkland</i> .....	16
Thermal Loss of Water on Young Planets: The Effect of a Strong Primitive Solar Wind <i>E. Chassefière</i> .....	17
Geochemical Cycles of CHNOPS and Other Potentially Important Biological Elements on Mars <i>B. C. Clark</i> .....	18
Hydraulic and Thermal Constraints on the Development of the Martian Valley Networks <i>S. M. Clifford</i> .....	18
The Origin of the Martian Intercrater Plains: The Role of Liquefaction from Impact and Tectonic-induced Seismicity <i>S. M. Clifford</i> .....	19
The Early History of Mars as Told by Degraded Highland Impact Craters <i>R. A. Craddock, T. A. Maxwell, and A. D. Howard</i> .....	20
The Radiative Effects of CO <sub>2</sub> Ice Clouds on the Early Martian Climate <i>D. Crisp and R. T. Pierrehumbert</i> .....	21
Degradation of the Martian Cratered Highlands: The Role of Circum-Hellas Outflow Channels and Constraints on the Timing of Volatile-driven Activity <i>D. A. Crown, S. C. Mest, and K. H. Stewart</i> .....	22
Mars on Earth: Antarctic Dry Valley Lakes and Their Deposits <i>P. T. Doran and R. A. Wharton</i> .....	24
Accretion of Earth and Mars: Implications for Bulk Composition and Volatile Inventories <i>M. J. Drake</i> .....	24
Volatile Inventories of Mars and Earth and Their Implication for the Evolution of Planetary Atmospheres <i>G. Dreibus, H. Wänke, and G. W. Lugmair</i> .....	26

Regarding a Wet, Early Noachian Mars: Geomorphology of Western Arabia and Northern Sinus Meridiani <i>K. S. Edgett and T. J. Parker</i> .....	27
Geologic Signature of Life on Mars: Low-Albedo Lava Flows and the Search for "Warm Havens" <i>K. S. Edgett and J. W. Rice Jr.</i> .....	29
Exopaleontology and the Search for a Fossil Record on Mars <i>J. D. Farmer and D. J. Des Marais</i> .....	30
Fossilization Processes in Modern Thermal Springs: Clues for Assessing the Biogenicity of Ancient Hydrothermal Deposits <i>J. D. Farmer, S. L. Cady, D. J. Des Marais, and M. R. Walter</i> .....	31
Cation Diffusion in Carbonate Minerals: Determining Closure Temperatures and the Thermal History for the Allan Hills 84001 Meteorite <i>D. K. Fiesler, R. T. Cygan, and H. R. Westrich</i> .....	32
Organic Matter Contributed to the Surface of Mars by Interplanetary Dust, Meteorites, Comets, and Asteroids <i>G. J. Flynn</i> .....	33
Highland Crater Basins as Evaporative/Sublimative Discharge Pumps for Driving Early Martian Groundwater to Atmosphere Water Transfers <i>R. D. Forsythe and C. R. Blackwelder</i> .....	34
Biogenic Activity in Martian Meteorite Allan Hills 84001: Status of the Studies <i>E. K. Gibson Jr., D. S. McKay, K. Thomas-Keprta, C. S. Romanek, S. J. Clemett, and R. N. Zare</i> .....	35
Major- and Trace-Element Distributions in Allan Hills 84001 Carbonate: Indication of a High Formation Temperature <i>J. D. Gilmour, R. A. Wogelius, G. W. Grime, and G. Turner</i> .....	37
Geochemical Evolution of the Crust of Mars <i>J. L. Gooding</i> .....	38
Geological Evolution of the Early Earth <i>P. F. Hoffman</i> .....	40
Microbial Fossils from Terrestrial Subsurface Hydrothermal Environments: Examples and Implications for Mars <i>B. A. Hofmann and J. D. Farmer</i> .....	40

Role of the Crust in the Evolution of the Martian Atmosphere <i>K. S. Hutchins and B. M. Jakosky</i> .....	42
Why the SNC Meteorites Might Not Come from Mars <i>E. Jagoutz</i> .....	42
Early Atmospheres of Earth and Mars: Importance of Methane to Climate and to Life's Origin <i>J. F. Kasting and L. L. Brown</i> .....	43
The Magnetic Properties Experiment on Mars Pathfinder <i>J. M. Knudsen, H. P. Gunnlaugsson, M. B. Madsen, S. F. Hviid, and W. Goetz</i> .....	45
Relative Ages of Maskelynite and Carbonate in Allan Hills 84001 and Implications for Early Hydrothermal Activity on Mars <i>D. A. Kring, T. D. Swindle, J. D. Gleason, and J. A. Grier</i> .....	46
Chemistry of Carbon, Hydrogen, and Oxygen During Early Martian Differentiation <i>K. Kuramoto and T. Matsui</i> .....	48
Thermal Emission Spectroscopy of Aqueously Precipitated Minerals Similar to Those in the SNCs <i>M. D. Lane and P. R. Christensen</i> .....	49
A Unique Mars/Early Mars Analog on Earth: The Haughton Impact Structure, Devon Island, Canadian Arctic <i>P. Lee</i> .....	50
Ice in Channels and Ice-Rock Mixtures in Valleys on Mars: Did They Slide on Deformable Rubble Like Antarctic Ice Streams? <i>B. K. Lucchitta</i> .....	51
Evidence for Volcanism Associated with Ismeniae Fossae Fretted Channels <i>G. E. McGill and M. W. Carruthers</i> .....	52
Mars Meteorites and Panspermian Possibilities <i>H. J. Melosh</i> .....	53
Active Carbohydrate Oligomers of Bacteria in Anoxic Environments <i>Y. Miura</i> .....	54
Chemical Evolution by Shock-Wave Energy in Anoxic Atmospheres <i>Y. Miura</i> .....	55



Goldenrod Pigment and the Occurrence of Hematite and Goethite on the Martian Surface <i>R. V. Morris and D. C. Golden</i> .....	56
Mössbauer Mineralogy on Mars <i>R. V. Morris and G. Klingelhöfer</i> .....	58
Chemical and Mineralogical Processes in Martian Soil <i>J. F. Mustard</i> .....	59
Hydrothermal Environments and Chemical Transport on Mars <i>H. E. Newsom</i> .....	60
Composition of the Martian Soil <i>H. E. Newsom and J. J. Hagerty</i> .....	62
The Shergottite Age Paradox <i>L. E. Nyquist, L. E. Borg, and C.-Y. Shih</i> .....	64
Fluvial and Lacustrine Degradation of Large Martian Basins During the Noachian <i>T. J. Parker</i> .....	65
Solar-Wind-induced Erosion of the Mars Atmosphere <i>H. Pérez-de-Tejada</i> .....	66
Elysium Basin, Mars: An Intermittent or Perennial Lake from Noachian to Amazonian Time <i>J. W. Rice Jr.</i> .....	68
Getting the First Crack at Noachian Clasts and Sediments: A Pathfinder's Prospectus <i>J. W. Rice Jr.</i> .....	69
Oxygen Isotope Ratio Zoning in Allan Hills 84001 Carbonates <i>J. M. Saxton, I. C. Lyon, and G. Turner</i> .....	70
Implications of Martian Life in an Antarctic Meteorite <i>W. R. Sheldon</i> .....	72
Carbonate Precipitation in Anoxic Environments: Implications for Atmospheric CO <sub>2</sub> Removal on Early Mars <i>D. Y. Sumner</i> .....	72
Studies of Weathering Products in the Lafayette Meteorite: Implications for the Distribution of Water on Both Early and Recent Mars <i>T. D. Swindle and D. A. Kring</i> .....	74

Distribution of Channels in the Thaumasia Region Indicates Hydrologic Activity Largely Due to Local Heating During Early Mars <i>K. L. Tanaka, J. M. Dohm, and T. M. Hare</i> .....	75
SEM Studies of Antarctic Lunar and SNC Meteorites with Implications for Martian Nanofossils: A Progress Report <i>A. E. Taunton</i> .....	76
What is Mars' Highlands Crust? <i>A. H. Treiman</i> .....	77
Effects of Cratering on the Early History of Mars <i>A. M. Vickery</i> .....	78
Subsurface Fluid Reservoirs on Mars: A Possible Explanation for the Fate of an Early Greenhouse Atmosphere <i>D. Vlassopoulos</i> .....	79
The Controversy of Young vs. Old Age of Formation of Carbonates in Allan Hills 84001 <i>M. Wadhwa and G. W. Lugmair</i> .....	79
Identification of Ancient Carbonaceous Cherts on Mars Using Raman Spectroscopy <i>T. J. Wdowiak, D. G. Agresti, S. B. Mirov, A. B. Kudryavtsev, L. W. Beegle, D. J. Des Marais, and A. F. Tharpe</i> .....	81
Progress in the Development of a Laser Raman Spectrometer System for a Lander Spacecraft <i>T. J. Wdowiak, D. G. Agresti, S. B. Mirov, A. B. Kudryavtsev, and T. R. Kinney</i> .....	82
The Nature of Fossil Bacteria <i>F. Westall</i> .....	84
Mars Geothermal and Volcanic Evolution: Volcanic Intrusions as Heat Sources to Maintain Viable Ecosystems? <i>L. Wilson and J. W. Head III</i> .....	85
Further Investigation of Isotopically Light Carbon in Allan Hills 84001 <i>I. P. Wright, S. Assanov, A. B. Verchovsky, I. A. Franchi, M. M. Grady, and C. T. Pillinger</i> .....	86

## Abstracts

### MÖSSBAUER SPECTROSCOPY OF THERMAL SPRINGS IRON DEPOSITS AS MARTIAN ANALOGS.

D. G. Agresti<sup>1</sup>, T. J. Wdowiak<sup>1</sup>, M. L. Wade<sup>1</sup>, L. P. Armendarez<sup>1</sup>, and J. D. Farmer<sup>2</sup>,  
<sup>1</sup>Astro and Solar System Physics Program, Department of Physics, University of Alabama at Birmingham, Birmingham AL 35294-1700, USA, <sup>2</sup>NASA Ames Research Center, Moffett Field CA 94035, USA.

We have been investigating iron-rich hot springs of Yellowstone National Park (YNP) as analogs for the hydrothermal systems that might have existed on an early warmer, wetter Mars. We report here on Mössbauer results for a suite of samples collected at Chocolate Pots, from a large Fe-rich vent mound located on the east bank of the Gibbon River, and their implications for understanding early processes and for prospecting for samples of exopaleontological interest.

Cores were taken along the outflow channel at several locations measured from the river's edge up to the vent, ~8 m away. Following collection, each core was sectioned into four depth increments, as in Table 1, except at the vent, where this could not be done. Thereafter the material was frozen and held below -5°C to inhibit subsequent change due to biological activity. For laboratory work, samples were thawed and ground to a fine powder, if necessary, and fixed in molten paraffin for ~20 mg/cm<sup>2</sup> Mössbauer absorbers or dispersed on a glass slide for XRD analysis.

Room-temperature Mössbauer spectra of each of the 13 samples was obtained (Figs. 1 and 2; the 5Cx and 6C1 spectra nearly match the 3C1.) Then selected samples were measured at temperatures down to ~12 K, as in Figs. 3 and 4. Several conclusions may be drawn from the spectra, assisted by XRD.

In the vicinity of the vent, the deposit (6C1 and the 5Cx series at all depths) is ferric (Mössbauer) and amorphous (broad, magnetically split lines at low temperature, Fig. 3, and flat XRD), apparently single phase. Physically, the material resembles a laminated glass that fractures readily on handling, appearing under the light microscope with multiple alternating clear (quartz?) and red (ferric) ~50-mm-thick bands.

Nearer the stream (2Cx and 3Cx series), the deposit is a fine powder at all depths. The surface layer, which includes a fibrous green mat component, is ferric and amorphous, as judged by XRD

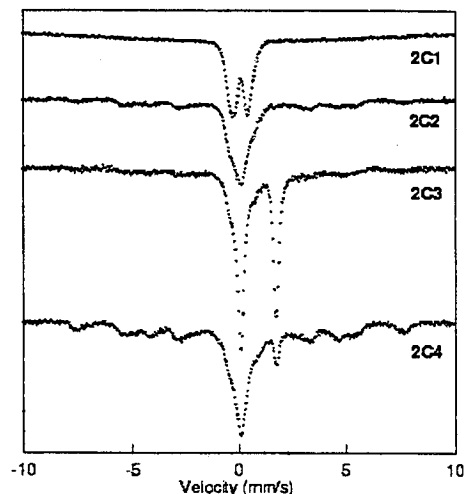


Fig. 1. Room-temperature spectra for the 2Cx series.

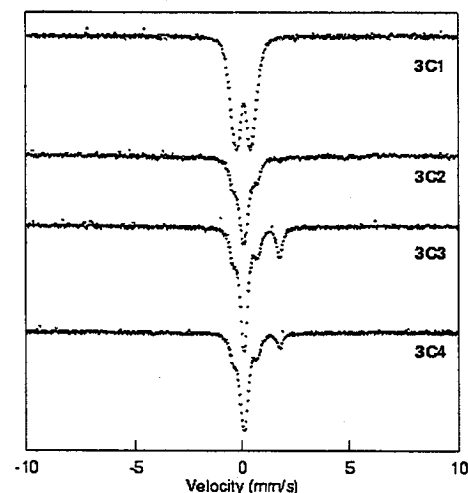


Fig. 2. Room-temperature spectra for the 3Cx series.

TABLE 1. Physical data for the 13 core samples examined in this study, including pH, temperature (T), and redox potential (Eh) of the water in the outflow channel immediately above the collection site.

Depth/Location	1 m	2 m	6 m	8 m
0-1 mm	2C1	3C1	5C1	—
1-4 mm	2C2	3C2	5C2	—
4-8 mm	2C3	3C3	5C3	—
>8 mm	2C4	3C4	5C4	—
0-1 cm	—	—	—	6C1
pH	7.9	7.8	7.2	5.8
T(°C)	48.0	53.2	54.2	55.0
Eh(mV)	-49.0	-45.7	-2.0	81.7

and Mössbauer, although the low-temperature spectra are not the same as those for 6C1 (Fig. 3). The 3Cx series shows some spectral variation with depth, unlike 5Cx, but the greatest variation, and hence biological diversity, is exhibited by the 2Cx series (Fig. 1).

We now focus on the strong ferrous doublet of the 2C3 spectrum of Fig. 1, which comprises approximately two-thirds of the total spectral area. Its splitting agrees within error to the published value of  $1.87 \pm 0.10$  mm/s at room temperature [1] for siderite ( $\text{FeCO}_3$ ), and increases in a known way as sample temperature is lowered to 45 K. Between 45 K and 30 K, the right peak of the pair appears to migrate from ~2.5 mm/s to ~5.0 mm/s below 30 K, similar to reported behavior [2,3] attributed to antiferromagnetic phase relax-

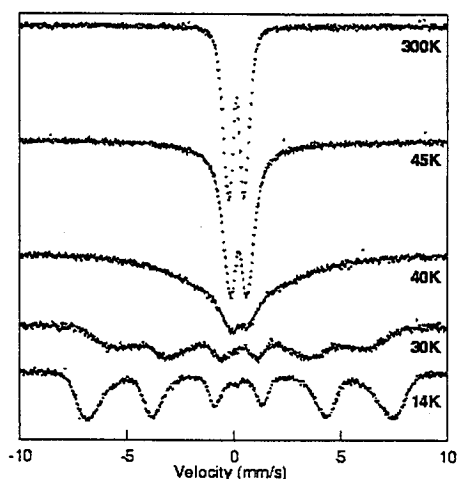


Fig. 3. Spectra of 6C1 taken at various temperatures.

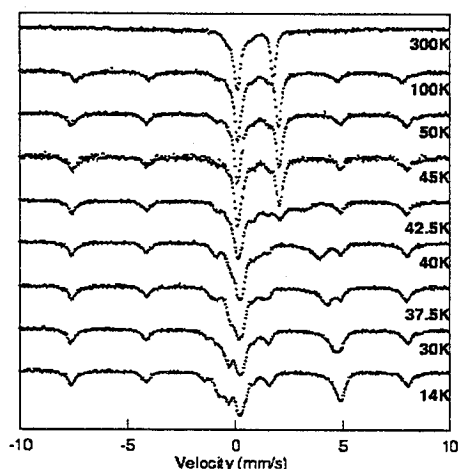


Fig. 4. Spectra of 2C3 taken at various temperatures.

ation in siderite. Meanwhile, XRD shows the four major peaks of siderite (Mineral Powder Diffraction File 29-696). Thus the data demonstrate that carbonate production is favored at 4–8 mm depth, 1 m from the stream, and is observed below 4 mm, both at the 1-m and 2-m sites.

We have observed a similar apparent loss at low temperatures of a ferrous peak at  $\sim 2.5$  mm/s for 2.09-Ga hematite stromatolite PPRG 2443, Gunflint Iron Formation. We will investigate whether this is related to the presence of preserved carbonate in the sample.

Isotopic data from SNC meteorites suggest an ongoing mechanism of crustal-atmosphere exchange that Jakosky and Jones [4] have attributed to active subsurface hydrothermal systems. It is generally assumed that  $\text{CO}_2$  of the primitive martian atmosphere was lost through a combination of escape to space and sequestering in the crust as carbonates. This is supported by the geochemical models [5], which indicate that hydrothermal mineralization could have been a highly effective means for sequestering carbonates in the early martian crust. The bulk composition of the martian crust is thought to be basaltic, and therefore enriched in Fe, Mg, and Ca. It is likely that solutes formed through hydrothermal circulation in

the martian crust would be comparatively enriched in these elements and that any carbonates precipitated from those solutions would tend to be Fe-rich varieties [6]. This view is supported by the Fe-rich hydrothermal carbonates observed in ALH 84001 [7]. Our ability to detect iron carbonate (siderite) iron-spring samples suggests an important potential application for the *in situ* analysis of martian crustal rocks during future landed missions. A systematic search for iron carbonates in martian rocks using Mössbauer would afford an opportunity to test the hypotheses discussed above regarding the evolution of the martian atmosphere and climate.

The occurrence of siderite within our subsurface profiles at Chocolate Pots suggests a potentially important connection to the microbiology of the system. Carbonate precipitation has been shown to be biologically mediated due to pH increases induced by sulfate reduction [8,9]. It is possible that a similar mechanism may account for the precipitation of iron carbonates within the deeper portions of our mat profiles. If the carbonates are being precipitated through biological controls, the isotopic signatures of the carbonates should reflect enrichment in the heavier isotope. It is also quite possible that these authigenic carbonates have captured microfossils or organic compounds as they precipitated. These comprise important areas for research that we will address in the future.

**Acknowledgments:** This research has been supported by grants from the NASA Exobiology and PIDD Programs.

**References:** [1] Mitra (1994) Chapter 10 in *Applied Mössbauer Spectroscopy*, Pergamon, 381 pp. [2] Forester et al. (1969) *J. Appl. Phys.*, 40, 1316. [3] Hang Nam Ok (1969) *Phys. Rev.*, 185, 472–476. [4] Jakosky and Jones (1994) *Nature*, 370, 328–329. [5] Griffeth and Shock (1995) *Nature*, 377, 406–408. [6] Farmer (1996) in *Evolution of Hydrothermal Ecosystems on Earth (and Mars?)*, pp. 273–299, Wiley. [7] McKay et al. (1996) *Science*, 273, 924–930. [8] Krumbein (1979) in *Biogeochemical Cycling of Mineral-forming Elements*, Elsevier, 612 pp. [9] Erlich (1990) *Geomicrobiology*, Dekker, 646 pp.

## GEOLOGIC ALTERATION AND LIFE IN AN EXTREME ENVIRONMENT: PU'U WAI'AU, MAUNA KEA, HAWAII.

C. C. Allen<sup>1</sup>, R. V. Morris<sup>2</sup>, D. C. Golden<sup>1</sup>, and C. S. Upchurch<sup>3</sup>,  
<sup>1</sup>Lockheed Martin Engineering and Sciences, Houston TX 77058, USA, <sup>2</sup>NASA Johnson Space Center, Houston TX 77058, USA, <sup>3</sup>Friendswood High School, Friendswood TX 77546, USA.

We are investigating Pu'u Waiau, a cinder cone located near the summit of Mauna Kea volcano. Lake Waiau occupies a portion of the crater. Volcanic ash and lapilli that form the cone have been hydrothermally altered to a material with a reflectance spectrum close to that of the martian bright regions. An extremely limited ecosystem, consisting mainly of bacteria, is found in the water and the rocks. Pu'u Waiau provides an opportunity to study geologic alteration and life in an environment approaching that on early Mars.

**Geology and Environment:** Pu'u Waiau is located 1 km southwest of the summit of Mauna Kea, at an altitude of approximately 4000 m. The cone was formed by eruptions of ash and lapilli. A hawaiite-mugearite lava flow from Pu'u Waiau has produced a K-Ar date of  $107 \pm 13$  k.y. [1].

Mauna Kea (White Mountain) has been glaciated at least four times, most recently around 12,000 yr ago. Several of the summit

cones and flows are characterized by hyaloclastites and pillow lavas indicative of eruption into glacial meltwater. Porter [2] contends that Pu'u Waiau was erupted subglacially, while Wolfe et al. [1] argue for subaerial eruption during an interglacial period.

The summit of Mauna Kea is a semi-arid, alpine desert tundra. Nighttime temperatures fall below freezing throughout the year [3]. The upper slopes are snow-covered each winter but the snow completely melts and ablates in the spring. Woodcock [4] described a 10-m-thick permafrost layer beneath the south wall of the Mauna Kea summit cone. The present investigation located interstitial ice within a few centimeters of the surface in the outward-facing east slope of Pu'u Waiau.

Lake Waiau, located in the Pu'u Waiau crater, is the only permanent body of water on Mauna Kea. The lake is fed by the melting of snow and subsurface ice, and the level is maintained by a small outflow channel. The lake is perched on a layer of relatively impermeable pyroclasts [2].

**Alteration:** Portions of the vesicular ash and lapilli that form Pu'u Waiau have been extensively altered. The major secondary mineral is clay, identified as montmorillonite mixed with saponite [3]. Minor alteration components include the zeolites phillipsite and possibly gismondine [1]. This suite of minerals is indicative of hydrothermal alteration at moderate temperatures, probably due to the percolation of warm water or steam through the cinders [1,3]. Alternatively, alteration could have been contemporaneous with eruption into subglacial meltwater [2].

Material on other portions of the upper slopes of Mauna Kea is much less altered. Fine ash and clay particles have been winnowed from much of the surface, leaving a lag deposit of millimeter- to centimeter-scale lapilli and rock fragments. The material below approximately 10 cm is finer grained than that at the surface and contains considerably more X-ray amorphous colloidal material (palagonite) than clay. The surface ash is extremely dry, while the palagonitic material below a depth of approximately 5 cm is distinctly moist. Much of this moisture evaporates within a few minutes upon exposure to the air.

**Life:** The summit of Mauna Kea is nearly devoid of life. The exception is the relative oasis created by Lake Waiau. The shoreline, particularly around short stream channels, is thinly fringed by grasses. Droppings from small mammals were observed near some of the grassy areas.

The lake also contains a limited population of micro-organisms. We cultured lake water in three agar media for 30 hr at 37°C. We also examined solids filtered from the lake water using optical and scanning electron microscopy. The lake sample contains 1–2- $\mu$ m bacilli and submicrometer coccoid forms.

We also collected material from a suspected bacterial mat at the shoreline, which was producing bubbles of an unidentified gas. This sample contains culturable bacteria in much higher concentrations than the lake water, as well as numerous sausage-shaped micro-organisms resembling diatoms.

The rim of Pu'u Waiau crater, approximately 100 m above lake level, consists of dry ash partially altered to smectite. A sample of this material yielded extremely small amounts of culturable bacteria. This result suggests that bacteria can survive at the surface anywhere on the mountain.

We also tested a sample of mixed volcanic ash and ice from the interstitial ice deposit on the outer slope of the cone. This material produced large colonies of micrometer-scale bacilli. The culture

pattern resembled that from the dry ash sample, but was orders of magnitude more vigorous. These bacteria are apparently adapted to existence near the freezing point at the interface between ash and ice. However, they thrive when exposed to elevated temperatures and abundant nutrients.

**Mars:** Hydrothermally altered volcanic ash has been proposed as a spectral analog to the fine-grained, eolian surface material that dominates the soil of Mars [5]. We measured the visible and near-infrared spectrum of altered, clay-bearing ash from the rim of Pu'u Waiau and compared it to a composite spectrum of martian bright regions [6]. Both spectra contain a relatively featureless ferric absorption edge through the visible and show essentially flat absorption in the near-infrared. Bands at 1400 and 1900 nm in the Pu'u Waiau spectrum result from higher levels of H<sub>2</sub>O and OH in the ash than on Mars. The presence of ferric absorption features near 600, 750, and 860 nm in the martian spectrum implies higher levels of red (well-crystalline and pigmentary) hematite on Mars [7] than in the Pu'u Waiau material.

Bacteria can exist in a range of environments at the 4000-m elevation on Mauna Kea. These micro-organisms survive in water, at the interface of ice and volcanic ash and even in the dry ash itself. Bacteria on a warmer, wetter early Mars might likewise survive in isolated bodies of water, within permafrost layers, or perhaps even in the near-surface regolith.

**References:** [1] Wolfe E. W. et al. (1997) *USGS Prof. Pap.* 1557, in press. [2] Porter S. C. (1979) *GSA Bull.*, 90, 980–1093. [3] Ugolini F. C. (1974) *Clays and Clay Min.*, 22, 189–194. [4] Woodcock A. H. (1974) *Arctic and Alpine Research*, 6, 49–62. [5] Allen C. C. et al. (1981) *Icarus*, 45, 347–369. [6] Mustard J. F. and Bell J. F. III (1994) *GRL*, 21, 3353–3356. [7] Morris R. V. et al. (1997) *JGR*, in press.

**THE EARLY MARTIAN CLIMATE WAS EPISODICALLY WARM AND WET.** V. Baker, Department of Hydrology and Water Resources (and Lunar and Planetary Laboratory), The University of Arizona, Tucson AZ 85721-0011, USA (baker@piri.lpl.arizona.edu).

In 1991 an "outrageous hypothesis" [1] was proposed that throughout its long-term geological history the climate of Mars alternated between two states as follows: (1) A long-term, stable state of general stability and cold, dry conditions, similar to those prevailing today at the planet's surface. (2) A short-term, quasi-stable state considerably warmer and wetter than those prevailing today. The necessity for postulating the past existence for state 2 derives from a great variety of geological evidence that otherwise seems inexplicable [2]. Among the geological phenomena explained by transitions between the two states are the following: extensive lacustrine and "marine" conditions (of relatively short duration) in the northern plains [3], extensive thermokarstic disruption of sedimentary deposits on the northern plains and in the outflow channels that fed water to them, extensive periglacial landform development (including especially near-surface ice flowage requiring much warmer temperatures than those prevailing today), valley networks developed on relatively young martian volcanos, and extensive evidence for glaciation [4] (notably in the southern hemisphere of Mars, but also on high volcanos, and perhaps in some of the outflow channels

that had earlier debouched flood water to the northern plains). Although these and many other landforms developed during state 2, the very short duration of that state and the small number of its repetitions are indicated by extensive evidence for very slow denudation in the martian cratered uplands. Crater morphologies are preserved such that prolonged precipitation, as occurring on Earth, could not have been possible. Clearly state 2 was a climate that on Earth would be classed as cold, dry, and glacial. However, on Mars, this contrasts with state 1, which was supercold and superdry, thereby precluding glacial conditions. The dry valleys of Antarctica are more similar to the ancient state 2 of Mars than they are to state 1.

The transition from the long-persistent state 1 conditions to the short-term glacial conditions (state 2) was induced cataclysmically. The outflow channels debouched absolutely phenomenal discharges of water [5], exceeding by an order of magnitude or more the largest known cataclysmic flood flows of Earth [6,7]. The energy for these immense floods could only have been supplied thermally, and a great phase of mantle plume activity was proposed, disrupting the permafrost and releasing both floods of water and immense bursts of radiatively active gases. The latter generated a transient greenhouse that facilitated the quasi-stable state 2 climate. A consequence of the above model/hypothesis is that extensive zones of the relatively warm, subsurface hydrosphere was delivered cataclysmically to the surface of the planet. If these zones, particularly those long-persistent beneath the permafrost, contained living organisms of the type tentatively identified in meteorite ALH 84001, then these organisms must have been extensively dispersed to the planet's surface. Although phase 2 conditions may have been too transient for their survival on the surface, they may have flourished long enough to leave extensive fossil evidence. The latter would be accessible to future lander missions to Mars.

**References:** [1] Kerr R. A. (1993) *Science*, 259, 910–911. [2] Baker V. R. et al. (1991) *Nature*, 352, 589–594. [3] Parker T. J. et al. (1993) *JGR*, 98, 11061–11078. [4] Kargel J. S. and Strom R. G. (1992) *Geology*, 20, 3–7. [5] Komatsu G. and Baker V. R. (1997) *JGR*, in press. [6] Baker et al. (1993) *Science*, 259, 348–350. [7] O'Connor J. E. and Baker V. R. (1992) *GSA Bull.*, 104, 267–279.

**DEVELOPING A CHEMICAL CODE TO IDENTIFY MAGNETIC BIOMINERALS (BIOMAGNETITE AND BIOGREIGITE) IN MARS SOIL AND ROCKS.** A. Banin<sup>1,2</sup> and R. L. Mancinelli<sup>2</sup>, <sup>1</sup>Department of Soil and Water Sciences, Hebrew University, P.O. Box 12, Rehovot, Israel, <sup>2</sup>SETI Institute, Mountain View CA, USA.

Life on early Mars is a plausible proposition. A recent review of the chemical make-up and physical environment of Mars, as we currently know and understand it, has shown that all the necessary ingredients for the evolution of life in a mode similar to that on Earth are in place [1,2]. This forms the basis for various propositions that life did arise on Mars. The search for life on Mars, extinct or extant, is receiving renewed attention with the detection in the ancient Mars meteorite ALH 84001 of several mineralogical, chemical, and morphological features that were attributed to evolved life [3]. Due to the lack of organic matter in the top soil of Mars, search for fossilized life relies heavily on mineral biomarkers. Therefore, the continued

exploration of Mars and the search for life on its surface calls for the development of protocols that will establish unequivocally that a certain mineral is biogenic in its origin and may be a proof for the early evolution and presence of life on Mars.

A primary observation that led to the suggestion that biological activity was fossilized in Mars meteorite ALH 84001, is the discovery of cuboid nanophase crystalline magnetite ( $\text{Fe}_3\text{O}_4$ ) of extremely small size in the meteorite. Currently, the only basis for the identification of these nanocrystals as biogenic is their morphology and small particle size [3]. This is not unequivocal nor unique evidence for biogenic origin because various abiotic chemical-mineralogical mechanisms may control and limit crystal growth, thus producing nanocrystals. For example, limited fluxes and a controlled supply of crystal components [4] and/or a physically restricting matrix [5] may be invoked as possible nonbiogenic mechanisms limiting crystal growth. Another possible mechanism for control of crystal growth is through high-temperature gas-solid deposition [6]. In the search for additional and unequivocal biomarkers, we propose to characterize the pattern of enrichment and/or depletion factors (distribution coefficients) of various major, minor, and trace metals in magnetic fractions separated from soils and crushed rocks on Mars. We hypothesize that a unique metal distribution pattern will be found in biogenic magnetite or greigite ( $\text{Fe}_3\text{S}_4$ ) nanocrystals due to the strict controls exerted by cell membranes and metabolic activity on the chemical composition of living organisms in general, and the highly controlled synthesis of magnetosomes in particular. If this is so, the patterns of elemental distribution in biogenically produced magnetic minerals will be different from those in magnetic minerals produced abiotically. These patterns may then be used to establish whether nanophase magnetite and greigite crystals found in Mars soil and rocks represent only a case of mineralogically limited crystal growth, or are fossilized residues of ancient life on Mars.

Biogenic magnetite is produced either by matrix-controlled or by biologically induced mechanisms. Biologically induced generation of magnetite involves dissimilatory Fe-reducing bacteria that couple Fe reduction to cellular energy and organic matter production. The process produces extracellular magnetite crystals of low crystallinity with a relatively wide grain-size distribution that are not clearly distinguishable from magnetite produced inorganically in partially reducing environments [7]. Matrix-controlled biomagnetites, on the other hand, are those produced within the cells of magnetotactic bacteria. These organisms are widespread in nature, being ubiquitous in aquatic environments and present in soils [8,9]. All the magnetotactic bacteria contain magnetosomes, intracellular membrane-bounded vesicles containing single-magnetic-domain magnetite crystals [8,14]. The controlled mode of synthesis of the individual crystals causes their magnetic dipole moments to orient parallel to each other in a chain, thus adding up and maximizing the dipole moment of the cell.

Petrogenic magnetite tends to form solid solutions with a number of low-solubility oxides of related elements. Metals that preferentially isomorphously substitute for Fe in the magnetite structure and form relatively stable solid solutions include Ti, Al (1–10%); Mg, Mn, V (0.1–1%); Cr, Zn, Cu (0.01–0.1%); and Ni, Co, Pb at lower concentrations [15]. The preference for substitution is determined by the element's ionic radii ratio to Fe and its valence. Because both  $\text{Fe}^{2+}$  and  $\text{Fe}^{3+}$  are replaceable in the magnetite structure, both divalent and trivalent metals are accommodated in the magnetite lattice. The ability to form continuous replacement series among the

major constituent cations, the easy formation of solid solutions with the Al and Fe oxides, and isomorphous substitution of trace elements within the O lattice, lead to large variations in the chemical composition of petrogenic magnetites.

Living organisms control their chemical composition within narrow limits. A chemical code is enforced on tissue composition and on internal and external biominerals produced by organisms [16]. As a result, the chemical composition of intracellular biominerals appears to be strictly controlled. Analyses of the chemical composition of magnetosome magnetites were conducted using analytical electron microscopy of single crystals and have shown the prevalence of Fe and lack of other metals in the biominerals [12–14,17,18]. It is assumed that the magnetosome membrane is the locus of control over the size and morphology of the magnetic particles [12]. The membrane acts as a controller for compositional, pH, and redox differentiation between the vesicle the intracellular environment. Specifically, the supersaturation level of the crystallizing mineral within the vesicle must be precisely controlled because the crystals exhibit a high degree of structural perfection. Even when cultured in the presence of sulfide, cells of the magnetotactic bacterium belonging to strain MC-1 have synthesized magnetite and not greigite crystals [19], showing strong magnetosome control of the chemical composition of the crystal. When *Magnetospirillum magnetotacticum* was incubated with Ti, Cr, Co, Cu, Ni, Hg, and Pb no transition metals other than Fe were detected in the magnetosome [18]. This suggests that the membrane exerts an extremely high degree of control over the flux of metals into the cell, totally preventing them from becoming minor components of the magnetite produced by the cell. The results reported by Gorby [18] are not definitive, however, due to the low sensitivity and high detection limits of the analytical procedure used. As a result, the work must be repeated using different techniques to establish the exact pattern of distribution coefficients of minor and trace constituents in biominerals.

A proposed protocol for *in situ* analysis of magnetic separates from Mars soil and rocks may involve the following steps: (1) Dry separation and concentration (beneficiating) of magnetic particles from Mars soil. Such separation has, in fact, been achieved during the Viking mission [19], and is easily performed. (2) The chemical composition of the magnetic separate will then be determined using the best chemical tools available on site. (3) Comparison of the detailed chemical enrichment factors of trace metals in the magnetic separates to those in the bulk soil (or rock) on the one hand, and to the typical pattern of enrichment/depletion factors in biogenically produced intracellular magnetite crystals, on the other hand, will lead to improved identification of the source and mode of formation of the magnetic minerals proving, or negating, claims for their biogenic origins.

**References:** [1] Banin A. and Mancinelli R. L. (1995) *Adv. Space Res.*, 3, 163. [2] Mancinelli R. L. and Banin A. (1995) *Adv. Space Res.*, 3, 171. [3] McKay D. S. et al. (1996) *Science*, 273, 924. [4] Banin A. et al. (1993) *JGR*, 98, 20831. [5] Morris R. V. et al. (1989) *JGR*, 94, 2760. [6] Bradley J. P. et al. (1996) *GCA*, 60, 5149. [7] Lovley D. R. et al. (1987) *Nature*, 330, 252. [8] Blakemore R. P. (1975) *Science*, 190, 377. [9] Fassbinder J. W. E. et al. (1990) *Nature*, 343, 161. [10] Frankel R. B. et al. (1979) *Science*, 203, 1355. [11] Mann S. N. et al. (1987) *Proc. R. Soc. London, B* 231, 469. [12] Mann S. N. et al. (1987) *Proc. R. Soc. London, B* 231, 477. [13] Bazylinski D. A. et al. (1993) *Arch. Microbiol.*, 160, 35.

[14] Bazylinski D. A. et al. (1993) *Nature*, 366, 218. [15] Correns C. W. (1969) *Introduction to Mineralogy*, Springer, New York, 484 pp. [16] Banin A. and Navrotsky Y. (1975) *Science*, 189, 550. [17] Towe K. M. and Moench T. T. (1981) *EPSL*, 52, 213. [18] Gorby Y. A. (1989) Ph.D. thesis, University of New Hampshire. [19] Meldrum F. C. et al. (1993) *Proc. R. Soc. London, B* 251, 231. [19] Hargraves R. B. et al. (1977) *JGR*, 82, 4547.

**EFFECT OF IMPACTS ON EARLY MARTIAN GEOLOGIC EVOLUTION.** N. G. Barlow, Department of Physics, University of Central Florida, Orlando FL 32816, USA.

The heavily cratered highlands of Mars attest to the heavy bombardment experienced by this planet early in its history. Impact cratering has been a major geologic process on Mars, both in the production of the craters distributed across the planet's surface, as well as affecting the overall surface and climatic evolution of the planet. The size and frequency of impacts were greater early in martian history (within about the first 3.5 k.y., according to most models), and analysis of the martian cratering record reveals clues to the evolution of the planet during this time period.

Crater size-frequency distribution analyses of the Moon and inner solar system planets reveal two distinct crater populations. The heavily cratered regions of Mercury, the Moon, and Mars all display a highly structured curve that cannot be represented by a single sloped distribution function at all crater diameters. The less heavily cratered lunar maria, martian plains, and surfaces of Venus and Earth display a crater size-frequency distribution that can be described by a distribution with a -2 cumulative (-3 differential) slope. Although some controversy still exists as to the reason for these two different distributions [1], several lines of evidence suggest these differences are real and represent a change in the size-frequency distribution of the impacting objects [2]. As such, the heavily cratered regions of inner solar system objects are interpreted to represent impacts from debris left over from the formation of the planets during the period of late heavy bombardment. The less heavily cratered regions record impacts from the current population of asteroids and comets. For Mars, analysis of the crater size-frequency distribution curves indicates that the heavily cratered (Noachian-aged) units date from the period of heavy bombardment; the ridged plains (primarily Lower Hesperian) also date from the period of heavy bombardment but their lower crater densities indicate they formed near the end of this period; and the lightly cratered terrain (Upper Hesperian through Amazonian) formed in the post-heavy bombardment period characterized by the present-day impact population [3].

The degree of degradation suffered by impact craters varies across the planet. Older craters are generally identified by a combination of superposition relationships and degree of degradation of features such as ejecta blankets and crater rims. Given the amount of geologic activity that the planet has undergone, one would expect that old craters on ancient terrain would show higher amounts of degradation than younger craters. This is exactly what is seen. However, the degree of degradation does not correlate with age of the terrain unit, indicating that the rate of degradation (erosion and/or deposition) has not been constant throughout martian history. Old

craters on Noachian terrain are much more degraded than is expected based on current erosional/depositional rates.

The crater size-frequency distribution of fresh impact craters can provide constraints on when the change from high degradation rates to the current level occurred. Fresh craters are defined here as those that still retain at least 90% of their surrounding ejecta blanket, still display a well-defined crater rim, and have little to no interior crater fill. These are craters that, by definition, have undergone little degradation since their formation. Although localized episodes of high degradation can occur over small areas [4], the overall crater size-frequency distribution curves for different terrain types can provide information about changes in the degradation history for the planet as a whole. The crater size-frequency distribution curve for fresh craters superposed on Noachian-aged ("ancient") units is statistically identical (Chi-squared distribution tests) to the fresh crater curve for the ridged plains [5]. The crater density difference between fresh crater and nonfresh crater curves for Noachian terrains is much greater than the corresponding curves for ridged plains and post-heavy-bombardment terrains. However, the fresh crater curves for the ancient Noachian terrain and the ridged plains still display the highly structured shape indicative of the heavy-bombardment-period impactor population.

The large difference in crater density between the curves for fresh craters and nonfresh craters on ancient terrain indicates much higher rates of degradation prior to the formation of the fresh craters than is seen for the younger terrain units. This is supported by photogeologic evidence of craters on Noachian-aged terrains showing much higher degrees of degradation than craters elsewhere [6]. The crater density of the fresh crater curve can provide constraints on when the period of high degradation ended. As already noted, this curve is statistically identical to the fresh crater curve for ridged plains and just slightly below the overall curve (fresh plus nonfresh but nonburied craters) for ridged plains. This curve still shows the highly structured nature of heavy-bombardment-aged terrains, but is one of the last size-frequency curves to do so—slightly younger terrains display size-frequency distribution curves indicative of formation in the post-heavy-bombardment era.

This analysis of the size-frequency distribution curves for fresh and nonfresh craters on martian terrain units of different ages indicates a period of high degradation ended prior to the end of the heavy-bombardment period, an idea presented by others subsequent to the Mariner 9 mission [7] and further supported by Viking analysis. The crater curve for the Argyre Basin rim material is statistically identical to the fresh crater curves of ancient and ridged plains material [5], indicating that the period of high degradation ceased about the time of the Argyre impact near the end of the heavy-bombardment period.

Many studies have suggested processes responsible for this early period of high degradation. Since this period was dominated by high impact rates, ejecta blanketing is one possible source of the degradation [8]. The coincidence of the end of this degradation period with the terminal stages of late heavy bombardment would seem to lend support to this idea. However, studies of how craters are degraded by various processes [9–11] indicate that the degraded craters in the martian highlands do not show shapes reflective of degradation by ejecta blanketing alone. Instead the shapes are most similar to what would be expected from fluvial erosion, including rainfall. This of course requires climatic conditions much different from those that currently exist on Mars, specifically the existence of

a thicker atmosphere that could support rainfall. A thicker atmosphere has also been suggested to explain some characteristics of the highland valley networks [12] as well as isotopic ratios within the current martian atmosphere [13].

The cessation of high degradation on Mars around the time of the Argyre impact correlates well with the cessation of highland valley network formation [14] as well as the terminal stages of late heavy bombardment. The large martian impact basins all formed during the heavy-bombardment period, with Hellas and Argyre forming near the end of this time [3]. Impact erosion models [15] suggest that the formation of such large basins was a very efficient method of eroding an initially thicker martian atmosphere to its present state. Thus the theoretical models and photogeologic evidence suggest the following scenario for the evolution of early Mars:

Mars initially had a thicker atmosphere that allowed rainfall and both surface and subsurface water. During this time, left-over material from the formation of the solar system impacted the surface and the resulting craters were subject to rapid degradation by fluvial processes. Large meteoroids were more abundant during this time than in the post-heavy-bombardment era, and as this large material passed through the martian atmosphere to produce large impact basins on the surface, they gradually eroded away the atmosphere. The final huge impacts of Hellas and then Argyre finished off the erosion of the initially thicker atmosphere, changing the climatic conditions to what prevails on Mars today. This caused a cessation of highland valley network formation and the end of the period of high degradation rates.

**References:** [1] Chapman C. R. and McKinnon W. B. (1986) in *Satellites*, pp. 492–580, Univ. of Arizona. [2] Strom R. G. et al. (1992) in *Mars*, pp. 383–423, Univ. of Arizona. [3] Barlow N. G. (1988) *Icarus*, 75, 285–305. [4] Barlow N. G. (1995) *JGR*, 100, 23307–23316. [5] Barlow N. G. (1990) *JGR*, 95, 14191–14201. [6] McGill G. E. and Wise D. U. (1972) *JGR*, 77, 2433–2441. [7] Chapman C. R. and Jones K. L. (1977) *Annu. Rev. Earth Planet. Sci.*, 5, 515–540. [8] Soderblom L. A. et al. (1974) *Icarus*, 22, 239–263. [9] Craddock R. A. and Maxwell T. A. (1990) *JGR*, 95, 14265–14278. [10] Grant J. A. and Schultz P. H. (1990) *Icarus*, 84, 166–195. [11] Grant J. A. and Schultz P. H. (1993) *JGR*, 98, 11025–11042. [12] Baker V. R. et al. (1992) in *Mars*, pp. 493–522, Univ. of Arizona. [13] Owen T. (1992) in *Mars*, pp. 818–834, Univ. of Arizona. [14] Schultz P. H. (1986) *NASA TM-88383*, pp. 188–189. [15] Melosh H. J. and Vickery A. M. (1989) *Nature*, 338, 487–489.

#### BIOMARKERS FOR ANALYSIS OF MARTIAN SAMPLES.

L. Becker<sup>1,2</sup>, G. D. McDonald<sup>3</sup>, and J. L. Bada<sup>1</sup>, <sup>1</sup>Scripps Institution of Oceanography, University of California, San Diego, La Jolla CA 92093, USA, <sup>2</sup>NASA Ames Research Center, Moffett Field CA 94035, USA, <sup>3</sup>Laboratory for Planetary Studies, Cornell University, Ithaca NY 14853, USA.

A central problem in organic analyses of martian samples (*in situ* or returned) is not only identifying and quantifying organic compounds that may be present, but also distinguishing those molecules produced abiotically from those synthesized by extinct or extant life. Terrestrial biology uses only a limited number of the large variety of organic compounds that can be synthesized abiotically under plausible cosmochemical conditions, and would have thus possibly



been available at the time of the origin of life. The detection on Mars of a small subset of these possible prebiotic compounds would be suggestive, but not compelling, evidence of past or present martian biochemistry. The most reliable indicator of the biological vs. abiotic origin of organic molecules is molecular homochirality [1]. The structural principles on which biomolecular activity is based lead us to believe that any functional biochemistry must use a single optical isomer, or enantiomer, of any optically active molecule. Proteins, for example, cannot fold into bioactive configurations such as the  $\alpha$ -helix if the amino acids of which they are composed are racemic (i.e., consist of equal amounts of D and L enantiomers). In contrast, all known laboratory abiotic synthetic processes result in racemic mixtures of chiral amino acids, and the amino acids in carbonaceous chondrites are almost entirely racemic [2]. Therefore an enantiomeric selection process would be required at some stage in the origin or evolution of life. Because there is no apparent biochemical reason why L amino acids would be selected over D amino acids, the selection of L amino acid homochirality on Earth has been considered to be simply a matter of chance.

Of the homochiral compounds used in terrestrial biochemistry, amino acids are the most suitable for use as biomarkers in extraterrestrial samples. Amino acids are in general less prone to decomposition than other chiral compounds such as ribose and deoxyribose. Detection techniques with sub-pmol sensitivities exist for amino acids, and are potentially adaptable for use on Mars lander or rover spacecraft [3]. Although we do not know whether amino acids were a component of the first self-replicating systems, or even required for the origin of life, a biochemical system of any significant complexity would probably evolve protein catalysis at an early stage. The detection of a nonracemic mixture of indigenous amino acids in a martian sample would be strong evidence for the presence of an extinct or extant biota on Mars. The finding of an excess of D amino acids would provide irrefutable evidence of unique martian life that could not have been derived from seeding the planet with terrestrial life. In contrast, the presence of amino acids with D/L close to 1.0, along with abiotic amino acids such as  $\alpha$ -aminoisobutyric acid (Aib), would be indicative of an abiotic origin, although we have to consider the possibility that the racemic amino acids were generated from the racemization of biotically produced amino acids [4].

We have used chiral amino acid analyses to investigate possible terrestrial organic contamination of the Antarctic shergottite EETA 79001 [5]. This meteorite contains several hundred parts per million low-temperature combustible C, which has been suggested to be endogenous martian organic material [6]. Analyses of a small fragment of the EETA 79001 carbonate material detected only the L enantiomers of the amino acids found in proteins. There is no indication of the presence of Aib, which is a common amino acid in carbonaceous meteorites and is readily synthesized in laboratory-based prebiotic experiments. However, Aib is not one of the amino acids normally found in the proteins of terrestrial organisms [7]. The amino acids in this martian meteorite are thus most likely terrestrial contaminants concentrated by sublimation of Antarctic ice and introduced into the meteorite by meltwater that percolated through the meteorite.

In addition, we have examined PAHs in the EETA 79001 carbonate and basaltic matrix material, as well as several Antarctic carbonaceous chondrites [8], using laser desorption/ionization mass spectrometry (LDMS). A similar technique was used by McKay et al. [9] for the detection of PAHs in the ALH 84001 meteorite. We found

that many of the same PAHs detected in the ALH 84001 carbonate globules are present in Antarctic carbonaceous chondrites and in both the matrix and carbonate (druse) component of EETA 79001. We also investigated PAHs in Antarctic Allan Hills ice and found that carbonate is an effective scavenger of PAHs in ice meltwater, and the distribution of PAHs extracted from the ice is similar to that found in both martian meteorites.

An important issue to consider is whether PAHs are useful "biomarkers" in the search for extinct or extant life on Mars. PAHs are ubiquitous on the Earth, derived by both the combustion of biomass and fossil fuels, and the slow geochemical aromatization (millions of years) of sterols and triterpenes present in many organisms [10,11]. This aromatization process can be accelerated by hydrothermal activity [12], and thus can occur over a much shorter geological timescale (thousands of years). PAH tracers of combustion have been identified in Greenland ice [13,14]. PAHs are also widespread in the cosmos [15] and are commonly found in carbonaceous chondrites [16] and interplanetary dust particles [17]. McKay et al. [9] argue that the simple distribution of PAHs found in the ALH 84001 is unique and different from that observed in terrestrial samples and carbonaceous chondrites and, thus, the observed PAHs provide evidence of extant or extinct life on Mars. In fact, we have observed similar distributions of PAHs in hydrothermal vent sediments and Antarctic carbonaceous chondrites.

On the Earth, PAHs do not play a major role in the biochemistry of any known organism. Moreover, with the possible exception of obtaining the stable C and H isotopic compositions for these compounds, the molecular architecture of PAHs cannot be used to distinguish between abiotic and biotic processes. Thus, whether the PAHs detected in ALH 84001 are diagenetic products of biologically derived compounds or are abiotic in origin is difficult, if not impossible, to establish.

In contrast to PAHs, amino acids play a major role in biochemistry on the Earth today and amino acid homochirality provides a reliable way of distinguishing between abiotic and biotic origins [3]. As has been discussed above, abiotic synthetic processes yield racemic mixtures of amino acids while terrestrial organisms use L amino acids for protein biosynthesis. Thus, amino acids may be the biomarker of choice in any search for past or present life on the surface of Mars. Future missions to Mars may provide us with a unique opportunity to test for these compounds *in situ*, and sample return missions will provide the pristine samples needed to conclusively evaluate the question of life on Mars.

**References:** [1] Bada J. L. (1995) *Nature*, 374, 594. [2] Cronin J. R. et al. (1988) in *Meteorites and the Early Solar System* (J. F. Kerridge and M. S. Matthews, eds.), p. 819, Univ. of Arizona, Tucson. [3] Bada J. L. and McDonald G. D. (1996) *Anal. Chem.*, 68, 668A. [4] Bada J. L. and McDonald G. D. (1995) *Icarus*, 114, 139–143. [5] McDonald G. D. and Bada J. L. (1995) *GCA*, 59, 1179. [6] Wright I. P. et al. (1988) *Nature*, 340, 220. [7] Bada J. L. (1991) *Phil. Trans. R. Soc. London*, B333, 349. [8] Becker L. et al. (1997) *GCA*, in press. [9] McKay D. S. et al. (1996) *Science*, 273, 924–930. [10] MacKenzie A. S. et al. (1982) *Science*, 217, 491–504. [11] Ramdahl T. (1983) *Nature*, 306, 580–582. [12] Simoneit B. R. T. (1990) *Appl. Geochem.*, 5, 3–15. [13] Jaffrezo J. L. et al. (1994) *Atmos. Environ.*, 28, 1139–1145. [14] Masclet P. et al. (1995) *Analysis*, 23, 250–252. [15] Allamandola L. J. et al. (1989) *Astrophys. J.*, 71, 733–775. [16] Hahn J. H. et al. (1988) *Science*, 239, 1523–1525. [17] Clemett S. J. et al. (1993) *Science*, 262, 721–723.

**APPLICATION OF THE CHEMIN XRD/XRF INSTRUMENT IN ANALYZING DIAGNOSTIC MINERALOGIES: QUANTITATIVE XRD ANALYSIS OF ARAGONITE AND BASALT.** D. Bish<sup>1</sup>, D. Vaniman<sup>1</sup>, P. Sarrazin<sup>2</sup>, D. Blake<sup>3</sup>, S. Chipera<sup>1</sup>, S. A. Collins<sup>3</sup>, and T. Elliott<sup>3</sup>, <sup>1</sup>Geology and Geochemistry, Mail Stop D469, Los Alamos National Laboratory, Los Alamos NM 87545, USA, <sup>2</sup>Mail Stop 239-4, NASA Ames Research Center, Moffett Field CA 94035, USA, <sup>3</sup>Imaging Systems Section, Jet Propulsion Laboratory, 4800 Oak Grove Drive, Pasadena CA 91109, USA.

We are developing a miniaturized X-ray diffraction and X-ray fluorescence (XRD/XRF) instrument for space exploration that will minimize the uncertainties in mineralogical and geochemical evaluation inherent in remote analysis. The instrument has been named CHEMIN, in reference to its role as a simultaneous CHEmical and MINeralogic analyzer. A functioning prototype of this instrument uses a Cu X-ray tube, transmission geometry, and an energy-selective CCD in single-photon-counting mode to collect simultaneous XRF (energy-dispersive) and flat-plate XRD data (see [1,2] for instrument descriptions). The ultimate goal of this instrument will be to obtain combined XRD and XRF data from planetary samples. Such an approach will greatly improve the accuracy of remote petrologic analysis by constraining the number of possible mineralogic interpretations. For example, although the Viking landers provided very useful XRF data on martian regolith, the complex chemistry reported (particularly the mixed-anion suite that includes S and Cl, as well as O) allows a wide range of mineralogic interpretations. Since remote XRF has provided proven results, we focus in this paper on preliminary tests in obtaining quantitative XRD data from the prototype CHEMIN instrument.

X-ray diffraction is the most direct and accurate analytical method for determining the presence of mineral species because the data obtained by this method are fundamentally linked to crystal structure. Other methods, based on chemical or spectral properties, are derivative and subject to much greater uncertainties. Moreover, significant progress has been made in the last decade in the development of quantitative XRD of multicomponent mixtures. The Rietveld method, which fits the entire observed diffraction pattern with a pattern calculated using the crystal structures of the constituent phases of the model mineral system, shows great promise for mineral analysis. This method can provide rapid quantitative estimates of mineral abundance as well as compositional, unit-cell parameters, and structural data on individual minerals [3,4]. In addition, recent advances in quadratic goal programming allow the solution of simultaneous linear equations using chemical and mineralogic data. Use of these techniques with combined bulk-sample XRD and XRF data makes it possible to extract considerable information on individual mineral compositions [5,6].

To test the capabilities of CHEMIN against realistically complex samples, we have used Rietveld analysis to determine mineral abundances from CHEMIN-derived diffraction patterns of a basalt and of a relatively pure sample of aragonite. These samples were chosen to represent a rock type that is known to be abundant on the martian surface and a mineral that in many terrestrial occurrences is biogenic.

XRD and XRF data for these samples were obtained with the prototype CHEMIN instrument using repetitive 30-s counts. After accumulation of numerous 30-s count datasets, the data were ana-

lyzed on a pixel-by-pixel basis. XRF data were obtained from the energy deposited in each pixel, and X-ray powder diffraction rings were generated by plotting the two-dimensional distribution of those pixels containing Cu K $\alpha$  photons. The powder rings were then integrated to generate conventional 2 $\theta$  vs. intensity powder diffraction patterns. The resulting XRD data were used as input to Rietveld refinements. During the refinements, the fit between observed and calculated patterns was optimized through a least-squares process in which parameters related to each phase, including their relative abundances, were varied.

Basalt is a common lithology of all terrestrial planets, fundamentally important in characterizing the nature of a planet's internal processes. Martian basalts have been fortuitously delivered to Earth as SNC meteorites, although these meteorites are quite diverse, ranging from fine-grained basalts to a variety of cumulate lithologies. This small suite of samples has generated considerable speculation about martian volcanism. Although basalts per se are not sought as lithologies likely to preserve fossil life on Earth, the debate about fossil life in martian meteorites provides impetus to the consideration of basalt in an exobiologic context. Indeed, volcanoclastic facies of some terrestrial basalts in systems cemented by calcite have yielded exceptionally well-preserved fossils of soft body parts [7]. For both planetary understanding and for exobiology goals, the ability to determine a martian basalt's chemistry and mineralogy is important.

A diffraction pattern of a terrestrial basalt was obtained using the prototype CHEMIN instrument. The quantitative mineral results from Rietveld analysis of these data are listed in Table 1, and the observed and calculated diffraction patterns are shown in Fig. 1. The X-ray fluorescence pattern is important in analyses of complex mixtures such as basalts because the chemical data provide constraints useful in limiting the mineralogies used in fitting the pattern. Despite the complexity of the basalt sample and the significant limitations in the prototype CHEMIN instrument, the Rietveld analysis is surprisingly good, with a calculated pattern that agrees well with the observed pattern. In addition, the resulting mineral analysis agrees well with optically determined modes for this sample. This level of success has only recently been obtained, and considerable improvement in the CHEMIN results are anticipated in the near future.

In contrast to the basalt, the aragonite sample was relatively pure and was easily characterized. Nevertheless, the XRD component of the CHEMIN analysis was capable of detecting and, with Rietveld processing, measuring impurities of 1.6% calcite and 0.2% quartz. These results illustrate the high sensitivity of the prototype CHEMIN

TABLE 1. Rietveld quantitative analysis of basalt sample.

Mineral	Wt%
Forsterite	7.5
Albite	28.9
Anorthite	17.5
Augite	4.7
Magnetite	1.9
Phlogopite	0.1
Fluorapatite	1.6
Sanidine	37.9

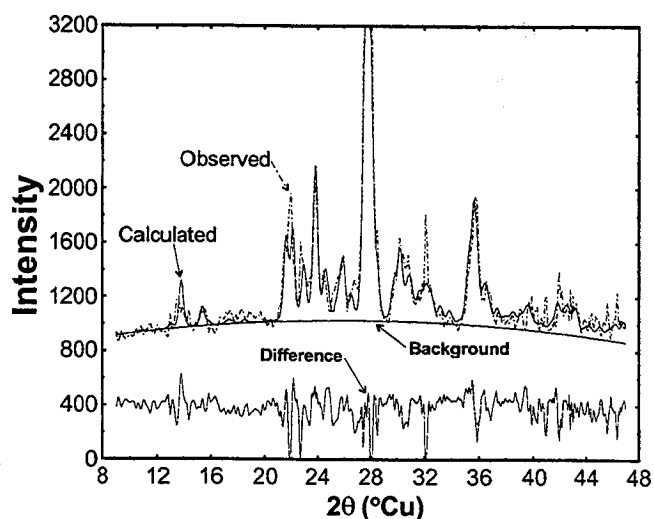


Fig. 1. Rietveld refinement results, showing observed CHEMIN data (dashed line), calculated data (solid line), and difference and background curves (solid lines) for a terrestrial basalt sample.

instrument in detecting very small quantities of diagnostic minerals. Contaminant detection that can distinguish between clastic, cemented clastic, and chemical sediments will be an important tool in remote petrologic and exobiologic studies. This capability will be very important in selecting appropriate samples with fossil-preservation potential for return to Earth and more detailed analysis.

**References:** [1] Blake D. F. et al. (1994) *LPS XXV*, 121–122. [2] Vaniman D. et al. (1994) *Proc. 43rd Annual Denver X-Ray Conference*, p. 43. [3] Bish D. L. and Howard S. A. (1988) *J. Appl. Cryst.*, 21, 86–91. [4] Bish D. L. and Post J. E. (1993) *Am. Mineral.*, 78, 932–942. [5] Braun G. E. (1986) *Clays Clay Mineral.*, 34, 330–337. [6] Braun G. E. et al. (1996) *Proc. 45th Annual Denver X-Ray Conference*, p. 209. [7] Briggs D. E. G. et al. (1996) *Nature*, 382, 248–250.

**SPECTROSCOPIC IDENTIFICATION OF MINERALS IN HEMATITE-BEARING SOILS AND SEDIMENTS: IMPLICATIONS FOR CHEMISTRY AND MINERALOGY OF THE MARTIAN SURFACE.** J. L. Bishop<sup>1</sup>, J. Friedl<sup>2</sup>, and U. Schwertmann<sup>2</sup>, <sup>1</sup>Mail Stop 239-4, NASA Ames Research Center, Moffett Field CA 94035, USA, <sup>2</sup>Lehrstuhl für Bodenkunde, Technische Universität München, D-85350 Freising, Germany.

Identifying the mineralogy of the martian regolith will provide information about the chemical environment on early Mars that controlled the weathering and other processes that generated the fine-grained surface material. Spectroscopic analysis of terrestrial soils and sediments with known weathering histories and/or formation conditions are essential in order to interpret the spectroscopic data from Mars. Here we present reflectance spectra from 0.3 to 25  $\mu\text{m}$  of several basaltic volcanic soils and Atlantis II Deep sediments.

**Introduction:** The soils on Mars are high in  $\text{Fe}^{3+}$  and Si [1] and contain 1–7% of a highly magnetic material [2]. The results of

numerous laboratory experiments and spectral observations suggest that hematite and smectite clays are present in the surface soil on Mars. Less clear is the identity of this magnetic component and how the soils were formed. One plausible scenario for this surface material includes particles of maghemite ( $\gamma\text{-Fe}_2\text{O}_3$ ) distributed in a clay-rich soil [2]. Nanophase (np)-hematite has also been found to be significantly more magnetic than bulk hematite [3] and mixtures of primarily np-hematite and a small amount of bulk hematite in a silicate matrix have been suggested as a possibility for the martian soil that would account for the visible spectral features and the magnetic component [4].

Mineralogical analyses have been performed on several Hawaiian soils formed from Fe-rich basaltic ash under varying moisture conditions [5]. All these soils contain ferrihydrite and hematite. The soils formed under humid conditions contain 20–35% ferrihydrite and a mixture of goethite, hematite, magnetite, and/or maghemite, while those formed under less humid conditions contain ~10% ferrihydrite and no goethite or magnetite.

**Samples:** Basaltic volcanic soils were collected from the Haleakala crater on Maui and from the Greek island Santorini. Although the Santorini climate is very dry, proximity to the Aegean sea allows more moisture to participate in the weathering processes here than at the high elevation of Haleakala. The Santorini soils were collected from a weathered lava flow (181) and near an active steam vent (182). Such soils result from oxidation and “palagonitization” of glassy basaltic lava flows. Palagonitic soil samples have been proposed as a possible analog material for the surface of Mars [6].

The sediment samples stem from a 4-m core of the Atlantis II Deep, Red Sea, representing a poorly (254-5) and a well-crystalline hematite (254-10) from the upper and lower part of the core. Sample 254-5d is a portion of sample 254-5 that was treated with dithionite to remove the Fe oxides.

**Measurements:** Reflectance spectra have been measured at RELAB (Brown University) as in previous investigations [7]. XRD and Mössbauer spectra have been measured as described in [8].

**Results for Palagonitic Soils (Dry Conditions):** These fine-grained soils are reddish-brown, contain 14–19 wt%  $\text{Fe}_2\text{O}_3$  and sample 72 is attracted by a strong permanent magnet. The reflectance spectrum of soil (72) from Haleakala is shown in Fig. 1. The visible region contains a weak feature near 0.93  $\mu\text{m}$  probably due to ferrihydrite and np-hematite (Fig. 1a). Features near 1.4, 1.9, and 2.2  $\mu\text{m}$  are assigned to phyllosilicates (Fig. 1b). In the mid-IR spectral region (Fig. 1c) are a water band near 6  $\mu\text{m}$  and a minimum near 8.5  $\mu\text{m}$  typical of silicates. The low reflectance and weak features at longer wavelengths are characteristic of fine-grained soils.

**Results for Palagonitic Soils (Less Dry Conditions):** The Santorini sample 181 has a reddish-brown color and 182 is slightly more orange. XRD and Mössbauer analyses indicate about equal amounts of hematite and goethite in 182, plus some additional  $\text{Fe}^{3+}$  and  $\text{Fe}^{2+}$ . Reflectance spectra of these two soils are shown in Fig. 1. The visible-region spectrum of 181 exhibits a weak shoulder near 0.8  $\mu\text{m}$  and a weak absorption feature near 0.88  $\mu\text{m}$  (Fig. 1a). Based on the strength of the features near 0.75 and 0.88  $\mu\text{m}$  in the spectrum of 182, this sample has more bulk hematite than the other soils. Sample 182 exhibits a stronger 2.2- $\mu\text{m}$  feature due to  $\text{AlOH}$  and sample 181 exhibits a stronger 1.9- $\mu\text{m}$  feature typical of water in phyllosilicates (Fig. 1b).

**Results for Thermal Oceanic Sediments:** XRD shows that the Atlantis Deep sediments contain hematite and nontronite. The grain size of the poorly crystalline np-hematite and the well-crystalline hematite as measured by XRD peak broadening is 5 and 120 nm respectively. Shown in Fig. 2 are reflectance spectra of two dried sediments and the clay fraction of sample 254-5. The visible-region spectra exhibit features near 0.6, 0.75, and 0.88  $\mu\text{m}$ , which are consistent with hematite, although the 0.88- $\mu\text{m}$  feature occurs at a longer wavelength than usual (Fig. 2a). Nontronite has an absorption near 9.4  $\mu\text{m}$  [9] that is shifting this band toward longer wavelengths. Sample 254-5 is attracted by a strong permanent magnet and exhibits weak features in this region characteristic of nanophase hematite. Sample 254-10 exhibits stronger features in accordance with its larger hematite grain sizes. The features near 2.3, 11–12, and 18  $\mu\text{m}$  (Fig. 2b) in each of these spectra are characteristic of nontronite. In the mid-IR region (Fig. 2c) the nontronite features are intensified in the dithionite-treated sample (254-5d).

**Applications to Mars:** Ferrihydrite and np-hematite are thought to be the most prevalent Fe oxides on the martian surface because of their weak visible features; both are observed in volcanic soils formed under dry to humid conditions. The presence of goethite indicates relatively more humid and/or cooler formation conditions. Although unlikely, if goethite is identified on Mars, it might suggest a moist climate reigned on the early Mars. For sample 182 the Fe is present roughly equally as goethite and hematite; however, the visible spectral features are characteristic of hematite and the typical martian bright regions. In order to confidently identify the mineralogy on Mars, and hence the former geochemical conditions, other techniques, such as IR and Mössbauer spectra and XRD data, will be needed.

**Acknowledgments:** J.L.B. expresses gratitude to the Institute for Planetary Exploration, DLR-Berlin and the Institute of Geochemistry, University of Vienna for support during recent months

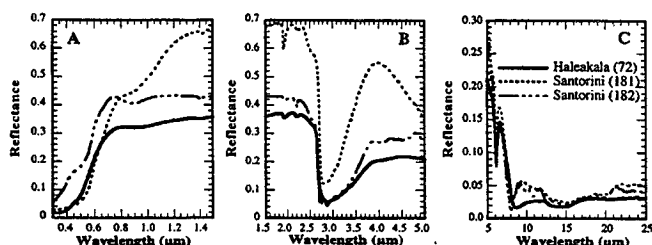


Fig. 1. Reflectance spectra of basaltic volcanic (palagonitic) soils (0.3–25  $\mu\text{m}$ ).

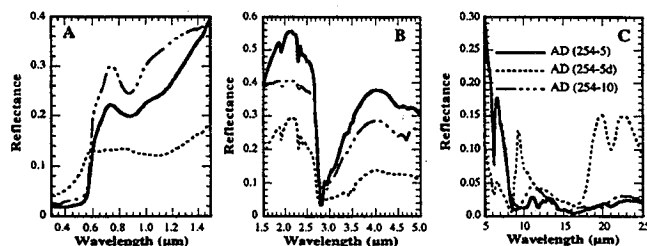


Fig. 2. Reflectance spectra of Atlantis Deep sediments (0.3–25  $\mu\text{m}$ ).

and to the National Research Council and NASA-ARC for support during completion of this work. J.F. and U.S. are grateful for funding from DFG grant Schw 90/47. RELAB is a multi-user facility at Brown University supported by NASA grant NAGW-748. J.L.B. thanks L. Gründler for assistance with sample collection.

**References:** [1] Toulmin P. et al. (1977) *JGR*, 82, 4625. [2] Hargraves R. et al. (1977) *JGR*, 82, 4547. [3] Morris R. et al. (1989) *JGR*, 94, 2760. [4] Morris R. and Lauer H. (1990) *JGR*, 95, 5101. [5] Parfitt R. et al. (1988) *Geoderma*, 41, 223. [6] Allen C. et al. (1981) *Icarus*, 45, 347. [7] Bishop J. et al. (1995) *Icarus*, 117, 101. [8] Friedl J. and Schwertmann U. (1996) *Clay Minerals*, 31, 455. [9] Sherman D. and Vergo N. (1988) *Am. Mineral.*, 73, 1346.

**$^{39}\text{Ar}$ - $^{40}\text{Ar}$  AGE OF ALLAN HILLS 84001.** D. D. Bogard<sup>1</sup> and D. H. Garrison<sup>1,2</sup>, Planetary Sciences, NASA Johnson Space Center, Houston TX 77058, USA (bogard@snmail.jsc.nasa.gov), <sup>2</sup>Also at Mail Code C23, Lockheed Martin, Houston TX 77058, USA.

**Background:** Martian meteorite ALH 84001 currently presents the only opportunity to directly study material that dates from the earliest history of Mars. Among the SNC meteorites, the nakhlites and Chassigny give radiometric ages of  $\sim 1.3$  Ga, and several shergottites give radiometric ages much younger than this [1]. Only ALH 84001 gives Rb-Sr and Sm-Nd isochron ages near 4.6 Ga, which implies that it initially formed very early in martian history [2]. A somewhat younger age of 3.92 Ga has been reported for ALH 84001 using the  $^{39}\text{Ar}$ - $^{40}\text{Ar}$  isotopic chronometer [3,4]. The feldspar in ALH 84001 has been shock melted, and Scott et al. [5] suggest that "plagioclase, silica, and the carbonate in ALH 84001 were probably all melted and partly mobilized during a single shock event of  $\sim 50$  GPa that also formed the brecciated zones." Experiments with eucrites and other shocked meteorites suggest that it is possible to reset the K-Ar chronometer without resetting the Rb-Sr or Sm-Nd chronometers [6]. Thus, precise definition of the  $^{39}\text{Ar}$ - $^{40}\text{Ar}$  age of ALH 84001 is of importance because it defines the time of plagioclase melting by shock impact on Mars and may define the carbonate formation time as well.

**New  $^{39}\text{Ar}$ - $^{40}\text{Ar}$  Results:** We made high-precision  $^{39}\text{Ar}$ - $^{40}\text{Ar}$  measurements of a 90-mg whole-rock sample of ALH 84001 (Fig. 1; "rectangles" are ages, continuous line is K/Ca). Our results are generally similar to Ar-Ar results previously reported [3,4], and we concur with these authors' conclusion that the  $^{39}\text{Ar}$ - $^{40}\text{Ar}$  age of this meteorite is much older than the determined isotopic chronologies of other martian meteorites. However, the Ar release profile of ALH 84001 is complex, and the meteorite contains trapped Ar, which necessitates an uncertain correction to the radiogenic  $^{40}\text{Ar}$  and thus to the derived age. With these considerations, we believe that the time of the shock event that melted feldspar in ALH 84001 is poorly constrained within the time period of  $\sim 3.8$ – $4.3$  Ga, but we suggest that the actual time may be  $\sim 4.2$  Ga. These conclusions differ from those of [3,4].

**Simple Age Interpretation:** Figure 1 indicates that Ar is released from two different phases, one with K/Ca ratios of  $\sim 0.18$ – $0.12$  (plagioclase) and one with ratios of  $< 0.02$  (pyroxene). The sudden decrease in ages over  $\sim 78$ – $93\%$  of the  $^{39}\text{Ar}$  release coincides with the onset of Ar degassing from pyroxene and is strongly suggestive of gain of  $^{39}\text{Ar}$  by recoil redistribution during the neutron irradiation, a phenomenon commonly observed. This redistributed

$^{39}\text{Ar}$  most likely derived from grain surfaces of feldspar, as the recoil distance of  $^{39}\text{Ar}$  is only  $\sim 0.16$  mm. An expected higher apparent age in the early extractions due to recoil loss of  $^{39}\text{Ar}$  is masked by recent diffusive loss of radiogenic Ar from grain surfaces. The slightly lower K/Ca ratios in the early extractions may reflect terrestrial weathering, but the sharply lower ratio at  $\sim 10\%$   $^{39}\text{Ar}$  release is probably due to carbonate decomposition. The sharp increase in ages for the last two extractions (5.3–5.8 Ga at  $>98\%$   $^{39}\text{Ar}$  release) is not likely due to system blanks nor to  $^{39}\text{Ar}$  recoil. The reasonable assumption is that the ages at  $<12\%$   $^{39}\text{Ar}$  release and  $\sim 78$ – $92\%$   $^{39}\text{Ar}$  release have been modified by  $^{39}\text{Ar}$  recoil redistribution and that the apparent “plateau” age of  $4.29 \pm 0.06$  Ga ( $\sim 12$ – $78\%$   $^{39}\text{Ar}$ ) is a measure of the degassing age. This approach differs, however, from that of [3,4], who implicitly assume that the recoil  $^{39}\text{Ar}$  derives from the interior of the high-K grains and prefer to sum all the Ar-Ar ages above  $\sim 12\%$   $^{39}\text{Ar}$  release to derive a somewhat lower age of  $\sim 4.13$  Ga. These ages, however, do not consider the effects of trapped Ar in ALH 84001 and thus may be only upper limits to the shock degassing time, as we next discuss.

**Derivation of Cosmogenic and Trapped Ar:** Argon isotopes in irradiated ALH 84001 have several sources. Part of the  $^{36}\text{Ar}$  and  $^{38}\text{Ar}$  are produced from cosmic rays and correlate in their release with  $^{37}\text{Ar}$ , which is produced in the reactor from Ca, the major target for production of cosmogenic  $^{36,38}\text{Ar}$ . At low and intermediate extraction temperatures,  $^{38}\text{Ar}$  produced in the reactor from  $^{37}\text{Cl}$  complicates the interpretation of  $^{38}\text{Ar}$  components. However, for the last three extractions, which released relatively large amounts of  $^{36,38}\text{Ar}$ , the  $^{36}\text{Ar}/^{38}\text{Ar}$  ratio is constant at 0.65, which is the expected value for pure cosmogenic Ar. For these same extractions, the  $^{36}\text{Ar}/^{37}\text{Ar}$  ratio is nearly constant at  $1.2 \times 10^{-3}$ , but it is considerably higher at lower extraction temperatures due to the presence of trapped Ar components. Thus, we used the concentration of  $^{37}\text{Ar}$  released at each temperature and the  $^{36}\text{Ar}/^{37}\text{Ar}$  ratio of  $1.26 \times 10^{-3}$  to correct the total  $^{36}\text{Ar}$  for cosmogenic  $^{36}\text{Ar}$  ( $3.6 \times 10^{-9}$  cm $^3$ /g). The remaining  $^{36}\text{Ar}$  ( $3.8 \times 10^{-9}$  cm $^3$ /g) is assumed to be a trapped component, either terrestrial or martian in origin, and presumably includes some amount of  $^{40}\text{Ar}$ .

A plot of  $^{36}\text{Ar}/^{40}\text{Ar}$  ratios vs.  $^{39}\text{Ar}$ - $^{40}\text{Ar}$  ages (Fig. 2) gives some insight into the nature of the trapped  $^{36}\text{Ar}/^{40}\text{Ar}$  ratio in ALH 84001. Open symbols represent the plateau extractions; solid symbols labeled with temperatures are all other extractions. Except for the 1200°–1550°C extractions, uncertainties in  $^{36}\text{Ar}/^{40}\text{Ar}$  are smaller than the symbol. The two arrows indicate expected mixing trends between a sample with an Ar-Ar age of 4.0 Ga and either trapped terrestrial air or martian atmosphere. The lower temperature extractions (300°–450°C) plot at lower ages because of recent diffusive loss of Ar (see Fig. 1). They do not define the nature of the trapped component, which at these lower temperatures was probably adsorbed terrestrial air. The 900°–1075°C extractions plot at slightly lower ages because of  $^{39}\text{Ar}$  recoil (Fig. 1), but they also released significant trapped  $^{36}\text{Ar}$ . For the 900°–1075°C extractions, this trapped  $^{36}\text{Ar}$  could reasonably be terrestrial, but could not be martian atmosphere, as this would require absurdly large ages in order for these data to plot on the 4.0-Ga/martian mixing line. Because the 900°–1075°C extractions represent early release of Ar from orthopyroxene, the presence of larger amounts of terrestrial Ar (compared to temperatures of  $\sim 500$ °– $850$ °C) might represent weathered surfaces of pyroxene grains. The 1300° and 1550°C extractions appear to suggest a trapped martian component, but uncertainties in these

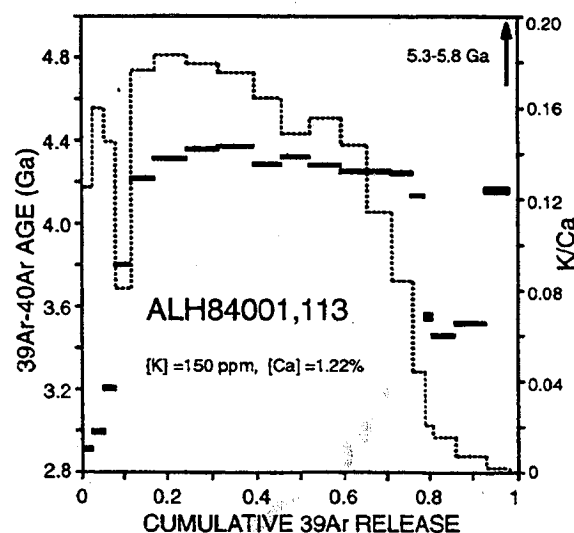


Fig. 1.

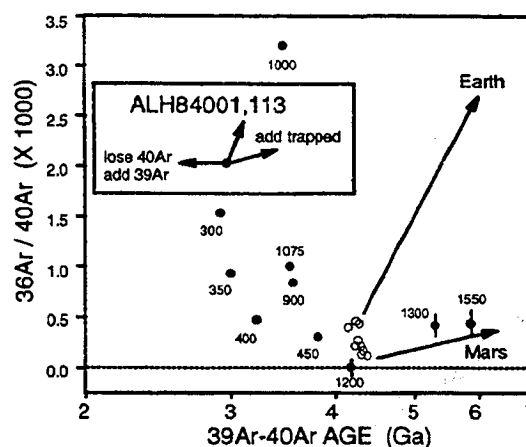


Fig. 2.

data are larger. These and other extractions may also contain relic radiogenic  $^{40}\text{Ar}$  (without  $^{36}\text{Ar}$ ) not entirely degassed by the shock event.

**Effects of Trapped Ar on Age:** Knowing the  $^{40}\text{Ar}/^{36}\text{Ar}$  ratio of the trapped component in ALH 84001 is critical, as the trapped  $^{40}\text{Ar}$  must be subtracted from the total  $^{40}\text{Ar}$  in order to derive a corrected  $^{39}\text{Ar}$ - $^{40}\text{Ar}$  age. If we correct the  $^{40}\text{Ar}$  data in Fig. 1 using the reasonable assumption that all trapped  $^{36}\text{Ar}$  is terrestrial air with  $^{40}\text{Ar}/^{36}\text{Ar} = 295$ , the  $^{39}\text{Ar}$ - $^{40}\text{Ar}$  age of the “plateau” decreases from  $4.29 \pm 0.06$  Ga to  $4.18 \pm 0.12$  Ga and the age summed over  $\sim 12$ – $100\%$   $^{39}\text{Ar}$  release decreases from 4.19 Ga to 3.87 Ga. The larger decrease for the  $\sim 12$ – $100\%$  age is caused by larger amounts of trapped  $^{36}\text{Ar}$  residing in those same extractions that exhibit the greatest  $^{39}\text{Ar}$  recoil effect ( $\sim 78$ – $93\%$   $^{39}\text{Ar}$  release). If instead we assume that the trapped Ar has a  $^{40}\text{Ar}/^{36}\text{Ar}$  ratio of 2400, characteristic of the martian atmosphere, the trapped  $^{40}\text{Ar}$  is larger than the total  $^{40}\text{Ar}$  for many temperature extractions and the ages become negative. This fact and Fig. 1 indicate that little, if any, of the trapped  $^{36}\text{Ar}$  in our

sample of ALH 84001 was derived from the martian atmosphere. Even with a correction for martian atmospheric, however, a quasi-plateau remains in the  $^{39}\text{Ar}$ - $^{40}\text{Ar}$  age spectrum, and two extractions of this "plateau" give the same age of 3.81 Ga. This is an absolute minimum for the shock degassing time of ALH 84001. Furthermore, all the trapped Ar in ALH 84001 need not be terrestrial or martian atmosphere. Some martian meteorites contain a trapped  $^{36}\text{Ar}$  component deriving from the martian mantle and having an unknown  $^{40}\text{Ar}/^{36}\text{Ar}$  ratio [7]. If this mantle  $^{40}\text{Ar}/^{36}\text{Ar}$  ratio is less than the terrestrial value of 295, the corrections to the ages shown in Fig. 1 would be less and the "plateau" age could lie in the range of 4.18–4.29 Ga. Thus we conclude that the limiting range in Ar-Ar ages for ALH 84001 is 3.8–4.3 Ga, with a fair probability of the age being  $\sim$ 4.2 Ga.

**References:** [1] McSween H. (1994) *Meteoritics*, 29, 757. [2] Nyquist L. et al. (1995) *LPS XXVI*, p. 1065. [3] Ash R. et al. (1996) *Nature*, 380, 57. [4] Turner G. et al. (1997) *GCA*, 61. [5] Scott E. et al. (1997) *LPS XXVIII*. [6] Bogard D. (1995) *Meteoritics*, 30, 244. [7] Bogard D. (1997) *JGR Planets*, 102, 1653.

**SCIENTIFIC ISSUES ADDRESSED BY THE MARS SURVEYOR 2001 GAMMA-RAY/NEUTRON SPECTROMETER (GRS/NS).** W. V. Boynton<sup>1</sup>, W. C. Feldman<sup>2</sup>, S. W. Squyres<sup>3</sup>, J. I. Trombka<sup>4</sup>, J. R. Arnold<sup>5</sup>, P. A. J. Englert<sup>6</sup>, A. E. Metzger<sup>7</sup>, R. C. Reedy<sup>2</sup>, H. Wänke<sup>8</sup>, S. H. Bailey<sup>1</sup>, J. Brückner<sup>8</sup>, L. G. Evans<sup>4</sup>, H. Y. McSween<sup>9</sup>, and R. Starr<sup>4</sup>, <sup>1</sup>Lunar and Planetary Laboratory, University of Arizona, Tucson AZ, USA, <sup>2</sup>Los Alamos National Laboratory, Los Alamos NM, USA, <sup>3</sup>Center for Radiophysics and Space Research, Cornell University, Ithaca NY, USA, <sup>4</sup>NASA Goddard Space Flight Center, Greenbelt MD, USA, <sup>5</sup>Department of Chemistry, University of California, San Diego, La Jolla CA, USA, <sup>6</sup>Institute of Geological and Nuclear Sciences, Lower Hutt, New Zealand, <sup>7</sup>Jet Propulsion Laboratory, California Institute of Technology, Pasadena CA, USA, <sup>8</sup>Max-Planck-Institut für Chemie, Mainz, Germany, <sup>9</sup>Department of Geological Sciences, University of Tennessee, Knoxville TN, USA.

The general observational goal of the Mars 2001 GRS/NS is to determine and map the abundances of elements needed to specify the physical and chemical environment of both present and past surface units of Mars. Using abundances determined by the Viking XRFs experiment, and those inferred from analyses of the SNC meteorites, the list of elements should, at the least, include H, O, Mg, Si, Cl, K, Fe, Th, and U. Some of the more important scientific questions that can be addressed by these data are presented.

**Crust and Mantle Composition:** Processes of crustal formation on Mars are very poorly known. Those inferred from observations of the Moon indicate considerable crustal differentiation leading to the concentration of Ca-Al silicates in the lunar highlands and mafic basalts that erupted to form the maria. Further differentiation is indicated by observed concentrations of incompatible elements such as K, U, and Th in the basalts. We do not have a good understanding of the extent to which these processes may have been active on Mars. Such differentiation is especially important for placing constraints on the magnitude of radiogenic heating of the crust and upper mantle. Measurements of the ratio of K to U and to Th are also important to establish the planetary abundance of K, and by inference other moderately volatile elements, in order to infer the

extent to which the volatile inventory of Mars may have been depleted by catastrophic impacts since the end of heavy bombardment, or interaction with the solar wind over the lifetime of the planet.

**Weathering Processes:** Much of the martian surface appears to be dominated by fine-grained dust. The elemental chemistry of this material was investigated to first order by the Viking landers. The composition was found to be very similar at the two Viking sites, suggesting global homogenization by eolian deposition through dust storms. Compared to most terrestrial materials, martian fines are high in Fe and Mg, low in Si and Al, and very low in K. These characteristics are consistent with weathering from mafic or ultramafic source rocks. It is not known whether these source rocks are representative of all of Mars, or just of a few distinct geochemical surface units. For example, if the fines were generated primarily by interaction of basaltic lavas with ground ice and water, the composition of the fines may be essentially unrelated to that of the most ancient highland rocks. Conversely, identification of the source rocks with the weathering products that constitute the martian dust cover will yield insight into the responsible weathering processes. An element particularly important in this regard is H. Viking results suggested that some water of hydration was present in martian fines, but the amount was poorly determined. Results from GRS/NS, particularly the neutron mode, should give the H concentration in martian soil with high accuracy, indicating the degree of hydration that the source rocks have undergone.

At both Viking landing sites, near-surface fines were found to be cemented by a caliche-like deposit called duricrust. Its enhanced abundance of S and Cl suggests formation by the leaching of soluble ions from within the regolith by flowing water. Transport to and redeposition at a remote location near the surface by the water should then produce a claylike, sedimentary deposit enhanced, perhaps, in NaCl when the water evaporated. Overlayed maps of Cl (the general signature of an ancient salt deposit) and H (the signature of a sediment deposit of claylike minerals) that will be provided by GRS/NS should allow a global search for the fossil remnants of run-off channels and/or underground (but near-surface) aquifers.

**Volcanism.** Volcanism has been a very important process in shaping the martian surface, and volcanic units are widespread on the planet. While the intensity of volcanic activity has generally diminished with time, volcanism appears to span almost all recorded martian geologic history. Volcanic activity has been dominated throughout the planet's history by the extrusion of very fluid lavas, with yield strengths and viscosities (where they can be estimated) comparable to or lower than those of terrestrial basalts. These properties, while at best a very nonspecific indicator of composition, are most consistent with ultramafic lavas of the sort one would expect to be derived from partial melting of an Fe-rich mantle. In many instances, lavas have been emplaced as broad, flat volcanic plains. These plains range in age from the very old units interspersed through the ancient cratered terrain and on the floor of the Hellas Basin, to the somewhat younger ridged plains of Lunae Planum, Chryse Planitia, and elsewhere, to the still younger plains of Elysium and, finally, Tharsis. It is not known to what extent there are systematic changes in the composition of these plains units with age, or what such changes might tell us about, say, changes in the depth of magma production with time. The Mars 2001 GRS/NS will be able to map the compositions of these units and to search for evidence of compositional changes.



**Volatile reservoirs and transport.** The Mars 2001 GRS/NS experiment will also address a number of problems having to do with volatiles (primarily  $\text{H}_2\text{O}$  and  $\text{CO}_2$ ) at and below the martian surface. Both cosmochemical considerations and widespread evidence for fluvial activity indicate that a substantial amount of  $\text{H}_2\text{O}$  was outgassed early in martian history. Much of that  $\text{H}_2\text{O}$  may now reside beneath the ground as ice. Using simple models of heat and vapor transport in the martian regolith, it is possible to show that ground ice may be stable within tens of centimeters of the martian surface at latitudes within  $30^\circ$ – $40^\circ$  of the poles. If this is correct, then it should be possible to use gamma-ray and neutron data together to make maps of both the depth to this ice and its concentration.

The one region where ice is known to be present at the martian surface is at the poles. The martian polar deposits are dominated by a sequence of layered deposits believed to be composed of a mixture of dust and  $\text{H}_2\text{O}$  ice. In the south polar region in particular, there are large areas of exposed layered deposits, and the GRS/NS experiment should be able to measure the ice/dust ratio in this material to a depth of several tens of centimeters.

Overlying the layered deposits at both poles are deposits of perennial ice. The thickness of these deposits is not known, nor is it known to what extent their ice/dust ratio differs from that of the underlying layered deposits. At the south pole there is evidence that during at least some years the perennial ice surface is  $\text{CO}_2$  rather than  $\text{H}_2\text{O}$ . The perennial ice at both poles covers large enough areas to be resolved by GRS, and it should be possible to determine the abundances of  $\text{H}_2\text{O}$ ,  $\text{CO}_2$ , and dust accurately. Again, gamma-ray and neutron data may be used together to establish whether there are any vertical variations in composition over depths of tens of grams per square centimeter.

Overlying both poles in the winter and extending down to middle latitudes are the seasonal frost caps, composed of  $\text{CO}_2$  condensed from the atmosphere. By using GRS/NS data it should be possible to make maps of polar cap thickness as a function of time through the martian year, and to observe the caps through their full cycle of advance and retreat. Thickness of the caps may be determined both by using neutron data and by observing the changing attenuation of strong gamma-ray lines from the underlying regolith.

#### EXPERIMENTAL STUDIES OF MARS-ANALOG BRINES.

M. A. Bullock<sup>1</sup>, J. M. Moore<sup>2</sup>, and M. T. Mellon<sup>2</sup>, <sup>1</sup>Laboratory for Atmospheric and Space Physics, Campus Box 392, University of Colorado, Boulder CO 80309, USA (bullock@sunra.colorado.edu), <sup>2</sup>Mail Stop 245-3, NASA Ames Research Center, Moffett Field CA 94035, USA.

Evaporite deposits may represent significant sinks of mobile anions (e.g., those of Ca, N, Mg, Fe) and cations (e.g., those of C, N, S, Cl) among the materials composing the martian surface and upper crust. Carbon and N are especially interesting because of their role as atmospheric gases that can become incorporated into crustal rocks [1,2]. The presence of water-soluble cations and anions in the martian regolith has been the subject of speculation for some time [3]. Viking lander data provided evidence for salt-cemented crusts on the martian surface in the form of lander imagery of friable soil layers and planar fragments of disturbed soil [4,5]. X-ray fluorescence analysis of martian soils that were cemented into clods and

crusts showed that they contained some 50% more S and Cl than did the loose surface soils [6,7]. Martian S is very likely to exist in the form of sulfate, and Cl in the form of chlorides [6], chlorates, or perchlorates [8]. Following the Viking landings, there was considerable discussion of other salt-forming materials that should exist on the martian surface, including carbonates [9] and nitrates [10, 11]. More recently, Earth-based IR spectroscopic evidence has been obtained indicating the presence of carbonates as well as sulfates and other hydrates on the martian surface [12]. However, even more recently, the case for carbonates on Mars has been complicated by the report of experiments on the photochemical instability of surface carbonates under Mars conditions [13]. Carbonates have also been detected in the SNC meteorites that are commonly believed to have a martian origin [14]. If the crusts observed at the two Viking landing sites are, in fact, cemented by salts, and these crusts are globally widespread as IRTM-derived thermal inertia studies of the martian surface seem to suggest [15], then evaporite deposits, probably at least in part derived from brines, are a major component of the martian regolith.

However, the nature of evaporite-precursor brines formed under martian conditions is poorly understood. To date, only a very limited number of laboratory investigations have been reported that have any bearing on a better understanding of various processes related to brine or evaporite formation on Mars. Moreover, recent attempts at modeling "warm, wet Mars" alteration and precipitate mineralogies would benefit enormously from laboratory data on the composition and formation rates of Mars-like brines and evaporites. Here, we report on a pilot laboratory experiment that investigates the formation of brines on Mars by determining the identity and production rate of water-soluble ions that form in initially pure liquid water in contact with Mars-mixture gases and unaltered Mars-analog minerals. The main components of the experimental apparatus consist of 10 identical, hermetically sealable sample containers made from Teflon, with interior volumes of 250 ml. The lids of each container have two stopcock-fitted ports to provide gas flow access to the headspace when needed. Individual pristine minerals were mixed to simulate the composition of martian rocks, chosen on the basis of SNC meteorite mineralogy [16]. Six of the samples were composed of 50 g of sorted and mixed minerals (57.2% augite, 25.26% forsterite, 13.14% anorthoclase, 3.14% ilmenite, 0.78% pyrite, and 0.48% chloroapatite) acting as unaltered Mars rock analogs immersed in 100 ml of deoxygenated, doubly distilled liquid  $\text{H}_2\text{O}$ . The head spaces of these six containers was filled with a martian gas mixture (95.5%  $\text{CO}_2$ , 2.7%  $\text{N}_2$ , 1.6% Ar, 0.13%  $\text{O}_2$ , and 0.07% CO) at 1 bar. Two other sample containers were filled with the Mars-analog rocks,  $\text{H}_2\text{O}$ , and terrestrial atmosphere to serve as controls, and the remaining two sample containers held Mars gas mixture and water, but no minerals. The rock/gas/water and gas/water mixtures were allowed to interact at  $20^\circ\text{C}$  for specific durations, up to one year, at which time the fluid was removed and analyzed for dissolved ions. The cations that were analyzed for were  $\text{Fe}^{2+}$ ,  $\text{Mg}^{2+}$ ,  $\text{Al}^{3+}$ ,  $\text{K}^+$ ,  $\text{Na}^+$ ,  $\text{Ca}^{2+}$ ,  $\text{Ti}^{4+}$ ,  $\text{Mn}^{2+}$ , and  $\text{Ba}^{2+}$  with a minimum quantity detection limit of 1 ppb. The anions we examined were  $\text{Cl}^-$ ,  $\text{F}^-$ ,  $\text{SO}_4^{2-}$ ,  $\text{SO}_3^-$ ,  $\text{NO}_3^{2-}$ ,  $\text{NO}_2^-$ , and  $\text{CO}_3^{2-}$  with minimum detection limits of 1 ppm. The analysis of the  $\text{Mg}^{2+}$ ,  $\text{Ca}^{2+}$ ,  $\text{Ti}^{4+}$ ,  $\text{Mn}^{2+}$ , and  $\text{Ba}^{2+}$  was done by emission spectroscopy (based upon plasma atomization);  $\text{Fe}^{2+}$ ,  $\text{Al}^{3+}$ ,  $\text{Na}^+$ , and  $\text{K}^+$  were evaluated using carbon furnace atomic absorption. The  $\text{Cl}^-$ ,  $\text{F}^-$ ,  $\text{SO}_4^{2-}$ ,  $\text{SO}_3^-$ ,  $\text{NO}_3^{2-}$ , and  $\text{NO}_2^-$  were measured using UV-visible spectrophotometry. The carbonate analysis pre-

TABLE 1.

Cation	Average Formation Rate (g cm <sup>-3</sup> yr <sup>-1</sup> )
Ca <sup>2+</sup>	4.0 × 10 <sup>-4</sup>
Ti <sup>4+</sup>	3.8 × 10 <sup>-5</sup>
Al <sup>3+</sup>	8.1 × 10 <sup>-6</sup>
Mg <sup>2+</sup>	4.9 × 10 <sup>-6</sup>
Na <sup>+</sup>	4.1 × 10 <sup>-6</sup>
Ba <sup>2+</sup>	2.8 × 10 <sup>-6</sup>
Anion	Average Formation Rate (g cm <sup>-3</sup> yr <sup>-1</sup> )
CO <sub>3</sub> <sup>2-</sup>	1.1 × 10 <sup>-4</sup>
Cl <sup>-</sup>	8.2 × 10 <sup>-6</sup>
SO <sub>4</sub> <sup>2-</sup>	1.4 × 10 <sup>-5</sup>
F <sup>-</sup>	1.9 × 10 <sup>-6</sup>
SO <sub>3</sub> <sup>-</sup>	8.0 × 10 <sup>-6</sup>
NO <sub>2</sub> <sup>-</sup>	1.4 × 10 <sup>-7</sup>

sumed alkalinity (when pH < 8.5) was due to carbonate. The measured formation rates for dissolved ions are shown in Table 1.

The presence of brines on Mars has been hypothesized, both as a crustal store of key volatile species and as an agent of chemical rock weathering. The physical properties of martian analog brines produced from future experiments will be evaluated by making brine solutions at various concentrations, guided by the results of this pilot experiment, and measuring such parameters as density and freezing point. The spectral signature of the resulting model evaporites can be compared with spectral data to be obtained from future missions and observations.

**References:** [1] Kahn R. (1985) *Icarus*, 62, 175–190. [2] Pollack J. B. et al. (1987) *Icarus*, 71, 203–224. [3] Malin M. C. (1974) *JGR*, 79, 3888–3894. [4] Moore H. J. et al. (1977) *JGR*, 82, 4497–4523. [5] Mutch T. A. et al. (1977) *JGR*, 82, 4452–4467. [6] Clark B. C. (1976) *Science*, 194, 1283–1288. [7] Arvidson R. E. et al. (1989) *Rev. Geophys.*, 27, 39–60. [8] Oyama V. I. et al. (1977) *Nature*, 265, 110–114. [9] Gooding J. L. (1978) *Icarus*, 33, 483–513. [10] Yung Y. L. et al. (1977) *Icarus*, 30, 26–41. [11] Yung Y. L. (1989) in *Bull. Am. Astron. Soc.*, 21, 979. [12] Pollack J. B. et al. (1990) *JGR*, 95, 14595–14627. [13] Mukhin L. M. et al. (1996) *Nature*, 379, 141–143. [14] Gooding J. L. et al. (1988) *GCA*, 52, 909–915. [15] Jakosky B. M. and Christensen P. R. (1986) *JGR*, 91, 3547–3559. [16] McSween H. Y. (1985) *Rev. Geophys.*, 23, 391–416.

**HYDROGEOLOGY AND EXOBIOLOGY SIGNIFICANCE OF MARTIAN LARGE CRATER LAKES.** N. A. Cabrol and E. A. Grin, Space Science Division, Mail Stop 245-3, NASA Ames Research Center, Moffett Field CA 94035-1000, USA (ncabrol@mail.arc.nasa.gov).

On Earth, lakes keep the record of local, regional, and global planetary changes in their sediments. They provide clues on varia-

tions of (1) climate and hydrologic regimes in their sediment grain-size distribution and (2) atmosphere changes in the composition of their sediments. Lakes are also favorable environments for the development of life. Because of this global memory, martian lakes must be targeted as priority objectives for the coming missions. Their importance was pointed out in previous studies [1–3]. From their comparison to terrestrial analogs, we should be able to reconstruct the hydrologic dynamics of their formation, thus unveiling part of the history of early Mars. Unfortunately, most of the ancient martian aqueous sedimentary basins that were localized are either too small to be studied at current resolution or are resurfaced. However, large lakes on Mars existed, like the 150-km-diameter Gusev Crater in the Aeolis region, which has been studied extensively for exploratory purposes [1–26]. Crater lakes of these dimensions offer an open window on 4 g.y. of hydrogeologic and atmospheric evolution of Mars. We thus started a global survey of Mars to localize and model major martian lakes. We present results of a coherent bathymetric model of Gusev Crater (–14.8°S latitude/182°W longitude) that shows the existence of a lake through 2 g.y. Then, we present preliminary results of a promising site, the 140-km-diameter Gale Crater (–5°S latitude/223°W longitude), that displays unique sedimentary exposures, with 21 layers on a 1000-m central deposit, with terracing and drainage systems arguing for an ice-covered lake. The comparison between Gusev and Gale allows us to sketch out a model of large crater lake formation and evolution.

Deep large impact craters (Newson 1996) and tectonic depressions such as Valles Marineris [27,28] hosted lakes formed by drainage from surrounding aquifers that were maintained by the geothermal heat flux [18]. In impact craters, water is proposed to have been sustained in a liquid state by the heat flux emanating from the melt-sheet material in the transient crater [29]. In the case of Gusev Crater, the surrounding impacted highland was infiltrated by the water from the Ma'adim Vallis flood plain. The fractured regolith provided significant permeability to recharge the underground reservoir during the formation of the lake inside the crater. In previous studies [18,19,21] we demonstrated that Ma'adim Vallis did not enter Gusev Crater until the late Hesperian. Before entering the crater, Ma'adim Vallis formed a flood plain surrounding Gusev and headed north toward the Elysium Basin [21,26]. However, a lake existed in Gusev before the entrance of Ma'adim Vallis, as demonstrated by the shape and morphology of the valley delta, which was formed under water and ice [18,23,24].

In the case of Gale Crater, the supply of water came from the overtopping of the northern rampart. Gale is located exactly at the boundary between the highlands and the lowlands. We propose that Gale Crater was submerged during the activation of the Elysium Basin, though the current mapped boundaries of the Elysium Basin are located north [22]. Our model of formation is illustrated by a strong asymmetrical shape of the sedimentary deposit in the crater center. The crater shows a deep topographic low in its northern section, bordered by a 2000-m-high central peak surrounded by layered sediments, suggesting a lacustrine deposition. The deep topographic low and the central peak may have provided access to the geothermal flux and helped to maintain the water in a liquid state [30,31] under ice, suggested by the presence of lateral drainage systems.

The recent survey of the ice-covered Lake Vostok in Antarctica [32] has shown sub-ice lacustrine movements in a closed liquid



water body. Association of rotary movements and geothermal flux, favorable to the development of microbiota in Antarctica [32], have been demonstrated. Curvilinear ridges observed in Gusev Crater could be relevant to comparable sub-ice movements due to differences in ice pressure. In addition, the relative chronologies established for both craters show that they were still active during the Early Amazonian, thus they must be considered to have a favorable late oasis.

**References:** [1] Goldspiel M. M. and Squyres S. W. (1991) *Icarus*, 89. [2] De Hon R. (1992) *Earth, Moon, Planets*, 56, 2. [3] Cabrol N. A. and Grin E. A. (1995) *Planet. Space Sci.*, 43, 179–188. [4] Cabrol N. A. (1990) *Proc. Journées du COSPAR* (K. Szégo, ed.), pp. 51–55, Sopron, Hungary. [5] *Landing Site Catalog* (1992) NASA RP-1238. [6] Cabrol N. A. et al. (1993) *LPS XXIV*, 241–242. [7] Cabrol N. A. and Grin E. A. (1994) *Astronom. Vestnik*. [8] Cabrol N. A. et al. (1994) *XIX EGS General Assembly*. [9] Grin E. A. et al. (1994) *LPS XXV*, 483–484. [10] Landheim R. et al. (1994) *LPS XXV*, 769–770. [11] Cabrol N. A. et al. (1994) *LPS XXV*, 213–214. [12] Landheim R. (1995) Master's thesis. [13] Cabrol N. A. (1995) MESR postdoctoral report. [14] Cabrol N. A. and Brack A. (1995) *LPS XXVI*, 201–202. [15] Cabrol N. A. et al. (1996) *Icarus*, 123, 269–283. [16] Cabrol N. A. and Grin E. A. (1996) in *ISSOL's '96 International Conference Report*. [17] Cabrol N. A. et al. (1996) *LPS XXVII*, 189–190. [18] Grin E. A. and Cabrol N. A. (1997) *Icarus*, submitted. [19] Cabrol N. A. et al. (1997a) *Icarus*, submitted. [20] Cabrol N. A. et al. (1997b) *Icarus*, submitted. [21] Cabrol N. A. et al. (1997) *LPS XXVIII*. [22] Cabrol N. A. (1997) *LPS XXVIII*. [23] Grin E. A. and Cabrol N. A. (1997) *LPS XXVIII*. [24] Grin E. A. and Cabrol N. A. (1997) *LPS XXVIII*. [25] Landheim R. et al. (1997) *Icarus*, submitted. [26] Kuzmin et al. (1997) in preparation. [27] Nedell S. S. et al. (1987) *Icarus*, 70. [28] Carr M. H. (1995) *JGR*, 84. [29] McKay C. P. et al. (1985) *Nature*, 313. [30] Newsom H. E. (1980) *Icarus*, 44. [31] Newsom H. E. et al. (1996) *JGR*, 101. [32] Kapista A. P. et al. (1996) *Nature*, 381.

**MICROBIAL DIVERSITY IN HYPERTHERMOPHILIC BIOFILMS: IMPLICATIONS FOR RECOGNIZING BIOGENICITY IN HYDROTHERMAL MINERAL DEPOSITS.** S. L. Cady<sup>1</sup>, C. E. Blank<sup>2</sup>, D. J. Des Marais<sup>1</sup>, M. R. Walter<sup>3</sup>, and J. D. Farmer<sup>1</sup>, <sup>1</sup>Exobiology Branch, Mail Stop N239-4, NASA Ames Research Center, Moffett Field CA 94035, USA, <sup>2</sup>Department of Molecular and Cellular Biology, University of California, Berkeley CA 94720, USA, <sup>3</sup>School of Earth Sciences, Macquarie University, North Ryde NSW 2109, Australia.

Whether life on Earth first evolved in hydrothermal environments remains debatable [1]. Molecular phylogenetic studies indicate that a geothermal environment supported the hyperthermophilic lifestyle of the last common ancestor of extant life on Earth [2–4]. This suggests that hydrothermal deposits could be excellent targets for future exopaleontological exploration on the surface of Mars [5]. Hydrothermal systems are common features of volcanic terranes on Earth, which were not only widespread during the Archean [6] but also appear to have been widespread on early Mars [7]. As mineralizing environments, hydrothermal systems have the potential to preserve evidence of biogenicity as stromatolites, chemofossils, or microfossils. Recent studies have shown, however, that while stro-

matolitic fabrics are preserved in ancient analogs of modern siliceous thermal spring deposits (e.g., Farmer et al., this volume), total organic C concentrations of ancient siliceous sinters are typically low (<0.01% TOC, D. Des Marais, personal communication), and organically preserved microfossils rare [8–10]. In addition, the accurate reconstruction of ancient microbial communities is complicated by the loss of microstructural detail of the sediments during diagenesis. To complement the work on ancient systems we are studying how modern hydrothermal ecosystems are converted to their fossilized counterparts. Using this methodology, Cady and co-workers [11,12] have shown that the morphological and microstructural development of geysers, the high-temperature form of siliceous sinter, is influenced by the presence of hyperthermophilic biofilms. Given the potential for life to exist at temperatures in excess of 113°C [13], it is apparent that we must reevaluate the contribution of hyperthermophilic biofilms to the formation of hydrothermal mineral deposits.

Geysers, previously considered abiogenic in origin, have been found to be colonized by discontinuous hyperthermophilic biofilms [11,12]. The biofilms (~1 µm thick), and the filamentous hyperthermophiles (~0.5 µm wide) they contain, influence the morphogenesis of geysers by localizing opaline silica deposition. The highest concentrations of filaments have been found in biofilms that colonize the tips of spicular geysers that form at the air-water interface around hot springs and geyser effluents. The interaction between opaline silica deposition, ultimately driven by evaporation, and the presence of filamentous hyperthermophilic biofilms, which provide a preferred substratum for opaline silica precipitation, has been found to influence the morphological and microstructural development of spicular geysers. The ability of submicrometer-scale features to propagate into larger-scale structures such as laminated spicules that are recognizable in fossil material underscores the importance of understanding the organosedimentary interactions by which they formed. That hyperthermophilic biofilms play a role in geyser formation is of paleobiological significance in that it reveals the potential for macroscale features of ancient siliceous hydrothermal deposits to record some aspects of the history of hyperthermophilic communities.

To determine whether unique macroscale features of geysers are associated with distinct microbial communities, we have surveyed different geyser lithotypes that occur in thermal springs venting near-boiling fluids (>90°C) at Yellowstone National Park using various microscopy techniques [14] and molecular phylogenetic analysis [15]. Our approach involves comparison of the microbial communities collected on various types of growth surfaces deployed in the springs, with the microbial communities that occur in sediments that accumulate in the bottoms of thermal springs, with those that colonize the surfaces of subaqueous and subaerial geysers. The biofilms were visualized by fluorescence microscopy and scanning and transmission electron microscopy. We have found that robust microbial consortia colonize the growth surfaces within a few days after deployment in the hot springs. Most organisms display filamentous morphologies, although we have observed that the densest microbial communities also contain small populations of rod- and coccus-shaped members. To characterize the taxonomic structure of the microbial communities without the need for cultivation, a molecular phylogenetic approach was taken. DNA was extracted from the organisms in the biofilms, and the polymerase chain reaction (PCR) was used to amplify ribosomal DNA using oligo-

nucleotides that are conserved for all known organisms. Ribosomal DNA analysis of biofilms collected on the growth surfaces and attached to geysers indicates that the hyperthermophilic consortia contain relatively few taxa. Some of the organisms are distant relatives of previously identified hyperthermophilic bacteria. In addition, a unique, novel lineage of bacteria was identified. This branch, which lies closer to the root of the phylogenetic "tree of life" than any other group identified to date, represents the oldest common ancestor of all extant bacteria. The discovery of this novel lineage by [15] demonstrates that there is much to be learned about the diversity of life at the high-temperature end of terrestrial thermal spring systems. Our findings also confirm that our combined field approach (to colonize different types of substrates in natural ecosystems) and laboratory protocol will most likely continue to reveal new taxa as we move our investigation into the epithermal parts of hydrothermal ecosystems [14].

**References:** [1] Forterre P. (1996) *Cell*, 85, 789. [2] Pace N. R. (1991) *Cell*, 65, 531. [3] Brown J. R. and Doolittle W. F. (1995) *Proc. Natl. Acad. Sci. USA*, 92, 2441. [4] Stetter K. O. (1994) in *Early Life on Earth* (S. Bengtson, ed.), pp. 143–151, Columbia Univ. [5] Kerridge J. F., ed. (1995) *NASA SP-530*. [6] Walter M. R. (1996) in *Hydrothermal Ecosystems on Earth (and Mars?)* (G. R. Bock and J. A. Goode, eds.), pp. 112–130, Wiley. [7] Farmer J. D. (1996) in *Hydrothermal Ecosystems on Earth (and Mars?)* (G. R. Bock and J. A. Goode, eds.), pp. 273–299. [8] Walter M. R. et al. (1996) *Palaos*, 11, 497. [9] Trewin N. H. (1994) *Trans. R. Soc. Edinb.*, 84, 433. [10] Trewin N. H. (1996) in *Hydrothermal Ecosystems on Earth (and Mars?)* (G. R. Bock and J. A. Goode, eds.), pp. 131–149, Wiley. [11] Cady S. L. et al. (1995) *GSA Abstr. with Progr.*, 27(6), A304. [12] Cady S. L. and Farmer J. D. (1996) in *Hydrothermal Ecosystems on Earth (and Mars?)* (G. R. Bock and J. A. Goode, eds.), pp. 150–173, Wiley. [13] Stetter K. O. (1996) in *Hydrothermal Ecosystems on Earth (and Mars?)* (G. R. Bock and J. A. Goode, eds.), pp. 1–18, Wiley. [14] Cady S. L. et al. (1996) *Eos Trans. AGU*, 77(46), F249. [15] Blank C. E. et al. (1997) *Am. Soc. Microbiol. Annual Meeting*, Miami, Florida, submitted.

**THE HIGHLANDS CRUST OF MARS AND THE PATHFINDER MISSION: A PROSPECTIVE VIEW FROM MARINER 6 INFRARED SPECTROSCOPY.** W. M. Calvin<sup>1</sup>, A. H. Treiman<sup>2</sup>, and L. Kirkland<sup>2</sup>, <sup>1</sup>U.S. Geological Survey, 2255 North Gemini Drive, Flagstaff AZ 86001, USA, <sup>2</sup>Lunar and Planetary Institute, 3600 Bay Area Boulevard, Houston TX 77058, USA.

The composition of the ancient martian crust, now seen as the highlands, is important to understanding the physical and chemical environments of early Mars. In July 1997, the Mars Pathfinder lander and rover are scheduled to land on the plains at the mouth of the Ares Vallis outflow channel and analyze highland rocks that were transported down Ares Vallis. There are few firm data on the composition of the highland crust [1]. However, infrared spectra from the Mariner 6 mission covered part of the highlands above Ares Vallis, and provide a prospective view of what Mars Pathfinder may discover.

**Geology:** Ares Vallis is a channel that begins in the highlands of Margaritifer Terra, extends northward between Xanthe and Arabia Terrae, and terminates in the lowlands of Chryse Planitia [2]. Ares

Vallis is among the largest such channels that debouch into Chryse; their tear-drop-shaped islands and other fluvial-like features suggest that they are the results of catastrophic flooding [3]. Surrounding Ares Vallis are highland plains and cratered units of Noachian age (Npl1, Npl2 of [2]) and older ridged plains (Hnr of [2]). The tributaries of Ares Vallis originate in regions of irregular, steeply hilly terrain: Margaritifer, Iani, and Aram Chaoses. Aram Chaos occupies part of a circular depression that may be a buried impact crater. Hillsides in these chaoses and in Ares Vallis itself expose near-horizontal layers that are thought to have formed by aqueous alteration or cementation of highlands rock [4].

**Infrared Spectroscopy:** The Mariner 6 spacecraft flew by Mars in July 1969, carrying an infrared spectrometer (IRS) that recorded spectra in the range 1.8–6.0  $\mu\text{m}$  [5], across southern Ares Vallis, including Aram and Iani Chaoses and Noachian-aged plains units (Fig. 1). The IRS entrance aperture was a slit, which yielded a ground footprint approximately 200 km  $\times$  10 km (depending on the distance from spacecraft to Mars) for each spectrum. Figure 1 shows the approximate locations of the center of each spectral scan near Ares Vallis, as well as the whole footprint for every other scan and the approximate instantaneous field of view for spectrum 178. Each spectrum is a composite of two wavelength segments in a continuous spatial scan. The area to the left of each central marked slit in Fig. 1 was scanned while the circular variable filter wheel rotated to cover the spectral range from 1.9 to 3.7  $\mu\text{m}$ ; the area to the right of the

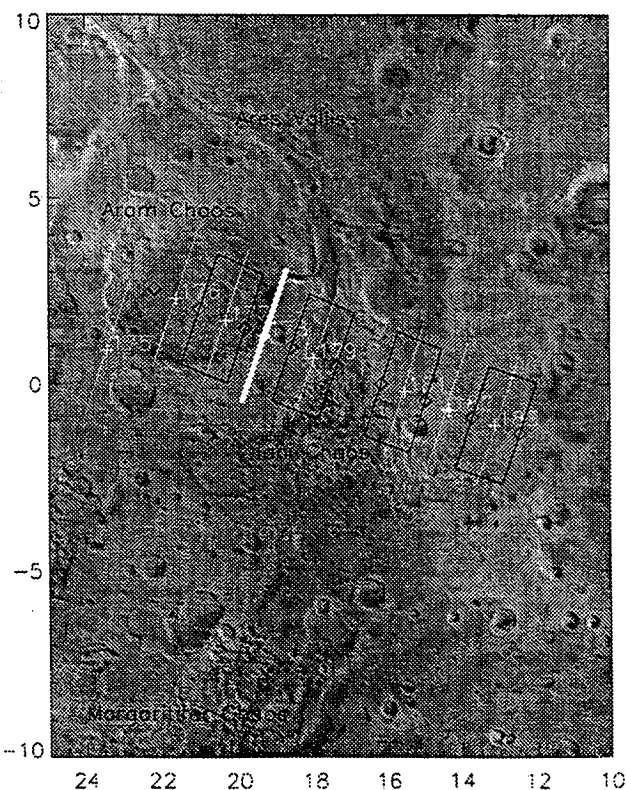


Fig. 1. Projection from the Mars Digital Image Map, Viking red filter with Mariner 6 IRS footprints overlain.

central slit was similarly scanned to cover the spectral range from 3 to 6  $\mu\text{m}$ . Measured wavelength increases from left to right in the spatial image. Spectra here were calibrated both in wavelength and in radiance [6], and periodic noise was removed via Fourier filtering.

**Results:** Previous analysis of IRS spectra in the nearby regions of Oxia Palus, Margaritifer Sinus, and Meridiani Sinus suggested the possible presence of hydrous magnesium carbonate minerals, such as hydromagnesite or artinite [7]. This interpretation was based on the consistency of these minerals with observed spectral features at 2.3, 3, and 5.4  $\mu\text{m}$ , as well as reasonable geochemical scenarios for the formation of such minerals on the surface of Mars. The Ares Vallis spectra also exhibit the 2.3- and 3- $\mu\text{m}$  absorption features. The 2.3- $\mu\text{m}$  feature is only partly associated with surface mineralogy [8,9], but the broad 3- $\mu\text{m}$  absorption is associated with bound molecular water [e.g., 5,6,10]. Recently, Calvin [6] proposed a simple method for calculating the band-integrated strength of this feature to examine the spatial variation in bound water abundance. In general, the Mariner 6 IRS spectra show little variation in the integrated strength of the feature; however, a few spectra show a 10% enhancement in band strength that is not correlated with albedo, thermal inertia, or topography. Two of these enhanced band depth spectra are of Aram Chaos (176 and 177, Fig. 1).

Aram Chaos is distinctly darker at visible and near-infrared wavelengths than the surrounding highlands. Of the eight IRS spectra that cover this region, spectra 176, 177, and 178 are the darkest, the other five being much brighter (Fig. 2). While most spectra are not sloped between 2.2 and 2.6  $\mu\text{m}$ , the Aram Chaos spectra (176 and 177) turn distinctly downward, with the longer wavelength 3–5% darker than the short. Unfortunately, the large footprint of the Mariner 6 spectra makes it difficult to assess if there are other weak absorption features characteristic of hydrated minerals on the surface. We are currently examining the spatial variation of the 2.3- $\mu\text{m}$  band strength. Given the past abundance of water in this area, it seems likely that the greater 3- $\mu\text{m}$  band strength is at least partly associated with the presence of hydrated minerals. These absorptions in IRS spectra of the Ares Vallis region suggest that highland rocks analyzed by Mars Pathfinder may contain detectable water and carbonate.

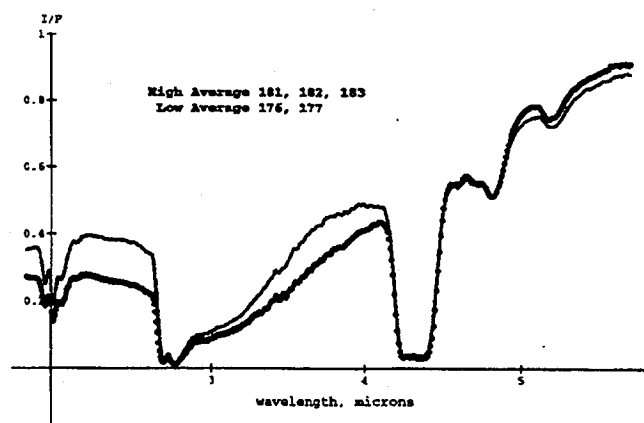


Fig. 2. Average IRS spectra from the Ares Vallis source region.  $I/F$  = measured/incident flux.

It is also interesting to note in the Termoskan data from the Russian Phobos spacecraft the center of Aram Chaos is associated with a localized high-inertia region with slightly brighter visible reflectance levels [11]. This high inertia region is associated with the two IRS spectra that have the larger 3- $\mu\text{m}$  band depth, and may suggest surface bonding or cementation by salts. However, it must be considered that the two observations are 20 years apart and mobile surface layers may alter the apparent association.

**Conclusions:** When Mars Pathfinder samples the martian highland crust, it will see material that is representative, at least at near- to mid-infrared wavelengths, of the highlands throughout the Xanthe/Arabia/Margaritifer region. Mariner 6/7 IRS spectra are consistent with ground surface exposure of hydrous carbonate minerals, and other minerals with bound molecular water such as clays and salts.

**References:** [1] Treiman A. H., this volume. [2] Sotro and Tanaka (1995) *USGS Map*, I-2441. [3] Carr M. (1996) *Water on Mars*, Oxford Univ. [4] Treiman A. H. (1997) *JGR*, 102, in press. [5] Pimentel et al. (1974) *JGR*, 79, 1623. [6] Calvin W. M. (1997) *JGR*, 102, in press. [7] Calvin et al. (1994) *JGR*, 99, 14659. [8] Clark et al. (1990) *JGR*, 14463. [9] Bell and Crisp (1993) *Icarus*, 2. [10] Erard et al. (1991) *Proc. LPS*, Vol. 21, 437. [11] Betts and Murray (1994) *JGR*, 99, 1983.

#### THERMAL LOSS OF WATER ON YOUNG PLANETS: THE EFFECT OF A STRONG PRIMITIVE SOLAR WIND.

E. Chassefière, Laboratoire de Météorologie Dynamique, Université P. et M. Curie, 4 Place Jussieu, 75252 Paris Cedex 05, France (eric.chassefiere@aero.jussieu.fr).

This work deals with the problem of thermal escape of H (and, in some cases, both H and O, i.e., water) on young planets, in earlier stages of planetary evolution. Although it is more specifically focused on the problem of Venus (and the present lack of O in Venus' atmosphere), it may also be applied to Mars.

It is first assumed that escape is stimulated only by the solar EUV radiation, which is known to have been more intense in the past [1]. From a simple energetic budget [2] it is shown that, in this case, O produced by photodissociation of water vapor in an earlier stage of evolution of the terrestrial planets may be lost by hydrodynamic escape (see [3] for theory), although in relatively modest amounts. If hydrodynamic escape of H contained in an ocean equivalent to a few present terrestrial oceans occurred at a relatively slow rate, over the first billion years of a planet's life, less than  $\approx 10\%$  of O is expected to be lost to space (typically  $\approx 10\%$  for Mars,  $\approx 2\%$  for Venus, and  $\approx 0\%$  for Earth). On the other hand, a short episode of intense escape ( $\approx 2 \times 10^7$  yr), during which the available solar EUV flux is fully consumed to drive escape, at the early stages when volatiles are supposed to have been outgassed ( $\approx 10^8$  yr) may yield more substantial O escape. For Venus and Mars, it is shown that primitive oceans of 1300 m and 600 m average depth respectively could be lost by EUV-stimulated hydrodynamic escape, with 30% and 50% respectively of O initially contained in the ocean released to space by hydrodynamic escape, the rest being involved in crustal oxidation. An important corollary is that if Venus had been supplied with more than  $\approx 0.45$  terrestrial ocean, it would have been left with an  $\text{O}_2$ -rich atmosphere, in good qualitative agreement with the previous suggestion of [4].

In a second step, the question of whether escape can work at high-energy-limited rates is assessed more specifically by using a devoted one-dimensional model of hydrodynamic escape [5], as previously made by [6]. This model is used to study the loss of H from a hot, water-rich atmosphere of the Venus type. A range of EUV heating rates corresponding to the present solar cycle fluctuations of the EUV flux and different possible heating efficiencies are first considered. The model takes into account the transition to the collisionless state at the exobase through a modified Jeans approach. For the fluid inner planetary corona, the conservation equations are solved from the base of the expanding flow ( $z \approx 200$  km) up to the exobase, generally located at an altitude of  $\approx 1$  planetary radius. Solutions are found in which the flux in the collisional region is equal to the Jeans escape flux at the exobase. It is shown that approximately two-thirds of the escape energy is supplied by energetic neutrals (ENs) formed by charge exchange between escaping H atoms and solar protons in the heliosphere, a fraction of which intercepts the exobase and heats by collision the upper layers of the fluid planetary corona. This mechanism differs somewhat from sputtering [e.g., 7], although basically of the same nature. Any planetary magnetic field pushing away the obstacle up to an altitude larger than  $\approx 3$  planetary radii would inhibit this effect. The ratio of the EUV flux to the solar wind strength is shown to be of prime importance, since the solar wind regulates the escape flux from the outer, through the action of energetic neutrals, and the EUV flux acts from the inner, by supplying atoms with the energy required to lift them up to the exobase.

The previous model is now being tested by using primitive enhanced values of the solar EUV flux. The most interesting result at the present stage is that, in early conditions, the radius of the fluid corona may reach  $\approx 4$  planetary radii, and a semicollisional region, inside which the mean free path and the scale height are close together, is established between 4 and  $\approx 10$  planetary radii [8]. Because the solar wind is an important source of escape energy, as previously shown, and because of the possibly large cross-sectional area of the venusian corona in early stages, this result suggests the potentially important role of the solar wind.

From a third specific model an enhanced primitive solar wind, such as may have prevailed during the first few 100 m.y. of solar system history [9], is shown to have had the potential to stimulate strong thermal atmospheric escape from the young Venus [10]. Due to heating by solar-wind bombardment of an extended dense planetary corona, an escape flux of pure atomic H as large as  $3 \times 10^{14} \text{ cm}^{-2} \text{ s}^{-1}$  is found to be possible, provided the solar wind was  $\approx 10^3$ – $10^4$  more intense than now. Even if escape was diffusion-limited, an enhanced primitive solar UV flux (a factor of  $\approx 5$  above present level), absorbed by  $\approx 0.3$  mbar of thermospheric water vapor, was able to supply the flow at the required rate. For these high escape rates, O was massively dragged off along with H, and water molecules could be lost at a rate of  $\approx 6 \times 10^{13} \text{ molecules cm}^{-2} \text{ s}^{-1}$ . Because, at this rate, a terrestrial-type ocean was completely lost in  $\approx 10$  m.y., short compared to typical accretion and outgassing times, water was lost "as soon" as it was outgassed. This mechanism could explain the present lack of O in the Venus atmosphere. Because it is expected to affect all Sun-like stars in the early phases of planet formation, abiotic O atmospheres could be rare in the universe. This result must be considered in relationship to the search for life (or at least clues to life) by spacebased IR interferometry [11]. Although Mars and the Earth are not thought to have given rise to a runaway

greenhouse effect of the Venus type, strong water escape, in addition to impact erosion, could perhaps occur in this way during an early accretional greenhouse phase [12].

**References:** [1] Zahnle K. J. and Walker J. C. G. (1982) *Rev. Geophys. Space Phys.*, 20, 280–292. [2] Chassefière E. (1996) *Icarus*, 124, 537–552. [3] Hunten D. M. et al. (1987) *Icarus*, 69, 532–549. [4] Kasting J. F. (1995) *Planet. Space Sci.*, 43, 11–13. [5] Chassefière E. (1996) *JGR*, 101, 26039–26056. [6] Kasting J. F. and Pollack J. B. (1983) *Icarus*, 53, 479–508. [7] Luhmann J. G. and Kozyra J. U. (1991) *JGR*, 96, 5457–5467. [8] Chassefière E. (1996) *GRL*, submitted. [9] Henney C. J. and Ulrich R. K. (1995) in *Proc. of Fourth SOHO Workshop*, pp. 3–7. [10] Chassefière E. (1997) *Icarus*, in press. [11] Léger A. et al. (1996) *Icarus*, 123, 249–255. [12] Matsui T. and Abe Y. (1986) *Nature*, 322, 526–528.

**GEOCHEMICAL CYCLES OF CHNOPS AND OTHER POTENTIALLY IMPORTANT BIOLOGICAL ELEMENTS ON MARS.** B. C. Clark, Mail Stop S-8000, Lockheed Martin Astronautics, P.O. Box 179, Denver CO 80127, USA (bclark@astr.lmco.com).

Utilizing available data on geochemical measurements of elements in martian soils, molecules in the martian atmosphere (including upper limits for many biochemically significant constituents), martian meteorite data, and occurrences of mineral phases on solar system bodies, certain constraints can be placed on the occurrence of elements critical to prebiotic and biological activity on Mars.

Although geochemical cycling may be restricted, compared to the extensive biogeochemical transport systems on Earth, certain conversions and cycling are inevitable. Concepts and potential schemes, as well as approaches to their further study in the martian context, will be presented.

**HYDRAULIC AND THERMAL CONSTRAINTS ON THE DEVELOPMENT OF THE MARTIAN VALLEY NETWORKS.** S. M. Clifford, Lunar and Planetary Institute, 3600 Bay Area Boulevard, Houston TX 77058, USA (clifford@lpi.jsc.nasa.gov).

The resemblance of the martian valley networks to terrestrial run-off channels, and their almost exclusive occurrence in the planet's heavily cratered highlands, suggested to many early investigators that the networks were the product of rainfall—relics of a significantly warmer and wetter climate that existed early in the planet's history. However, in response to mounting geologic and theoretical arguments against the existence of a warm early Mars, efforts to explain the genesis of the networks have refocused on potential contributing endogenetic conditions and mechanisms. This abstract examines the hydraulic and thermal constraints that would have been imposed on the development of the networks by the existence of a colder climate.

An inherent assumption in many recent studies has been that, at the time of valley network formation, the position of the groundwater table in the cratered highlands was determined by crustal temperature alone. By this reasoning, the water table was essentially

coincident with the base of the overlying frozen ground—implying a local depth beneath the terrain of as little as 100 m, given the expected 5–6 $\times$  greater geothermal heatflow that is thought to have characterized the planet at this time (~4 b.y. ago). Under these conditions it is argued that subpermafrost groundwater may have contributed to the formation of the valley through sapping.

However, in the absence of an active process of groundwater recharge at high elevations, the assumption of a terrain-following water table, given a planetwide subfreezing climate, appears seriously flawed. While the groundwater table on Earth often conforms to the shape of the local landscape, it does so only because it is continuously replenished by atmospheric precipitation and infiltration into the soil (e.g., Fig. 1a). However, under subfreezing conditions, the condensation of ice in the near-surface crust will effectively isolate the underlying groundwater from any possibility of atmospheric resupply (Fig. 1b). Under such conditions, groundwater will flow until any residual hydraulic head has decayed—leaving the system in hydrostatic equilibrium (Fig. 1c).

For the above reason, the identification of a vigorous recharge mechanism for groundwater in the martian highlands is a critical consideration if the valley networks were formed by the flow of liquid water. Given the concurrent existence of a subfreezing climate, the only viable candidate for this process that appears consistent with the geologic evidence is hydrothermal convection [1–3].

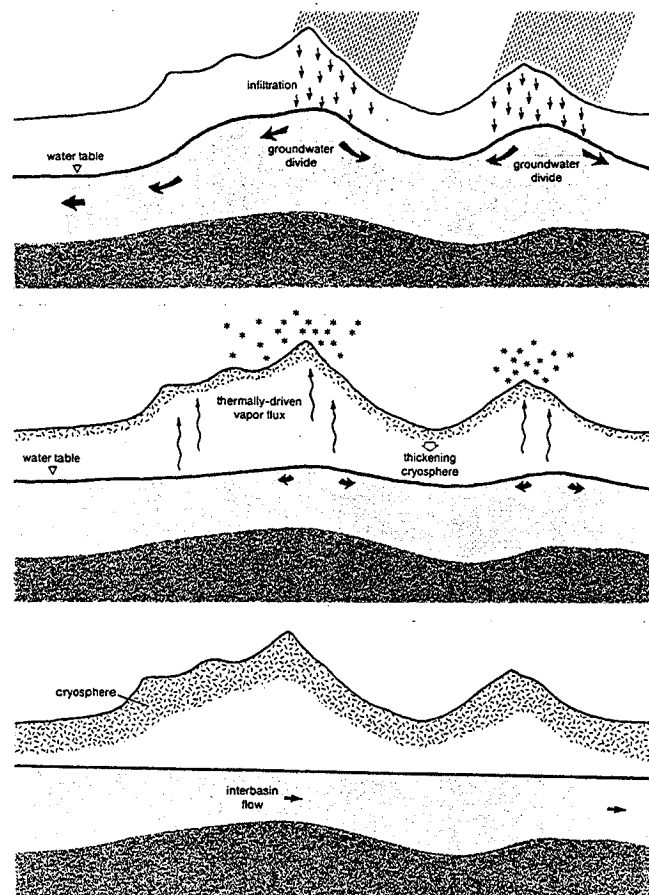


Fig. 1. The subsurface hydrologic response of Mars to the onset of a colder climate (after Clifford [3]).

The arguments in favor of a hydrothermal origin of the valley networks are persuasive. Given a water-rich early crust, and the inevitable production of impact melt resulting from the formation of the craters found throughout the highlands, the development of vigorous hydrothermal systems in association with large impacts appears inescapable [1,3]. Indeed, calculations of impact melt production based on the crater size-frequency distribution of the highland's crust indicate that planetwide, impact-generated hydrothermal systems may have discharged a volume of water equivalent to a global ocean ~130 m ([3], section 4.4.3)—a volume more than sufficient to have carved the networks. (Note that [4] has recently proposed an alternative mechanism for generating the valley networks based on headward extension by groundwater-assisted mass-wasting. A major strength of this idea is that the quantity of liquid water required to erode the valleys is significantly less than that required by a sapping origin, although some groundwater is still required at the base of the debris to help lubricate its transport downstream.)

Under the climatic conditions that are currently thought to have prevailed on Mars at the time of valley network formation, hydrothermal convection appears to be the only process capable of supplying significant volumes of water to the surface and near-surface environment of elevated regions within the cratered highlands. Although the role of hydrothermal systems in the generation of the networks is far from proven, given a water-rich Mars, it is difficult to conceive of a scenario where the development of such systems does not naturally arise from the impact and volcanic evolution of the planet's surface [1–3].

**References:** [1] Newsom H. E. (1980) *Icarus*, 44, 207–216. [2] Gulick V. C. and Baker V. R. (1990) *JGR*, 95, 14325–14345. [3] Clifford S. M. (1993) *JGR*, 98, 10973–11016. [4] Carr M. H. (1995) *JGR*, 100, 7479–7507.

**THE ORIGIN OF THE MARTIAN INTERCRATER PLAINS: THE ROLE OF LIQUEFACTION FROM IMPACT AND TECTONIC-INDUCED SEISMICITY.** S. M. Clifford, Lunar and Planetary Institute, 3600 Bay Area Boulevard, Houston TX 77058, USA (clifford@lpi.jsc.nasa.gov).

Since images of the martian cratered highlands were first returned by Mariner 4, investigators have puzzled over the origin of the intercrater plains (e.g., Öpik, 1965; Hartmann, 1966). The apparent deficit of craters with diameters <30 km within the plains and the poor preservation state of many of the larger craters throughout the highlands are often attributed to the possible existence of a dense early atmosphere whose presence may have warmed the early climate and accelerated the rates of fluvial and eolian erosion. While such conditions may have existed and contributed to the development of the intercrater plains, the evidence for abundant water in the early crust and the frequency of major seismic disturbances estimated from the planet's impact and tectonic record, suggests another possibility.

Under conditions where the pressure of water in a soil's pores exceeds the local lithostatic stress, there can be a sudden and catastrophic loss of soil strength called liquefaction. On Earth, liquefaction is often triggered when a saturated soil experiences a sudden acceleration due to the passage of a seismic shear or compressional wave. This occurrence can cause massive slumping,

folding, and faulting on slopes, violent eruptions of water and sediment, and the formation of extensive collapse depressions arising from the liquefaction and lateral extrusion of susceptible underlying layers. Examples of such phenomena are well documented, having been observed in association with major earthquakes all over the world. In one of the most destructive events on record, flow slides triggered by the 1920 Kansu earthquake ( $M_w = 7.8$ ) buried 10 large cities and numerous villages in an  $\sim 8 \times 10^4$  km<sup>2</sup> area of China, killing almost 200,000 people [1]. In areas that have experienced such extensive liquefaction, the landscape is often left as complex mass of depressions and ridges—creating a hummocky texture that closely resembles the appearance of the martian intercrater plains.

On Mars, the propagation of crustal shock waves generated by impacts, earthquakes, and explosive volcanic eruption is likely to have repeatedly shaken, dilated, and forcefully compressed water-bearing formations on a global basis—producing transient pressures sufficient to cause widespread liquefaction, the disruption of confined aquifers, and the ejection of water and sediment through crustal fractures and pores. During the great Alaska earthquake of 1964 ( $M_w = 9.2$ ), these processes caused extensive flow slides and resulted in water and sediment ejection from shallow aquifers as far as 400 km away from the earthquake's epicenter, with some eruptions rising over 30 m into the air [2].

As discussed by Golombek et al. [3], Tanaka and Clifford [4], and Clifford [5], the martian geologic record provides abundant evidence that Mars has experienced seismic events of a similar, and sometimes much greater, magnitude. A recent analysis suggests that at the maximum distance that water and sediment ejections were observed during the Alaska earthquake, pore-pressure changes of as much as several bars (200–300 kPa) were generated in near-surface silt and clay sediments [6]. On Mars, an impact of equivalent seismic energy ( $D \sim 87$  km, assuming a kinetic-to-seismic energy conversion efficiency of  $10^{-4}$ ) will produce this same pressure change in a basalt aquifer at a distance of  $\sim 225$  km, while a 200-km impact (equivalent to an  $M_w = 10$  quake) extends this range to  $\sim 1000$  km. For impacts  $\geq 600$  km ( $M_w \geq 11$ ), pore pressures in excess of 100 kPa are generated on a global scale, with substantially higher pressures occurring within several crater radii of the point of impact and at the impact's antipode.

Terrestrial field and laboratory studies have demonstrated that a soil's susceptibility to liquefaction is dependent on a variety of factors and conditions, including particle size, soil density, extent of lithification, pore and confining pressure, as well as the magnitude and frequency of ground acceleration. All other things being equal, the soils most susceptible to liquefaction are well-sorted angular sands, although soils of virtually any particle size—from clays to gravel—can liquefy under appropriate conditions of pore pressure and confinement. This is especially true in confined aquifers at low elevations, where initial pore pressures may already approach lithostatic values.

On Mars, the intense impact and volcanic activity of the Noachian period is likely to have resulted in the production of a several-kilometers-thick layer of interbedded ejecta, pyroclastics, lavas, and weathering products [5]. Given a crust with this composition, the presence of abundant water, surface temperatures resembling those of today, and an internal heat flow  $\sim 5$ – $6 \times$  its present value, conditions were right for the global occurrence of near-surface aquifers confined by up to several hundred meters of frozen ground. Under such conditions, liquefaction generated by the occurrence of

more than  $3 \times 10^4$  impact events with a seismic energy equal to (or up to  $10^6$  times greater than) that associated with the 1920 Kansu earthquake [6] could well explain the origin of the intercrater plains alone—without the need to invoke a more massive early atmosphere.

**References:** [1] Seed H. B. (1968) *Proc. Am. Soc. Civil Engineers*, 94, 1055–1122, J. Soil Mech. Found. Div. [2] Waller R. M. (1968) in *The Great Alaska Earthquake of 1964*, pp. 97–116, National Academy of Sciences, Washington, DC. [3] Golombek M. P. et al. (1992) *Science*, 258, 979–981. [4] Tanaka K. L. and Clifford S. M. (1993) in *Workshop on the Martian Northern Plains*, pp. 17–18, LPI Tech Rpt. 93-04, Part 1. [5] Clifford S. (1993) *JGR*, 98, 10973–11016. [6] Clifford S. M. and Leyva I. A. (1997) in preparation.

#### THE EARLY HISTORY OF MARS AS TOLD BY DEGRADED HIGHLAND IMPACT CRATERS.

R. A. Craddock<sup>1,2</sup>, T. A. Maxwell<sup>1</sup>, and A. D. Howard<sup>2</sup>, <sup>1</sup>Center for Earth and Planetary Studies, National Air and Space Museum, Smithsonian Institution, Washington DC 20560, USA (craddock@ceps.nasm.edu), <sup>2</sup>Department of Environmental Sciences, University of Virginia, Charlottesville VA 22903, USA.

From Mariner 4 data, Leighton et al. [1] first observed that martian highland impact craters are preserved at various states of degradation. Successive Mariner flights provided additional data, and because of the predominance of present-day eolian activity, it was first suggested that loose crater ejecta had been removed and redistributed to explain the modified appearance of the martian craters [2,3]. Alternatively, Jones [4] and Chapman and Jones [5] suggested that water acted as a major erosive agent during an early martian crater obliteration event. Volcanism is another potential process suggested for crater modification [6]. Because the geologic materials that contain degraded impact craters are the oldest exposed units on the planet [7,8], these hypotheses obviously imply very different geologic histories for early Mars. Our work has focused on determining the mechanism(s) responsible for modifying the highland impact craters as well as assessing both the temporal and spatial variations experienced by these processes. Our important findings are summarized below. These observations support the idea of an early “warm and wet” Mars, which may have resulted from the gradual collapse of the primordial atmosphere into the martian crust.

**Previous Observations:** While it is inarguable that eolian deposition has modified impact craters in the highlands, these processes appear to be restricted to specific regions on Mars (e.g., Arabia [9] or Ismenius Lacus [10]) and are separable from the more global event recorded in dissected highland materials (Npld, as mapped by [7,8]). Only erosional processes are capable of explaining the observed crater morphology and, more importantly, the size range of modified craters [11]. Because crater rim heights increase as a function of diameter [12], craters with rim heights greater than the thickness of an overlying deposit will retain sharp rims, whereas those with rim heights less than the thickness of the deposit will be buried or subdued. Such morphologies are not observed in most areas, implying that degradation, as opposed to pure aggradation, was the dominant process operating in the early martian environment. This rules out processes such as global volcanic resurfacing or eolian deposition.



Based on the analysis of superposed fresh crater populations located in highland material between  $\pm 30^\circ$  latitude, it appears that crater degradation ceased at higher elevations (e.g., 3–4 km, Late Noachian) before it did at lower elevations (e.g., 1–2 km, Early Hesperian) [13]. This observation is consistent with the cessation of fluvial activity due to desiccation of a volatile reservoir with time, and with decreasing martian atmospheric pressures that caused cloud condensation—and thus precipitation—to occur at progressively lower elevations.

Dendritic ancient valley networks in the equatorial highlands show evidence of drainage into smooth, intracrater basins. Such areas have been interpreted as containing sedimentary deposits [14]. In many instances, comparisons of the fresh impact crater populations contained in these basins with those in the surrounding highlands concur with this interpretation [15]. These analyses indicate that extensive sedimentary deposits may have resulted from highland degradation, implying that materials eroded from impact craters were transported great distances (tens of kilometers), which requires overland flow of water. It also implies that the ancient valley networks are the result of surface run-off and not sapping.

Recent photoclinometric analyses of craters in the Sinus Sabaeus and Margaritifer Sinus regions [16] and two-dimensional computer simulations of a variety of erosional processes indicate that a combination of diffusional creep and fluvial erosion and deposition is capable of describing the observed degraded crater morphology. However, extensive seepage and backwasting is also needed to explain the up to 30% enlargement in crater diameter observed at the terminal stage of degradation. These results argue that early Mars experienced widespread precipitation, fluvial processes, and near-surface groundwater flow.

Ion microprobe analyses of the SNC meteorites [17] suggest that martian lavas contained  $\sim 0.1$ – $0.5\%$  water, a value comparable to quenched Hawaiian and mid-ocean ridge basalts [18]. Assuming that the gas content of martian lavas was comparable to terrestrial basalts in both the composition of constituents and their abundances, Craddock and Greeley [19] calculate that a cumulative layer between 3 m and 21 m of acid rain ( $\text{H}_2\text{SO}_4$ ) may have precipitated onto the martian surface as the result of volcanic degassing of  $\text{SO}_2$ . Also, their revised estimates of the amount of juvenile water released through volcanism,  $1.1 \times 10^{18}$  kg ( $\sim 8 \pm 1$  m), fall short of the estimated volume of water contained in the north polar layered deposits [20]. This implies that Mars experienced an earlier episode of outgassing that probably occurred during accretion (i.e., the early Noachian). This possibility is further supported by the release factor for nonradiogenic volatiles that was derived by Scambos and Jakosky [21] from their model of the release factor of Ar. In their model Mars must have outgassed  $\sim 10$  m of water if the planet retained some early Noachian volatiles (Table 2 in [21]), which agrees well with results in [19].

**Summary Interpretations:** The principal interpretation that can be made from our observations is that it probably rained like hell on early Mars. The systematic decrease in age with elevation indicates that this was not a series of punctuated events but a single, long-lived event that waned gradually through time. Currently, our working hypothesis is that the primordial martian atmosphere slowly condensed and collapsed (i.e., precipitated) into the martian regolith, while simultaneously degrading the highland impact craters, redistributing eroded materials, and carving the ancient valley networks. The warm, wet climate on early Mars may have failed due

to escape of volatile material into space and the lack of adequate replenishment from volcanic outgassing as suggested in [22]. The waning stage of atmospheric collapse during the Hesperian is also closely related to the ages of martian outflow channels. Although it is difficult to draw direct conclusions based solely on our work in the martian highlands, this temporal relation does suggest that perhaps precipitation and percolation of water into the martian regolith eventually created a hydrostatic head that, once high enough, provided the conditions necessary for outflow channel formation.

**References:** [1] Leighton R. B. et al. (1965) *Science*, 149, 627–630. [2] Hartmann W. K. (1971) *Icarus*, 15, 410–428. [3] Chapman C. R. (1974) *Icarus*, 22, 272–291. [4] Jones K. L. (1974) *JGR*, 79, 3917–3931. [5] Chapman C. R. and Jones K. L. (1977) *Annu. Rev. Earth Planet. Sci.*, 5, 515–540. [6] Arvidson R. E. et al. (1980) *Rev. Geophys. Space Phys.*, 18, 565–603. [7] Greeley R. and Guest J. E. (1987) *U.S. Geol. Surv. Misc. Invest. Ser. Map*, I-1802-B. [8] Scott D. H. and Tanaka K. L. (1986) *U.S. Geol. Surv. Misc. Invest. Map*, I-1802-A. [9] Moore J. M. (1990) *JGR*, 95, 14279–14289. [10] Grant J. A. and Schultz P. H. (1990) *Icarus*, 84, 166–195. [11] Craddock R. A. and Maxwell T. A. (1990) *JGR*, 95, 14265–14278. [12] Pike R. J. and Davis P. A. (1984) *LPS XV*, 645–646. [13] Craddock R. A. and Maxwell T. A. (1993) *JGR*, 98, 3453–3468. [14] Goldspiel J. M. and Squyres S. W. (1991) *Icarus*, 89, 392–410. [15] Maxwell T. A. and Craddock R. A. (1995) *JGR*, 11765–11780. [16] Craddock R. A. et al. (1997) *JGR*, in press. [17] Watson L. L. et al. (1994) *Science*, 265, 86–90. [18] Gerlach T. M. and Graeber E. J. (1985) *Nature*, 313, 273–277. [19] Craddock R. A. and Greeley R. (1997) *JGR*, submitted. [20] Malin M. C. (1986) *GRL*, 13, 444–447. [21] Scambos T. A. and Jakosky B. M. (1990) *JGR*, 95, 14779–14787. [22] Haberle R. M. et al. (1994) *Icarus*, 109, 102–120.

**THE RADIATIVE EFFECTS OF  $\text{CO}_2$  ICE CLOUDS ON THE EARLY MARTIAN CLIMATE.** D. C. Crisp, Jet Propulsion Laboratory, California Institute of Technology, Pasadena CA 91109, USA.

Morphological evidence of fluvial erosion on the martian surface indicates that Mars may have once had a much warmer, wetter climate. These conditions have been attributed to atmospheric greenhouse effects associated with a much more massive primordial  $\text{CO}_2$ - $\text{H}_2\text{O}$  atmosphere. However, recent modeling studies [1] suggest that no atmosphere composed entirely of  $\text{CO}_2$  and  $\text{H}_2\text{O}$  can maintain surface temperatures above the  $\text{H}_2\text{O}$  frost point. These models show that even though 1–5-bar  $\text{CO}_2$ - $\text{H}_2\text{O}$  atmospheres have enough thermal opacity to effectively prevent the escape of thermal radiation from the surface, their radiative equilibrium temperatures at tropopause levels would fall below the  $\text{CO}_2$  ice clouds at these levels. Kasting [1] did not explicitly model the radiative effects of these clouds, but concluded that they would cool the planet because they would reflect a large fraction of the incident solar insolation back to space, and contribute little absorption to enhance the atmospheric greenhouse effect. More recently, Pierrehumbert and Erlick [2] have proposed that infrared multiple scattering by these clouds may have actually produced a significant amount of warming, by reflecting a much larger fraction of the upwelling thermal radiation back into the surface and lower atmosphere.

To more completely assess the radiative forcing by  $\text{CO}_2$  ice clouds, we created a series of plausible model atmospheres for early

Mars and used a spectrum-resolving (line-by-line) multiple scattering model to derive the solar and thermal fluxes and heating rates for cases with and without CO<sub>2</sub> ice clouds. The model atmospheres had surface pressures of 1 and 5 bars respectively. Their temperatures decreased adiabatically from 273 K at the surface to the CO<sub>2</sub> frost point (~715 for the 1-bar case, and ~190 K for the 5-bar case), and then followed the frost point profile at higher altitudes. Each model atmosphere included CO<sub>2</sub>, a small amount of H<sub>2</sub>O (~40 ppmv) and CO (600 ppmv). CO<sub>2</sub> ice clouds with a range of optical depths ( $10 \leq \tau \leq 1000$ ) and particle sizes ( $0.1 \leq r_e \leq 10 \mu\text{m}$ ) were considered.

At solar wavelengths, optically thick CO<sub>2</sub> ice clouds can reduce the globally averaged net solar flux at the top of the atmosphere by about a factor of 10 (from ~82.6 W/m<sup>2</sup> to less than 8.74 W/m<sup>2</sup> for a  $\tau_s = 100$  cloud). These clouds also reduce the downward solar flux at the surface (from 65.6 to only 2.4 W/m<sup>2</sup> for  $\tau_s = 100$ ). The effects of these clouds on the thermal radiation field are almost as dramatic, however. When cloud absorption is included, but multiple scattering is neglected at thermal wavelengths, the CO<sub>2</sub> ice clouds have a negligible effect on the thermal radiative balance as Kasting [1] asserts. However, when thermal multiple scattering is included, optically thick CO<sub>2</sub> clouds can reduce the spectrally integrated thermal flux significantly (from ~55 to ~14 W/m<sup>2</sup> for  $\tau_s = 100$ ). The largest reductions in the outgoing thermal flux occur in the spectral windows, centered near 20  $\mu\text{m}$  (400 cm<sup>-1</sup>) and 8.5  $\mu\text{m}$  (1150 cm<sup>-1</sup>). The cloud has no effect in the vicinity of the CO<sub>2</sub> 15- $\mu\text{m}$  band, where the atmosphere is optically thick. These results suggest that even though CO<sub>2</sub> ice clouds may have produced a small net radiative cooling in the early martian atmosphere, the "reflective" greenhouse mechanism proposed by Pierrehumbert and Erlick [2] may have significantly reduced their impact on the early martian climate.

**References:** [1] Kasting J. (1991) *Icarus*, 94, 1-13. [2] Pierrehumbert and Erlick (1997) *J. Atmos. Sci.*, submitted.

**DEGRADATION OF THE MARTIAN CRATERED HIGHLANDS: THE ROLE OF CIRCUM-HELLAS OUTFLOW CHANNELS AND CONSTRAINTS ON THE TIMING OF VOLATILE-DRIVEN ACTIVITY.** D. A. Crown, S. C. Mest, and K. H. Stewart, Department of Geology and Planetary Science, University of Pittsburgh, Pittsburgh PA 15260, USA.

The cratered highlands east of the Hellas Basin preserve landforms representative of much of Mars' history and record the effects of volcanism, tectonism, fluvial erosion and deposition, eolian activity, and mass-wasting. Previous mapping studies and geomorphic analyses have provided a general understanding of the evolution of this region [1-3], placed constraints on the volcanic activity associated with Hadriaca and Tyrrhena Paterae [3-7], and characterized Dao and Harmakhis Valles and the terminus of Reull Vallis [3,8,9]. Recent geologic mapping studies have been extended from the Hadriaca/Tyrrhena Paterae region into the highlands of Promethei Terra [10-13] in order to examine the entire Reull Vallis outflow system and to analyze highland evolution outward from the Hellas Basin. The present study summarizes results relevant to determining the timing and nature of volatile-related depositional and erosional events.

**Formation of Circum-Hellas Outflow Channels:** Three major outflow channel systems, Dao, Harmakhis, and Reull Valles, extend from the cratered highlands toward Hellas Basin (see Table 1 for outflow channel characteristics). Dao and Harmakhis Valles have similar morphologic attributes and have previously been interpreted to be collapsed regions of volcanic and sedimentary plains that were eroded by a combination of surface and subsurface flow [3,14,15]. Spatial and temporal associations between source regions for Dao and Harmakhis Valles and volcanic materials associated with the paterae suggest that volcano-ice interactions may have contributed to and possibly triggered outflow channel formation [3,14]. Both Dao and Harmakhis Valles are trough-shaped canyons whose source regions are scarp-bounded collapse depressions adjacent to slumped areas of surrounding plains. Reull Vallis exhibits similar but more varied morphologic characteristics. Its source region consists of several small channels that converge in a large irregular depression in Hesperia Planum. The age of the ridged plains and their interpretation as voluminous lava flows is consistent with the apparent relationship between outflow channel formation and volcanism.

Analyses of the morphologic properties of Dao, Harmakhis, and Reull Valles indicate that these circum-Hellas outflow channels were the result of a series of erosional and depositional events over an extended time period. Lineations parallel to canyon walls are evidence for flow of fluids through the outflow systems, and Reull Vallis exhibits some streamlined features in its source region. Evidence for subsurface flow is present in the zones of subsided plains separating the main canyons of Dao and Harmakhis Valles from their source regions. Reull and Harmakhis Valles may have at one time had a subsurface connection, but their intersection is obscured by a large debris apron. Collapse is clearly a primary process in the formation of Dao and Harmakhis Valles; the lack of preserved evidence for collapse and subsurface flow along Reull Vallis suggests that this may be a more mature system. Secondary collapse of wall materials has enlarged all three valles. Depositional features are not typically observed in conjunction with martian outflow channels [14]. All three circum-Hellas valles exhibit evidence for resurfacing of their floors, the most prominent example being Reull Vallis, which contains a distinctive, lineated mantle of appreciable thickness. At Dao Vallis' terminus, an apparent depositional lobe of material emanates from its main canyon onto Hellas Planitia [3].

**Timing of Volatile-Driven Processes:** Formation of valley networks in small, relatively isolated drainage basins in the cratered highlands and on rugged highland massifs presumably represents the oldest preserved evidence of fluvial erosion in the region. Dissection of Hadriaca Patera's flanks preceded the formation of run-off channels in the adjacent channeled plains rim unit (unit AHh<sub>5</sub> in [1,3,11] that are truncated by both Dao and Harmakhis Valles. All three valles dissect extensive plains units of Hesperian and Amazonian/Hesperian age. The initial stages of outflow channel development may have begun as early as mid-Hesperian or as late as Early Amazonian. Crater statistics for large craters (>5 km in diameter) suggest that outflow channel floors are Hesperian in age; other studies including smaller diameter craters suggested that the floors of Dao and Harmakhis Valles were Amazonian/Hesperian in age [3]. Debris aprons are locally the youngest geologic features



TABLE 1. Characteristics of Circum-Hellas Outflow Channel Systems.

		Dao Vallis	Harmakhis Vallis	Reull Vallis
Length		~1200 km	~800 km	~1500 km
Width		6–50 km	8–60 km	5–50 km
Orientation	Segment 1	NE-SW	NE-SW	N-S
	Segment 2	E-W	E-W	NE-SW
	Segment 3	N/A	N/A	NW-SE
Morphology		Canyon system	Single canyon	Discontinuous channel/canyon system
Source		Two collapse depressions	Collapse depression	Small channels, irregular depression, and tributary canyon
Layering		None apparent	None apparent	Several scales observed
Ages of surrounding units*		AH, H	AH, N	AH, H, N
Evidence for:				
	Surface flow			
	Streamlined features	None apparent	None apparent	Yes
	Flow lineations	Yes	Yes	Yes
Subsurface flow		Yes	Yes	Connection to Harmakhis?
Collapse				
	During formation	Yes	Yes	?
	Secondary (i.e., wall)	Yes	Yes	Yes
Deposition				
	At terminus	Yes	?	Connection to Harmakhis?
	On floor	Yes	Yes	Yes
	Adjacent to vallis	None apparent	None apparent	Probably?

\*A = Amazonian, H = Hesperian, N = Noachian; ages from geologic map of [11].

in the region and overlie valles floor materials. Debris aprons have relatively uncratered surfaces suggesting formation in the Amazonian Period. Due to limited areal extents, crater ages for valles floor materials and debris aprons are subject to significant uncertainties.

The initial stages of outflow channel development appear to have involved catastrophic collapse events in or near their source regions. However, based on the morphologic properties and diversity of valles walls and floors, the circum-Hellas outflow channel systems were apparently long-lived, particularly in the case of Reull Vallis. Dao, Harmakhis, and Reull Valles all exhibit evidence for fluid flow within their canyons and various wall erosion and failure events downstream from their source regions. Small-scale layering in Reull Vallis reflects different erosional events within the channel. In addition, downstream from the junction of segments 2 and 3 of Reull Vallis, a tributary side canyon with layered walls is observed. Here, Reull Vallis becomes wider, presumably due to the release of additional fluids from this secondary source region. The identification of pitted plains near the source of Harmakhis Valles [3], a series of smooth sedimentary plains units adjacent to Reull Vallis [11], and a series of prominent debris aprons/flows in the highlands near Harmakhis and Reull Valles [11–13], all with similar surface characteristics, is indicative of a relatively young, regional style of degradation. The abundance of irregular pits suggests volatile-rich materials subjected to deflation. The apparent continuity and similar surface characteristics of a smooth plains unit with materials on the floor of a basin within Reull Vallis, the lobate terminations of smooth plains against the surrounding highlands, and the mesas and channels south of Reull Vallis suggest that fluids moving through

the channel may have had a significant role in both the resurfacing of low-lying regions of the highlands and erosion of plains units adjacent to the channel [10,11]. Furthermore, detailed geomorphologic characterization of young (Amazonian?) debris aprons reveals subsequent fluvial erosion indicating at least the local presence of water postdating emplacement of the youngest geologic features in the region [13]. Further analyses of the highlands of the eastern Hellas region of Mars will continue to refine the hydrologic evolution and sedimentary history of the region and document climate change on Mars.

**References:** [1] Greeley R. and Guest J. E. (1987) *U.S. Geol. Surv. Misc. Inv. Ser. Map I-1802B*. [2] Tanaka K. L. and Leonard G. J. (1995) *JGR*, 100, 5407–5432. [3] Crown D. A. et al. (1992) *Icarus*, 100, 1–25. [4] Greeley R. and Crown D. A. (1990) *JGR*, 95, 7133–7149. [5] Crown D. A. and Greeley R. (1993) *JGR*, 98, 3431–3451. [6] Crown D. A. and Greeley R. (1997) *Geologic Map of MTM Quadrangles—30262 and—30267, Hadriaca Patera Region of Mars*, U.S. Geol. Surv., in review. [7] Gregg T. K. P. et al. (1997) *U.S. Geol. Surv. Misc. Inv. Ser. Map I-2556*, in press. [8] Price K. H. (1993) *LPS XXIV*, 1179. [9] Price K. H. (1997) *Geologic Map of MTM Quadrangles—40262, —40267, and—40272: Dao, Harmakhis and Reull Valles Region of Mars*, U.S. Geol. Surv., in review. [10] Crown D. A. and Mest S. C. (1997) *LPS XXVIII*, 269–270. [11] Mest S. C. and Crown D. A. (1997) *LPS XXVIII*, 945–946. [12] Mest S. C. and Crown D. A. (1996) *Geol. Soc. Am. Abstr. with Progr.*, A-128. [13] Stewart K. H. and Crown D. A. (1997) *LPS XXVIII*, 1377–1378. [14] Baker V. R. (1982) *The Channels of Mars*. [15] Squyres S. W. et al. (1987) *Icarus*, 70, 385–408.

**MARS ON EARTH: ANTARCTIC DRY VALLEY LAKES AND THEIR DEPOSITS.** P. T. Doran and R. A. Wharton Jr., Biological Sciences, Desert Research Institute, P.O. Box 60220, Reno NV 89506, USA (pdoran@maxey.unr.edu).

Images of proposed fluvial systems on Mars suggest that there must have existed downstream locations where water pooled, and the sediment load deposited (i.e., lakes) [1,2]. As Mars became progressively colder over geological time, any lakes on its surface would have become seasonally, and eventually perennially, ice-covered. The notion that martian life's last stand may have been a swim in an ice-covered lake was born from this proposed progression. In turn, the study of perennially frozen Antarctic lakes as martian analogs has become important, especially in light of proposed sample return missions to Mars. If we go to Mars to look for evidence of lacustrine life, where is the best place to look and what are we looking for?

Much of our work has been performed in the McMurdo Dry Valleys of Antarctica ( $\sim 77^\circ\text{S}$ ). Lakes in this region mostly have perennial ice covers 3–6 m thick. Although the ice restricts up to 99% of the incident light, microbial mat communities flourish on the lake bottoms. Some lakes at higher elevations, previously believed to be frozen solid, have recently been discovered to contain water at depth. One lake, Lake Vida, has 16 m of ice cover, underlain by an undetermined amount of wet saline ice, and possibly an ice-free saline water body. The temperature at the dry ice/wet ice interface is  $\sim 10^\circ\text{C}$  warmer than the local mean annual temperature, suggesting some warming mechanism at depth. The mechanisms behind the formation and persistence of this type of lake are still under investigation. Plans are also being made to penetrate and aseptically sample the saline water and underlying sediment. The significance of these deeply frozen lakes is profound. What does it take to freeze a lake solid and extinguish the life it contains?

The main thrust of our present research is to relate modern lake environments to the sediments being deposited, and to use this relationship to make inference from paleolake deposits concerning the environment of the ancient lake. In the dry valleys there are two main types of paleolake deposit; perched deltas and lacustrine sand mounds. Both contain preserved (freeze-dried) organic matter and carbonates.

We have analyzed carbonate and organic matter in sediment cores from modern Lake Hoare, "perched" deltas remaining from Glacial Lake Washburn that occupied the Taylor Valley up to  $\sim 8000$  yr ago [3], and lacustrine sediment mounds near Lake Vida (perched deltas are also associated with the Vida mounds, but we have not yet sampled them). The lacustrine sand mounds and associated deltas were left by a Greater Lake Vida.

Strata in Lake Hoare sediments have a mean carbonate  $^{13}\text{C}$  value of 5.6‰, very close to the predicted value (5.4‰) for Antarctic lakes precipitating carbonate near saturation [4]. Organic matter  $^{13}\text{C}$  is variable, but overall is isotopically light. Heavier organic  $^{13}\text{C}$  values are generally associated with coarse-grained material, suggesting the material originated in shallower waters or is allochthonous. A depth transect of surface microbial mat samples in Lake Hoare clearly shows that  $^{13}\text{C}$  gets lighter with depth in the lake, at a much greater rate than does the DIC in the water column. These data suggest that  $^{13}\text{C}$  of microbial mat may be a useful indicator of paleohydrology (e.g., lake level, ice thickness, etc.).

We find that  $^{13}\text{C}$  of modern deltas and shallow lacustrine mats are quite variable considering they are from the same lake at the same time. All these samples are near a major inflow to the lake, and therefore are influenced by both lake and stream dynamics. Comparison of these results with the depth transect in Lake Hoare reported above leads us to suggest that lake bottom environments are more stable and predictable than lake edge deltaic environments, and therefore lake bottom deposits are more useful as paleoindicators.

Distinct authigenic (as opposed to detrital) carbonate is absent in the deltas, since the thermodynamics of the stream/lake system does not allow for saturation of calcite near stream inflows (i.e., where the deltas are forming). Lacustrine sand mounds, on the other hand, contain abundant and readily identifiable authigenic carbonate, since these deposits are characteristic of lake bottom environments. Identifying authigenic carbonate will be important for the martian case, since carbonate is more likely to be preserved in the harsh ambient environment than organic matter, and it will contain isotopic signatures (e.g.,  $^{13}\text{C}$ ,  $^{18}\text{O}$ ) indicative of the lake environment at the time of deposition. We are presently defining this relationship. Our work in the dry valleys suggests further that the larger the delta, the less likely the chance of finding nonclastic material. This is presumably a result of the high-energy environment that produces the larger deltas.

Deltas may not be ideal locations to look for evidence of past life on Mars. Nevertheless, large deltaic features visible in Viking imagery (e.g., in the Ma'adim Vallis/Gusev Crater system) are useful in that they indicate a possible region of discovery for smaller-scale features of potential, such as lacustrine sand mounds.

**References:** [1] Carr M. H. et al. (1987) *LPS XVIII*, 155–156. [2] Wharton R. A. Jr. et al. (1995) *J. Paleolimnology*, 13, 267–283. [3] Doran P. T. et al. (1994) *J. Paleolimnology*, 10, 85–114. [4] Doran P. T. et al. (1995) *Antarc. J. U.S.*, 24(5), 234–237.

**ACCRETION OF EARTH AND MARS: IMPLICATIONS FOR BULK COMPOSITION AND VOLATILE INVENTORIES.** M. J. Drake, Lunar and Planetary Laboratory, University of Arizona, Tucson AZ 85721, USA.

The dominant paradigm for the formation of the Earth has been the heterogeneous accretion hypothesis [e.g., 1]. Support for this hypothesis comes principally from the stepped pattern of lithophile, moderately siderophile, and highly siderophile elements in the Earth's mantle (Fig. 1), and the inability of metal/silicate partition coefficients obtained at low pressures and temperatures to produce a match to the pattern under conditions of metal-silicate equilibrium. The abundance pattern in the martian mantle is quite different (Fig. 2), leading Dreibus and Wänke [2] to the conclusion that Mars accreted from the same distinct chemical components, but in different proportions. These components either came in as a homogeneous mixture, or were homogenized subsequent to accretion. Treiman et al. [3] concluded independently that Mars accreted homogeneously.

Other hypotheses, such as inefficient core formation [4], have also been proposed to account for the elemental abundance pattern of the Earth's mantle, but have been largely discounted because of the special conditions required to match observed abundances.

However, a detailed examination of abundance patterns in the Earth shows that the heterogeneous accretion hypothesis also requires special pleading. For example, Ga belongs to the moderately siderophile group of elements like Ni and Co in Fig. 1, yet it plots with the refractory lithophile elements, an observation difficult to explain by heterogeneous accretion.

The shortcomings of the accretion hypotheses discussed above, coupled with the recognition that planetary accretion involved extremely energetic impacts, and advances in large-volume, high-pressure technology in the 1990s, have led to a reexamination of homogeneous accretion in the context of a magma ocean. Several groups have reported metal/silicate partition coefficients at high pressures and temperatures. Righter et al. [5] and Li and Agee [6] show that moderately siderophile elements in the Earth's mantle can be matched by equilibrium between metal and silicate in a magma ocean with a depth corresponding to about 250 kbar (approximately 800–900 km deep). Righter and Drake [7] extended this conclusion to include the highly siderophile element Re (Fig. 1). Righter and Drake [8] showed that abundances in the Moon, Mars (Fig. 2), and Vesta are also consistent with planetary-scale magma oceans. In the case of Mars, the magma ocean extended to a pressure of about 60–90 kbar (approximately 450–675 km deep).

Both Earth and Mars are depleted in volatile elements relative to chondrites, with Mars being somewhat less depleted than the Earth [2]. The most important volatile species for the purposes of this conference is water. On geochemical grounds the bulk martian mantle abundance is 36 ppm, which, if fully outgassed, is equivalent to a global ocean 130 m deep [2]. Estimates based on geological considerations [9] and D/H ratios [10] are generally higher. Water is highly soluble in magmas. For example, at the modest temperature and pressure of 1200°C and 1 kbar, basaltic magma can dissolve

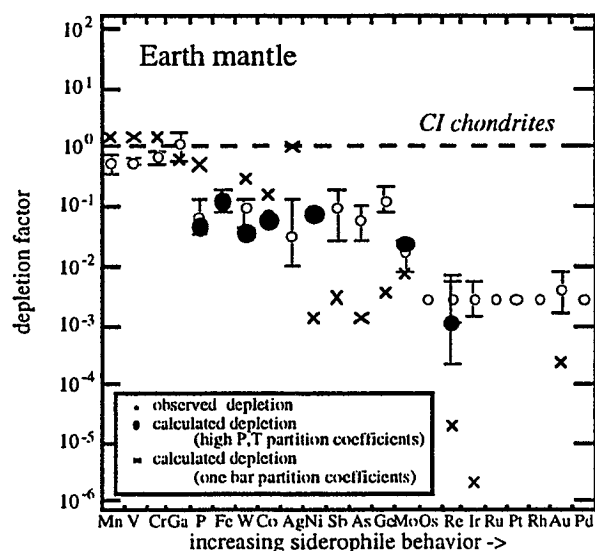


Fig. 1. Comparison of the observed siderophile-element depletions in Earth's upper mantle (open circles) with those calculated using one-bar partition coefficients (crosses) and high-pressure/high-temperature calculated partition coefficients (solid circles). Earth mantle abundances can be fit for equilibrium between metal and silicate at the base of a magma ocean at 250 kbar, 2225°C, relative redox state  $DIW = -0.5$ , S content of the molten metal  $X_S = 0.18$ , and peridotitic magma.

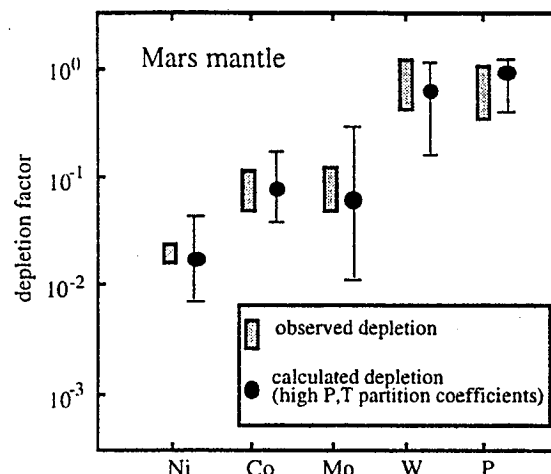


Fig. 2. Comparison of the observed siderophile-element depletions in the martian mantle (shaded bars) with those calculated using high-pressure/high-temperature calculated partition coefficients (solid circles). In this example, martian mantle abundances can be fit for equilibrium between metal and silicate at the base of a magma ocean at 75 kbar, 1900°C, relative redox state  $DIW = -0.7$ , S content of the molten metal  $X_S = 0.2$ , and peridotitic magma.

up to 3 wt% water [11]. Thus abundant water was available for outgassing on both Earth and Mars, in addition to any subsequent addition to the inventory from cometary impacts.

At least some fraction of the atmosphere of Mars outgassed very early in Mars history, as indicated by the presence of distinct atmospheric and solid-body reservoirs of  $^{129}\text{Xe}/^{132}\text{Xe}$ .  $^{129}\text{Xe}$  is produced by beta decay of  $^{129}\text{I}$ , with a half-life of 16 m.y. Had more than 5–7 half-lives of  $^{129}\text{I}$  passed before atmospheric outgassing, different reservoirs would not have been produced. Musselwhite and Drake [12] have shown that the  $^{129}\text{Xe}/^{132}\text{Xe}$  ratios in martian reservoirs can be produced by outgassing of a magma ocean followed by atmospheric erosion and additional outgassing. It is clear from Xe isotopes that the Earth's atmosphere also began outgassing while  $^{129}\text{I}$  was still "alive" [13].

On both Earth and Mars, water would have outgassed along with Xe and other atmophile species. If the paradigm for the origin of life is correct, namely that the presence of liquid water, organic material, and an energy source ineluctably lead to self-replicating organisms, it seems likely that life began on both planets as soon as liquid water became permanently stable, and that it persisted on Mars at least until the atmospheric pressure dropped below the water triple point.

**Acknowledgments:** Supported by NASA grant NAGW-3348.

**References:** [1] Wänke (1981) *Phil. Trans. R. Soc. London*, A303, 287. [2] Dreibus and Wänke (1987) *Icarus*, 71, 225. [3] Treiman et al. (1987) *Proc. LPSC 17th*, in *JGR*, 92, E627. [4] Jones and Drake (1986) *Nature*, 322, 221. [5] Righter et al. (1997) *Phys. Earth Planet. Inter.*, in press. [6] Li and Agee (1986) *Nature*, 381, 686. [7] Righter and Drake (1997) *EPSL*, 146, 541. [8] Righter and Drake (1996) *Icarus*, 124, 513. [9] Baker et al. (1991) *Nature*, 352, 589. [10] Donahue (1995) *Nature*, 374, 432. [11] Holloway and Blank (1994) *Rev. Mineral.*, 30, 187. [12] Musselwhite and Drake (1997) *Icarus*, in press. [13] Allègre et al. (1983) *Nature*, 303, 762.

**VOLATILE INVENTORIES OF MARS AND EARTH AND THEIR IMPLICATION FOR THE EVOLUTION OF THE PLANETARY ATMOSPHERES.** G. Dreibus, H. Wänke, and G. W. Lugmair, Max-Planck-Institut für Chemie, Postfach 3060, D-55020 Mainz, Germany (dreibus@mpch-mainz.mpg.de).

From the data of SNC meteorites it is evident that the abundance ratios of moderately volatile and volatile elements are about a factor of 2–3 higher for Mars than for the Earth [1]. However, at present, the abundance of atmophilic volatiles and water on Mars is very low, in spite of the geological evidence of an early period in the history of Mars during which abundant water existed on its surface [2].

Gas loss from the primitive atmosphere during accretion could be the explanation for the estimated low water concentration of

36 ppm for the martian mantle [1] and the 2-orders-of-magnitude lower primordial rare gas concentrations in the martian atmosphere compared to the terrestrial values. There is no doubt that accretion is the most effective degassing stage in the evolution of planets. The huge quantities of  $H_2$  produced by the reaction of  $H_2O$  with metallic Fe during accretion act as a carrier for the extraction of gaseous species from the planetary interior and also remove them from the gravity field of the planet due to hydrodynamic escape [3]. The present atmospheres of Earth and Mars were mainly formed by degassing of the planets after the end of accretion.

Such a loss of volatiles is manifested by the low abundance of halogens and  $^{129}Xe_{rad}$  on Earth. From the amount of I in the bulk earth = 8.8 ppb [4] and the  $^{129}I/^{127}I$  ratio of  $1.09 \times 10^{-4}$  for Bjurböle [5], assuming 100% outgassing of  $^{129}Xe_{rad}$ , we determine an amount

TABLE 1.

	$^{129}Xe/^{132}Xe$	$^{132}Xe$ [ $10^{-12}cm^3/g$ ]	I [ppb]	Br [ppb]	Cl [ppm]	La [ppm]	Br/I	Br/La ( $\times 10^{-3}$ )
<b>Mars</b>								
Atmosphere	2.5 <sup>[6]</sup>	0.75 <sup>[6]</sup>						
Basalts								
Shergotty	1.19 <sup>[11]</sup> ; 1.36 <sup>[11]</sup> 1.34 <sup>[12]</sup>	9.21 <sup>[11]</sup> ; 5.56 <sup>[11]</sup> 4.03 <sup>[12]</sup>	36	890	108	2.44	25	400
Zagami	1.51 <sup>[13]</sup> 1.50 <sup>[14]</sup>	9.6 <sup>[13]</sup> 4.13 <sup>[14]</sup>	15 5.2	640 670	130 133	2.02 2.98	43 130	320 225
EETA 79001A	0.977 <sup>[15]</sup>	3.66 <sup>[15]</sup>	<100*	189	26	0.37	—	510
EETA 79001B			960*	287	48	0.80	—	360
EETA 79001C-glass (trapped atmosphere)	2.422 <sup>[12]</sup> 2.231 <sup>[15]</sup>	37.4 <sup>[12]</sup> 24.6 <sup>[15]</sup>	<12	378	35	0.30	>31	1180
QUE 94201			4600*	350	91	0.35	—	1000
<i>Lherzolites</i>								
ALHA 77005	1.11 <sup>[12]</sup>	6.02 <sup>[12]</sup>	1720*	69	14	0.32	—	220
LEW 88516	1.284 <sup>[16]</sup>	15.2 <sup>[16]</sup>	60	50	29	0.27	—	190
<i>Cumulates</i>								
Lafayette	1.26 <sup>[13]</sup> ; 1.29 <sup>[13]</sup>	18.7 <sup>[13]</sup> ; 8.8 <sup>[13]</sup>	54	590	101	2.0	11	295
Nakhla	1.56 <sup>[11]</sup> ; 1.38 <sup>[11]</sup> 1.90 <sup>[13]</sup> ; 1.18 <sup>[13]</sup>	3.01 <sup>[11]</sup> ; 3.78 <sup>[11]</sup> 5.7 <sup>[13]</sup> ; 2.8 <sup>[13]</sup>	17 24	3460 <sup>†</sup> 3410 <sup>†</sup>	1890 <sup>†</sup> 563 <sup>†</sup>	2.18	200 140	1590
ALH 84001	1.83 <sup>[7]</sup> ; 1.97 <sup>[7]</sup>	6.7 <sup>[7]</sup> ; 24.6 <sup>[7]</sup>	17	65	12	0.14	3.8	464
Chassigny	1.029 <sup>[11]</sup>	22.9 <sup>[11]</sup>	<10	97	34	0.59	>10	165
<b>Earth</b>								
Atmosphere	0.98 <sup>[6]</sup>	15.6 <sup>[6]</sup>						
Basalts – MORB								
CH98 DR10			12	159	71	2.7	13	59
CH98 DR11	1.002 <sup>[17]</sup>	1.37 <sup>[17]</sup>	11	90	28	2.7	8	33
CH98 DR12	1.015 <sup>[17]</sup>	0.57 <sup>[17]</sup>	<6	64	22	2.8	>11	23
CH98 DR15			8	62	43	2.3	7	27
CH98 DR17			5	196	89	2.8	38	70
OIB								
1699	0.988 <sup>[17]</sup>	1.16 <sup>[17]</sup>	20	344	177	10	17	34
1701	0.989 <sup>[17]</sup>	1.68 <sup>[17]</sup>	27	310	233	10	11	31
1712	0.989 <sup>[17]</sup>	0.64 <sup>[17]</sup>	61	550	200	9.7	9	57
Spinel-lherzolite			4.2	12	1.4	0.36	3	33
CI (Orgueil)	1.07 <sup>[18]</sup>	8.13 <sup>[18]</sup>	560	2530	678	0.245	4.5	10326

\*Meteorites from Antarctica are generally heavily contaminated with I [19]. Hence, these I data and the one for Lafayette (a find) have to be considered as upper limits only.

<sup>†</sup> Terrestrial contamination?

of  $\sim 167 \times 10^{-12} \text{ cm}^3/\text{g}$   $^{129}\text{Xe}_{\text{rad}}$  produced by decay of  $^{129}\text{I}$ . Compared with  $1.04 \times 10^{-12} \text{ cm}^3/\text{g}$  in the Earth's atmosphere, one calculates an interval between Bjurböle and the onset of  $^{129}\text{Xe}_{\text{rad}}$  retention in the Earth's atmosphere of  $\sim 115 \text{ m.y.}$  for the retention of  $^{129}\text{Xe}_{\text{rad}}$  in the Earth's atmosphere.

In contrast to Earth, on Mars the halogen inventory is about a factor of 3 higher (i.e., 25 ppb I), but a similar concentration of  $^{129}\text{Xe}_{\text{rad}}$  ( $1.12 \times 10^{-12} \text{ cm}^3/\text{g}$ ) was measured in the atmosphere [6]. Either the I-Xe formation interval relative to Bjurböle for the retention of  $^{129}\text{Xe}_{\text{rad}}$  in the martian atmosphere is  $\sim 137 \text{ m.y.}$ , or some Xe was retained in the interior of Mars. Retention of a considerable portion of  $^{129}\text{Xe}_{\text{rad}}$  in the martian mantle seems less likely due to the low  $^{129}\text{Xe}/^{132}\text{Xe}$  ratios in the martian basalts (Table 1), which may still be considered upper limits because of possibly insufficient subtraction of trapped atmosphere. We note that an independent estimate of the I-Xe systematic for the martian interior also yields a similar interval of  $\sim 110 \text{ m.y.}$  However, incomplete outgassing of rocks near the surface containing high concentrations of  $^{129}\text{Xe}_{\text{rad}}$  (see below) is still possible when we consider the high  $^{129}\text{Xe}/^{132}\text{Xe}$  ratio of about 1.83 and 1.97 in ALH 84001 [7]. With its crystallization age of close to 4.56 Ga [8], it is at least possible that  $^{129}\text{Xe}_{\text{rad}}$  from *in situ* decay of  $^{129}\text{I}$  is present. Table 1 shows that all other, much younger martian meteorites (except one Nakhla sample) have  $^{129}\text{Xe}/^{132}\text{Xe}$  ratios between 1.03 and 1.51.

Because of the short  $^{129}\text{I}$  half-life of 15.7 m.y.,  $^{129}\text{Xe}_{\text{rad}}$  is produced early in the history of planets. Iodine, a highly volatile and also highly incompatible element, is easily extracted from heated rock samples in the presence of  $\text{H}_2\text{O}$ , as are all halogens. Hence, it is likely that during accretion, I was removed from the interior of Mars very efficiently and incorporated into the crustal rocks present at that time [1]. Clearly, primordial rare gases, including Xe, would have been extracted together with I. However, rare gases would mostly have entered the atmosphere and been lost. After the end of accretion,  $^{129}\text{Xe}_{\text{rad}}$  produced from the extant  $^{129}\text{I}$  in the crust would have been released into the present atmosphere over geologic time. This led to the observed  $^{129}\text{Xe}/^{132}\text{Xe}$  ratio of 2.5 [6] compared to the interior value of about 1.5 [9]. The comparison of the Br/I ratio in Shergotty and Zagami with terrestrial basalts (MORB) indicates the preferred extraction of I from the martian mantle (Table 1). Shergottites are young basalts and probably reflect the composition of the martian mantle in modern times. Thus, their I depletion could be an indication of an early extraction of I from the mantle into the crust as proposed by [1] in order to explain the observation that  $^{129}\text{Xe}/^{132}\text{Xe}$  in martian rocks is lower than in the atmosphere [9]. In terrestrial MORB and mantle xenoliths one finds Cl, Br, and I close to CI abundance ratios (Table 1). Contrary to Mars, plate tectonics on Earth, with its continuous recycling of hydrosphere and crust into the mantle, might have led to this preservation of the CI ratio of halogens in mantle-derived samples.

In summary, Mars initially was almost certainly a very volatile-rich planet but has suffered a huge gas loss from the primitive atmosphere during accretion through hydrodynamic escape and removal by large impacts [10]. As is apparent from Table 1, in contrast to the Earth, Mars contains most of its complement of Xe in its interior.

**References:** [1] Dreibus and Wänke (1987) *Icarus*, 71, 225. [2] Carr M. H. (1986) *Icarus*, 68, 187. [3] Hunten et al. (1986) *Icarus*, 69, 532. [4] Wänke et al. (1984) in *Archaeon Geochemistry*,

p. 1. [5] Podosek F. A. (1970) *GCA*, 34, 341. [6] Anders and Owen (1977) *Science*, 198, 453. [7] Swindle et al. (1995) *GCA*, 59, 793. [8] Jagoutz et al. (1994) *Meteoritics*, 29, 478. [9] Ott and Begemann (1985) *Nature*, 317, 509. [10] Watkins and Lewis (1984) in *Workshop on Water on Mars*, p. 91. [11] Ott U. (1988) *GCA*, 52, 1937. [12] Swindle et al. (1986) *GCA*, 50, 1001. [13] Ott et al. (1988) *Meteoritics*, 23, 295. [14] Marti et al. (1995) *Science*, 267, 1981. [15] Becker and Pepin (1984) *EPSL*, 69, 225. [16] Ott and Löhner (1992) *Meteoritics*, 27, 271. [17] Staudacher and Allègre (1982) *EPSL*, 60, 389. [18] Mazar et al. (1970) *GCA*, 34, 781. [19] Dreibus and Wänke (1985) *Meteoritics*, 20, 367.

**REGARDING A WET, EARLY NOACHIAN MARS: GEOMORPHOLOGY OF WESTERN ARABIA AND NORTHERN SINUS MERIDIANI.** K. S. Edgett<sup>1</sup> and T. J. Parker<sup>2</sup>, <sup>1</sup>Department of Geology, Arizona State University, Box 871404, Tempe AZ 85287-1404, USA (edgett@esther.la.asu.edu), <sup>2</sup>Mail Stop 183-501, Jet Propulsion Laboratory, 4800 Oak Grove Drive, Pasadena CA 91109, USA (timothy.j.parker@jpl.nasa.gov).

**Introduction and Background:** This is a paper about the environment of Mars during the time when heavy bombardment was coming to an end and shortly thereafter. The exact date of this period is not known, but based on the Earth-Moon experience, it can be assumed to be  $\sim 4.1\text{--}3.8 \text{ b.y.}$  ago. A common assumption made about the early history of Mars is that the surface environment was similar to Earth [e.g., 1]. The common image of Earth during this period is that of an ocean-covered world dotted by islands of volcanic and impact origin [e.g., 2,3]. The oldest rocks on Earth date back to about 3.9 b.y. and include many volcanic and immature sedimentary rocks that were deposited in subaqueous environments [2,4].

If early Earth was a "Water World," could the martian surface also have been largely underwater at the same time? Estimates of the amount of water available on Mars relative to Earth  $\sim 4 \text{ b.y.}$  ago range from very little to more than on Earth. A typical assumption is that both planets had the same amount of water in proportion to the planet size [e.g., 5], although Mars could have had more water because it formed at a greater distance from the Sun [6]. If both planets began with the same proportion of water per planet mass, the depth of water on Mars, spread out over the surface, would have been about 1.2 km [5].

There is considerable evidence, largely in the form of valley networks, to suggest that erosion by water was vigorous during the Noachian Epoch [7]. Also, some of the largest impact basins, such as Isidis, Chryse, Argyre, and Ladon, have very deeply eroded rims [8,9]. Erosion by surface run-off nearly ceased as Mars entered the Hesperian Epoch [7].

Large, ancient seas have been proposed to have occurred at times in the martian past. Most attention is usually focused on the question as to whether the northern plains of Mars filled with water as a result of the formation of the giant Hesperian/Amazonian outflow channels [10], but there might also have been seas in Argyre and Hellas Basins [e.g., 9].

While the case has been made that seas might have once covered vast portions of Mars [10], little attention has been given to the question of seas in the earliest martian environments—seas that

could have been larger than those proposed, for example, by Parker et al. [10] for the northern plains. Such Noachian seas would have existed at the same time that life was emerging on the ocean-covered Earth.

This paper explores the possibility that a portion of western Arabia and Sinus Meridiani might have been under water at about the same time that heavy bombardment was ending and the valley networks were eroding the cratered highlands of Mars.

**Observations:** We focus on the region that is mainly between 10°S northward to 30°N, and from 10°W eastward to 330°W. The region includes the three main color units of western Arabia and Sinus Meridiani, identified as "bright red," "dark red," and "dark gray" [11]. The elevation of this region is low (<2 km) compared to other heavily cratered Noachian surfaces on Mars [12]. The topography at the kilometer scale is very flat across the region, dropping about 0.7 m/km from east to west over 3000 km. Frey and Roark [12] called this the "Western Arabia Shelf." While their focus was on the geophysical explanation for the low, flat topography of western Arabia [12], our focus is on the surface geomorphology.

Our observations can be summarized as follows: (1) There are horizontally bedded sediments in various states of eolian erosion throughout the region. These include mesas and "white rock"-like landforms on crater floors [13,14], yardangs and pedestal craters [15], and craters buried by bright layered material in Sinus Meridiani. (2) The sedimentary layers overlie most of the large impact craters in the region. (3) Some portion of the sediments must consist of sand, because recent dark streaks and dunes are common among these wind-eroded landforms. (4) There are almost no valley networks in the region (see M. H. Carr's Fig. 4-6 in [7]). (5) As noted by Frey and Roark [12], the regional topography is presently low and flat relative to other regions in the martian cratered highlands.

The portion of western Arabia that has a "dark red" surface [11] is characterized by the presence of many large, dark depositional wind streaks that originate at small dune fields on crater floors. In many of these craters there are small mesas and yardang landforms that resemble "White Rock" in Sinus Sabaeus. (Note that "White Rock" has been proposed to be a possible lacustrine deposit [16] with exobiological implications [17]). Also in the "dark red" part of western Arabia, there are many examples of yardangs and pedestal craters in the intercrater plains [15], both of which are characteristic of eolian erosion of fine-grained, semiconsolidated sedimentary rock. In the northern part of the "pipe bowl" of Sinus Meridiani, craters are buried under sediment that is probably 100–1000 m thick. The sediment appears to be the same as that which is largely wind-eroded in the "dark red" areas to the north. It is interesting to note that some of the sediment that buries craters in Sinus Meridiani appears to be very bright, similar to "White Rock." In the "bright red" portion of western Arabia, there are several craters that contain large mesas of layered sediment; the largest of these is in Henry Crater [14].

**Discussion:** Western Arabia appears to have been buried by up to 1 km of fine-grained sediment. Some large craters in the region postdate this deposit, thus it is likely that the sediment was deposited during the time when heavy bombardment was ending or had just recently ended. The origin of the sediment is unknown, but a case can be made to suggest that the sediment was deposited in

standing water. Moore [18] was confronted with a similar dilemma regarding wind-eroded mantle deposits in northeastern Arabia. The primary difference between the western Arabia region discussed here and the northeastern Arabia region discussed by Moore [18] is elevation. The region described by Moore [18] lies at modern elevations between 2 km and 5 km. If not for the great elevation, Moore [18] said that "a reasonable conclusion would be that it is [a] water-laid sedimentary deposit." Moore then discussed the merits and difficulties of interpreting the mantle in terms of tephra airfall vs. eolian dust deposition.

The elevation problem confronted by Moore [18] for northeastern Arabia does not apply in western Arabia and Sinus Meridiani. In addition, northeastern Arabia has valley networks, while western Arabia does not. The entire region lies below the present-day 2-km contour, and a portion of this region is lower than the 0-km datum. With a low, broad slope, the region could easily be inundated by water if enough were present to fill the northern plains up to the 2-km contour level. The fact that the entire western Arabia region has almost no valley networks may be an important clue that this may have been the case. This observation is most easily explained if the region was underwater at the same time that valley networks were eroding the martian highlands.

**Conclusion:** The low, relatively flat expanse of western Arabia and northern Sinus Meridiani bears evidence of a post-heavy-bombardment event in which layered sediments of up to 1 km thick were deposited in and surrounding the older impact craters. The sediments have subsequently been eroded by wind. The region, with its low elevation and relative lack of valley networks, could very plausibly have been under water early in martian history. Our scenario assumes the regional elevation has been about the same for 4 b.y.—however, it is equally possible that the region has been upwarped (toward eastern Arabia) over time.

If western Arabia and northern Sinus Meridiani were under water during the (perhaps appropriately named) Noachian Epoch, the observed layered sediments might include carbonate and evaporite deposits, as well as airfall from volcanic eruptions and meteorite impacts. The summary presented here is a framework in which future observations can be made and the origin of the sedimentary layers can be ultimately determined.

**References:** [1] McKay C. P. and Stoker C. R. (1989) *Rev. Geophys.*, 27, 189–214. [2] Goodwin A. M. (1981) *Science*, 213, 55–61. [3] Jenkins G. S. et al. (1993) *JGR*, 98, 8785–8791. [4] Lowe D. R. (1980) *Annu. Rev. Earth Planet. Sci.*, 8, 145–167. [5] Squyres S. W. and Kasting J. F. (1994) *Science*, 265, 744–749. [6] Lewis J. S. (1974) *Science*, 186, 440–443. [7] Carr M. H. (1996) *Water on Mars*, Oxford Univ. [8] Schultz P. H. et al. (1982) *JGR*, 87, 9803–9820. [9] Parker T. J. (1996) *LPS XXVII*, 1003–1004. [10] Parker T. J. et al. (1993) *JGR*, 98, 11061–11078. [11] Presley M. A. and Arvidson R. E. (1988) *Icarus*, 75, 499–517. [12] Frey H. V. and Roark J. H. (1997) *LPS XXVIII*. [13] Forsythe R. D. and Zimbelman J. R. (1995) *JGR*, 100, 5553–5563. [14] Zimbelman J. R. (1990) *LPS XXI*, 1375–1376. [15] Presley M. A. (1986) M.A. thesis, Washington Univ., St. Louis. [16] Williams S. H. and Zimbelman J. R. (1994) *Geology*, 22, 107–110. [17] An Exobiological Strategy for Mars Exploration (1995) *NASA SP-530*. [18] Moore J. M. (1990) *JGR*, 95, 14279–14289.

**GEOLOGIC SIGNATURE OF LIFE ON MARS: LOW ALBEDO LAVA FLOWS AND THE SEARCH FOR "WARM HAVENS."** K. S. Edgett<sup>1</sup> and J. W. Rice Jr.<sup>2</sup>, <sup>1</sup>Department of Geology, Arizona State University, Box 871404, Tempe AZ 85287-1404, USA (edgett@esther.la.asu.edu), <sup>2</sup>Department of Geography, Arizona State University, Box 870104, Tempe AZ 85287-0104, USA (asjwr@asuvm.inre.asu.edu).

**Introduction:** The possibility that Mars had living organisms in its past has become the focus of much attention in the wake of observations of the ALH 84001 meteorite presented by McKay et al. [1]. Regardless of the final outcome of the vigorous debate that has ensued, the possibility that Mars had life in the past was already regaining interest and support prior to this announcement [2–4]. It is often argued that if Mars ever developed life, living organisms might still exist somewhere under the planet's surface. The focus of this paper is on the search for geologic settings for extant martian life.

A key component of the search for martian organisms is the search for credible evidence of geologically young hydrothermal environments [4,5]. Mars Global Surveyor, scheduled to reach the planet on September 12, 1997, carries the Thermal Emission Spectrometer (TES). With 3–9-km/pixel resolution, TES data will play a major role in the search for minerals and geothermal heat associated with present and relatively recent hydrothermal systems [6]. Cameras on Mars Global Surveyor and the Mars Surveyor '98 orbiter will also aid in this search; and instruments will surely be proposed for the Mars Surveyor '01 orbiter that have higher spatial resolution for detecting hydrothermal environments. However, potential targets relevant to the search for young hydrothermal systems can already be identified. These are found on the basis of the presence of relatively young, low-albedo lava flows.

To date, the youngest features on Mars that are proposed to have a volcanic origin are dark, sandy spots associated with faults in the Valles Marineris, which Lucchitta suggested might be relatively young pyroclastic deposits [7,8]. However, landing a spacecraft in these valleys to search for evidence of life might be difficult. A plain with hundreds of kilometers of relatively flat surface might make a preferable future landing site. In this paper, we note the presence of two low-albedo lava flows that occur on vast plains that are large enough to consider a safe spacecraft landing, should either location prove (upon further examination by instruments such as TES) to be a viable place to look for extant life.

**Why Low-Albedo Lava Flows?** Dark-hued surfaces on Mars tend to be sandy, eolian environments, not lava flows [9]. Indeed, the surfaces with the lowest albedos are dune fields [e.g., 9–11]. The reason that dune fields and sandy surfaces tend to have low albedos is attributed to the probable mafic composition of the sand and the removal of fine dust via saltation [e.g., 12], a process that is well understood and documented in the terrestrial literature [e.g., 13]. Thus, there is a general assumption about Mars that dark surfaces lack dust, while other surfaces have at least a thin coating of dust [e.g., 14]. In this context, how would a low-albedo lava flow on Mars be explained? A low-albedo lava flow would be a surface that lacks an optically thick coating of fine, bright dust. The lack of dust could be the result of sand saltating across the lava flow, or it could be

explained if the flow is extremely young and has not had time to develop a thick enough mantle of dust. In either case, a dark lava flow would also be a surface that has not undergone significant chemical weathering. The lack of a dust coating and lack of weathering might indicate that the lava flow is extremely young.

**Dark Flow in Syria Planum:** The first low-albedo flow we describe is located in Syria Planum at 20.6°S, 98.6°W (see Viking orbiter image 643A64). Its presence was noted by Hodges and Moore [15], but they did not discuss the implication of its low albedo. The flow covers about 100 km<sup>2</sup> and appears to have erupted from a fissure that trends northwest-southeast. Many other lava flows are present in the region, and some of them are also associated with fissures. None of the other flows in the region are as dark as the low-albedo flow at 20.6°S, 98.6°W, but some flows in the region have dark margins. The flow is not entirely dark, however, as part of it has a bright surface. This bright patch could be caused by dust trapped on a small portion of the flow's presumably rough surface, but it could also be a local tephra deposit. Hodges and Moore [15] noted the similarity between this particular flow and the Kings Bowl Lava Field on the Snake River Plain in Idaho. The feature known as "Kings Bowl" is a small volcanic crater in the center of the lava field, from which a deposit of bright tephra was erupted about 2100 yr ago [16]. The explosive phase of the Kings Bowl eruption was caused by magma interaction with groundwater. Could the flow in Syria Planum have also involved explosive interaction with groundwater? Higher-resolution images (e.g., better than 20 m/pixel) would be helpful in determining the surface characteristics of this dark flow.

**Dark Flow in Cerberus:** The second low-albedo lava flow lies at the northeastern end of the classical low-albedo feature, Cerberus. The flow originates at one of the Cerberus Rupes fissures at 16.1°N, 199.5°W [17]. The flow extends about 250 km to the southwest (see Viking orbiter images 883A 04, 06). The flow appears to have a lower albedo (i.e., <0.10) than the dark eolian material in the same region. The Cerberus Rupes fissures might have been the source of other relatively young volcanic flows and possible pyroclastic deposits [15,17], but this flow is the only one that appears to be dark. The Cerberus Rupes extend into the Elysium Basin. In addition to being sources of volcanism, the Cerberus Rupes might have been a source for water that carved streamlined islands located near 9°N, 204.8°W [17]. The Elysium Basin in general appears to have been both the site of an Amazonian sea [18] and very late Amazonian volcanism [19].

**Discussion:** How did these two lava flow surfaces remain dark since the time of their eruption, when all other lava flows on Mars observed to date do not appear to be dark hued? For some reason, they did not retain a coating of fine, bright dust following the major global dust storms (1973, 1977) observed in the same decade that the flows were imaged by the Viking orbiters.

The lava flow in Cerberus is associated with the dark Cerberus albedo feature, which might be a sandy eolian environment [20]. It is therefore possible that abrasion by windblown sand could have helped keep the Cerberus flow dark. However, the dark Cerberus albedo feature overlies many other lava flows that are not dark and appear to be older than the dark flow described here. How could sand blasting cause one lava flow to appear dark but not the others?



The lava flow in Syria Planum is not associated with any other low-albedo surface features. Thus, the possibility of sand blasting is difficult to invoke in the case of Syria Planum.

We conclude that both dark lava flows described here are very young relative to most other lava flows on Mars. The flow at Cerberus has a few small superposed craters (<3 km diameter), suggesting that it might not be extremely young; however, all the volcanic features associated with the Cerberus Rupes and Elysium Basin are very young relative to other volcanic landforms on Mars [19]. The lava flow in Syria Planum is too small relative to the available image resolution to determine if there are any superposed craters. It is entirely possible that this flow is less than  $10^6$  yr old, perhaps less than  $10^3$  yr if the low albedo is due to lack of net deposition of dust on its surface.

**Conclusion:** Low-albedo lava flows might be good indicators of the geographic locations of relatively recent martian volcanism. Places where volcanism was most recent have the highest potential for finding geothermal and hydrothermal processes that are active today. The association of volcanic, fluvial, and lacustrine features in the Cerberus and Elysium region [17–19] make this area more likely than Syria Planum to be a site of recent or active hydrothermal systems. However, both regions described here warrant additional examination using Mars Global Surveyor and future Mars Surveyor orbiter spectrometers and cameras.

**Acknowledgments:** The term "Warm Havens" was borrowed, with respect, from Jakosky's paper "Warm havens for life on Mars" [5].

**References:** [1] McKay D. S. et al. (1996) *Science*, 273, 924–930. [2] McKay C. P. and Stoker C. R. (1989) *Rev. Geophys.*, 27, 189–214. [3] Klein H. P. (1996) *Icarus*, 120, 431–436. [4] An Exobiological Strategy for Mars Exploration (1995) *NASA SP-530*. [5] Jakosky B. M. (1996) *New Scientist*, 150, 38–42. [6] Christensen P. R. et al. (1992) *JGR*, 97, 7719–7734. [7] Lucchitta B. K. (1987) *Science*, 235, 565–567. [8] Lucchitta B. K. (1990) *Icarus*, 86, 476–509. [9] Edgett K. S. and Christensen P. R. (1994) *JGR*, 99, 1997–2018. [10] Thomas P. and Weitz C. (1989) *Icarus*, 81, 185–215. [11] Bell J. F. III et al. (1997) *LPS XXVIII*. [12] Thomas P. (1984) *Icarus*, 57, 205–227. [13] Rice M. A. et al. (1996) *Sedimentol.*, 43, 21–31. [14] Christensen P. R. (1986) *JGR*, 91, 3533–3545. [15] Hodges C. A. and Moore H. J. (1994) *U.S. Geol. Surv. Prof. Paper* 1534. [16] King J. S. (1977) in *Volcanism on the Snake River Plain, Idaho* (R. Greeley and J. S. King, eds.), pp. 153–163, NASA. [17] Edgett K. S. and Rice J. W. Jr. (1995) *LPS XXVI*, 357–358. [18] Scott D. H. and Chapman M. G. (1991) *Proc. LPS*, Vol. 21, pp. 669–677. [19] Plescia J. B. (1990) *Icarus*, 88, 465–490. [20] Edgett K. S. et al. (1994) *LPI Tech. Rpt. 94-04*, p. 25.

**EXOPALEONTOLOGY AND THE SEARCH FOR A FOSSIL RECORD ON MARS.** J. D. Farmer and D. J. Des Marais, Mail Stop 239-4, NASA Ames Research Center, Moffett Field CA 94035-1000, USA.

There is substantial geological evidence to indicate that Mars was more like Earth early in its history, with a denser, warmer atmosphere and abundant surface water [1]. Under such conditions, life could have developed in surface environments on Mars, eventually retreating into the deep subsurface as the planet lost its

atmosphere and began to refrigerate [2,3]. If life developed on Mars, it is likely to have left behind a fossil record. A record of ancient martian life could potentially include the organic remains of organisms (body fossils), biosedimentary structures (stromatolites) and associated biofabrics, as well as chemofossils (e.g., biomarker compounds, isotopic signatures).

In developing a strategy to explore for fossils on Mars, we have been guided by the nature of the Precambrian fossil record on Earth, as well as microbial fossilization processes in modern environments that are thought to be good analogs for the early Earth and Mars [4,5]. Such studies indicate that microbial fossilization is favored by (1) rapid entombment of micro-organisms within aqueously deposited minerals (chemical precipitates) and (2) by the rapid burial of organic materials within fine-grained, clay-rich sediments. And even if life did not develop on Mars, the same processes described above are key for preserving a record of prebiotic chemical evolution. This record has been lost on the Earth due to crustal recycling, active hydrological cycling, and resulting chemical weathering. However, on Mars heavily cratered highland terranes preserve extensive tracts of ancient crust that provide an unparalleled record of the early events of planetary and prebiotic evolution similar to that which led to life on Earth.

The concept of early mineralization and the rapid entombment of microorganisms by sediments is central in defining a site selection strategy to explore for a fossil record on Mars. Geological environments where microbial communities are commonly preserved by either chemical precipitates or fine-grained detrital sediments include (1) mineralizing spring systems (ranging from sub-aerial, subaqueous, and shallow subsurface hydrothermal, to cold spring systems on the floors of alkaline lakes); (2) lake basins where fine-grained shales or marls accumulate under anoxic conditions, and terminal (saline) lake basins where salts are deposited through evaporation; and (3) mineralized horizons or hard-pans (e.g., calcretes, silcretes, ferracretes) formed by the selective leaching and reprecipitation of minerals within soil profiles. To this we can also add permafrost terranes where ground ice produces frozen soils that capture and cryopreserve organisms and associated organic materials.

Chemical sedimentary deposits are often simple in composition, consisting of a fairly narrow range of pure endmember mineralogies. This should make them easy to detect from orbit or on the ground using high-resolution remote sensing techniques. Of the common chemical sediments, the most stable minerals include silica, phosphate, and carbonate. These mineralogies tend to have long crustal residence times and are the most common host sediments for microbial fossils in the Precambrian record on Earth. Other potential host minerals include evaporite minerals that are relatively unstable (they dissolve easily) and therefore tend to be lost from the record quickly if not replaced during early diagenesis by more stable minerals, such as barite or silica. As mentioned above, ice is another potential host mineral for fossils, but tends to have a very short residence time in the crust and is therefore most appropriate as a target for a recent fossil record.

In exploring Mars for molecular fossils, priority should be given to fine-grained, low-temperature sedimentary systems that are likely to have maintained a closed chemical system after deposition. On Earth, the fine-grained sediments (e.g., shales, mudstones) of the deeper parts of sedimentary basins tend to form low-permeability host rocks that retain a comparatively high total organic C content.



With the compaction of such fine-grained sediments, and their early cementation by silica, phosphate, or carbonate, permeability is greatly reduced, thus promoting the long-term preservation of organic materials. By terrestrial analogy, likely targets on Mars for such deposits include deep-water (basin-central) facies of terminal lake basins. On Earth, these fine-grained deposits are often important source rocks for petroleum. And it is also worth noting that organic preservation is often enhanced in fine-grained sediments owing to an abundance of absorbant clay minerals that selectively bind organic molecules on their surfaces or as interlayer cations.

Implementation of the proposed strategy for Mars exopaleontology will depend heavily on the targeting of favorable landing sites on Mars based on recognition of the geological environments outlined above. This will enable the optimization of missions for *in situ* robotic exploration to target the best rocks for sample return. This effort can best be accomplished through high-resolution spectral mapping from orbit. Mineralogy provides the most direct means for interpreting ancient environments and for selecting those sites that have the best chance of having preserved a record of ancient life. The aqueous minerals listed above, along with similar potential host deposits, have characteristic spectral signatures within the near- (1–3  $\mu\text{m}$ ) and mid-infrared (5–12  $\mu\text{m}$ ), which suggests they can be unambiguously identified from orbit at spatial resolutions of 100–200 m/pixel.

**References:** [1] Carr M. H. (1996) *Water on Mars*, Oxford Univ., 229 pp. [2] McKay C. P. and Stoker C. R. (1989) *Rev. Geophysics*, 27, 189–214. [3] Boston P. J. et al. (1992) *Icarus*, 95, 300–308. [4] Farmer J. D. and Des Marais D. J. (1994) *LPS XXV*, 367–368. [5] Farmer J. D. (1995) *Palaios*, 10, 197–198.

**FOSSILIZATION PROCESSES IN MODERN THERMAL SPRINGS: CLUES FOR ASSESSING THE BIOGENICITY OF ANCIENT HYDROTHERMAL DEPOSITS.** J. D. Farmer<sup>1</sup>, S. L. Cady<sup>1</sup>, D. J. Des Marais<sup>1</sup>, and M. Walter<sup>2</sup>, <sup>1</sup>Mail Stop 239-4, NASA Ames Research Center, Moffett Field CA 94035-1000, USA, <sup>2</sup>School of Earth Sciences, Macquarie University, North Ryde, NSW, Australia.

Hydrothermal systems have been cited as important targets in the search for evidence of an ancient biosphere on Mars [1,2]. Indeed, such environments appear to have been widespread on Mars earlier in its history [3], while subsurface hydrothermal systems may have provided clement environments for life throughout the subsequent history of the planet. Comparative studies of modern and ancient hydrothermal systems on Earth have the potential to provide important constraints on long-term evolutionary trends in hydrothermal ecosystems [4], and the results of such studies also assist in refining strategies to explore Mars for a fossil record of ancient hydrothermal life.

To create a comparative framework for interpreting the fossil record of ancient hydrothermal deposits on the Earth, and possibly Mars, we have carried out parallel studies of the microbial bio-sedimentology, taphonomy, and geochemistry of active hydrothermal environments in Yellowstone National Park. One goal of the research is the development of highly integrated biosedimentological and paleontological models for siliceous [5,6], carbonate [7], and Fe-oxide-precipitating springs ([8] and Farmer et al., work in progress). In this report we emphasize fossilization processes in

subaerial siliceous thermal springs over a broad range of temperatures. Although such studies are primarily intended to provide a basis for evaluating the microbial contributions to the fossil record of ancient hydrothermal deposits on Earth, they also have implications for the biogenicity of suspect “nanofossils” in martian meteorite ALH 84001 [9].

The microbial contributions to sedimentary fabric in subaerial hydrothermal deposits take on importance where population growth rates keep pace with, or exceed rates of inorganic mineral precipitation, thus allowing for the development of continuous biofilms or mats. The micro-organisms of mineralizing thermal springs are typically entombed while they are still viable. But the precise modes of preservation reflect a balance between rates of organic matter degradation, primary mineral precipitation, and secondary infilling during early diagenesis. At the cellular level, the biological information of siliceous thermal spring deposits results from the encrustation of individual cells and filaments primarily within undermat environments. Subaerial sinters are initially quite porous and permeable, and at temperatures higher than about 20°–30°C organic materials are rapidly degraded prior to the infilling (cementation) of sinter frameworks. This appears to explain why organically preserved microfossils are rare in sub-Recent and ancient siliceous sinters [10] and why observed values for total organic C in ancient siliceous sinters are very low (Des Marais, unpublished data).

In ancient sinter deposits, the diagenetic transformation of primary amorphous silica to secondary quartz usually results in the loss of all cellular-level information. However, taxes within microbial communities often lead to clumping of cells and/or preferred filament orientations that together define higher-order composite mat fabrics (e.g., network, coniform, and palisade). For the photoautotrophic cyanobacterial communities that dominate subaerial systems below 73°C, such composite (community-level) fabrics frequently survive diagenesis, providing important clues for biogenicity in ancient deposits [10]. Similarly, at temperatures >90°C, siliceous spring communities are dominated by filamentous hyperthermophiles that form biofilms covering most near-vent surfaces. Biofilms localize silica nucleation and appear to contribute significantly to the morphogenesis of various types of geyserite deposits [11]. Although certain aspects of the laminated microstructure of geyserites may reflect biogenesis, cellular-level preservation is extensively overprinted and lost during infilling, recrystallization, and the ordering of amorphous silica during early diagenesis [6].

**References:** [1] Walter M. R. and Des Marais D. J. (1993) *Icarus*, 101, 129–143. [2] Farmer J. and Des Marais D. (1994) *LPS XXV*, 367–368. [3] Farmer J. D. (1996) in *Evolution of Hydrothermal Ecosystems on Earth (and Mars?)* (G. Bock and J. Goode, eds.), pp. 273–299, Wiley. [4] Walter M. R. (1996) in *Evolution of Hydrothermal Ecosystems on Earth (and Mars?)* (G. Bock and J. Goode, eds.), pp. 112–127, Wiley. [5] Farmer J. D. et al. (1995) *Geol. Soc. Am. Abstr. with Progr.*, 27(6), 305. [6] Cady S. L. and Farmer J. D. (1996) *Evolution of Hydrothermal Ecosystems on Earth (and Mars?)* (G. Bock and J. Goode, eds.), pp. 150–173, Wiley. [7] Farmer J. D. and Des Marais D. J. (1994) in *Microbial Mats: Structure, Development and Environmental Significance* (L. J. Stal and P. Caumette, eds.), pp. 61–68, NATO ASI Series in Ecological Sciences, Springer-Verlag. [8] Agresti D. G. et al. (1995) *LPS XXVI*, 7–8. [9] McKay D. S. et al. (1996) *Science*, 273, 924–930. [10] Walter M. R. et al. (1996) *Palaios*, 11(6), 497–518. [11] Cady S. et al. (1995) *Geol. Soc. Am., Abstr. with Progr.*, 27(6), 305.

**CATION DIFFUSION IN CARBONATE MINERALS: DETERMINING CLOSURE TEMPERATURES AND THE THERMAL HISTORY FOR THE ALLAN HILLS 84001 METEORITE.** D. K. Fiesler, R. T. Cygan, and H. R. Westrich, Geochemistry Department, Sandia National Laboratories, Albuquerque NM 87185-0750, USA.

The diffusion rates of cations in carbonate minerals can be used to help constrain the thermal conditions expected for the formation and subsequent history of the ALH 84001 martian meteorite. Since homogenization of the carbonate globules readily occurs at elevated temperatures—the extent being a function of grain size and diffusion coefficient for a given temperature—one can examine the measured compositional zoning patterns of the carbonate phases to see how the profiles might be preserved or modified [1–6]. Of course, thermal cooling histories of rocks can be quite complex and will need appropriate diffusion models in order to correctly interpret the compositional zoning patterns [7]. A convenient method based on the concept of closure temperature is provided by Dodson [8]. He derived an approximation for the relationship between cooling rate, grain size, and closure temperature for thermally activated diffusion in geological systems. The diffusion-based cooling model is given by the following nonlinear equation

$$\frac{E_a}{RT_c} = \ln \left( \frac{-ART_c^2 D_0}{a^2 E_a s} \right)$$

where  $E_a$  is the activation energy for diffusion,  $R$  is the gas constant,  $T_c$  is the closure temperature,  $D_0$  is the diffusion coefficient,  $A$  is a geometric factor (equal to 55 for a sphere), and  $s$  is the cooling rate. This equation provides a series of closure temperatures as a function of cooling rate and grain radius. The closure temperature represents the temperature below which a cation zoning pattern would be essentially frozen or preserved, as observed in the carbonate globules found in the martian meteorite. The approximation includes the assumption that the system under consideration cools to a temperature low enough that diffusion is no longer significant over the life of the system.

Unfortunately, few data for the diffusion rates of cations in carbonate minerals are available that can be directly used to determine closure temperatures. However, our experimental approach, which uses thin-film-mineral-diffusion couples [9], provides an accurate means of obtaining relatively low-temperature diffusion data for cations. We have used a high-vacuum evaporator to deposit a thin film (~1000 Å) coating of an isotopically enriched tracer onto a cleaved (104) calcite surface. The calcite samples were then annealed in 1 atm of  $\text{CO}_2$  for 500–1000 hr and then analyzed using a Cameca IMS 4f ion microprobe. The resulting plot of tracer concentration (as  $^{44}\text{Ca}/^{40}\text{Ca}$ ) vs. analysis time is presented in Fig. 1 and clearly shows the diffusion penetration.

The interface between the enriched coating and the mineral surface is identified by a discontinuity in the depth profile. The raw concentration profile is then transformed to concentration vs. depth using a sputtering rate (2.85 Å/s) determined by measuring the depth of a sputtered crater using a profilometer on an uncoated sample. The diffusion coefficient is obtained by fitting the final diffusion profile to an error function solution to Fick's diffusion

equations, dependent on surface concentration  $C_s$ , bulk concentration  $C_b$ , and the diffusion coefficient  $D$  [10]. The variation of concentration as a function of depth  $x$  and experimental time  $t$  is described by

$$C_x = C_s + (C_b - C_s) \operatorname{erf} \left( \frac{x}{4\sqrt{Dt}} \right)$$

Figure 2 provides an example of the Ca diffusion profile from one of our preliminary experiments performed at 650°C for 510 hr. The profile exhibits the expected decrease of the Ca tracer ( $^{44}\text{Ca}$ ) content up to a depth of approximately 0.15  $\mu\text{m}$ . The best fit of the observed profile to the diffusion model given above is also shown in the figure, and provides a Ca self-diffusion coefficient of  $1.1 \times 10^{-21} \text{ m}^2 \text{ s}$ .

Experiments were performed for Ca and Mg diffusion in calcite at temperatures from 500° to 700°C. Values for the activation energy  $E_a$  and preexponential term  $D_0$  for the Arrhenius relation were obtained and then used to calculate the expected closure temperatures for various grain sizes and cooling rates expected for the carbonate globules in the ALH 84001 meteorite.

Using the data for Ca diffusion in calcite [11], cooling rates must be more rapid than 1000°/m.y. for the cation zoning to have been preserved if the martian carbonates formed at more than 650°C. Our preliminary experimental data indicate that Mg diffusion rates in calcite ( $D = 10^{-19} \text{ m}^2/\text{s}$  at 700°C) are more than 2 orders of magnitude faster than those for Ca. The closure temperatures based on the Mg diffusion data are lower and therefore require a more rapid cooling rate than those calculated based on the Ca diffusion data (see Fig. 3). This analysis demonstrates that any model for the high-temperature formation of the carbonate assemblage requires rapid cooling for the preservation of the observed chemical zoning. However, a low-

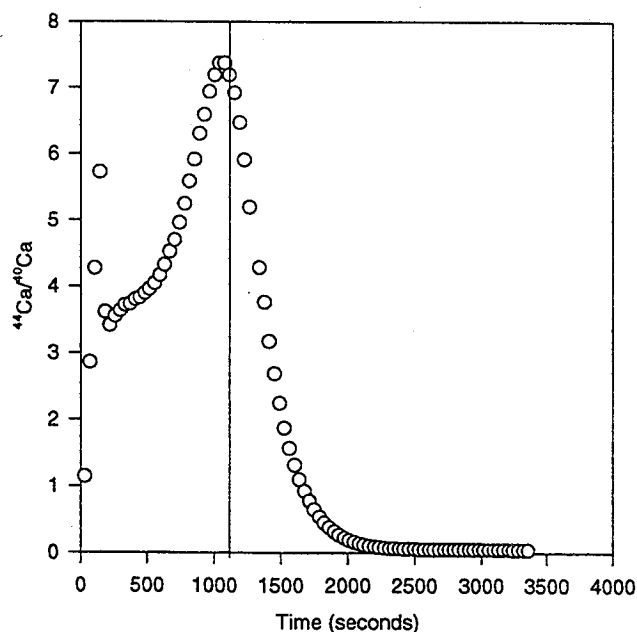


Fig. 1. Raw ion microprobe profile as function of sputtering time for  $^{44}\text{Ca}$  in calcite annealed at 650°C for 510 hr. The vertical line shows the location of the interface between the enriched coating and the calcite interface.

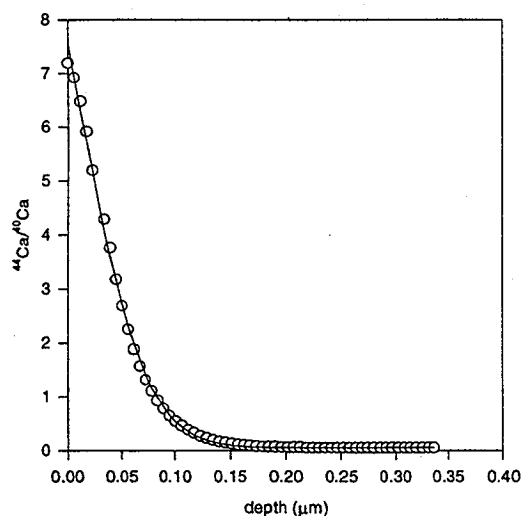


Fig. 2. Diffusion profile for  $^{44}\text{Ca}$  in calcite annealed at  $650^\circ\text{C}$  for 510 hr. The best fit (solid line) of the diffusion model to the observed data is based on the optimization of the  $C_b$ ,  $C_s$ , and  $D$  parameters.

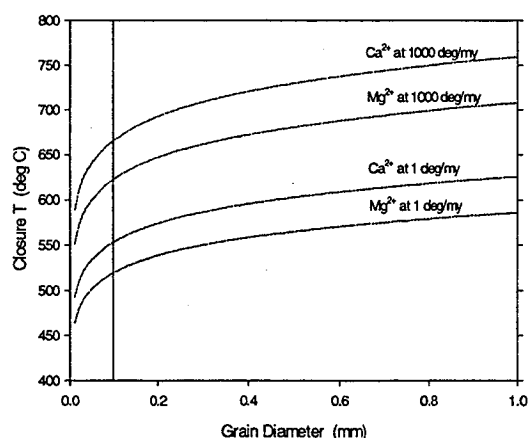


Fig. 3. Closure temperatures as a function of grain diameter and cooling rate calculated for Ca and Mg diffusion in calcite. The vertical line represents the mean diameter of the carbonate globules in the ALH 84001 meteorite.

temperature model for formation is not constrained by the experimental diffusion data.

**Acknowledgments:** We are grateful for the technical discussions with K. Thomas-Keprta and C. Schwandt that led to the application of our experimental diffusion data to the martian meteorite. This research was supported by the U.S. Department of Energy, Office of Basic Energy Sciences, Geosciences Research, under contract DE-AC04-94AL85000 with Sandia National Laboratories.

**References:** [1] Harvey R. and McSween H. Y. (1996) *Nature*, 382, 49–51. [2] Mittlefehldt D. W. (1994) *Meteoritics*, 29, 214–221. [3] Treiman A. H. (1995) *Meteoritics*, 30, 294–302. [4] Thomas-Keprta K. L. et al. (1997) *LPS XXVIII*, 1433–1434. [5] McKay D. S. et al. (1996) *Science*, 273, 924–930. [6] Romanek

C. S. et al. (1994) *Nature*, 372, 655–657. [7] Ganguly J. and Tazzoli V. (1994) *GCA*, 58, 2711–2723. [8] Dodson M. H. (1973) *Contrib. Mineral. Petrol.*, 40, 259–274. [9] Schwandt C. S. et al. (1993) *Pure Appl. Geophys.*, 103, 631–642. [10] Crank J. (1975) *The Mathematics of Diffusion*, Oxford Univ., London. [11] Farver J. R. and Yund R. A. (1996) *Contrib. Mineral. Petrol.*, 123, 77–91.

**ORGANIC MATTER CONTRIBUTED TO THE SURFACE OF MARS BY THE ACCRETION OF INTERPLANETARY DUST, METEORITES, COMETS, AND ASTEROIDS.** G. J. Flynn, Department of Physics, State University of New York-Plattsburgh, Plattsburgh NY 12901, USA.

Organic material has been detected in interplanetary dust particles (IDPs), in meteorites believed to be derived from carbonaceous asteroids, and in the comae of comets. The accretion of IDPs, carbonaceous meteorites, comets, and asteroids deposits this organic matter onto the surfaces of the planets. Depending on the peak temperature reached during the accretion, this organic matter may survive intact or be degraded.

Modeling of the rate of addition of organic matter to the surface of the Earth by the accretion of IDPs has been performed by Anders [1] and by the impact of comets by Chyba et al. [2]. In both cases these studies concluded that significant quantities of organic matter were added to the surface of the Earth, and that this organic matter may have been important in the development of life on the ancient Earth.

In the terrestrial case, only the smallest IDPs are accreted without being heated above the pyrolysis temperature ( $\sim 600^\circ\text{C}$ ) of typical organic matter. However, modeling of the accretion of IDPs onto Mars by Flynn and McKay [3] demonstrated that, because Mars has a significantly lower escape velocity and a larger atmospheric scale height than does the Earth, larger IDPs experience significantly less heating on Mars' atmospheric entry than they would on Earth. The effect is to allow much larger IDPs to accrete onto Mars with their organic matter intact than is possible for accretion onto the Earth [4]. Because the mass-frequency distribution of the IDPs increases steeply over the mass range from  $10^{-9}$  to  $10^{-4}$  g (see Table 1), a small increase in the maximum size of the particles not heated above the pyrolysis temperature results in a large increase in the mass of the IDPs accreted with their organic matter intact.

The atmospheric entry heating experienced by IDPs accreting onto Mars was modeled using the entry heating model developed by Whipple [5] and the Mars entry velocity distribution modeled by Flynn and McKay [3], who transformed the terrestrial velocity distribution of radar meteors to Mars using a technique developed by Zook [described in 6]. The fraction of the IDPs in each mass decade that experience peak temperatures  $<600^\circ\text{C}$  was determined (column 3 of Table 1). About 24% of the IDPs in the  $10^{-5}$ -g mass decade ( $\sim 120$ – $270\ \mu\text{m}$  in size) are accreted onto Mars without being heated above  $600^\circ\text{C}$ . In the terrestrial case, particles in the  $10^{-7}$ -g mass decade experience comparable heating, with larger particles being more severely heated.

This modeling indicates that about  $2.4 \times 10^6$  kg/yr of IDPs are accreted onto Mars without experiencing a thermal pulse  $>600^\circ\text{C}$ . The surface density (mass/unit area) of IDPs accreted onto Mars without being heated above  $600^\circ\text{C}$  is about an order of magnitude greater than for the Earth.

TABLE 1. IDP accretion onto Mars.

Mass Decade (g)	IDP Mass Accreted (kg/yr)	Fraction with $T_{\max} < 600^{\circ}\text{C}$
$10^{-3}$	$2 \times 10^6$	0.01
$10^{-4}$	$3 \times 10^6$	0.07
$10^{-5}$	$3 \times 10^6$	0.24
$10^{-6}$	$1.5 \times 10^6$	0.46
$10^{-7}$	$6 \times 10^5$	0.75
$10^{-8}$	$2 \times 10^5$	0.88
$10^{-9}$	$7 \times 10^4$	0.96

The estimated mass-frequency distribution of objects accreted by the Earth shows two peaks, one near  $10^{-5}$  g (in the IDP region), and a second near  $10^{17}$  g (corresponding to the infrequent impact of kilometer-sized objects). Anders [1] points out that the mass contributed by meteorites is inconsequential compared to the IDPs and the large impactors. Since typical IDPs recovered from the Earth's stratosphere contain ~12 wt% C [7], and much of this C is accreted without thermal alteration, the meteoritic contribution to C on Mars must be small by comparison to the IDP contribution. Anders [1] argues that the bulk of the surviving organic matter is contributed to the Earth by C-rich IDPs, rather than the large objects modeled by Chyba et al. [2] because the severity of the impact of kilometer-sized objects is likely to destroy any organic material they carry. While this seems likely, the flux of large objects, comets, and asteroids impacting Mars is estimated to be about  $2.6\times$  the terrestrial flux for objects of the same size [8] because there are more objects that cross the orbit of Mars than cross the orbit of Earth. Thus, the accretion of organic material by the impact of large objects onto Mars is also likely to exceed the terrestrial accretion rate.

The surface densities of both IDPs and large objects accreted onto Mars exceed those on Earth, and a much greater fraction of the IDPs accreted onto Mars are not heated above the pyrolysis temperature of typical organic matter than in the terrestrial case. If, as suggested by Anders [1] and Chyba et al. [2], the accretion of interplanetary matter is an important source of prebiotic organic matter on the early Earth, then it is likely to have been an even more important source of organic matter on the early surface of Mars.

**References:** [1] Anders E. (1989) *Nature*, 342, 255–257. [2] Chyba et al. (1990) *Science*, 249, 632–635. [3] Flynn G. J. and McKay D. S. (1990) *JGR*, 95, 14497–14509. [4] Flynn G. J. (1996) *Earth Moon Planets*, 72, 469–474. [5] Whipple F. L. (1950) *Proc. Natl. Acad. Sci.*, 36, 687–695. [6] Morgan T. H. et al. (1988) *Icarus*, 75, 156–170. [7] Thomas K. L. et al. (1993) *GCA*, 57, 1551–1566. [8] Shoemaker E. M. (1977) in *Impact and Explosion Cratering*, pp. 617–628, Pergamon.

**HIGHLAND CRATER BASINS AS EVAPORATIVE/SUBLIMATIVE DISCHARGE PUMPS FOR DRIVING EARLY MARTIAN GROUNDWATER TO ATMOSPHERE WATER TRANSFERS.** R. D. Forsythe<sup>1</sup> and C. R. Blackwelder<sup>1</sup>, <sup>1</sup>Department of Geography and Earth Sciences, University of North Carolina–Charlotte, Charlotte NC 28223, USA (rdfsyt@email.uncc.edu).

New fluvial geomorphic evidence is being assembled from the southwestern Memnonia and southern Aeolis regions within the

southern hemisphere's highlands on Mars to help identify and model the processes under which water was transferred within the early martian atmosphere and ground water reservoirs.

Previous work [1–3] has identified the presence of salts on Mars, and thus the likely important role evaporation (as well as sublimation) has played in transferring water back to the martian atmosphere. Also, prior work has shown that surface waters ponded and flowed under dynamic conditions that were largely controlled by groundwater-supported fluvial base levels [4]. Under the implied terrestrial-like relationships between surface channels and ground water systems, one visualizes channels as piercing lines of a water table, and channel grade as a measure of groundwater potentiometric gradient. In arid regions on Earth, water, rather than reaching the ocean, ponds in intrabasin low points where it evaporates back to the Earth's atmosphere. In these basins, such as those of the U.S. Great Basin or Atacama Desert of South America, the discharge of groundwater solely by this means is established by the presence of inflowing channels, the lack of outflow channels, and the presence of evaporites. The continual discharge of groundwater to the atmosphere by this means creates a dynamically supported draw down within the regional water table.

Approximately 20 crater basins have been identified in the low latitudes of Mars' southern hemisphere in the southwestern Memnonia and southern Aeolis regions that have clear inflowing channels, but no outlets. Seven of these examples are shown in Fig. 1. These seven crater basins all lie at elevations between 2000 and 4000 m. Channels feeding these basins tend to be short and have steep gradients. In general these basins have infilling deposits bringing the floors to within, on average, 1.2 km of the surrounding highland regolith. All inflow channels have head reaches within the upper highland surface, and debouch at crater basin floors, found generally lying 0.6–2.3 km lower in elevation. The geometry of these channels is tabulated in Table 1 (basins depths estimated from shadow length measurements). The channels include sinuous sections (arguing against a sapping origin) and are generally oriented at very high, if not perpendicular, angles to crater basin margins. In addition, select basins have more than one inflow channel (e.g., Fig. 1d) that have different orientations, but still perpendicular orientations to the basin margins. The latter cases form compelling evidence that the underlying water table is potentiometrically depressed 0.6–2.3 km beneath its level within the surrounding regolith and that this depression is symmetric to the basins. These gradients imply high rates of groundwater flux into the depression. This flow would quickly (within a few months) relax the potentiometric field if it were not dynamically maintained by continual discharge from within the basin. Impacts during Mars' early history would have penetrated the groundwater table, and thus have created local conditions for accelerated evaporation and sublimation. Thus, inferences drawn from the existence of these inflow channels, lends support to the view that early crater basins operated as evaporative/sublimative discharge pumps. These discharges probably dominated groundwater flow conditions during Mars' early period of Noachian landform development, and provided a major avenue for water transfer from groundwater to the atmosphere.

The steep gradients of the short inflow stream channels (minimum 0.02, maximum 0.15, average 0.07) for these early crater basins is in marked contrast to the gradients of the younger ~1000-km-long "outflow" channels. Ma'Adim, Al-Qahiri, and Mangala Valles, all found in this region, have gradients 4–6 times lower (maximum 0.004, minimum 0.003, average 0.0035) than the crater



Fig. 1. Crater basins of the southwestern Memnonia and southern Aeolis region of Mars with fluvial inflow channels and no outlets. The channels are used here to model groundwater flow conditions developed as a response to evaporative and sublimative losses within these basins. Locations are given in Table 1.

basin inflow channels, and are found with base levels approximately 2000 km lower than the surrounding highlands. The major outflow channels also generally fed waters consistently northward, in conformance with global-scale topographic relief. By the time the major outflow channels had developed, groundwaters had also been lowered by at least 1 km on a regional scale within the southwestern Memnonia and southeast Aeolis region. The lowered water table conditions would have eliminated discharges in most of the crater basins by this time. Concurrently, the potentiometric gradient relaxed to a more regional or hemispheric trend, sloping gently to the north. Overall, one can conclude that groundwater conditions within the highlands evolved from an earlier regime wherein a higher, near-surface, water table had its potentiometric surface controlled largely by the evaporative discharges within crater basins to one dominated by hemispheric-scale groundwater flow at depths of 2 km or more toward the northern plains. The discharge flux within the crater basins may have been the driving mechanism responsible for the lowering of the water table during Mars' early evolution.

**References:** [1] Clark B. C. and Van Hart D. C. (1981) *Icarus*, 45, 370–378. [2] Malin M. C. (1974) *JGR*, 79, 3888–3894. [3] Zent

A. P. and Fanale F. P. (1986) *Proc. LPSC 16th*, in *JGR*, 91, D439–D445. [4] Forsythe R. D. and Zimbleman J. R. (1995) *JGR*, 100, 5553–5563.

**BIOGENIC ACTIVITY IN MARTIAN METEORITE ALLAN HILLS 84001: STATUS OF THE STUDIES.** E. K. Gibson Jr.<sup>1</sup>, D. S. McKay<sup>2</sup>, K. Thomas-Keptra<sup>3</sup>, C. S. Romanek<sup>4</sup>, S. J. Clemett<sup>5</sup>, and R. N. Zare<sup>5</sup>, <sup>1</sup>Mail Code SN4, Planetary Sciences Branch, NASA Johnson Space Center, Houston TX 77058, USA, <sup>2</sup>Earth Science and Solar System Exploration Division, Mail Code SN, NASA Johnson Space Center, Houston TX 77058, USA, <sup>3</sup>Lockheed Martin, NASA Johnson Space Center, Houston TX 77058, USA, <sup>4</sup>Savannah River Ecology Laboratory, Drawer E, University of Georgia, Aiken SC 29802, USA, <sup>5</sup>Department of Chemistry, Stanford University, Palo Alto CA 94305, USA.

Several lines of evidence were given by McKay et al. [1] to suggest the presence of biogenic activity within the martian meteorite ALH 84001: (1) The presence of secondary carbonate globules were found within fractures and cracks of the 4.5-g.y.-old igneous rock; (2) the formation age of the carbonates is believed to be younger than the crystallization age of the host igneous rock; (3) SEM and TEM images of the carbonate globules and associated mineralogical phases resemble terrestrial biogenic structures and fossilized nanobacteria; (4) the presence of magnetite and iron sulfide phases may have resulted from oxidation and reduction reactions known to be important in terrestrial microbial systems; and (5) the presence of polycyclic aromatic hydrocarbons (PAHs) and associated carbonate globules indicating potential indigenous organic molecules. As noted in [1], none of these observations is in itself conclusive proof for the existence of past life on Mars. Although there are alternative explanations for each of these phenomena taken individually, when they are considered collectively, particularly in view of their close spatial association, we concluded that they may represent the first direct evidence for primitive life on early Mars.

Since the initial report, additional supporting evidence [2–8] and opposing views [9–14], including alternative inorganic explanations, have been offered. Major controversies continue over the age of the carbonates, the temperature at which they formed, and the source of the PAHs.

Knott et al. [15] suggested the carbonates were formed around 3.6 g.y., whereas Wadhwa and Lugmair [16] noted the formation may be as late as 1.3 g.y. Turner et al. [17] later argued that the 3.6-

TABLE 1. Spatial data for inflow channels to internally drained crater basins.

Project ID (Fig. 1 ID)	Viking Frame	Latitude (approx.)	Longitude (approx.)	Crater Depth (km)	Channel Length (km)	Channel Gradient
B-3-1 (G)	629A49	218.5	-19.5	2.3	16	0.15
B-3-2 (C)	631A13	216.5	-18.5	0.8	30	0.03
B-4-1a (D)	631A11	217.0	-14.5	1.1	16	0.07
B-4-1b (D)	631A11	217.0	-14.5	1.1	15	0.07
C-2-1 (H)	631A15	210.0	-25.0	0.6	28	0.02
F-2-1 (F)	595A60	196.5	-21.5	1.0	24	0.04
H-3-1 (B)	596A53	188.0	-20.5	1.6	18	0.09
H-4-1 (A)	596A55	188.5	-18.0	1.1	14	0.07

g.y. date is not well defined and additional studies are needed to define the carbonate formation date. In particular, [17] argued that their Ar-Ar age is really the age of the maskelynite, and would only be an upper limit on the age of the carbonate providing that the carbonate formed at low temperatures.

Formation temperatures for the carbonates were initially proposed to be between 0° and 80°C based upon O isotopic compositions [18]. It was suggested [9] that the formation temperatures were greater than 650°C and formed during impact processes and remobilization. Valley et al. [19] have made *in situ* O isotope measurements and show that the combination of isotopic and chemical data indicate low temperatures in the range estimated by [18]. Bradley et al. [11] reported the presence of ribbonlike forms with screw dislocations and twinned magnetite within carbonate phases from ALH 84001. Based upon the whisker morphologies and the screw dislocations, they suggested the magnetite formed at greater than 500°C from fumarolelike processes. However, other workers [20] have reported similar whiskerlike magnetites produced by bacteria. Dobeneck et al. [21] have reported twinned magnetite can be produced by bacteria at room temperatures. As yet, no one has reported screw dislocations in biogenic magnetite, and defect-free magnetite seems to be the norm for biogenic magnetite. However, no one has yet looked at the whisker-shaped biogenic magnetite for screw dislocations. Thomas et al. [22] present evidence for a chain of magnetite crystals within the ALH 84001 carbonate that appears to be similar to magnetotactic-like magnetite chains produced by terrestrial bacteria. It is clear that magnetites can be produced by a variety of processes and caution must be applied when interpreting these components. Undoubtedly, the spatial relationships among mineral grains and the microenvironments in which these precipitates formed provide a very important clue to their origins. Studies of the minor- and trace-volatile elements within the carbonates by Flynn and coworkers [23] fail to find volatile elements normally associated with terrestrial fumaroles or volcanic events.

Microstructures and "nanobacteria"-like features within ALH 84001 are spherical, elongated, and segmented in shape. The small sizes were criticized [24] as being too small to be bacteria. However, it was noted that nanobacteria of sizes down to 100 nm and possibly as small as 50 nm are common within the terrestrial environment [5,25,26]. Dwarf bacteria, bacteria desiccated after death and during mineralization, bacteria spores, and even viruses have been proposed to explain some of these nanosize forms. Studies of organisms recovered at 0.3 to 1 km depth within the Columbia River basalts [27,28], have shown features that have the same sizes and morphologies as those observed within ALH 84001 and that are probably formed by micro-organism activity. Some of these features are threadlike Fe-rich forms and fragments probably produced by larger bacteria. Some of the ALH 84001 features similarly may be fossilized fragments and forms that are the products of micro-organisms rather than the micro-organisms themselves.

Recognition of biofilms produced by bacteria within terrestrial environments has recently shown that three-dimensional organic networks can be produced by microbial communities [26,28]. Presence of biofilms within subsurface Columbia River basalts, which are associated with the subsurface organisms, along with biofilms from travertine deposits [26,28], show the microbial production and importance of such processes. McKay et al. [29] and Steele and colleagues [30] have documented the occurrence of possible biofilms within ALH84001. Other features that may be biogenic include possible mineralized organisms in the 1–2- $\mu$ m size range.

Ion microprobe studies by Valley et al. [19] noted the presence of C enriched in  $^{12}\text{C}$  composition occurring within selected regions of the carbonate globules. Flynn et al. [23] noted the irregular distribution of a C phase (either graphite or organic C) within the carbonate globules. The C isotopic values of –65‰ for a component within ALH 84001 is suggestive of a microbial bacteria signature [2]. The measured range of >100‰ in C isotopic compositions (+40‰ to –65‰) within the carbonate globules [2,18,31] shows the wide variety of C phases present within ALH 84001.

Indigenous organic components within ALH 84001 were shown to be present as polycyclic aromatic hydrocarbons (PAHs). The PAHs are typically associated with the carbonate phases [8]. The signature of the PAHs spectra within ALH 84001 is unique and not identical to those of carbonaceous chondrites, ordinary chondritic meteorites, interplanetary dust particles, and typical terrestrial soils or contaminants. Becker et al. [10] suggested that cycling of Antarctic melt water containing trace concentrations of organic components through the meteorite would enrich PAHs within the carbonate phases. They proposed that the PAHs observed within ALH 84001 were terrestrial components and not from Mars. If the quantities of Antarctic melt water required by [10] cycled through ALH 84001, the isotopic systematics of the sample would probably be altered and alteration products formed. Alteration products are minimal in this meteorite. Additionally, Clemett et al. [32] have measured PAHs within micrometeorites and IDPs collected from both north and south polar ices of widely different ages. They failed to find any enrichment of PAHs in the samples and documented 2 order-of-magnitude variation in PAH concentration among particles collected from the same site on the same day. Because of the porosity of these particles, one might expect the particles to absorb PAHs from polar ices.

In the five months since the publication of our hypothesis about possible evidence for past biogenic activity within ALH 84001 [1], we feel that our arguments have been strengthened with the new data. Researchers from other fields of science have acquired supporting data for this hypothesis. Additional experiments are needed to further clarify the hypothesis on the origin of the carbonate globules. Many of these studies are underway and will be reported in the future.

**References:** [1] McKay D. S. et al. (1996) *Science*, 273, 924–930. [2] Wright I. P. et al. (1997) *LPS XXVIII*. [3] Arrhenius G. and Mojzsis S. (1996) *Current Biology*, 6, 1213–1216. [4] Jull A. J. T. et al. (1997) *JGR Planets*, 102, 1663–1669. [5] Folk R. L. (1993) *J. Sediment. Petrol.*, 63, 990, and (1996) *Science*, 274, 1288. [6] McKay D. S. et al. (1996) *Science*, 274, 2123–2125. [7] Gibson E. K. Jr. et al. (1996) *Science*, 274, 2125. [8] Clemett S. J. and Zare R. N. (1996) *Science*, 274, 2122–2123. [9] Harvey R. P. and McSweeney H. Y. Jr. (1996) *Nature*, 382, 49–51. [10] Becker L. et al. (1997) *GCA*, 61, 475–481. [11] Bradley J. P. et al. (1996) *GCA*, 60, 5149–5155. [12] Galimov E. M. (1997) *Science*, in press. [13] Anders E. (1996) *Science*, 274, 2119–2121. [14] Shearer C. K. and Papike J. J. (1996) *Science*, 274, 2121. [15] Knott S. K. et al. (1995) *LPS XXVI*, 765–766. [16] Wadhwa M. and Lugmair G. W. (1996) *Meteoritics*, 31, A145. [17] Turner G. et al. (1997) *GCA*, in press. [18] Romanek C. S. et al. (1994) *Nature*, 372, 655–656. [19] Valley J. W. et al. (1997) *LPS XXVIII*, 1475–1476, and (1997) *Science*, in press. [20] Vali H. and Kirschvink J. L. (1990) in *Iron Biominerals* (R. B. Frankel and R. P. Blakemore, eds.), pp. 97–115, Plenum, New York. [21] von Dobeneck T. et al. (1987) *Geowissenschaften Unserer Zeit*, 5, 27–36. [22] Thomas-Keprta K. (1997) *LPS XXVIII*.



[23] Flynn G. J. et al. (1997) *LPS XXVIII*. [24] Schopf J. W. (1996) NASA Press Conference, August 7, 1996. [25] Chafetz H. S. and Buczynski C. (1992) *Palaios*, 7, 277–293. [26] Defarge C. et al. (1996) *J. Sediment. Res.*, 66, 935–947. [27] Stevens T. O. and McKinley J. P. (1995) *Science*, 270, 450–456. [28] Allen C. C. et al. (1997) *LPS XXVIII*. [29] McKay D. S. et al. (1997) *LPS XXVIII*. [30] Steele A. et al. (1997) *LPS XXVIII*. [31] Grady M. M. et al. (1994) *Meteoritics*, 29, 469. [32] Clemett S. et al. (1997) *GCA*, in press.

**MAJOR- AND TRACE-ELEMENT DISTRIBUTIONS IN ALLAN HILLS 84001 CARBONATE: INDICATION OF A HIGH FORMATION TEMPERATURE.** J. D. Gilmour<sup>1</sup>, R. A. Wogelius<sup>1</sup>, G. W. Grime<sup>2</sup>, and G. Turner<sup>1</sup>, <sup>1</sup>Department of Earth Sciences, University of Manchester, Manchester, M13 9PL, UK (mbejdg@man.ac.uk), <sup>2</sup>Department of Nuclear Physics, University of Oxford, Keble Rd, Oxford, UK.

As part of an ongoing study of the ancient martian meteorite ALH 84001 we have performed preliminary proton microprobe (PIXE: Proton-Induced X-ray Emission) analyses of a carbonate region and an adjoining maskelynite grain. Major-element zoning is similar to that previously reported, while some unusual trace-element abundances in the carbonate seem most easily explicable if the carbonate formed at high temperature from a CO<sub>2</sub>-rich fluid. In this case, the period of elevated temperature during carbonate formation would have reset the Ar-Ar age of the maskelynite, so the two phases would have similar ages. Our preferred age for the carbonate of  $3750 \pm 150$  Ma is based on the Ar released by laser ing a submicrogram carbonate grain [1] and is indistinguishable from the Ar-Ar age of the maskelynite ( $3920 \pm 80$  Ma—weighted mean of stepped heating data [2]).

The proton microprobe [3] employs a focused beam of protons to stimulate X-ray emission in a polished section; analyses are similar to those from an electron probe, except that bremsstrahlung background is greatly reduced allowing a lower detection limit for many elements. The spot size of the proton beam is typically less than 1 mm; however, the beam penetrates 20 mm or more below the sample surface so care must be taken to ensure data are not influenced by subsurface mineral grains. This is achieved with reference to Rutherford back scattering (RBS) spectra acquired simultaneously with point analyses.

Three types of PIXE analyses have been performed: elemental mapping, line scans, and point analyses. All data were acquired without an X-ray filter to allow simultaneous analysis of light and heavy elements. A back-scattered electron image of the region upon which we have focused our attention is shown in Fig. 1. It consists of an area of carbonate that appears to have grown within a crack in a grain of maskelynite. Both carbonate and maskelynite are adjacent to a chromite grain. Major-element maps showing the location of the line scan relative to maskelynite and carbonate are shown in Fig. 2.

The major-element variations along the scan are shown in Fig. 3. The scan covers the rim of a carbonate region and the interface with maskelynite (the extent of the maskelynite can be seen from the silicon scan). These data do not represent a complete traverse from carbonate core to rim. However, in the region of overlap close to the carbonate rim they are comparable to previously published electron

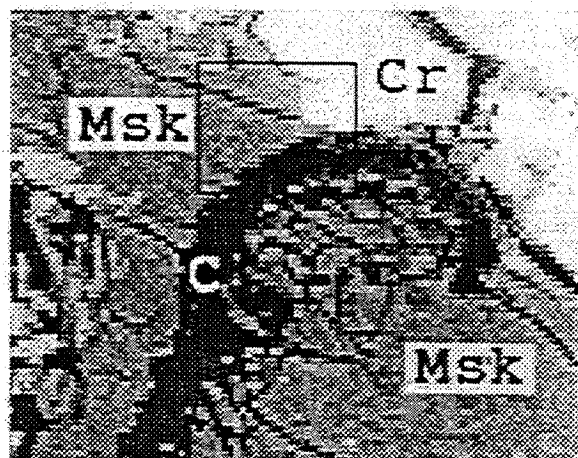


Fig. 1. A BSE electron micrograph of a section of sample ALH 84001,110. The box highlights the approximate region of Fig. 2. Key: Msk = maskelynite, Cr = chromite, C = carbonate.

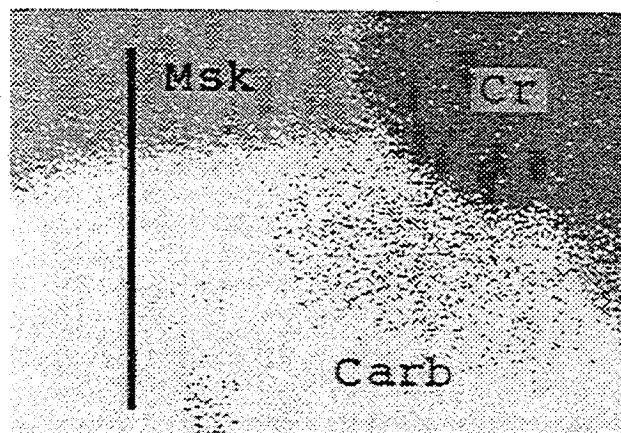
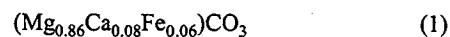


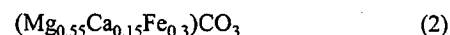
Fig. 2. Overlain major-element maps (Si = light gray, Cr = black) showing the extent of maskelynite (Msk), chromite (Cr), and carbonate (Carb). The line shows location of the line scan from Fig. 3. The width of the image is 50 mm.

probe data [4], albeit at higher resolution. The magnesite-rich region close to the carbonate rim is clearly bounded by zones with higher calcite and siderite components.

Calibration of scans proceeds via Rutherford back-scattering point analyses located along the scan line. Two analyses of the most Mg-rich region (close to the rim) yield



while the Fe-rich end of the traverse has composition



PIXE point analyses of the carbonate clearly reveal the presence of two unusual trace elements: K and Cr (Fig. 4a; the presence of Cr in these carbonates has been reported previously [7]). Estimated concentrations of both Cr and K are 500 ppm. The possibility of

contamination by subsurface maskelynite or chromite grains or both is unlikely given the stoichiometries derived from the RBS spectra (Fig. 4b) and by the uniform distribution of Cr and K counts in the PIXE map of the analyzed region of the carbonate. All point analyses show peaks for both these elements, indicating that both K and Cr may be widespread in the carbonate. Furthermore, simulations of our RBS spectra incorporating a thin layer of maskelynite (<0.5mm) are not in good agreement with our data, suggesting that contamination from this source is not the cause. However, further work is underway to verify and further quantify our K and trace-element abundances. Figure 4a also shows a significant rhodochrosite component in the carbonate.

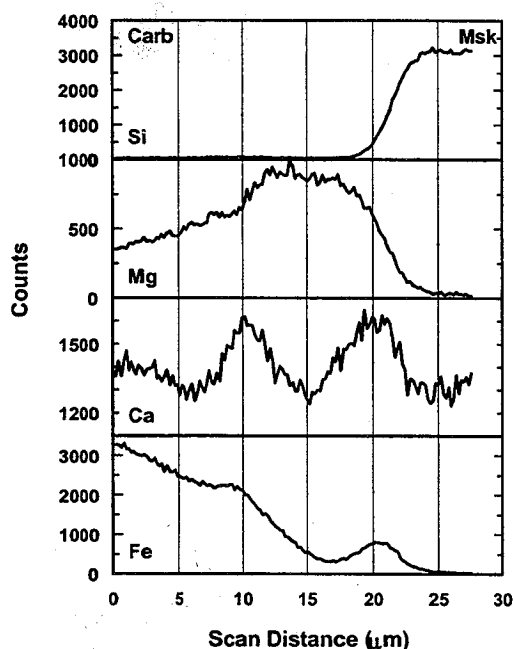


Fig. 3. Major-element variations along a traverse across a carbonate rim.

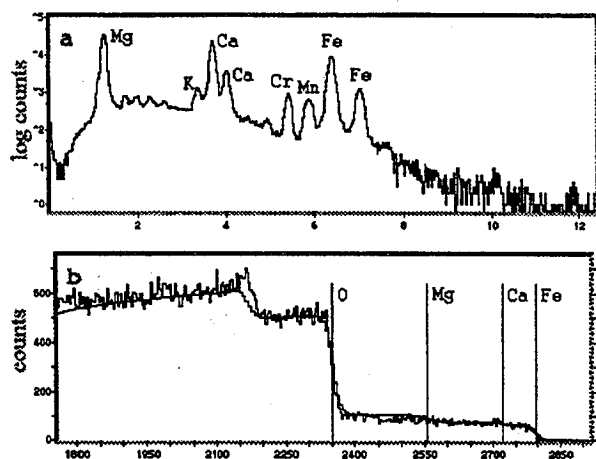


Fig. 4. (a) A PIXE spectrum and (b) Rutherford backscattering spectrum for a carbonate analysis.

The presence of K and Cr in the carbonate would be hard to account for were the carbonate precipitated from a low-temperature aqueous fluid: K and Cr concentrations in terrestrial carbonates are usually below the PIXE detection limit (<110 ppm and <40 ppm respectively [5]) and Na is present at concentrations between 100 and 200 ppm in marine calcite [6]. In addition,  $\text{Cl}/^{36}\text{Ar}$  in ALH 84001 is unrealistically low for a martian hydrothermal fluid [1]. However, both the previously reported presence of Na in the carbonate ( $0.33 \pm 0.07$  wt% oxide [7]) and our K content are easier to understand if the carbonates were formed rapidly from a (possibly impact-derived)  $\text{CO}_2$ -rich melt (as suggested in [8] and [9]). In short, our preliminary trace-element results are more consistent with the origin of the carbonates being at high temperature than at low temperature.

**References:** [1] Gilmour et al. (1997) *LPS XXVIII*. [2] Turner et al. (1997) *GCA*, in press. [3] Grime et al. (1991) *Nucl. Instrum. Meth. Phys. Res., B54*, 52–63. [4] McKay and Lofgren (1997) *LPS XXVIII*. [5] Wogelius, unpublished data. [6] Veizer (1983) *Rev. Mineral.*, 265–300. [7] Mittlefehldt (1994) *Meteoritics*, 29, 214–221. [8] Harvey and McSween (1996) *Nature*, 382, 49–51. [9] Scott et al. (1997) *LPS XXVIII*.

#### GEOCHEMICAL EVOLUTION OF THE CRUST OF MARS.

J. L. Gooding, Mail Code SN2, Planetary Missions and Materials Branch, NASA Johnson Space Center, Houston TX 77058-3696 USA (jgooding@ems.jsc.nasa.gov).

**Introduction:** *Crust* is defined here as the solid outer portion of Mars that includes crystallized magmas, produced by igneous differentiation of the planet, as well as other volcanic deposits and any clastic or chemical sedimentary rocks formed by weathering and diagenesis. Implicit in this definition is the rock rubble known as the *regolith*, including un lithified evaporites.

In the context of the search for life, the evolution of the Mars crust is important for the thermal and chemical environmental controls that it imposed upon the approach of biogenic chemical elements toward molecular self-replication. Prematurely arrested crustal evolution would be bad news for the emergence and evolution

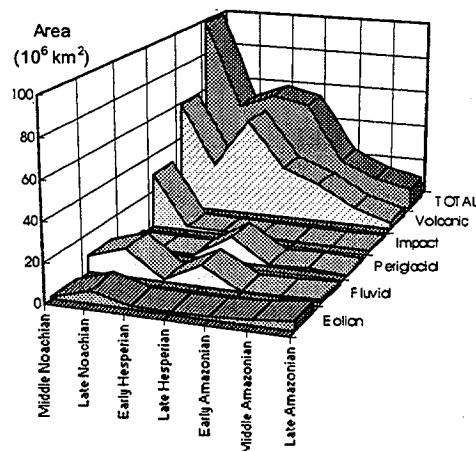


Fig. 1. Summary of processes that affected evolution of the martian crust through geologic time, based on photogeologic interpretations [1].



of life. On the other hand, extensive crustal evolution probably would foster the mature evolution of biogenic compounds.

**The Big Picture:** From photogeologic evidence, resurfacing of Mars—including all endogenous and exogenous processes recognized thus far—occurred most rapidly during the first ~1 g.y. of planetary history (Fig. 1). The abundance of asteroid impacts and the extent of volcanism during Noachian time indicates early crustal evolution characterized by hot, high-energy environments. Thereafter, the rates of all endogenous processes apparently declined until a resurgence during Hesperian time. It was not until the later rekindling that water- and ice-related sedimentation appear correlated in the record.

**Igneous Evolution:** Thermal models suggest that Mars experienced substantial internal melting and differentiation shortly after accretion [2]. It is inferred from compositions of martian meteorites that internal heating of Mars was enabled by abundances of natural radionuclides (K, Th, and U) that are broadly similar to those in the mantle of Earth. Allowing for uncertainties in the rate of convection in the early martian mantle, the resultant igneous crust of Mars is predicted from thermal models to be about 50–150 km thick.

The radioisotope systematics of martian meteorites, all of which are mafic igneous rocks, indicate that the martian igneous crust is rather highly evolved in the geochemical sense. Based on the Nd-Sm and Rb-Sr systems, the martian meteorites represent rocks that are more highly evolved than basalts on the Moon. Based on our understanding of Earth, measurable radioisotope indicators such as the parameters  $\epsilon(\text{Nd})$  and  $(^{87}\text{Sr}/^{86}\text{Sr})_0$  numerically increase as differentiation and igneous crustal evolution proceed. Therefore, taken at face value, the evidence from available samples indicates comparable degrees of igneous evolution on Mars and Earth (Fig. 2).

In the absence of rock cycling through plate tectonics, which has dominated the last 0.2–0.6 g.y. of Earth history but appears to be absent from Mars, the mechanism for accomplishing radioisotope maturation of martian lavas remains unidentified. Nonetheless, the isotopic records demonstrate that igneous heat sources extensively drove the chemical refinement of the crust to Earth-like degrees of maturity. In fact, the shergottite meteorites yield radiometric ages, which can be interpreted as lava-flow ages, on the order of <0.2 g.y., indicating a continuing martian internal heat engine through Late Amazonian time.

**Sedimentary Evolution:** None of the martian meteorites recognized to date are sedimentary rocks. Therefore, we lack direct evidence, in the form of samples, to enlighten us with regard to the sedimentary geology of Mars.

From photogeologic evidence, water-related sedimentation peaked twice during martian history—neither time in clear correlation with volcanism (Fig. 1). Therefore, it is not obvious whether the episodes of fluvial dominance involved hot or cold water. Furthermore, photogeologic evidence for sedimentary basins, which might have contained standing bodies of water for prolonged periods of time, is limited.

Hypotheses for the transmigration of an early dense atmosphere into the crust, possibly mediated by surface water, are intuitively appealing but not yet supportable with observational evidence. The first-order problem is to account for a putative inventory of hundreds to thousands of millibars of  $\text{CO}_2$  that presumably was outgassed during igneous differentiation (Fig. 3 [5]). The same volcanic outgassing is predicted to have released water equivalent to a globally condensed layer of tens of meters [6].

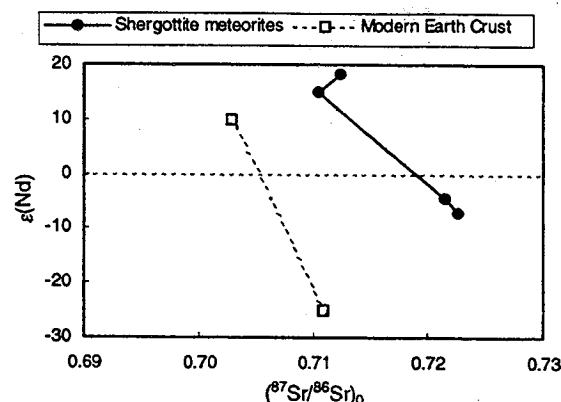


Fig. 2. Sm-Nd and Rb-Sr data that indicate comparable degrees of radioisotopic evolution for the crusts of Mars [3] and Earth [4].

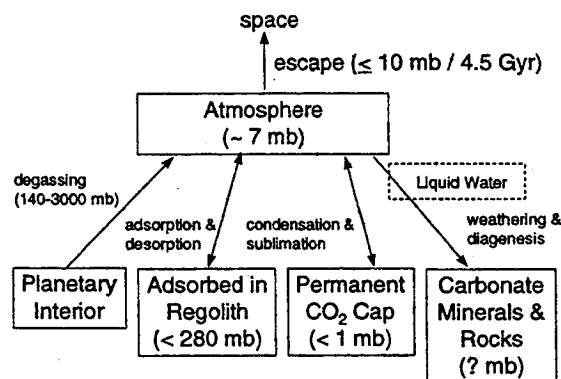


Fig. 3. Box model for the transmigration of  $\text{CO}_2$  into the Mars crust, as modified after [5].

Because only a tiny fraction of the  $\text{CO}_2$  inventory can be attributed to icy condensate, model mechanisms for sequestering the  $\text{CO}_2$  have included adsorption on a thick, fine-grained regolith or chemical reactions to form carbonate minerals. Adsorbed  $\text{CO}_2$  is effectively invisible by remote sensing, leaving the remote search for carbonate minerals as the main method for testing the  $\text{CO}_2$  transmigration hypotheses. Among the various spacecraft- or ground-based, remote sensing experiments that have been conducted, all but one have failed to find definitive evidence for carbonate minerals [7]. The single positive identification is interpreted as 1–3 vol% of unidentified carbonate mineral(s) in martian atmospheric dust [8]. The Viking landers were ill equipped to identify minerals and, therefore, shed no light on the possible occurrence of carbonates in Mars soils [9].

Even though they are igneous rocks, the martian meteorites contain trace amounts of carbonate minerals [10] that prove the viability, if not the actual capacity, of chemical reactions to fix  $\text{CO}_2$  into the crust. At least some of the carbonates found in the martian meteorites can be understood as products of groundwater chemistry. What remains to be determined is whether there exist massive, bedded carbonates that would have required for their formation substantial and long-lived bodies of surface water.

**Conclusions:** The igneous portion of the Mars crust appears to be geochemically highly evolved. Unfortunately, the maturity of the

sedimentary evolution of the crust remains largely unknown. Indications from the igneous record suggest that geochemical evolution included biologically favorable energy sources during at least the first ~1 g.y. of history. But given the current lack of information, almost nothing can be said about whether sustained bodies of liquid water occurred at the surface or left behind rock records of chemical sedimentation.

**References:** [1] Tanaka K. et al. (1988) *Proc. LPSC 18th*, p. 665. [2] Schubert G. et al. (1992) in *Mars* (H. H. Kieffer et al., eds.), p. 147, Univ. of Arizona, Tucson. [3] Jones J. H. (1989) *Proc. LPSC 19th*, p. 465. [4] McCulloch M. T. and Bennett V. C. (1994) *GCA*, 58, 4717. [5] Kahn R. (1985) *Icarus*, 62, 175. [6] Greeley R. (1987) *Science*, 236, 1653. [7] Soderblom L. A. (1992) in *Mars* (H. H. Kieffer et al., eds.), p. 557, Univ. of Arizona, Tucson. [8] Pollack J. B. et al. (1990) *JGR*, 95, 14595. [9] Arvidson R. E. et al. (1989) *Rev. Geophys.*, 27, 39. [10] Gooding J. L. (1992) *Icarus*, 99, 28.

## GEOLOGICAL EVOLUTION OF THE EARLY EARTH.

P. F. Hoffman, Department of Earth and Planetary Sciences, Harvard University, Cambridge MA 02138, USA.

For the purpose of studying early planetary crust, the Earth was not the best choice of campsites. Its crust is ravaged from below by mantle convection and from above by the hydrologic cycle. These forces were, if anything, more destructive in the past than at present. Therefore, the milestones observed in the geological record, listed below, should not be construed as first happenings but rather as oldest preserved examples.

**Narryer, Western Australia (4.3 Ga):** Detrital submillimeter grains of Zr ( $\text{ZrSiO}_4$ ) having  $^{207}\text{Pb}/^{206}\text{Pb}$  ages of 4.3–4.1 Ga occur in sandstones deposited at 3.0 Ga. Although their source is unknown, these grains are the oldest tangible evidence of early terrestrial crust.

**Acasta, Northwest Canada (4.0 Ga):** Granitic (potassium feldspar-plagioclase-quartz) and tonalitic (plagioclase-quartz) gneisses having U-Pb Zr ages of 4.0 Ga, with associated mafic and ultramafic rocks, occur as enclaves up to 40 km<sup>2</sup> in areal extent in a 3.6-Ga granitic terrain. As the oldest known crustal rocks, they are notable for having a compositional diversity, interpreted to reflect intracrustal recycling, essentially indistinguishable from much younger continental crust. Based on Nd and Pb isotopic data, the felsic components had variable crustal prehistories of up to about 200 m.y. and the mafic components were derived from mantle sources variably depleted by melt removal.

**Isua, West Greenland (3.9 Ga):** A 35-km-long belt of metasomatically altered mafic volcanic rocks and banded Fe formation, perhaps tectonically interleaved, is included within and intruded by extensive 3.9–3.6-Ga tonalitic gneisses. The banded Fe formation is taken as evidence for liquid water on the Earth's surface and contemporaneous photosynthesis is inferred from C isotopic compositions. Unlike the Acasta gneisses, the ancient gneiss terrain in West Greenland represents juvenile crust lacking significant crustal prehistory.

**Coonterunah, Western Australia (3.5 Ga):** In the central Pilbara shield, the 3.46-Ga Warrawoona basalt-chert sequence is

underlain unconformably by basaltic-dacitic volcanics (3.52 Ga), quartzose sandstones and intrusive granites (3.47 Ga). The unconformity represents a subaerial erosion surface, the oldest known example of demonstrably emergent continental crust.

**Barberton, South Africa (3.4 Ga):** Oceanic crust, formed ca. 3.48 Ga and hydrothermally altered, similar to that occurring at modern mid-ocean ridges, was thrust over an ensimatic island arc at about 3.44 Ga, implying that subduction-powered plate convergence was then in operation. At 3.16 Ga, the assembled intra-oceanic accretionary complex was thrust onto the ancestral Kaapvaal continental margin, providing further evidence of the gravitationally driven subduction process. By 3.1 Ga, the Kaapvaal craton represented a tectonically coherent continent at least  $1.2 \times 10^6$  km<sup>2</sup> in area. Mantle xenoliths from beneath the Kaapvaal craton include diamondiferous eclogites interpreted as partially subducted relics of Archean oceanic crust.

**Witswatersrand, South Africa (3.1–2.7 Ga):** A cratonic basin, at least  $4.4 \times 10^5$  km<sup>2</sup> in area, formed on the Kaapvaal craton between 3.07 and 2.72 Ga. Possible glacial deposits occur at four stratigraphic horizons, the oldest between 2.97 and 2.91 Ga. If truly glaciogenic, they place constraints on global surface temperatures. The next oldest glacial sediments are the three Huronian (2.45–2.22 Ga) glaciations of southern Canada and their possible correlates in Wyoming, Finland, and Western Australia.

**Superior, Central Canada (2.7 Ga):** A composite continent at least  $2.8 \times 10^6$  km<sup>2</sup> in area (presumed extensions having been lost through subsequent continental break-up) was constructed at 2.7 Ga of island arcs, some built on oceanic plateaus, sediment accretionary complexes, and older continental blocks. The presence at this time of narrow transcurrent shear zones up to 1000 km long has been cited as evidence for the existence of torsionally rigid tectonic plates.

**Hamersley, Western Australia–Transvaal, South Africa (2.7–2.4 Ga):** Long-lived, broadly conformable sequences of banded Fe formation, carbonates, and shales slowly accumulated between 2.68 and 2.43 Ga on the Pilbara and Kaapvaal cratons, which may have been joined together at that time. The cratons perhaps resembled modern oceanic plateaus, underlain by more-or-less stretched continental crust.

**Vredefort, South Africa (2.025 Ga):** Geological evidence for impacts is notably lacking in the Archean record, but the Vredefort dome is surely related to a circular impact structure, 200–300 km in diameter, formed at  $2.023 \pm 4$  Ma.

**MICROBIAL FOSSILS FROM TERRESTRIAL SUBSURFACE HYDROTHERMAL ENVIRONMENTS: EXAMPLES AND IMPLICATIONS FOR MARS.** B. A. Hofmann<sup>1</sup> and J. D. Farmer<sup>2</sup>, <sup>1</sup>Natural History Museum Bern, Bernastrasse 15, CH-3005 Bern, Switzerland (hofmann@nmbe.unibe.ch), <sup>2</sup>Mail Stop 239-4, NASA Ames Research Center, Moffet Field CA 94035-1000, USA (jfarmer@mail.arc.nasa.gov).

The recognition of biological signatures in ancient epithermal deposits has special relevance for studies of early biosphere evolution and in exploring for past life on Mars [1–3]. Recently, proposals for the existence of an extensive subsurface biosphere on Earth, dominated by chemoautotrophic microbial life, has gained prominence [4,5]. However, reports of fossilized microbial remains or

biosedimentary structures (e.g., stromatolites) from the deposits of ancient subsurface systems are rare. Microbial preservation is favored where high population densities coexist with rapid mineral precipitation [2,6]. Near-surface epithermal systems with strong gradients in temperature and redox are good candidates for the abundant growth and fossilization of micro-organisms, and are also favorable environments for the precipitation of ore minerals. Therefore, we might expect microbial remains to be particularly well preserved in various kinds of hydrothermal and diagenetic mineral precipitates that formed below the upper temperature limit for life ( $\sim 120^{\circ}\text{C}$ ).

Under rapid precipitation, fossilization is known to occur by the coating of external organic surfaces by various kinds of metalliferous precipitates. The glycoproteins of bacterial cell walls are known to bind metal ions [7,8]. This type of passive mediation has been documented in modern hydrothermal systems that exhibit very high precipitation rates, including the vent areas of subaerial springs [9] and black smokers of the deep sea [10]. However, elements such as Fe, Mn, Ni, and V are also known to be important components of metalloenzymes in many heterotrophic micro-organisms, being required cofactors for cell growth [11]. In these groups, the precipitation of Fe oxides and Mn oxides is directly mediated by physiological processes, with fine-grained metal oxides forming either intracellularly (e.g., in magnetotactic bacteria [12]), or accumulating within exopolymer matrixes [13,14].

Examples of well-preserved fossil microbiotas from subsurface environments have previously been published only from Warstein,

Germany [15]. Other occurrences containing possible microbial remains include salt dome caprocks from the Texas Gulf area [16] and epithermal U-bearing veins at Menzenschwand, Germany [17]. Here we present a number of newly recognized occurrences of well-preserved subsurface microbiotas, all enclosed in opal, chalcedony, or megaquartz, from localities in California, Oregon, Texas, Brazil, Germany, the Czech Republic, the Faeroer Islands, India, the Kerguelen Islands, New Zealand, and Mongolia (Hofmann and Farmer, in preparation). Many of these occurrences are within amygdulites in basaltic-to-acid volcanic rocks or in vein-type epithermal mineralizations. Subsurface microfossils from these localities are remarkably well preserved, commonly as heavily encrusted branched filament molds with a primary internal diameter of 2–10 mm. The encrusted filaments typically have an outer diameter of 50–200 mm. In the examples studied, microbial filaments (cell walls and/or sheaths) were apparently coated and/or replaced by very fine-grained goethite, iron-silicate minerals and/or chalcedony, and subsequently embedded in chalcedony or megaquartz. In some large amygdulites, mineralized filamentous structures are as much as 10 cm long. In the absence of filamentous morphologies, a biological origin for structures from Menzenschwand and some other sites include finely banded stromatolitic fabrics with lamina shapes resembling the surfaces of some microbial mats, homogeneous fine-grain size, and isolated patches of reduced minerals (reduction spots) in an oxidized host rock [18–20].

Many of the subsurface microbiotas so far identified are from volcanic environments, commonly amygdulites. Similar environments are very likely to be found on Mars. Our findings suggest that vesicular textures, along with late-stage aqueous minerals deposited within fractures of a variety of host rocks, should be considered important potential targets for a fossil record of subsurface microbial life on Mars.

**References:** [1] Walter M. R. and Des Marais D. J. (1993) *Icarus*, 101, 129–143. [2] Farmer J. D. and Des Marais D. J. (1994) *LPS XXV*, 367–368. [3] McKay D. S. et al. (1996) *Science*, 273, 924–930. [4] Stevens T. O and McKinley J. P. (1996) *Science*, 270, 450–454. [5] Pedersen K. (1993) *Earth Sci. Rev.*, 34(4), 243–260. [6] Farmer J. D. et al. (1995) *Geol. Soc. Am. Abstr. with Progr.*, 27(6), 305. [7] Ehrlich H. L. (1996) *Geomicrobiology*, 2nd edition, Marcel Dekker Inc., New York. [8] Ferris F. G. et al. (1988) *Geology*, 16, 149–152. [9] Farmer J. D. and Des Marais D. J. (1994) in *Microbial Mats: Structure, Development and Environmental Significance* (L. J. Stal and P. Caumette, eds.), pp. 61–68, NATO ASI Series in Ecological Sciences, Springer Verlag. [10] Zierenberg R. A. and Schiffman P. (1990) *Nature*, 348, 155–157. [11] Beveridge T. and Doyle, eds. (1989) *Metal Ions and Bacteria*, Wiley, New York. [12] Frankel R. B. et al. (1983) *Biochim. Biophys. Acta*, 763, 147–159. [13] Ghiorse W. C. (1980) *Annu. Rev. Microbiol.*, 38, 515–550. [14] Ghiorse W. C. and Hirsch P. (1979) *Arch. Microbiol.*, 123, 213–226. [15] Kretzschmar M. (1982) *Facies*, 7, 237–260. [16] Sassen R. et al. (1988) *Org. Geochem.*, 14, 381–392. [17] Hofmann B. (1989) *Nagra (Swiss Natl. Cooperative for the Storage of Radioactive Waste) Technical Report 88-30*, Baden, Switzerland. [18] Hofmann B. (1990) *Proc. First Intl. Symp. Microbiology of the Deep Subsurface*, Orlando 1990. [19] Hofmann B. (1990) *Chem. Geol.*, 81, 55–81. [20] Hofmann B. (1991) *Mineral. Petrol.*, 44, 107–124.

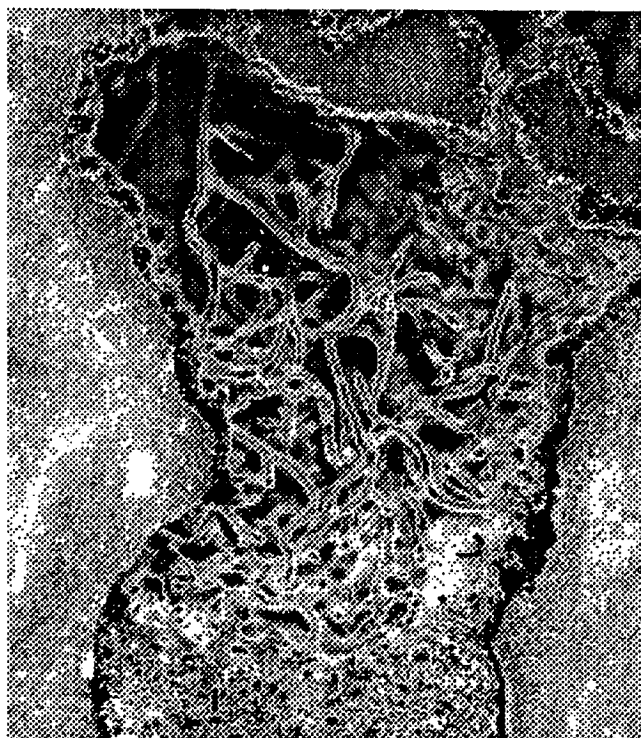


Fig. 1. Mineralized microbial filaments in rhyolite amygdule, Central Oregon. Open space is filled with chalcedony. Arnoth collection. Field of view 3 mm.

**ROLE OF THE CRUST IN THE EVOLUTION OF THE MARTIAN ATMOSPHERE.** K. S. Hutchins and B. M. Jakosky, Laboratory for Atmospheric and Space Physics and the Department of Geological Sciences, University of Colorado, Boulder CO 80309, USA.

We have examined the plausibility of the martian crust as a source of atmospheric volatiles, particularly  $^{40}\text{Ar}$ ,  $^{36}\text{Ar}$ , and  $^{20}\text{Ne}$ . Previously, we developed an atmospheric evolution model for martian Ar and Ne that included fluxes of volatiles from the mantle via intrusive and extrusive volcanic outgassing and loss of volatiles to space by collisional sputtering from the exobase [1]. Due to the importance of sputtering loss on the lighter noble gases (independent of the possibility of an early intrinsic magnetic field [2]), we found that additional sources of  $^{40}\text{Ar}$ ,  $^{36}\text{Ar}$ , and  $^{20}\text{Ne}$  would be required to match the present-day abundances measured in the martian atmosphere. Our previous model results indicated that the additional sources must supply 4–100 $\times$  the Ar and 40–1800 $\times$  the Ne outgassed by intrusive and extrusive volcanic activity.

Release and transport of volatiles from the crust via groundwater circulation represent a likely candidate for the required additional source. Volatiles trapped by incomplete magma degassing (particularly for intrusions) and volatiles produced radiogenically ( $^{40}\text{Ar}$ ) are released from crustal minerals by diffusion and chemical alteration. Once released, the volatiles are available for transport to the surface and the atmosphere via groundwater circulation that can reasonably extend to depths of 10–15 km [3].

Using our previous model of Ar evolution (including  $^{40}\text{Ar}$ ,  $^{36}\text{Ar}$ , and  $^{38}\text{Ar}$ ) and a crustal concentration of K ranging from 350 ppm to 2500 ppm (the lower limit represents no preferential crustal partitioning of K during differentiation, while the upper limit is that inferred from a shergottite model of the crust), we calculated the crustal production of  $^{40}\text{Ar}$  directly from our model. Thus, the production and release of radiogenic Ar from the crust is directly constrained by an independent assessment of the crustal concentration of K.

Based on preliminary model calculations, we find that between 5 and 25 km of crust must have released  $^{40}\text{Ar}$  to the atmosphere. This corresponds to approximately 5–70% of the total crust depending on the estimate of crustal thickness, which is poorly constrained at present.

Having calculated the  $^{40}\text{Ar}$  supplied by crustal outgassing, we can apply the observed atmospheric  $^{40}\text{Ar}/^{36}\text{Ar}$  ratio as a constraint on crustal outgassing of  $^{36}\text{Ar}$ . Using this constraint, we found that crustal concentrations of  $^{36}\text{Ar}$  ranging from  $\sim 6.0 \times 10^{-9} \text{ cm}^3 \text{ STP/g}$  to  $1.5 \times 10^{-8} \text{ cm}^3 \text{ STP/g}$  were necessary for the same volumes of crust. These concentrations are not inconsistent with the concentration of  $^{36}\text{Ar}$  measured in the Shergotty or Nakhla meteorites [4]. Higher crustal concentrations of noble gases may be possible given the lack of volatile recycling via plate tectonic activity.

Crustal release of Ne is not as rigorously constrained. In order to match the observed atmospheric abundance of Ne given our previous sputtering model and the above model of crustal release, the same volume of crust must (1) have a  $^{20}\text{Ne}$  abundance of between  $\sim 2.5 \times 10^{-9} \text{ cm}^3 \text{ STP/g}$  and  $3.5 \times 10^{-8} \text{ cm}^3 \text{ STP/g}$ , which is not unreasonable with respect to the concentrations measured by Ott [4], and (2) have been outgassed within the last 100 m.y. in order to be consistent with the short residence time of Ne in the crust and the atmosphere and the measurement of the atmospheric Ne abundance.

In summary, sputtering has dramatically influenced the evolution of the martian atmosphere. In light of this loss, sources in addition to intrusive and extrusive volcanic outgassing are required to satisfy the available constraints of the measured abundances of  $^{36}\text{Ar}$ ,  $^{38}\text{Ar}$ , and  $^{40}\text{Ar}$ , and the ratios of  $^{36}\text{Ar}/^{38}\text{Ar}$  and  $^{40}\text{Ar}/^{36}\text{Ar}$ . Crustal outgassing by martian groundwater systems appears to be a plausible and defensible source of the necessary additional atmospheric Ar. Application of observable constraints on outgassing such as the crustal K concentration and the observed  $^{40}\text{Ar}/^{36}\text{Ar}$  ratio, allows for more rigorous justification of these results (a substantial improvement over our previous efforts). Groundwater outgassing also may provide a viable source of additional Ne, but is not as rigorously constrained. Groundwater cycling of volatiles may also have played a distinct role in the evolution of martian climate as  $\text{CO}_2$  was sequestered [5] and, possibly, later released back to the atmosphere.

**References:** [1] Hutchins K. S. and Jakosky B. M. (1996) *JGR*, 101, 14933. [2] Hutchins K. S. and Jakosky B. M. (1997) *JGR*, in press. [3] Clifford S. M. (1993) *JGR*, 98, 10993. [4] Ott U. (1988) *GCA*, 52, 1937. [5] Griffith L. L. and Shock E. L. (1995) *Nature*, 377, 406.

**WHY THE SNC METEORITES MIGHT NOT COME FROM MARS.** E. Jagoutz, Max Planck Institut für Chemie, Postfach 3060, D-55020 Mainz, Germany (jagoutz@mpch-mainz.mpg.de).

For many years the reasons why the SNC meteorites might come from Mars were discussed in the literature. The most important argument for their martian origin was that SNC meteorites are young magmatic rocks and Mars is most likely the place where such rocks might originate. However, recently considerable doubt is growing. The first suspicion arose when a 4.55-Ga age of ALHA 84001 was measured [1]. Under these circumstances, reviewing available and new SNC data makes them appear in a different light.

**Revisiting the Young Ages:** From the examination of their Rb-Sr, Sm-Nd, and U-Pb isotope systematic we must conclude that only two differentiation processes dominated the evolution of the SNC meteorites. The first and primary differentiation occurred 4.5 Ga ago, the second between 150 Ma and 1.4 Ga. The first differentiation formed chemically distinctive reservoirs from primary accreted material. Those reservoirs might further be called planetary reservoirs. The second differentiation process mainly created the final chemical and mineralogical composition of the SNC meteorites as they are today.

The isotope data were calculated to the present-day value and the effect of the second differentiation was corrected out to obtain a comparable set of data for modeling the primary differentiation. For ALHA 84001 the present-day isotope values are taken considering that this meteorite did not experience a second differentiation while all the other SNCs must be corrected.

**Primary Differentiation:** The Sr and Nd isotopes plot with a clear negative trend (Fig. 1). While ALHA 84001 and EETA 79001 plot outside this trend, this will be discussed later. There is a common hypothesis that the Sm/Nd ratio of the accreting matter was chondritic. Therefore we are able to interpolate the present-day Sr isotopic composition of the average accreting matter using the Sr-Nd isotopic correlation. In Fig. 2 the  $^{87}\text{Rb}/^{86}\text{Sr}$  and  $^{147}\text{Sm}/^{144}\text{Nd}$  ratios of the primary matter are indicated by the field "Chondrites." The evolution path of the melt and the residuum at different degrees of

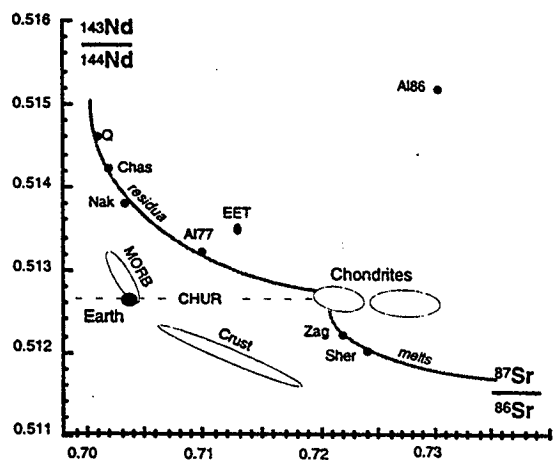


Fig. 1.

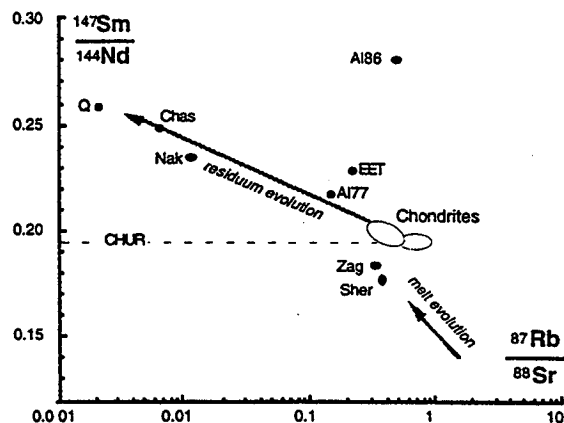


Fig. 2.

partial melting were calculated. The residue moves along the track indicated as "residuum evolution" and the composition of the melt is indicated by "melt evolution." The first increment of melt having a high Rb/Sr ratio will move like the residue mainly in the direction of lower Rb/Sr ratio with increasing partial melting (note: the  $^{87}\text{Rb}/^{86}\text{Sr}$  scale is logarithmic!). A higher degree of partial melting will also move the residue to higher Sm/Nd, while the melt gets closer to the primary composition. The melt will reach the primary composition at a high degree of partial melting. After 4.5 Ga this chemical change will be reflected in the Sr and Nd isotopes. These isotopic compositions are indicated in Fig. 1. There is surprising agreement in the isotopes with the result of a simple melting model. EETH and ALHA 84001 fall outside this magmatic trend, but both these meteorites show evidence of hydrothermal activity. Rb-Sr and Sm-Nd seem to follow a magmatic fractionation trend but U-Th-Pb fractionation seems to be independent from this fractionation. Sr-Nd-Pb isotopes are plotted in a three-dimensional plot (not shown here). The Sr-Nd correlation as seen in Fig. 1 is noticeable and there is scatter in the Pb direction. All data form a plane. This plane is perpendicular to the Sr-

Nd correlation (Sr-Nd plane), indicating that the U-Pb fractionation was independent of the fractionation that caused the Sr-Nd correlation.

**Second Differentiation:** Details of the second differentiation process will be given. While the first differentiation follows the pattern of partial melting, the second differentiation cannot be explained by any melting processes. While major elements and the modal composition still reflect the trend of the first differentiation, the second differentiation mainly resets the minerals isotopically, but the chemical changes in the whole rocks are not consistent with a melting process. Especially the Rb-Sr, but also the U-Pb systematics, are not much affected by the second differentiation at all. Moreover, the initial Pb is close to the geochron, which is not expected if the excess U existed for a long time. The gain of U (or loss of Pb) might be caused by the second differentiation. The Sm-Nd system is drastically changed by the second differentiation.

It is tempting to see the secondary differentiation as an internal resetting of the isotopes. However, there is a drastic change in the total rock Sm/Nd ratio from the second differentiation as well. In Nakhla and Chassigny (the most depleted residues) Sm/Nd was decreased, while in the shergottites and hercynitic shergottites the Sm/Nd ratio was increased. There is no magmatic evolution that can explain these changes without changing the Rb-Sr system. A suggestion to understand the chemical changes of the second differentiation: a dispersed trace mineral with highly fractionated REE and low Sr/Nd ratio was equilibrated to the surrounding minerals and then mobilized out of the sample. Inhomogeneities found in different whole-rock splits of the SNC meteorites could also point in this direction.

**Conclusions:** There was a magmatic event at 4.5 Ga that formed the SNC meteorites. The young disturbance cannot be classified as a magmatic process. The assumption that the young Nd ages might be truth ages and Sr and Pb might be produced by a mixing process is not valid, because Sr and Nd isotopes are still showing the magmatic sequence from the differentiation at 4.5 Ga. Only ALHA 84001 and EETA 79001 might have gained some Sr.

Brandenburg [2] suggested that CI chondrites have some affinities to SNC meteorites. It is not suggested here that C chondrites come from Mars but it is conceivable that the SNC might be the achondritic counterparts of the C chondrites. Bogdanovski and Jagoutz [3] found some minerals in Allende that plot left of the 4.5-Ga Sm-Nd isochron. This might also point toward a recent Sm-Nd disturbance in C chondrites. Furthermore, the organic compounds found in SNC meteorites resemble the organics from C chondrites.

**References:** [1] Brandenburg (1996) *Meteoritics*, 31, A20. [2] Jagoutz (1995) *Eos Trans. AGU*, 75, 400. [3] Bogdanovski and Jagoutz (1997) *LPS XXVIII*, 129-130.

**EARLY ATMOSPHERES OF EARTH AND MARS: IMPORTANCE OF METHANE TO CLIMATE AND TO LIFE'S ORIGIN.** J. F. Kasting and L. L. Brown, Department of Geosciences, 211 Deike, Pennsylvania State University, University Park PA 16802, USA (kasting@essc.psu.edu).

For the past 20 years, modelers of Earth's early atmosphere have assumed that it consisted of a weakly reducing mixture of  $\text{CO}_2$ ,  $\text{N}_2$ , and  $\text{H}_2\text{O}$ , with smaller amounts of  $\text{CO}$ ,  $\text{SO}_2$ , and  $\text{H}_2$  [e.g., 1-3]. The argument was twofold: (1)  $\text{CO}_2$  and  $\text{H}_2\text{O}$  are the major gases emitted

by volcanos today and (2) highly reduced gases, like  $\text{CH}_4$  and  $\text{NH}_3$ , would have been irreversibly converted to more oxidized species by photolysis followed by escape of H to space. Essentially the same arguments should apply to early Mars. The hypothesized presence of weakly reduced atmospheres on both planets has led to two perceived problems: (1) Earth's atmosphere may have been too oxidizing to permit synthesis of organic molecules needed as precursors for life's origin [4] and (2) Mars' atmosphere may not have been able to generate a large enough greenhouse effect to explain the geologic evidence for a warm early climate [5].

An assumption that is implicit in all these models of atmospheric evolution is that the redox state, or oxygen fugacity, of Earth's upper mantle has remained constant over time. Today, Earth's mantle appears to be near equilibrium with the QFM (quartz-fayalite-magnetite) mineral buffer, which is to say it is near the boundary between  $\text{Fe}^{+2}$  and  $\text{Fe}^{+3}$  [e.g., 6]. The gases emitted by surface volcanos under these conditions are relatively oxidized. For example, the predicted ratio of  $\text{H}_2/\text{H}_2\text{O}$  is  $\sim 0.01$  and the ratio of  $\text{CO}/\text{CO}_2$  is  $\sim 0.03$ , in good agreement with observed values (p. 50 of [2]).  $\text{CH}_4$  and  $\text{NH}_3$  are not observed in such volcanic emissions.

There are reasons to believe, however, that Earth's primitive mantle may have been significantly more reduced. Theoretically, one would expect that in the immediate aftermath of core formation, the oxygen fugacity should have been near equilibrium with the IW (iron-wüstite) buffer, that is, close to the boundary between  $\text{Fe}^0$  and  $\text{Fe}^{+2}$ . The gases released by surface volcanos under such circumstances would have been considerably more reduced, e.g., ratios of  $\sim 1$  for  $\text{H}_2/\text{H}_2\text{O}$  and 3 for  $\text{CO}/\text{CO}_2$  are predicted (p. 50 of [2]).  $\text{CH}_4$  would still have been a minor component of these gases.

For many years, it has been argued that the early mantle was not as reduced as predicted above. The evidence in favor of a more oxidized mantle is the putative excess abundance of siderophile (Fe-loving) elements in the mantle. This has led to planetary formation models in which Earth was veneered by an oxidized layer of material during the latter stages of accretion [e.g., 7]. Now, however, new studies of metal-silicate partition coefficients [8,9] indicate that siderophile elements may not be overabundant after all. Righter et al. [9] argue that the abundances of five moderately siderophile elements can be explained by assuming equilibration between molten silicates and Fe at the base of a 1000-km-deep magma ocean. Such an ocean may have been formed as a consequence of the giant impact event that is thought to have formed the Moon [10].

Additional evidence in favor of a more reduced early mantle for Earth comes from thermodynamic analyses of sulfide and chromite inclusions in 3.3-b.y.-old diamonds [6]. These inclusions point to a mantle oxidation state intermediate between IW and QFM at that time. Kasting et al. [6] argue that the mantle was gradually oxidized over time by the subduction of hydrated seafloor, followed by outgassing and escape of  $\text{H}_2$ .

As pointed out above,  $\text{CH}_4$  would still have been only a minor component of surface volcanic emissions, even if the upper mantle was initially near equilibrium with IW. This is true primarily because the effective pressure at which such gases are released is relatively low (1–10 bar) and the temperatures are high (1400–1500 K) [2]. Gases released from submarine volcanism, however, last equilibrate with rocks at much higher pressures and lower temperatures; hence,  $\text{CH}_4$  can be a more abundant constituent. Thermodynamic calculations [11] indicate that  $\text{CH}_4$  could have been the dominant C species released by mid-ocean ridge submarine

volcanism if the mantle oxygen fugacity was as little as 1 log unit below QFM. At modern outgassing rates [12,13], the  $\text{CH}_4$  source could have been of the order of  $10^{12}$  mol/yr. Calculations with a photochemical model [11] show that this could have supported an atmospheric  $\text{CH}_4$  mixing ratio of  $\sim 50$  ppm. This value might be increased by a factor of several if volcanic outgassing rates on the primitive Earth were higher than today, as seems likely.

Such high atmospheric  $\text{CH}_4$  concentrations would have been important for two reasons: (1) They would have allowed atmospheric synthesis of HCN by a mechanism in which N atoms produced in the ionosphere combine with the byproducts of  $\text{CH}_4$  photolysis in the stratosphere [14]. HCN and  $\text{H}_2\text{CO}$  are the two key starting blocks for the synthesis of RNA and amino acids.  $\text{H}_2\text{CO}$  is produced in substantial amounts by photochemical reactions in a  $\text{CO}_2$ - $\text{H}_2\text{O}$  atmosphere [15]. (2) Atmospheric  $\text{CH}_4$  concentrations of 50 ppm or more could have made a substantial contribution to the atmospheric greenhouse effect. According to calculations made using a radiative-convective climate model (thesis by L. Brown, in preparation), 50 ppm of  $\text{CH}_4$  would produce  $\sim 15$  W/m<sup>2</sup> of additional downward radiative forcing at the tropopause. If atmospheric  $\text{CO}_2$  was as low as estimated by Rye and Holland [16], this climatic contribution may have been important in countering the faintness of the young Sun.

Extending these calculations to early Mars is, of course, problematical. It seems reasonable to assume, though, that the martian upper mantle was not greatly different from Earth's upper mantle at a time shortly following the main accretion period. Analyses of SNC meteorites indicate that the martian upper mantle is depleted in siderophile elements relative to Earth [e.g., 17], which would be consistent with its equilibrating with the IW buffer. We do not know what volcanic outgassing rates might have been on early Mars, but they may not have been greatly lower than for early Earth. Perhaps more importantly, we do not know whether early Mars had oceans and, if so, how deep they might have been. Because of the lower surface gravity and possibly much shallower oceans, submarine outgassing of  $\text{CH}_4$  would have been less favored than on Earth. Nevertheless, a mantle oxygen fugacity near IW could still have allowed  $\text{CH}_4$  to be outgassed as the dominant C species. Photochemical calculations for hypothetical early Mars atmospheres predict that  $\text{CH}_4$  concentrations of  $\sim 100$  ppm or more may have been possible (thesis by L. Brown, in preparation). Atmospheric  $\text{CH}_4$  levels could, of course, have been even higher if early Mars was inhabited by bacteria [18] and if some of those bacteria made their metabolic living by methanogenesis.

If  $\text{CH}_4$  was a significant component of the primitive martian atmosphere, it could have affected climate and facilitated life's origin just as on Earth. Climate calculations that we have performed to date do not indicate that  $\text{CH}_4$  would have been able to bring the global average surface temperature above freezing. However, we have recently recognized that  $\text{CH}_4$  absorption in the visible/near-IR (which has not been considered in our model) may have lowered the planetary albedo significantly. It remains to be seen whether the effect is large enough to produce a warm early Mars. High-altitude  $\text{CO}_2$  ice clouds may also have produced a significant warming effect on the martian climate [19]. Additional radiative-convective climate modeling and, ultimately, GCM modeling is needed to study both these possibilities.

**References:** [1] Walker J. C. G. (1977) *Evolution of the Atmosphere*, Macmillan, New York. [2] Holland H. D. (1984) *The*



*Chemical Evolution of the Atmosphere and Oceans*, Princeton Univ., Princeton. [3] Kasting J. F. (1993) *Science*, 259, 920–926. [4] Stribling R. and Miller S. L. (1987) *Origins of Life*, 17, 261–273. [5] Kasting J. F. (1991) *Icarus*, 94, 1–13. [6] Kasting J. F. et al. (1993) *J. Geol.*, 101, 245–257. [7] Jones J. H. and Drake M. J. (1986) *Nature*, 322, 221–228. [8] Walter M. J. and Thibault Y. (1995) *Science*, 270, 1186–1189. [9] Richter K. et al. (1996) *Phys. Earth Planet. Inter.*, submitted. [10] Hartmann W. K. et al. (1986) *Origin of the Moon*, Lunar and Planetary Institute, Houston. [11] Kasting J. F. and Brown L. L. (1997) in *The Molecular Origins of Life: Assembling the Pieces of the Puzzle* (A. Brack, ed.), Cambridge Univ., New York, submitted. [12] Des Marais D. J. and Moore J. G. (1984) *EPSL*, 69, 43–57. [13] Marty B. and Jambon A. (1987) *EPSL*, 83, 16–26. [14] Zahnle K. J. (1986) *JGR*, 91, 2819–2834. [15] Pinto J. P. et al. (1980) *Science*, 210, 183–185. [16] Rye R. et al. (1995) *Nature*, 378, 603–605. [17] Longhi J. et al. (1992) in *Mars* (H. H. Kieffer et al., eds.), pp. 184–208, Univ. of Arizona, Tucson. [18] McKay D. S. et al. (1996) *Science*, 273, 924. [19] Pierrehumbert R. T. and Erlick C. (1997) *J. Atmos. Sci.*, submitted.

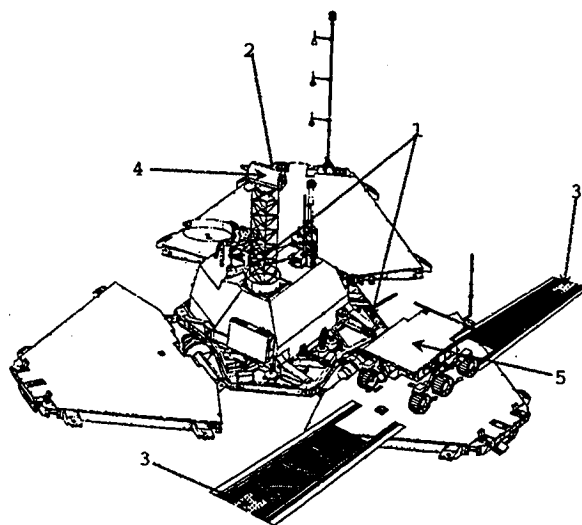


Fig. 1. The Pathfinder lander. The labels refer to (1) the two sets of magnet arrays; (2) tip plate magnet; (3) ramp magnets; (4) imager (IMP); and (5) the Sojourner rover.

**THE MAGNETIC PROPERTIES EXPERIMENT ON MARS PATHFINDER.** J. M. Knudsen, H. P. Gunnlaugsson, M. B. Madsen, S. F. Hviid, and W. Goetz, Niels Bohr Institute for Astronomy, Physics and Geophysics Department, Universitetsparken 5, DK-2100 Copenhagen, Denmark.

**Introduction:** A remarkable result from the Viking missions to Mars in 1976 was the discovery that the martian soil is highly magnetic, in the sense that the soil is attracted by small permanent magnets [1,2].

The Viking landers carried two types of permanent magnets, a weak and a strong magnet. The surface magnetic field and surface magnetic field gradient of the strong-type magnet were 250 mT and 100 Tm<sup>-1</sup> respectively. The corresponding numbers for the weak magnet were 70 mT and 30 Tm<sup>-1</sup>. Both types were mounted on the backhoe of the soil sampler, where they were exposed to the soil. A strong-type magnet was mounted in the Reference Test Chart (RTC), which was exposed to wind-borne particles exclusively.

At both landing sites both backhoe magnets were saturated with magnets. It was estimated that the martian dust contains between 1% and 7% of a strongly magnetic phase, most probably a ferrimagnetic ferric oxide intimately dispersed throughout the soil. Limits for the saturation magnetization  $\sigma_s$  were advanced: 1 Am<sup>2</sup> (kg (soil))<sup>-1</sup> <  $\sigma_s$  < 7 Am<sup>2</sup> (kg (soil))<sup>-1</sup>.

**Scientific Goal:** The Magnetic Properties Experiment (MPE) on Mars Pathfinder consists of two magnet arrays located at different sites on the lander (see Fig. 1), a tip plate magnet (TPM) and two ramp magnets. The TPM is mounted on the tripod base (tip plate) of the imager for Mars Pathfinder (IMP), at a distance of only 10 cm from the eye of the imager. The two ramp magnets are located at the ends of the ramps where the Sojourner rover will drive off the lander. The Sojourner rover is expected to return to one of the ramps, and measure the elemental composition of the dust that has been attracted to the ramp magnets, using the onboard APX spectrometer.

The scientific goal of the MPE on Mars Pathfinder is to identify the strongly magnetic phase on the surface of Mars.

The inclusion of weaker magnets on Mars Pathfinder—as compared with the Viking missions—will enable us to give a more precise estimate of the magnetization of the grains in the dust on Mars.

The spectroscopic capabilities of the IMP are so much better than those of the Viking cameras that it may be possible to distinguish a difference in mineralogy between loose soil/dust on the ground and the material that has been magnetically attracted to one of the magnetic properties instruments. This will give information of crystallite size and the degree of intergrowth of different crystallites in a single dust particle, i.e., it may be able to distinguish single-phase particles from multiphase particles. Specifically, a color difference between the material adhering to the five magnets of a magnet array will be expected if not all particles in the dust are essentially identical to one another.

Grossly stated, two major pathways for the formation of the martian soil may be distinguished, and the resulting magnetic phase will be different for the two pathways.

If the magnetic phase has formed in abounded water via precipitation, it will be almost pure iron oxide, and will not contain the element Ti. If, however, the magnetic phase has formed via comminution of the underlying rocks, which, like the Mars meteorites are assumed to contain titanomagnetite, the resulting magnetic phase will contain the element Ti.

An identification of the magnetic phase in the surface dust on Mars (or identification of its properties) will enhance our understanding of the alteration processes that have shaped the surface of the planet, particularly the role of water.

The identification will be based on three results:

1. The pattern of dust on the two magnet arrays and the TPM. Both the magnet array and the TPM have been constructed with a variety of values of the magnetic field and magnetic field gradient at the surface of the instrument on which magnetic dust is attracted. By observing on which site on the surface of the instrument magnetic dust is attracted one can estimate the effective magnetization of the attracted dust grains.

2. The optical properties of the attracted dust. The IMP is capable of acquiring images in 12 distinct spectral bands (the imager is described in detail in an article that will be published in *Journal of Geophysical Research* [3], special issue on the Pathfinder mission). Using these filters, a rough reflection spectrum can be obtained. The optical properties of Fe(III) compounds are very sensitive to, e.g., particle size [4].

3. Elemental analyses of the dust attracted to the ramp magnet performed using the APX instrument on the Sojourner rover.

Figure 2 shows a front view of the magnet array. The positions of the magnets below the surface of the instrument are indicated (dashed lines) as well as typical values of the magnitude of the magnetic field gradient  $\nabla(B)$  and the magnetic field  $B$  at the surface. Each magnet assembly consists of a ring magnet with outer diameter 19 mm and inner diameter 13 mm magnetized opposite to a centrally aligned disc magnet of diameter 6.5 mm.

Figure 3 shows the design of the TPM. The magnet itself is essentially a bull's-eye-pattern magnet, of the same type as the magnets used for the magnet array but 4.0 mm thick. The active surface of the instrument is tilted  $7^\circ$  with respect to the underlying magnet to ensure sufficient variation of  $\nabla(B)$  and  $B$ .

Figure 4 shows three samples on the magnet array. The pattern of particles is significantly influenced by the detailed magnetic properties of the particles. From the images, essential facts on their magnetic properties can be deduced.

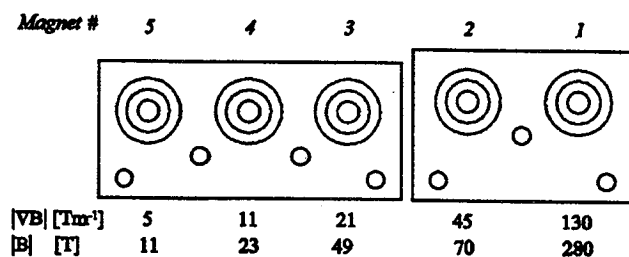


Fig. 2. Front view of the magnet array. The positions of the magnets below the surface are indicated by dashed lines.

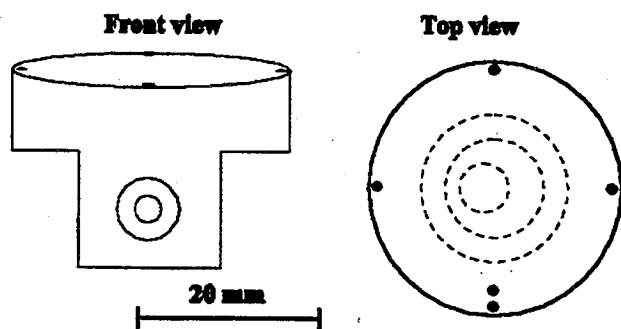


Fig. 3. Front view and top view of the tip plate magnet. The top view shows the "active" surface of the instrument with indication of the position of the magnet assembly below the surface (dashed lines) and five marks that define a local coordinate system on the surface.

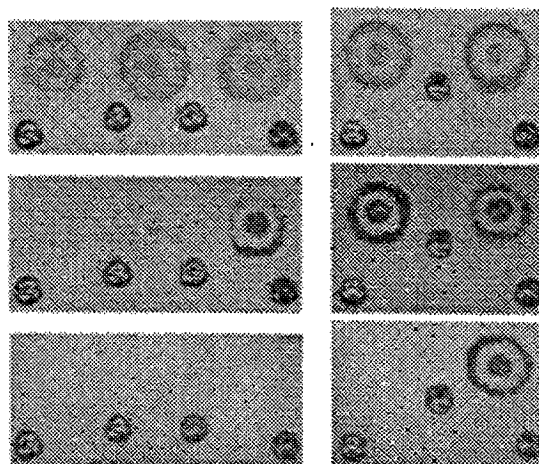


Fig. 4. Three different samples on the magnet array. At the top we have pure maghemite ( $\gamma\text{-Fe}_2\text{O}_3$ ), which is strongly magnetic ( $\sigma_s \approx 70 \text{ Am}^2\text{kg}^{-1}$ ) and hence sticks to all magnets. In the middle we have basaltic beach sand ( $\sigma_s \approx 2.0 \text{ Am}^2\text{kg}^{-1}$ ) and at the bottom we have synthetic hematite ( $\alpha\text{-Fe}_2\text{O}_3$ ,  $\sigma_s \approx 0.4 \text{ Am}^2\text{kg}^{-1}$ ), sticking to the strongest magnet only.

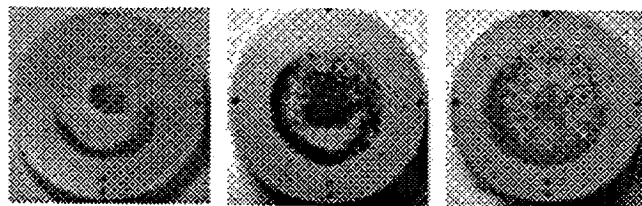


Fig. 5. Three samples on the tip plate magnet. Left: Black basaltic sand from Brædratunga, Iceland. This sample contains particles of relatively low-saturation magnetization ( $\sigma_s \approx 1 \text{ Am}^2\text{kg}^{-1}$ ). Middle: Beach sand from Skerfjafjordur, Iceland ( $\sigma_s \approx 10 \text{ Am}^2\text{kg}^{-1}$ ), displaying chain formation. Right: Synthetic maghemite ( $\gamma\text{-Fe}_2\text{O}_3$ ,  $\sigma_s \approx 70 \text{ Am}^2\text{kg}^{-1}$ ).

Figure 5 shows three different samples on the TPM. Note the impressive variations of patterns formed on the TPM. Detailed analysis of such patterns will give information on magnetization and crystallite dimensions.

**References:** [1] Hargraves R. B. et al. (1976) *JGR*, 82, 4547–4558. [2] Hargraves R. B. et al. (1979) *JGR*, 84, 8379–8384. [3] Morris R. V. et al. (1989) *JGR*, 94, 2760–2778. [4] Smith P. H. et al. (1997) *JGR Planets*, submitted.

**RELATIVE AGES OF MASKELYNITE AND CARBONATE IN ALLAN HILLS 84001 AND IMPLICATIONS FOR EARLY HYDROTHERMAL ACTIVITY ON MARS.** D. A. Kring, T. D. Swindle, J. D. Gleason, and J. A. Grier, Lunar and Planetary Laboratory, University of Arizona, 1629 E. University Boulevard, Tucson AZ 85721, USA.

ALH 84001 is the first SNC-related orthopyroxenite [1] and apparently the first sample from the ancient cratered highlands of Mars. Isotopic analyses indicate it crystallized  $\sim 4.5 \text{ Ga}$  [2,3], forming some of the original crust of Mars only a few hundred million



years after planetary differentiation. Subsequently, the cumulate was repeatedly shock-metamorphosed and invaded by  $\text{CO}_2$ -charged hydrothermal fluids, which produced secondary carbonate. One of the shock-metamorphic events appears to have occurred  $\sim 4.0$  Ga [e.g., 4], although the timing of other impact events and the precipitation of secondary carbonate is uncertain [cf. 5–7]. To further constrain the timing of these events, we have examined the textural relationship between the cumulate minerals and features produced by secondary metamorphic and hydrothermal processes.

The original cumulate fabric of the rock (split, 140) is crosscut with cataclastic zones of anhedral to subhedral orthopyroxene, chromite, and feldspathic glass [8]. Carbonate occurs in these cataclastic zones and in fractures between and within surviving orthopyroxene. It is clear that the carbonate precipitated after the impact event that produced the cataclastic zones of material, because the carbonate is not disaggregated. Rather, its crystal fabric crosscuts the disorganized structure of the cataclastic zones and fractured orthopyroxene.

Where igneous textures are best preserved, the feldspathic glass occurs interstitially between euhedral to subhedral orthopyroxene grains. The morphology and stoichiometry of the glass indicates it is maskelynite, a diaplectic glass produced from plagioclase ( $\text{Ab}_{60}\text{An}_{36}\text{Or}_4$ ) by shock pressures  $>29$  GPa [9]. Carbonate is intimately associated with the feldspathic glass. They occur together in the cataclastic zones, occupying the same morphological niches, and elsewhere patches of carbonate invade larger grains of maskelynite. Like Treiman [10], we believe these types of textures indicate the carbonate was produced in a dissolution-precipitation reaction. Unlike Treiman [10], however, we think the carbonate grew at the expense of maskelynite rather than plagioclase. As several investigators have noted [e.g., 1, 10, 11], the carbonate has a radial crystalline texture that produces spherical or semispherical globules. This morphology is consistent with the replacement of a glassy phase [e.g., 12–15] or growth into liquid or vapor. In contrast, when carbonate replaces plagioclase, it usually attacks boundaries between crystal twins, grain boundaries, and cracks. This produces linear traces or skeletal frameworks of carbonate rather than semispherical globules of radiating carbonate. Consequently, the texture of the carbonate suggests it replaced maskelynite and is thus younger than maskelynite. Carbonate replacement of maskelynite has previously been documented in shock-metamorphosed rocks associated with the Clearwater West impact crater on Earth [16, 17].

The duration of hydrothermal activity needed to produce the carbonate can be estimated by considering the dissolution rate of maskelynite. The dissolution rate is dependent on the pH of the hydrothermal fluid. Previous assessment of the assemblage of carbonate, ZnS, Fe-sulfides, and Fe-sulfates in ALH 84001 suggests the dissolution occurred in a system where  $\text{pH} > 7$  [18]. In a mildly to strongly alkaline system, experimental results [19] indicate that plagioclase with the ALH 84001 composition of  $\text{Ab}_{60}\text{An}_{36}\text{Or}_4$  would dissolve at a rate of  $1.9 \times 10^{-10}$   $\mu\text{m/s}$  ( $\text{pH} = 7$ ,  $T = 22^\circ\text{C}$ ) to  $1.4 \times 10^{-12}$   $\mu\text{m/s}$  ( $\text{pH} = 12$ ,  $T = 22^\circ\text{C}$ ). At these rates, 50  $\mu\text{m}$  of plagioclase (equivalent to the approximate radius of carbonate globules) could be dissolved in 8300 yr to 1.1 m.y. Since we believe carbonate replaced maskelynite rather than plagioclase, the applicable dissolution rate may have been a little faster, but not as fast as the dissolution rate of a completely disordered glass. If hydrothermal fluids were hotter than  $\sim 22^\circ\text{C}$ , then the dissolution rate would have been even faster. For example, experimental dissolution of tektite

glass at  $90^\circ\text{C}$  [20] and andesitic glass at  $300^\circ\text{C}$  [21] suggests timescales as short as a few years are possible. According to Wentworth and Gooding [18], the carbonate may have been produced at temperatures of  $\sim 100^\circ\text{C}$ – $300^\circ\text{C}$ , in which case the hydrothermal system that affected ALH 84001 may have been very short lived. If the temperatures were even higher, like those ( $>650^\circ\text{C}$ ) proposed by Harvey and McSween [11], then the dissolution-precipitation reaction would have occurred very quickly.

If the temperatures of the hydrothermal system were  $>650^\circ\text{C}$ , then the  $^{40}\text{Ar}$ – $^{39}\text{Ar}$  systematics in the maskelynite would have been reset while the carbonate precipitated [7]. In this case, the age of the carbonate would correspond to the last degassing age of the maskelynite,  $\sim 4.0$  Ga [4, 5, 7]. On the other hand, if the temperature of the hydrothermal system was  $<300^\circ\text{C}$ , then the  $^{40}\text{Ar}$ – $^{39}\text{Ar}$  systematics in the maskelynite may have only been disturbed and the carbonate could have an age significantly less than 4.0 Ga. Previous attempts to determine the timing of the carbonate precipitation have suggested younger ages, with estimates ranging from 3.6 Ga [5] to 1.39 Ga [6]. The youngest age is based on a poorly constrained two-point Rb–Sr “isochron” produced during a leaching experiment. The older age is based on a preliminary laser  $^{40}\text{Ar}$ – $^{39}\text{Ar}$  analysis that the authors now conclude was misleading [7]. They feel that the Ca/K ratio in that analysis is lower than they expect in carbonate, and conclude that their sample must have included some phase richer in K. We tried to measure the abundances of K in maskelynite and carbonate with an electron microprobe to see if we could extract the age of the carbonate based on the Ca/K ratios of this and other  $^{40}\text{Ar}$ – $^{39}\text{Ar}$  analyses. We determined that maskelynite contains  $\sim 6000$  ppm K and has a Ca/K ratio of  $\sim 8$ . The Mg,Fe-carbonate and Mg-carbonate have  $<80$  ppm K and Ca/K ratios  $>380$  and  $>310$  respectively. Most of the carbonate-bearing material analyzed by Turner et al. [7] has much larger K abundances than we measured in carbonate and consequently we confirm their conclusion that they were probably not dating the carbonate. However, we also note that they have three samples with K  $<120$  ppm, approaching the values expected of carbonate, and that these three samples also have systematically lower apparent ages, suggesting the carbonate is younger than the  $\sim 4.0$ -Ga degassing age of maskelynite. We conclude that dating of carbonate using the  $^{40}\text{Ar}$ – $^{39}\text{Ar}$  technique may be feasible, but probably requires larger and/or purer samples.

Finally, we note that if carbonate were produced at the expense of maskelynite in an atom-by-atom dissolution-precipitation reaction, then it is not likely to have involved microbial life [cf. 22]. The radiating globular textures of the carbonate are consistent with the nucleation and growth kinetics of reactions involving glassy materials like maskelynite. We also point out that Ca-carbonate, with radiating crystal fibers in globular forms with about the same dimensions (50  $\mu\text{m}$  diameter) as seen in ALH 84001, have been described in CI chondrites [23]. In the case of the CI carbonate, it seems clear that the textures were produced by simple aqueous activity; one cannot, therefore, appeal exclusively to microbial intervention for the textures seen in ALH 84001 unless one also argues that CI-chondrite parent bodies harbored life.

**References:** [1] Mittlefehldt D. W. (1994) *Meteoritics*, 29, 214–221. [2] Jagoutz E. et al. (1994) *Meteoritics*, 29, 478–479. [3] Nyquist L. E. et al. (1995) *LPS XXVI*, 1065–1066. [4] Ash R. D. et al. (1996) *Nature*, 380, 57–59. [5] Knott S. F. et al. (1995) *LPS XXVI*, 765–766. [6] Wadhwa M. and Lugmair G. W. (1996) *Meteoritics & Planet. Sci.*, 31, A145. [7] Turner G. et al. (1997) *GCA*, in

press. [8] Gleason J. D. et al. (1997) *GCA*, submitted. [9] Stöffler D. et al. (1986) *GCA*, 50, 889–903. [10] Treiman A. (1995) *Meteoritics*, 30, 294–302. [11] Harvey R. P. and McSween H. Y. Jr. (1996) *Nature*, 383, 49–51. [12] Keith H. D. and Padden F. J. Jr. (1963) *J. Appl. Phys.*, 34, 2409–2421. [13] Keith H. D. and Padden F. J. Jr. (1963) *J. Appl. Phys.*, 35, 1270–1285. [14] Keith H. D. and Padden F. J. Jr. (1963) *J. Appl. Phys.*, 35, 1286–1296. [15] Lofgren G. (1971) *JGR*, 76, 5635–5648. [16] Dence M. R. (1965) *Ann. New York Acad. Sci.*, 123, 941–969. [17] Bunch T. E. et al. (1967) *Am. Mineral.*, 52, 244–253. [18] Wentworth S. J. and Gooding J. L. (1995) *LPS XXVI*, 1489–1490. [19] Welch S. A. and Ullman W. J. (1996) *GCA*, 60, 2939–2948. [20] LaMarche P. H. et al. (1984) *J. Non-Crystal. Solids*, 67, 361–369. [21] Guillemette R. N. et al. (1980) *Proc. Intl. Symp. Rock-Water Interaction*, 3rd edition, pp. 168–169. [22] McKay D. S. et al. (1996) *Science*, 273, 924–930. [23] Fredricksson K. and Kerridge J. F. (1988) *Meteoritics*, 23, 35–44.

**CHEMISTRY OF CARBON, HYDROGEN, AND OXYGEN DURING EARLY MARTIAN DIFFERENTIATION.** K. Kuramoto<sup>1</sup> and T. Matsui<sup>2</sup>, <sup>1</sup>Center for Climate System Research, University of Tokyo 153, Japan (keikei@ccsr.u-tokyo.ac.jp), <sup>2</sup>Department of Earth and Planetary Physics, University of Tokyo, Tokyo 113, Japan.

Study of the chemical reprocessing of C-H-O-bearing volatiles during differentiation of Mars into the atmosphere, mantle, and core has a key significance in understanding the surface environment of early Mars. We assess this issue based on our recently developed thermodynamic model [1]. In this model, we numerically estimate equilibrium partitioning of C-H-O-bearing chemical species among gas, magma, and molten metallic iron that presumably differentiate eventually into the proto-atmosphere, mantle, and core respectively. On Mars, C-H-O-bearing volatiles are estimated to be reprocessed in a different way from the case of Earth, because both planets have different building blocks with respect to composition [1,2]. It is suggested that Mars initially has a proto-atmosphere of a substantially reduced chemical composition and a wet mantle that bears elemental C phases at great depths. Early Mars may have a surface environment suitable for the occurrence and evolution of life.

The SNC meteorites retain some evidence for homogeneous accretion of Mars in their abundance pattern of siderophile elements, i.e., most of the martian building blocks are considered to be a homogeneous mixture of metals, silicates, and volatiles. Dreibus and Wänke [3] found that the two-component model can successfully explain the geochemical constraints on these meteorites. According to them, the martian building blocks are modeled as a mixture of reduced, volatile-free component A and CI-chondritic component B with a mixing ratio of A:B = 60:40. This composition is adopted in our volatile partitioning model below.

The differentiation of the rocky planets required a high temperature to cause melting and/or vaporization of the planetary materials. The heat source is likely to be the release of accretional energy. Recent theory of planetary formation suggests that the terrestrial planets are grown by high-speed impacts of massive planetesimals at

their intermediate to final growth stage [e.g., 4]. Each of such impacts is considered to bury not only heat but also accreting materials into great depths of the planetary interior. We assume, therefore, that C-H-O-bearing volatiles are partitioned under relatively high temperatures and pressures among gas, silicate melt, and molten metallic iron.

We estimate the volatile partitioning for the system of the same bulk composition with the martian building blocks as mentioned above. T and P ranges are taken to be 2000–3000 K and 0.2–5.0 GPa respectively. The results can be summarized as follows: (1) The oxygen fugacity is kept nearly  $10^{-1}$  times that of the IW buffer case over the calculated T and P range. (2) Gas (or fluid) accommodates the largest fraction of H and C in the system, even though we take into account the solubilities of volatiles into magma and molten metallic iron. (3) Gas has significantly reduced compositions:  $H_2/H_2O \approx 5$ ,  $CO_2$  is minor, and  $CH_4$  and CO dominate at high pressures. (4) Graphite saturates at pressure higher than a critical level, which depends on temperature. For example, the critical level is estimated to be 0.6 GPa when  $T = 2000$  K. Saturation of diamond instead of graphite is expected at P higher than about 5 GPa. (5) Magma is wet. It is estimated to contain  $H_2O$  by 3–5 wt% depending on T and P. Dissolution of the other volatile components into magma (e.g.,  $CO_2$ ) is negligible. (6) Molten metallic iron contains light elements. The mol ratios of H/Fe, C/Fe, and S/Fe of the metal are estimated to be nearly 0.1, 0.1, and 0.4 respectively, which depends slightly on T and P. It is to be noted that the solubilities of H and C into the metal are significantly reduced due to repulsive interactions with S because its concentration is large.

The above results have quite important implications for the evolution of the surface environment of early Mars. The estimated gas composition suggests the possibility of a proto-atmosphere with a reduced chemical composition that is appropriate for abiotic synthesis of precursor materials of life. The existence of such a reduced-type proto-atmosphere is consistent with extensive loss of H (or  $H_2O$ ) from Mars inferred from D/H ratios in the atmosphere and SNC meteorites [5]. This is because surface  $H_2O$  is considered to be gradually consumed by photochemical reactions with reduced C species ( $CO$ ,  $CH_4$ ), producing  $CO_2$  and  $H_2$ , which easily escape into space. Such  $H_2O$  loss possibly results in a relatively  $CO_2$ -rich and  $H_2O$ -poor surface environment. This is consistent with isotopic data of atmospheric components [6].

Our partitioning model also suggests that the martian mantle may be originally wet and contain a significant amount of elemental C species. That the early warm climate of Mars may be sustained by volcanic degassing from a wet mantle may also explain the relatively high oxygen fugacity estimated for the present martian mantle, because redox reactions among  $H_2O$  and silicates occur in association with degassing. The light elements partitioned to the metal may affect the structure of the martian core. This may be testable by future explorations of the martian interior using, for example, a seismic method.

**References:** [1] Kuramoto K. and Matsui T. (1996) *JGR*, 101, 14909–14932. [2] Kuramoto K. (1997) *Phys. Earth Planet. Inter.*, in press. [3] Dreibus G. and Wänke H. (1987) *Icarus*, 71, 225–240. [4] Lissauer J. J. and Stewart G. R. (1993) in *Protostars and Planets III*, pp. 1061–1088, Univ. of Arizona, Tucson. [5] Donahue T. M. (1995) *Nature*, 372, 432–434. [6] Jakosky B. M. (1991) *Icarus*, 94, 14–31.

**THERMAL EMISSION SPECTROSCOPY OF AQUEOUSLY PRECIPITATED MINERALS SIMILAR TO THOSE IN THE SNCs.** M. D. Lane and P. R. Christensen, Department of Geology, Box 871404, Arizona State University, Tempe AZ 85287-1404, USA (lane@olivia.la.asu.edu; phil@alex.la.asu.edu).

Photographic data from the Mariner and Viking missions suggest that liquid water once flowed on Mars and probably pooled within topographic lows such as large regional basins and impact craters. Standing water, however, is no longer present on the martian surface due to low pressure and temperature conditions that lie outside the range of liquid water stability. The water is likely to have evaporated, during which process the ions dissolved within the martian water would have combined and precipitated as minerals when their concentrations reached saturation. Presently it is not known what the exact compositions of the ancient waters were that globally scarred the surface, nor what minerals precipitated as evaporation took place; however, analyses of the martian shergottite, nakhlite, and chassignite (SNC) meteorites have proven that on Mars host rock interacted with saline, oxidizing, alkaline solutions causing precipitation of secondary minerals [1–5]. Although the fluid interaction in the geologically young meteorites could have occurred in the subsurface and/or with water of locally restricted chemistry and therefore may not be representative of other or ancient martian water systems, the meteorites provide the only unambiguous data regarding the martian minerals derived through precipitation from an aqueous fluid. Determining the extent to which aqueous mineral deposits are present on Mars' surface will be a goal of the Thermal Emission Spectrometer (TES) instrument aboard the Mars Global Surveyor (MGS) spacecraft. The TES will measure the radiation emitted from Mars' surface, after which the raw data will be calibrated to produce emissivity spectra. Emissivity spectra are analogous to finger prints in that they are unique for each mineral and thus may be used during data analysis to uniquely identify the minerals that are present. If minerals that were precipitated from an aqueous fluid are detected on Mars, their identification will allow for inferences to be made concerning the initial water chemistry. The purpose of this study is to present the emissivity spectra of minerals similar to those identified in the martian meteorites to demonstrate the utility of thermal emission spectroscopy for identifying and differentiating aqueously precipitated minerals.

The aqueously precipitated salt minerals that have been identified in the SNCs include carbonate, sulfate, phosphate, and chloride [1,3–12]. The carbonates and sulfates represent the most abundant precipitates [4]. Calcite ( $\text{CaCO}_3$ ) is the dominant carbonate in the Mars meteorites [4] and is present in each of the shergottite [1], nakhlite [2], and chassignite [5,9,10] classes. Carbonates of cations other than Ca have been identified as well. These other carbonates include magnesite ( $\text{MgCO}_3$ ) [10,13], siderite ( $\text{FeCO}_3$ ) [13], Mg-Ca carbonates in shergottite EETA 79001 [5], and carbonates containing both Fe and Mn suggestive of a siderite-rhodochrosite solid solution [8]. The vibrational, mid-infrared emission spectra of the Ca-, Mg-, Fe-, and Mn-carbonates are shown in Fig. 1. The various associated cations distinctively shift the positions of the absorption features and thus allow for discrimination between the carbonates [14]. The absorption band positions for carbonates that contain more than one cation lie between the two endmember carbonate band positions [14]. The dominant sulfate species present in the SNC

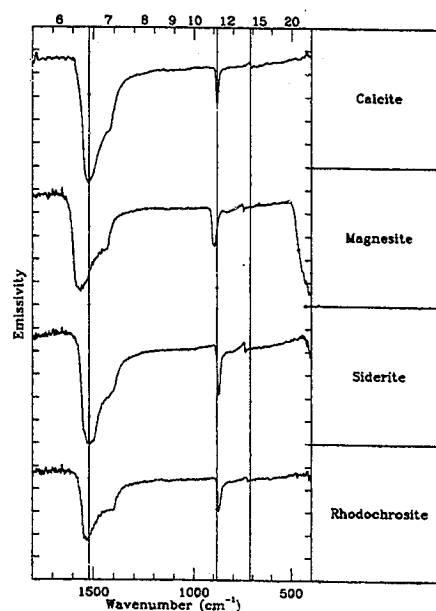


Fig. 1. Thermal emissivity spectra of carbonate minerals. Vertical lines are drawn through the calcite absorption band minima for comparison to other carbonate minima.

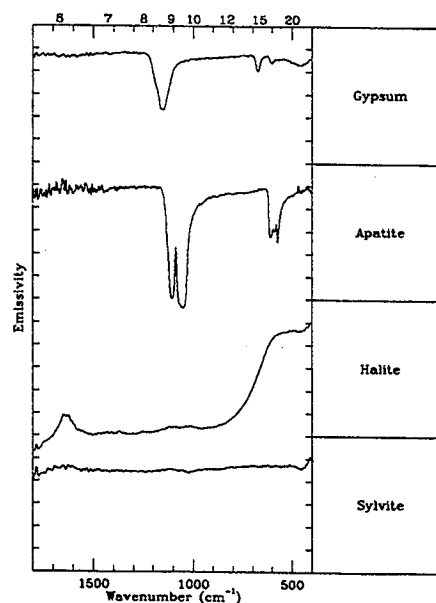


Fig. 2. Thermal emissivity spectra of sulfate, phosphate, and chloride minerals.

meteorites is gypsum ( $\text{CaSO}_4 \times 2\text{H}_2\text{O}$ ) [1,2,5,9,10]. The emissivity spectrum of gypsum is shown in Fig. 2. Additional minerals identified in the SNCs include Mg-rich phosphate [1], halite ( $\text{NaCl}$ ), and sylvite ( $\text{KCl}$ ) [2,7]. The vibrational emissivity spectra for the phos-

phate (apatite) and the chlorides are shown in Fig. 2. At this time chemical analysis of the apatite is unavailable, thus the amount of constituent Mg is unknown. The spectra in Figs. 1 and 2 show the variety of spectral absorptions associated with the carbonate, sulfate, and phosphate anions that will allow identification of the minerals. An additional result is that chlorides may be difficult to identify due to the absence of discrete spectral absorption bands.

Although aqueously precipitated minerals are only trace constituents of any of the SNC meteorites, their presence provides resounding evidence for hydrous activity on Mars. Identification of carbonate, sulfate, phosphate, or chloride from the TES data will enable a clearer understanding of the temporal and spatial scale of active martian hydrology as well as provide insight into the fluid chemistry and the chemical reactions that took place on the surface.

**References:** [1] Gooding J. L. et al. (1988) *GCA*, 52, 909–915. [2] Gooding J. L. et al. (1991) *Meteoritics*, 26, 135–143. [3] Gooding J. L. (1992) *LPI Tech. Rept. 92-04, Part 1*, pp. 16–17. [4] Gooding J. L. (1992) *Icarus*, 99, 28–41. [5] Wentworth S. J. and Gooding J. L. (1994) *Meteoritics*, 29, 860–863. [6] Gooding J. L. and Muenow D. W. (1986) *GCA*, 50, 1049–1059. [7] Treiman A. H. and Gooding J. L. (1991) *Meteoritics*, 26, 402. [8] Chatzi-theodoridis E. and Turner G. (1990) *Meteoritics*, 25, 354. [9] Wentworth S. J. and Gooding J. L. (1991) *LPS XXII*, 1489–1490. [10] Wentworth S. J. and Gooding J. L. (1991) *Meteoritics*, 26, 408–409. [11] Gooding J. L. and Wentworth S. J. (1991) *LPS XXII*, 461–462. [12] Jull A. J. T. et al. (1997) *JGR*, 102, 1663–1669. [13] Mittlefehldt D. W. (1994) *Meteoritics*, 29, 214–221. [14] Lane M. D. and Christensen P. R., in preparation.

**A UNIQUE MARS/EARLY MARS ANALOG ON EARTH: THE HAUGHTON IMPACT STRUCTURE, DEVON ISLAND, CANADIAN ARCTIC.** P. Lee, NASA Ames Research Center, Moffett Field CA 94035-1000, USA (lee@astrosun.tn.cornell.edu).

Haughton is a 20-km-diameter impact structure located on Devon Island, N.W.T., Canada. The structure formed 23 m.y. ago, and is the highest-latitude terrestrial crater known (~75°N, 90°W). It lies in the “frost rubble zone,” in an environment similar in several respects to that prevailing at the surface of Mars at present and/or on early Mars, if wetter and warmer conditions existed then [1]. Locales on Earth where similar, predominantly cold, relatively dry, windy, and unvegetated conditions prevail serve as valuable “Mars analogs” [2–4]. They (1) provide insight into the various geologic and possibly biologic processes that may have operated or still operate on Mars, (2) help interpret the meteoritical, Earth-based remote-sensing, and spacecraft data available for Mars, and (3) help plan the next steps in the exploration of Mars.

From this perspective, Haughton is a site of exceptional interest, as (1) it is an impact structure, a common and fundamental geologic feature of the martian surface; (2) it is currently, and has been for much of its existence (although not at the time of its formation), exposed to the present “Mars-like” and/or “early Mars-like” environment of the terrestrial high latitudes [5]; (3) it exhibits geologic features of fluvial, periglacial, eolian, and possibly hydrothermal origin that may have analogs on Mars; (4) it formed in carbonates, a rock type believed to occur on Mars and that has been associated with the recently proposed evidence for past life in martian meteor-

ites [6–10]; (5) it once contained a lake, as may have many impact craters and other basins on early Mars [11–13]; and (6) its earliest postimpact paleolacustrine sediments have been preserved and retain a fossil record [5], as might be preserved at paleolake sites on Mars if these ever harbored biologic activity [14–16]. Haughton is unique in that it is the only site known on Earth where all these Mars-like conditions and features occur together.

A study of the Haughton impact structure as a Mars analog, the “Haughton-Mars 97” (HM-97) Project, will begin this year with field observations at the crater. The objective of the project is to characterize those aspects of Haughton’s morphologic and physical evolution that are relevant to Mars’ geologic (in particular hydrologic) and possibly biologic evolution. The study will focus on (1) fluvial, (2) periglacial, (3) paleolacustrine, and (4) hydrothermal features and processes, and will complement investigations carried out by the Haughton Impact Structure Study (HISS) Project [17]. Both similarities and differences between Haughton and Mars are of interest and will be considered during HM-97. Fluvial investigations will include examining the nature of the drainage network at and near Haughton, in particular determining the possible role of headward sapping, a fluvial process suspected to have given rise to the small valley networks on early Mars [e.g., 18]. Periglacial investigations will include an inventory of periglacial formations at and near Haughton, and a comparison of these features with those attributed to periglacial processes on Mars [e.g., 18–20]. Periglacial investigations will also include a study of how materials specific to the crater (e.g., its “regolith-like” processes). Paleolacustrine investigations will include a study of the physical evolution of Haughton’s paleolake (e.g., inference of climatic variations from the varves preserved in its paleolacustrine sediments [e.g., 5]). Hydrothermal investigations will include a search for evidence of hydrothermal activity in the initial postimpact stage of Haughton’s history, and an attempt to determine how long this activity might have lasted.

The rationale, approach, and objectives of HM-97 will be presented in more detail during the Early Mars conference. Ideas and suggestions for optimizing the scientific return of this study will be welcome. It is hoped that HM-97 will advance our understanding of what early Mars was like, of how Mars has evolved through time, and of how best to explore that planet in the near future.

**Acknowledgments:** HM-97 is supported by NASA and the National Research Council.

**References:** [1] Squyres S. W. and Kasting J. F. (1994) *Science*, 265, 744–749. [2] Gibson E. K. et al. (1983) *JGR*, 88, 912–928. [3] McKay C. P. et al. (1985) *Nature*, 313, 561–562. [4] NASA and NSF Rept., Dec. 1990, 19 pp. [5] Hickey L. J. et al. (1988) *Meteoritics*, 23, 249–254. [6] Kahn R. (1985) *Icarus*, 62, 175–190. [7] McKay C. P. and Nedell S. S. (1988) *Icarus*, 73, 142–148. [8] Pollack J. B. et al. (1990) *JGR*, 95, 14595–14628. [9] Mittlefehldt D. W. (1994) *Meteoritics*, 29, 214–221. [10] McKay D. S. et al. (1996) *Science*, 273, 924–930. [11] Goldspiel J. and Squyres S. W. (1991) *Icarus*, 89, 392–410. [12] Scott D. et al. (1992) *Proc. LPS, Vol. 22*, pp. 53–62. [13] Lee P. (1993) *LPI Tech. Rpt. 93-03, Part 1*, p. 17. [14] Wharton R. A. et al. (1987) *Nature*, 325, 343–345. [15] Wharton R. A. et al. (1995) *J. Paleolim.*, 13, 267–283. [16] McKay C. P. and Davis W. L. (1991) *Icarus*, 90, 214–221. [17] Grieve R. A. F. (1988) *Meteoritics*, 23, 249–254. [18] Carr M. H. (1996) *Water on Mars*, Oxford Univ., 229 pp. [19] Lucchitta B. K. (1981) *Icarus*, 90, 264–303. [20] Squyres S. W. (1989) *Icarus*, 79, 229–288.

# ICE IN CHANNELS AND ICE-ROCK MIXTURES IN VALLEYS ON MARS: DID THEY SLIDE ON DEFORMABLE RUBBLE LIKE ANTARCTIC ICE STREAMS?

B. K. Lucchitta, U.S. Geological Survey, 2255 N. Gemini Drive, Flagstaff AZ 86001, USA (blucchitta@flagmail.wr.usgs.gov).

Recent studies of ice streams in Antarctica reveal a mechanism of basal motion that may apply to channels and valleys on Mars. The mechanism is sliding of the ice on deformable water-saturated till under high pore pressures. Ice in outflow channels on Mars [1] may have slid on rubbly weathering products. However, elevated heatflow is needed to melt the base of the ice. Either volcanism or higher heatflow more than 2 b.y. ago [2] could have raised the temperature at the base of the ice and generated water to fill pores. Regarding valley networks, higher heatflow 3 b.y. ago could have allowed sliding of ice-saturated overburden at a few hundred meters depth. If the pristine valleys were somewhat deeper than they are now, they could have formed by the same mechanism.

Recent sounding of the seafloor in front of the Ross Ice Shelf in Antarctica reveals large persistent patterns of longitudinal megaflutes and drumlinoid forms [3], which bear remarkable resemblance to longitudinal grooves and highly elongated streamlined islands found on the floors of martian outflow channels. The flutes are interpreted to have formed at the base of ice streams during the last glacial advance [3]. Additional similarities of Antarctic ice streams with martian outflow channels are apparent. Antarctic ice streams are 30–80 km wide and hundreds of kilometers long. Martian outflow channels have similar dimensions. Ice stream beds are below sea level [4]. Carr [5] determined that most common floor elevations of martian outflow channels lie below martian data, which may have been close to or below past martian sea levels [6,7]. The Antarctic ice stream bed gradient is flat and locally may go uphill, and surface slopes are exceptionally low [8]. Martian channels also have floor gradients that are shallow or go uphill locally and have low surface gradients [9]. The depth to the bed in ice streams is 1–1.5 km [10]. At bankful stage, the depth of the fluid in outflow channels was 1–2 km, according to the height of bordering scarps [1]. The similarity between Antarctic ice streams and martian outflow channels suggests that ice may have flowed through and shaped the outflow channels [1], and that perhaps the mechanism of motion of Antarctic ice streams also operated in outflow channels. In addition, sliding on deformable rubble may explain the formation of small valley networks.

The large Siple Coast Antarctic ice streams are thought to slide over longitudinally grooved, deforming till, where much of the movement is within the till [10,11]. The till is saturated with water at high pore pressures that supports nearly the entire weight of the ice [10,4]. The small differential between overburden pressure and pore pressure at the bed is more important than the volume of water, but water needs to be supplied to the till interface [4]. For pore pressures to remain high, the ice streams have to act as a seal that blocks the flow of water through them, and the rock underneath has to be of low permeability to prevent the water from draining away. The water is thought to have been derived from melting ice due to geothermal heat and perhaps volcanic heat [10]. Once moving, frictional heat will tend to keep the water from refreezing.

A similar mechanism of sliding on deformable rubble may have operated at the base of outflow channels and small valleys on Mars. Indeed, such a mechanism has recently been proposed by Carr [5] for

fretted channels and valleys on Mars. Most of the conditions for the Antarctic sliding mechanism are met for martian outflow channels. *In situ* rubble from weathering products may have served as the deformable layer. The channel ice may have come from ice dams and jams [1], from frozen or partially frozen lakes [12], from segregated masses akin to ice sills or laccoliths [13], from glacier ice [7,14], or from icings above springs [1]. The channel ice forms the seal above the sliding horizons, the bedrock the seal below so that water could accumulate under high pore pressures. For small valleys in highlands, deformable breccia with mechanical properties similar to till [15,16] probably occurs at 1–2 km depth. Layers that may represent impermeable horizons have also been recognized in many places at these depths [17,18]. Such layers may form the seal below the sliding horizons. The ice-saturated ground above [19,5] would provide the seal in the overburden and furnish the water needed to pressurize the pores.

Water needs to be liberated at the base of the sliding masses to generate high pore pressures. The depth to melting can be calculated from the heatflow equation  $z = k/Q (t_p - t_s)$ ; where  $z$  = thickness of the measured layer, here the depth to melting;  $k$  = thermal conductivity;  $Q$  = heatflow;  $t_p$  = temperature at the lower boundary of the layer, here the melting temperature; and  $t_s$  = annual mean surface temperature. Depth to melting can be measured to the 273 K isotherm for water ice, or to the 252 K isotherm for NaCl brines, which are likely to occur on Mars [21]. The depth at which water ice overburden would melt on Mars under current equatorial surface temperatures (218 K [20]) is nearly 5 km, using a heatflow of  $30 \text{ mWm}^{-2}$  [20] and a thermal conductivity of ice of  $k = 2.6 \text{ J m}^{-1} \text{ s}^{-1} \text{ K}^{-1}$  (after [21]). Clearly, this depth is in excess of the common depth of outflow channels. Evidently, warmer climates would be needed to make the ice-stream mechanism work. However, outflow channels date from the martian mid-history or even late history [22], when the existence of warmer climates is conjectural. Therefore, elevated heatflow is needed to liberate water from ice at the base of the outflow channels.

The possible association of channels and valleys with regions of elevated heatflow is suggested by proximity to grabens [23], dark, most likely mafic, materials [24], and volcanos [25]. Assuming a heatflow of  $90 \text{ mWm}^{-2}$ , representative of some volcanic regions on Earth [26], and using the other parameters given for ice above, melting of ice overburden would have occurred at a depth of 1.6 km using the 273 K isotherm (water ice) and at 1.0 km using 252 K (NaCl brines). Thus, on the floor of ice-filled, 1–2-km-deep outflow channels, water could have been liberated in the equatorial areas of Mars if the region had elevated heat flow due to volcanism.

Past heat flows have been addressed by Schubert and Spohn [2]. Their model estimates mantle heat flows of about  $40 \text{ mWm}^{-2}$ , 1 b.y. ago; of about  $70 \text{ mWm}^{-2}$ , 2 b.y. ago; and of about  $100 \text{ mWm}^{-2}$ , 3 b.y. ago. Accordingly, 2 b.y. ago and earlier, melting would occur at depths of 2.0 km or less (273 K isotherm, water) or 1.3 km or less (252 K isotherm, NaCl brine), and ice could have flowed in outflow channels.

Most valleys on Mars are ancient (upper Noachian [22]) and formed during a time when heat flow was elevated and melting occurred at much shallower levels than today. The depth to melting critically depends on the thermal conductivity used for the martian highlands. Clifford [20] proposed a thermal conductivity of  $2.0 \text{ J m}^{-1} \text{ s}^{-1} \text{ K}^{-1}$  (an average between frozen soils and vesicular basalt). Rossbacher and Judson [19] used a thermal conductivity of  $0.8 \text{ J}$

$\text{m}^{-1} \text{s}^{-1} \text{K}^{-1}$  (frozen limonitic soil). Applying current surface temperatures, Schubert and Spohn's [2] heatflow values of 3 b.y. ago, and Clifford's [20] thermal conductivity, the depth to melting of ice-rich rock overburden would have been 1.1 km (273 K isotherm, water) or 0.7 km (252 K isotherm, NaCl brine). Using Rossbacher and Judson's [19] thermal conductivity, the depth to melting of ice-rich overburden would have been 0.4 km or 0.3 km respectively. The latter depths fall within the range of depths of small valleys on Mars [27], especially if one assumes that the valleys have been infilled with erosional debris. Thus, about 3 b.y. ago, during times of elevated heatflow, water may have been liberated at the floor level of small valleys, allowing pore pressures to build. Given lack of restraint at the bottom of slopes and local concentration of fluids, the ice-rich ground could have become mobilized and slid in the manner of Antarctic ice streams.

**References:** [1] Lucchitta (1982) *JGR*, 87, 9951–9973. [2] Schubert and Spohn (1990) *JGR*, 95, 14095–14104. [3] Shipp and Anderson (1997) in (Davies et al., eds.), Chapman and Hall, London, in press. [4] Paterson (1994) Pergamon Press. [5] Carr (1995) *JGR*, 100, 7479–7507. [6] Parker et al. (1989) *Icarus*, 82, 111–145. [7] Baker et al. (1991) *Nature*, 352, 589–594. [8] Drewry (1983) Scott Polar Res. Inst., Cambridge. [9] Lucchitta and Ferguson (1983) *Proc. LPSC 13th*, in *JGR*, 88, A553–A568. [10] Blankenship et al. (1986) *Nature*, 322, 54–57. [11] Alley et al. (1986) *Nature*, 322, 57–59. [12] DeHon (1992) *Earth, Moon, Planets*, 56, 95–122. [13] Howard (1990) *NASA TM-4300*, pp. 120–122. [14] Kargel and Strom (1992) *Geology*, 20, 3–7. [15] Clow and Moore (1988) *LPS XX*, 201–202. [16] MacKinnon and Tanaka (1989) *JGR*, 94, 17359–17370. [17] Soderblom and Wenner (1978) *Icarus*, 34, 622–637. [18] Davis and Golombek (1990) *JGR*, 95, 14231–14248. [19] Rossbacher and Judson (1981) *Icarus*, 45, 39–59. [20] Clifford (1993) *JGR*, 98, 10973–11016. [21] Glen (1974) *Cold Regions Sci. Engin. Monograph II-C2a*, CRREL, Hanover, New Hampshire. [22] Tanaka (1986) *Proc. LPSC 17th*, in *JGR*, 91, E139–E158. [23] Zimbelman et al. (1992) *JGR*, 97, 18309–18317. [24] Geissler et al. (1990) *JGR*, 95, 14399–14413. [25] Gulick and Baker (1990) *JGR*, 95, 14325–14344. [26] Sclater et al. (1980) *Rev. Geophys.*, 18, 269–311. [27] Goldspiel et al. (1993) *Icarus*, 105, 479–500.

**EVIDENCE FOR VOLCANISM ASSOCIATED WITH ISMENIAE FOSSAE FRETTE CHANNELS.** G. E. McGill<sup>1</sup> and M. W. Carruthers<sup>1,2</sup>, <sup>1</sup>Department of Geosciences, University of Massachusetts, Amherst MA 01003, USA, <sup>2</sup>Now at the American Museum of Natural History, New York NY, USA.

Fretted channels [1] characterize much of the modified highlands of northern Arabia Terra. These are wide, steep-sided, flat-floored canyons most commonly occurring within the highlands adjacent to areas where the dichotomy boundary is transitional and fretted [2,3]. Many of the fretted channels connect directly with the lowlands to the north, but others are completely closed canyons not connected with the lowlands. The area also includes surface depressions with more gently convex walls and floors that appear similar to the highland surface; some of these open into fretted channels, others are entirely closed.

The importance of ground ice in the development of these channels has been suspected since they were first described [e.g., 2,4,6],

but there is little consensus concerning several important aspects of fretted channel development: (1) the dominant erosional process responsible, (2) the mechanism for releasing water, (3) the role of impact craters, (4) the origin of closed canyons, and (5) the controls on channel loci. Although our work has addressed most of these questions, here we concentrate primarily on a possible mechanism for providing liquid water and for explaining the existence of closed canyons as well as through-going channels.

Several workers have noted that fretted channels transect and incorporate craters [2,7,8], and many of the fretted channels follow arcuate courses apparently controlled by ancient crater and basin structures [8–10]. Schultz and Glicken [10] further proposed that igneous activity localized by impact craters could be responsible for melting and mobilizing ground ice and thus providing water for channel development. Some troughs and canyons are probably controlled by faults related to the dichotomy boundary [11].

A number of features within the area of Ismeniae Fossae in northern Arabia Terra have been interpreted by Carruthers [12,13] as due to volcanic or intrusive activity including at least some of the craters incorporated into fretted channels. The evidence supporting these interpretations ranges from very good to circumstantial. Other interpretations are clearly possible for the weaker cases, but a more coherent regional model results from the volcanic and intrusive interpretations. Here we will restrict the discussion to two features for which the evidence favoring a volcanic origin seems most convincing to us. Both occur in association with a complex fretted channel with branches heading in depressions at 35.5°N, 334.5°W and 34.5°N, 332°W. The channel flows in a general east-northeast to east direction to about 38°N, 325.5°W, where it turns abruptly north through a degraded crater to debouch onto the northern lowlands within the southern part of the fretted terrain of Deuteronilus Mensae. The channel is interrupted immediately downstream of the eastern head and again at 36°N, 326.5°W by ejecta blankets of younger craters. Several stubby tributaries join the channel along its course, and two substantial tributaries join at the point where it turns abruptly northward. The channel walls are scalloped into arcuate embayments in many places, and more complete craterlike depressions are locally incorporated. Two of these craterlike depressions provide morphological evidence suggestive of a volcanic origin, the depression at the western head of the channel, and a depression at 37°N, 332°W.

The western channel head is a depression 10 × 15 km across and 600–700 m deep. It is separated from the downstream reaches of the channel by a fracture-bounded block, and thus any fluid flow out of the depression was probably subsurface within the fractures. The depression lies on a broad rise with smooth upper flanks, and with lower flanks on the north, west, and south sides that are characterized by lobate deposits cut by radial valleys a few hundred meters wide and up to 30 km long. On the floor of the depression is a dark, fractured dome-shaped mound ~4 km wide and 100 m high. The broad, low profile and steep inner slopes of the crater suggest a comparison with terrestrial maar craters. The lobed and gullied lower flank resembles early wet base surge deposits from phreatomagmatic eruptions; the smooth upper flank is similar to later, dryer ash deposits [e.g., 14,15]. The dome-shaped mound is interpreted as a late-stage lava dome, such as is present in the East Ukinrek maar in Alaska [16]. The evidence favoring a volcanic origin for this depression is very good; its morphology and the



probable basaltic composition of the magma support interpreting it as a maar. A hydrovolcanic origin was suggested [17,18] for the morphologically comparable gullied deposits on the flanks of Tyrrhena and Hadriaca Paterae.

About 120 km downstream from its western head the channel incorporates an elongate, scallop-walled depression about 20 × 35 km across and 1100 m deep. The northeastern and southern flanks of the depression slope outward at 5°–10°; these flanks are lighter and smoother than the surrounding highland surface. Lobate and gullied lower flank deposits are not apparent. Within the depression is a dark, gullied mound 8 km wide and 400–500 m high. Because it is distinctly darker than the walls of the depression, this mound is not likely to be an erosional remnant. We infer that it, too, is a late-stage lava dome. The irregular shape, complex scalloped walls, smooth outward sloping flanks, and dark interior dome all support a volcanic rather than an impact origin for this depression. Again its general morphology suggests a comparison with terrestrial maar craters. The depth of the depression and the multiple scallops on the walls imply that if it is a maar, it resulted from more than one explosive event.

Phreatovolcanism on Mars would probably involve magma-ice interaction rather than magma-water interaction. There is an analog on Earth: the Espenberg maars in northwestern Alaska [19,20]. These are large (4–8 km in diameter) compared to other maars on Earth, and there is evidence from bathymetric data [21] for multiple explosive events during their formation.

As noted above, the courses of fretted channels appear to be controlled by older fractures related to impact craters and basins and to the dichotomy boundary. These fractures would tend to concentrate ground ice into large masses, as commonly happens within permafrost terrains on Earth. The evidence for volcanic activity presented here thus suggests a ready source of heat to melt ground ice over a large region, and it would be entirely logical for future surface channels to be initiated as collapse troughs above ice-filled fractures. This not only accounts for the apparent structural control of channel courses, but also provides an explanation for closed canyons and incompletely developed valleys. For these latter features, the water generated by melting ice in fractures cannot have escaped by surface run-off. It is possible that the water escaped as groundwater in fracture porosity, but it also could have been driven to the surface by intrusive heating and sublimated into the atmosphere. If the volcanic depressions here described (and others likely present but without surviving diagnostic characteristics) are maars, as we suspect, then at least some of the widening and deepening of the fretted channels could be due to water released by phreatomagmatic eruptions. Mass wasting processes, for which much evidence exists [4–6,22], very likely have widened the channels and modified their floors, obscuring much of the evidence for earlier processes of erosion and transportation.

**References:** [1] Sharp R. P. and Malin M. C. (1975) *GSA Bull.*, 86, 593–609. [2] Sharp R. P. (1973) *JGR*, 78, 4073–4083. [3] Parker T. J. et al. (1989) *Icarus*, 82, 111–145. [4] Squyres S. W. (1978) *Icarus*, 34, 600–613. [5] Squyres S. W. (1979) *JGR*, 84, 8087–8096. [6] Lucchitta B. K. (1984) *Proc. LPS 14th*, in *JGR*, 89, B409–B418. [7] Malin M. C. (1976) *JGR*, 81, 4825–4845. [8] Schultz P. H. et al. (1982) *JGR*, 87, 9803–9820. [9] Lucchitta B. K. (1978) *U.S. Geol. Surv. Map I-1065*. [10] Schultz P. H. and Glicken H. (1979) *JGR*, 84, 8033–8047. [11] Dimitriou A. (1990) M.S. thesis,

Univ. of Massachusetts. [12] Carruthers M. W. (1995) *LPS XXVI*, pp. 217–218. [13] Carruthers M. W., *JGR*, in review. [14] Aranda-Gomez J. J. et al. (1992) *Bull. Volcanol.*, 54, 393–404. [15] Godchaux M. M. et al. (1992) *J. Volcanol. Geotherm. Res.*, 52, 1–25. [16] Kienle J. et al. (1980) *J. Volcanol. Geotherm. Res.*, 7, 11–37. [17] Greeley R. and Crown D. A. (1990) *JGR*, 95, 7133–7149. [18] Crown D. A. and Greeley R. (1993) *JGR*, 98, 3431–3451. [19] Beget J. E. and Mann D. (1992) *Eos Trans. AGU*, 73, 636. [20] Beget J. E. et al. (1996) *Arctic*, 49, 62–69. [21] Charron S. D. (1995) M.S. thesis, Univ. of Massachusetts. [22] Carr M. H. (1995) *JGR*, 100, 7479–7507.

**MARS METEORITES AND PANSPERMIAN POSSIBILITIES.** H. J. Melosh, Lunar and Planetary Laboratory, University of Arizona, Tucson AZ 85721, USA (jmelosh@lpl.arizona.edu).

It is now widely accepted that the SNC meteorite clan, including the rogue ALH 84001, originated on Mars. However, only two decades ago, no less an authority than Gene Shoemaker had confidently asserted that any material ejected from the surface of a planet at escape velocity would be either vaporized or completely melted. Certainly, any micro-organisms residing in it would be destroyed by the heat. So what has changed in the meantime that now permits us to think that, not only may rocks be launched into space from another planet, but that these rocks might, just possibly, carry viable micro-organisms from one planet to another?

The principal argument that impacts can eject nearly intact rocks into interplanetary space is derived from the rocks themselves. In the wake of much argument and measurement, a convincing case has been built that the SNC meteorite clan, in particular the gas-containing EETA 79001, originated on the planet Mars. The case for meteorite ejection of intact rocks from a planetary-scale body was further bolstered by the recognition of meteorites from the Moon in 1983. Although some of these rocks show signs of high shock pressures (Shergotty, the type shergottite, contains the first diaplectic glass—maskelyenite—recognized by terrestrial mineralogists), others, such as Nakhla, exhibit no trace of shock metamorphism.

These observations are now supported by both theoretical understanding of how lightly shocked planetary surface material can be launched at high speed by large impacts as well as by laboratory experiments that demonstrate that the process works as expected. The most characteristic feature of this process is that the high-speed lightly shocked ejecta must originate from close to the surface of the target planet.

The old (and still mostly correct) argument against the possibility of high-speed ejection of intact rocks revolves around the Hugoniot relation that connects the pressure jump across a shock wave with the corresponding velocity jump. This relation has been measured directly for a wide variety of geologic materials and in general shows that, if the velocity jump is comparable to the escape velocity of Mars (5.0 km/s), then the pressure jump must exceed about 150 GPa for basalt—easily enough to melt and partly vaporize the rock.

However, although the Hugoniot relation holds for the bulk of the rocks in the vicinity of a large impact, a small volume very close to the surface can escape its constraints. At a free surface the pressure must stay rigorously at zero, no matter how close to the impact site the surface rocks may lie. Thus, surface rocks very close

to the site where the impactor strikes (which is generally well inside the final crater) remain at zero pressure while other rocks a short distance below the surface are compressed to high pressure by the impact. This produces a large pressure gradient in the rocks just below the surface. Since the acceleration of this material is directly proportional to the pressure gradient, these rocks, protected from high pressure by their proximity to the free surface, achieve high velocities without being subjected to high pressures [1,2].

This theoretical picture was augmented by an experiment performed by Gratz et al. at the Lawrence-Livermore National Laboratory [3]. In this experiment the ejecta from the face of a block of Westerly Granite that had been impacted at 4 km/s with a penny-sized aluminum disk was collected. The result confirmed theoretical expectations: millimeter-sized fragments of unshocked quartz were blasted out at speeds of more than 1 km/s, a substantial fraction of the impact speed itself.

The case for high-speed ejection of lightly shocked material is also supported by observations of the ejecta of Ries Crater in Germany. In addition to the usual highly shocked and melted debris (for example, the Moldavite tektites were produced from melted target rocks and showered over the terrain that would become Czechoslovakia), lightly shocked blocks of Malm limestone, the uppermost geologic rock unit at the site of the impact, were ejected at least 200 km from the impact site at a speed of more than 1.4 km/s. Although these blocks did not actually leave the Earth, their ejection speed is far higher than the Hugoniot relation would predict from their observed shock damage.

It is thus clear that at least some of the ejecta from a large meteorite impact is both lightly shocked and swift, some of it capable of leaving the planet it originated on. Moreover, this material comes from close to the planet's surface. Since this is just where biological, specifically microbial, activity is most intense, it seems possible that some of this ejecta may carry micro-organisms into space.

It is easy to establish some limits on the maximum shock pressure that a rock carrying viable micro-organisms might endure. At relatively low shock pressures,  $P$ , the main effect of the shock wave is to crush the rock, eliminating any initial porosity,  $\phi$ , that may be present. The irreversible work done on the rock as it is crushed is  $P\phi$ . It seems likely that if this work raises the rock's temperature much above 100°C it will be sterilized: no viable micro-organisms will survive. The shock pressure  $P$  that can just raise the temperature of a typical rock with density 2700 kg/m<sup>3</sup> and heat capacity 700 J/kg-K from 0° to 100°C is about 1 GPa. This pressure corresponds approximately with the Hugoniot Elastic Limit of typical rocks, a pressure where substantial crushing is noted experimentally and where shatter cones may appear.

Given this limit on the maximum pressure that a rock may experience without being sterilized (I will call such unsterilized ejecta "fecund" material in the following discussion), it is possible to estimate the total mass and fragment size of ejecta from Mars (or the Earth!) that may achieve escape velocity and could potentially transport life from one planet to another. This estimate shows that impacts that produce craters more than about 30 km in diameter are capable of ejecting large numbers of fecund fragments larger than 1 m in diameter [4].

Upon reaching space many micro-organisms entrained in the ejecta will die. However, the combination of freeze-drying in hard vacuum (lopholization) and the preservation of microbial spores

may make it possible for an ejecta fragment to inoculate any other world it falls on with a sample of life from its planet of origin. The large size of many ejecta fragments (1 m or more in diameter) can easily shield its microbial passengers from UV radiation, although shielding from cosmic rays would require a much larger fragment (10 m or more in diameter). One unanswered question is just how much radiation various micro-organisms can tolerate in a dormant state. The many measurements of the radiation tolerance of metabolizing organisms are not relevant here, because such organisms have active systems that repair radiation damage to their DNA.

Upon arrival at a new planet, the few-meter size of such fragments is nearly ideal for deceleration in the atmosphere of one of the terrestrial planets (early Mars would have been more favorable for this scenario than the present planet) and arrival at the surface at relatively low velocity (near terminal velocity for the atmosphere). Such a rock would have experienced crushing aerodynamic forces during its deceleration and the former interior would thus be exposed. A better vector for inoculating planets with life probably could not have been designed intentionally.

Recent work by Gladman et al. [5] has suggested that the transfer of ejecta from Mars to Earth is assisted by a "fast track" through a series of orbital resonances that cuts the expected transfer time of ejecta from more than 10 m.y. (estimated from Monte Carlo orbital evolution models) to the order of 1 m.y. Earth to Mars evolution is generally slower and more difficult, so a smaller proportion of Earth ejecta hit Mars than Mars ejecta hit Earth, although both processes do take place. Similarly, much ejecta finds its way to Venus as well.

It thus seems plausible that a significant amount of exchange of ejecta between the terrestrial planets has occurred, especially during the era of heavy bombardment when cratering rates were at least 1000× higher than at present. Recent discoveries of ancient fossils on Earth suggest that life was extant here, at least, during this era, so a very real possibility exists that early Mars and Venus had the possibility of being colonized by terrestrial life (or perhaps life originated on Mars or Venus and terrestrial life is its offspring!). The proof of this proposal would be the discovery of life (either extant or fossil) that showed affinities with terrestrial life.

**References:** [1] Melosh H. J. (1984) *Icarus*, 59, 234. [2] Melosh H. J. (1985) *Geology*, 13, 144. [3] Gratz A. J. et al. (1993) *Nature*, 363, 522. [4] Melosh H. J. (1988) *Nature*, 332, 687. [5] Gladman B. J. et al. (1996) *Science*, 271, 1387.

**ACTIVE CARBOHYDRATE OLIGOMERS OF BACTERIA IN ANOXIC ENVIRONMENTS.** Y. Miura, Department of Chemistry and Earth Sciences, Faculty of Science, Yamaguchi University, Yoshida, Yamaguchi 753, Japan.

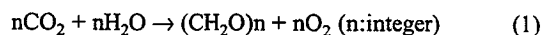
A new type of oligomer  $SO_3$  was found in natural and synthetic materials from the L-lactic acid monomer ( $C_3H_6O_3$ ) by heating to 180°C and rapidly mixing under decreased pressure [1-3]. Oligomers with various degrees of polymerization are obtained from 2 to 23 in the formulae  $(C_3H_4O_2)_z$  with an open-ring structure and with characteristic biological activity, as observed in supramolecules [4]. The oligomer  $SO_3$  provides a significant clue for analyzing the origin of life [5-9] arising from copying system and enzymelike activity in anaerobic and photosynthetic bacteria on the anoxic water planets, Earth and Mars.



**Chemical Evolution of Life:** The chemical evolution of life [5–9] can be summarized in the following steps: (1) conversion of inorganic  $\text{CO}_2$ ,  $\text{H}_2\text{O}$  to organic compounds  $(\text{CH}_2\text{O})_n$  by fermentation of spheroidal prokaryotes, or by primitive photosynthesis; (2) conversion of inorganic  $\text{CO}_2$ ,  $\text{H}_2\text{O}$ , and  $\text{N}_2$  to simple organic monomers of  $\text{HCHO}$  and  $\text{HCN}$ , sugars, amino acids and bases, and nucleic acids and proteins; and (3) conversions of protein and nucleic acids to life precursors and primitive organisms.

Although the monomers  $(\text{CH}_2\text{O})_n$  are important energy-transferring molecules, intermediate organic oligomers with biological activity have not been reported previously in terrestrial rocks [6,7] or meteorites [11], nor in synthetic experiments [5,8]. In spite of the important roles of sugars and RNA or DNA giant molecules, there are few detailed studies of carbohydrate molecules with biological activity from low to high degrees of polymerization. A large amount of carbohydrate oligomers can be explained more detailed reaction in the above (1) process.

**Various Primitive Life Materials:** The following various species of primitive life are considered to be formed in primordial Earth and Mars [13]: (1) anaerobic bacteria (3.8 Ga–2.9 Ga), (2) photosynthetic bacteria (3.3 Ga–2.9 Ga), (3) anaerobic prokaryotes (2.9 Ga–2.4 Ga), (4) aerobic prokaryotes by modern photosynthesis (1.8 Ga–1.0 Ga), (5) eukaryotes (1.5 Ga–1.3 Ga, 0.8 Ga–0.7 Ga, and 0.5 Ga–0.0 Ga), and (6) algae and metazoans (0.7 Ga–0.5 Ga). Before producing the first primitive life on Earth and Mars, it takes ~1 g.y. due to its complex chemical evolution. During anaerobic or photosynthetic bacteria, the main organic materials are  $(\text{CH}_2\text{O})_n$  composition as follows (cf. Table 1)



**New Carbohydrate Oligomers with Characteristic Ring Structure:** Trace amounts of lactic acid  $\text{SO}_3$  oligomers have been extracted from human organisms [1–3]. Large amounts of synthetic  $\text{SO}_3$  are formed from L-lactic acid monomer with inert gas of  $\text{N}_2$ , rapidly stirred (360 rpm) at  $180^\circ\text{C}$  for 10 hr. After cooling the molten solution, the fractions of lactic acid oligomers are measured by the proton-NMR (H-NMR), high-performance liquid chromatography (HPLC), and field-desorption mass spectrometry (FD-MS) to obtain the polymerization indexes ( $z$ ) of the oligomers.

Two types of the oligomer were obtained: a closed ring (CR)  $(\text{C}_3\text{H}_4\text{O}_2)_z$ , and an open chain (OC)  $[(\text{C}_3\text{H}_4\text{O}_2)_z\text{H}_2\text{O}]$ . The computed program CHEM3D for energy-minimizing indicates that  $z = 5$  oligomers have a zig-zag CR structure with a large cavity, or OC feature, and that the  $z = 11$  oligomers have a C-shaped curled CR with an OC, or simple curled OC. The CR structures are confirmed by adding  $\text{Na}^+$  ions or  $\text{H}_2\text{O}$  molecules into the vacant hole of the CR structure.

**Active Carbohydrate Oligomers as Enzymelike Characteristics:** Among  $(\text{CH}_2\text{O})_n$  carbohydrates of formaldehyde ( $n = 1$ ), acetic acid ( $n = 2$ ), lactic acid ( $n = 3$ ), ribose ( $n = 5$ ), and glucose ( $n = 6$ ), the characteristic oligomer structure and biological activity can be found only in the lactic acid ( $n = 3$ ) oligomer. The lactic acid monomer has the three distinct characteristics of the recycling process: (1) change from monomer to oligomer and polymer by natural dehydration [12], (2) alteration from polymer to monomer by natural hydrolysis, and (3) replacement from organic monomer to inorganic compounds of water and  $\text{CO}_2$  by primitive fermentation or photosynthesis in anoxic conditions as shown in equation (1).

TABLE 1. Characteristic cyclic system of  $\text{SO}_3$  oligomers in primitive Earth and Mars [1,9,10].

---

Water and carbon dioxide  $\rightarrow$  (anaerobic or primitive photosynthetic bacteria)  $\rightarrow (\text{CH}_2\text{O})_n$  monomers  $\rightarrow (\text{CH}_2\text{O})_3 \rightarrow$  (dehydration)  $\rightarrow \text{SO}_3$  lactic acid oligomer  $\rightarrow$  (copying)  $\rightarrow$  polylactic acid  $\rightarrow$  (hydrolysis)  $\rightarrow$  lactic acid monomer  $\rightarrow \text{H}_2\text{O}$  and  $\text{CO}_2$

---

The supramolecule  $(\text{C}_3\text{H}_4\text{O}_2)_z$  derived from  $(\text{C}_3\text{H}_6\text{O}_3)$  has effects similar to the recognition of elements or molecules, transformation, and translocation of an enzymelike reaction as the following characteristics: (1) host (by CR oligomers) and guest (by  $\text{Na}^+$ ,  $\text{H}_2\text{O}$  and OC oligomer) relation by carbohydrate compounds similar to biological effect by enzymes of protein compounds. This suggests that life precursors can evolve from the main composition of carbohydrates by slow polymerization during the first chemical evolution of the origin of the life. (2) Production of chemical energy from oligomers  $(\text{CH}_2\text{O})_n$  to lactic acid monomers by enzymelike reaction in the CR ring structure. This indicates that chemical energy by  $\text{SO}_3$  fermentation can produce in anoxic conditions among  $(\text{C}_3\text{H}_6\text{O}_3)_z$  and materials expressed in equation (1). This result suggests that the  $\text{SO}_3$  fermentation in anaerobic bacteria does not require the formation of phosphorous compounds (ATP or ADP) during primitive Earth and Mars. (3) The CR structure can duplicate to polylactic acid [1–3,12]. This indicates that primitive copying ability starts by polymerization from monomers to oligomers or polymers before establishing duplication ability such as the RNA or DNA complex.

**References:** [1] Miura Y. (1996) *Proc. 29th ISAS Lunar Planet. Symp. (ISAS, Japan)*, 29, 289–292. [2] Miura Y. (1996) in *Japanese Govt. Rept. KK-B1 of Formation and Metamorphic Process of Primordial Organisms in the Solar System (Hokkaido Univ)*, Grain Formation Workshop Vol. XVIII, 5–8. [3] Miura Y. (1997) *Proc. New Frontiers in Biochemical Fluid Engineering (JSME, Japan)*, p. 4, in press. [4] Lehn J.-M. (1995) *Supramolecular Chemistry*, VCH, Weinheim, Germany, 271 pp. [5] Miller S. L. (1953) *Science*, 117, 528–529. [6] Walter M. R. et al. (1980) *Nature*, 284, 443–446. [7] Schopf J. W. (1993) *Science*, 260, 640–646. [8] Chyba C. and Sagan C. (1992) *Nature*, 355, 125–132. [9] McKay D. S. et al. (1996) *Science*, 273, 924–930. [10] Miura Y. (1994) *Astron. Soc. Pacific Conf. Series*, 63, 259–264. [11] Hayatsu R. et al. (1977) *GCA*, 41, 1325–1339. [12] Gilding D. K. and Reed A. M. (1979) *Polymer*, 20, 1459–1466. [13] Schopf J. W. (1977) *Precambrian Res.*, 5, 143–173.

**CHEMICAL EVOLUTION BY SHOCK-WAVE ENERGY IN ANOXIC ATMOSPHERES.** Y. Miura, Department of Chemistry and Earth Sciences, Faculty of Science, Yamaguchi University, Yoshida, Yamaguchi 753, Japan.

Nitrogen-bearing organic compounds are obtained by impacting shock-wave energies of thunder, volcanic eruption, asteroids, and cosmic-ray bombardments in anoxic atmospheres. It takes a long time for chemical evolution to N-bearing compounds in an anoxic atmosphere because shock-wave events are extremely localized for chemical evolution even in asteroid impacts. Carbohydrates in primitive oceans are widely formed in anoxic atmospheres on Earth and Mars.

**Active Carbohydrates in Anoxic Atmospheres:** Miura [1–4] reported that some  $(\text{CH}_2\text{O})_n$  carbohydrates show oligomers and that lactic acid ( $\text{C}_3\text{H}_5\text{O}_3$ ) reveals  $\text{SO}_3$  molecules of oligomer structure  $\{(\text{C}_3\text{H}_5\text{O}_3)_z\}$  with biological activity characteristic of supramolecules [5]. The  $\text{SO}_3$  molecules can be synthesized under acid liquid conditions and a high temperature of  $180^\circ\text{C}$ . This suggests that active carbohydrates can be formed widely on primitive seawaters on Earth and Mars without strong shock-wave energy.

**Nitrogen-bearing Compounds by Shock-Wave Energy:** Miller [6] synthesized a N-bearing amino acid from inorganic compounds by the shock-wave energy of spark. Similar organic compounds of N-bearing composition are formed by other shock-wave energy such as thunder storms, volcanic eruptions, hydrothermal vents in deep sea, and asteroids or cosmic-ray bombardments. However, it takes a long time to form anaerobic bacteria for chemical evolution.

The first life on primitive Earth and Mars is considered to be formed by tiny RNA organisms of N-bearing compounds in large amounts of active carbohydrate solution. The difference in amounts between large carbohydrates and small N-bearing organic compounds results in a long history of about 1 g.y. to form life precursors of prokaryotic cell on primordial Earth and Mars.

**Circulation of C-bearing Materials on the Earth and Mars:** From the recycle system of C-bearing materials on Earth, the constituent organic compounds of life materials are considered to be one material-state of the various compounds between inorganic and organic compounds. Therefore, supramolecules of lactic acid oligomers  $\text{SO}_3$  are significant intermediates to produce enzyme-like activity on Earth and Mars. If seawater and the atmosphere necessary for recycling C-bearing materials between inorganic and organic compounds cannot exist for long geological history, then the chemical evolution required for producing life-complex from prokaryotic (in anoxic environments) to eukaryotes (in O-rich environments) cells is considered to be intercepted probably on primordial martian surface.

**Mineralized Fossils from Organic Compounds:** Light elements of CHON organisms can remain as fossils of carbonates, phosphates, or sulfides in anoxic primordial environments by secondary reaction. Martian meteorite ALH 84001 [7] with carbonates, magnetite, and pyrothite as fossilized minerals is considered to be replaced fossil of anaerobic or photosynthetic bacteria. Almost all fossils on Earth are found in sedimentary rocks, though the ALH 84001 rock is primordial igneous brecciated rock. Therefore it is considered that the rock with carbonate globules is captured in the interior by meteoritic impacts on the martian sea or hot spring.

**References:** [1] Miura Y. (1994) *Astron. Soc. Pacific Conf. Series*, 63, 259–264. [2] Miura Y. (1996) *Proc. 29th ISAS Lunar Planet. Symp. (ISAS, Japan)*, 29, 289–292. [3] Miura Y. (1996) in *Japanese Govt. Rept. KK-B1 of Formation and Metamorphic Process of Primordial Organisms in the Solar System (Hokkaido Univ.) Grain Formation Workshop Vol. XVIII*, pp. 5–8. [4] Miura Y. (1997) *Proc. New Frontiers in Biochemical Fluid Engineering (JSME, Japan)*, in press. [5] Lehn J.-M. (1995) *Supramolecular Chemistry*, VCH, Weinheim, Germany, 271 pp. [6] Miller S. L. (1953) *Science*, 117, 528–529. [7] McKay D. S. et al. (1996) *Science*, 273, 924–930.

**GOLDENROD PIGMENT AND THE OCCURRENCE OF HEMATITE AND GOETHITE ON THE MARTIAN SURFACE.** R. V. Morris<sup>1</sup> and D. C. Golden<sup>2</sup>, <sup>1</sup>Mail Code SN3, NASA Johnson Space Center, Houston TX 77058, USA (richard.v.morris@jsc.nasa.gov), <sup>2</sup>Dual Inc., Houston TX 77058, USA.

**Introduction:** “Goldenrod iron oxide” is the name for a commercial mineral pigment produced by blending red hematite ( $\alpha\text{-Fe}_2\text{O}_3$ ) and yellow goethite ( $\alpha\text{-FeOOH}$ ) pigments. Evidence for both components of this goldenrod-colored pigment has been extracted from visible and near-IR reflectivity spectra of martian bright regions. The general structure of reflectivity spectra of martian bright regions is a nearly featureless absorption edge from  $\sim 400$  nm to 750 nm and nearly flat reflectivity between 750 nm and 2200 nm. This structure is observed in certain palagonitic soils and is associated with nanophase ferric oxides [1]. Superimposed on this general structure are certain weak features that can be associated with either well-crystalline hematite or goethite. The inflections in the absorption edge near 520 nm and 610 nm, the local reflectivity maximum near 740 nm, and the minimum near 850 nm are consistent with the presence of red (i.e., well-crystalline and pigmentary) hematite [e.g., 2–5]. The assignment of red hematite to the martian spectral data is consistent with low-temperature spectral data for red hematite in synthetic and natural samples [3]. The contribution of red hematite is estimated to be less than 5% [3]. Other martian bright regions, whose areal extent is apparently much less than hematitic regions, have a shallow minimum near 900 nm [5]. Unfortunately, these spectra (ISM data from Phobos-2) do not extend to wavelengths less than  $\sim 750$  nm. One mineralogy suggested by [5] for the 900-nm minimum is goethite. Other possible mineralogies include maghemite, ferrihydrite, jarosite, and schwertmannite [5–7].

In this paper, we document the mineralogy and other physico-chemical properties of goldenrod pigment and describe the spectral properties of its mixtures with a palagonitic tephra from Mauna Kea, Hawai'i. The tephra itself is pigmented by nanophase ferric oxide (np-Ox) [3]. Reflectivity spectra were obtained at temperatures appropriate for the martian surface. The spectra of these mixtures and their temperature dependence have implications for the abundance of hematite and goethite on Mars.

**Properties of Goldenrod Pigment (BLS1):** As shown in Fig. 1, two sextets are present in the Mössbauer spectrum (293 K) of BLS1. Their Mössbauer parameters are within error of literature values [e.g., 8]. Relative areas of hematite and goethite sextet are 0.3 and 0.7. TEM photomicrographs show a mixture of particles with acicular (goethite) and equant (hematite) morphologies. Selected area electron diffraction and lattice imaging was used to associate mineralogy with morphology. Mean dimensions of hematite ( $90 \pm 40$  nm) and goethite ( $510 \pm 160 \times 70 \pm 30$  nm) particles were determined by measuring dimensions of discrete particles on photomicrographs.

The reflectivity spectrum of BLS1 at 293 K is shown between 400 nm and 1200 nm in Fig. 2a. A minimum and a local reflectivity maximum occur at  $882 \pm 6$  nm and  $750 \pm 6$  nm respectively. The BLS1 spectrum could reasonably be attributed to a single ferric-bearing phase even though two phases are actually present. Evidence that the BLS1 spectrum has more than one phase is the

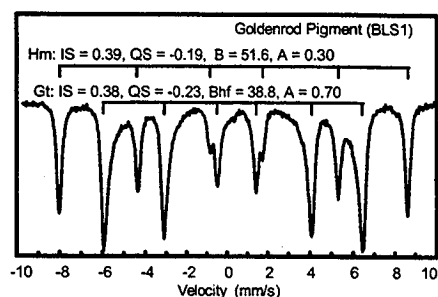


Fig. 1.

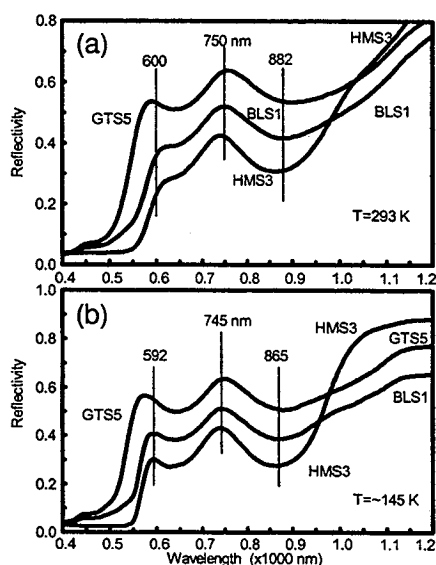


Fig. 2.

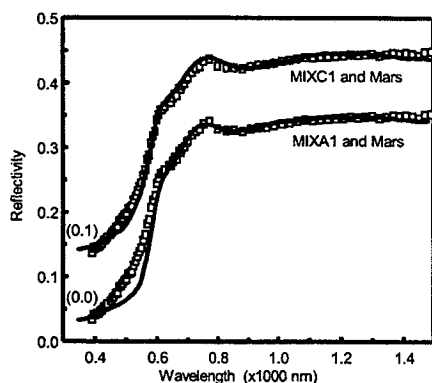


Fig. 3.

presence of the two inflections near 500 nm and 550 nm. Also shown for comparison in Fig. 2a are reflectivity spectra for hematite HMS3 and goethite GTS5, which are synthetic powders described by [8]. Both oxides are well crystalline and are the closest match we have

for the morphology and size of the hematite and goethite components of BLS1.

The BLS1 spectrum is readily understood in terms of spectral features associated with hematite and/or goethite. The 882-nm minimum and 750-nm maximum are intermediate to the corresponding features in hematite and goethite. The 600-nm shoulder and strong inflection near 550 nm correspond to hematite features. And the weak inflection near 500 nm and the 440-nm shoulder correspond to goethite features. Figure 2b shows the same spectra except that the sample temperature is  $\sim 145$  K, which corresponds to the minimum temperature expected on Mars. BLS1, like HMS3 and GTS5, has two minima (865 nm and 640 nm) and two maxima (745 nm and 592 nm) at this temperature. The two minima and 745-nm maximum are intermediate to the corresponding hematite and goethite features. The 592-nm maximum and strong inflection correspond to hematite features, and the 440-nm shoulder corresponds to a goethite feature. The features of BLS1 whose positions are most dependent on temperature are the  $\sim 880$ -nm minimum and the  $\sim 600$ -nm shoulder (at 293 K) to maximum (low temperatures). The former can be attributed to the temperature dependence of the corresponding goethite feature, and the latter results from the temperature dependence of the corresponding hematite feature.

**Application to Martian Spectral Data:** In Fig. 3, we show spectral data for mixtures of palagonitic tephra HWMK530 ( $<150$  nm) [3] with BLS1 (MIXC1: 4.8%) and HMS3 (MIXA1: 2.4%) at 293 K and the martian bright regions spectrum [9], for which estimated martian surface temperature is  $\sim 228$  K [3]. For both mixtures, the depth of the minimum approximates that for the martian spectrum. Although the position of the minimum for the hematite mixture and Mars are the same ( $\sim 860$  nm), the MIXA1 reflectivity is too low near 550 nm, although the difference is less but still significant at low temperatures [3]. The mixture with BLS1 has better agreement near 550 nm, but the minimum is located at longer wavelengths than the martian one. Although we do not yet have low-temperature spectra for MIXC1, we can infer from the temperature dependence of BLS1 (Fig. 2b) that, at low temperatures, the position of the minimum will approximate the martian position and that the reflectivity near 550 nm will also be in better agreement.

These results show that, at low temperatures, martian spectral data like that in Fig. 3 are permissive of considerable goethite (BLS1 is 70% goethite and 30% hematite) even though the positions of the spectral features are compatible with hematite alone. It could be that goethite formed early in martian history when the planet was possibly wetter and warmer and that production of hematite has been favorable since then. It is also possible that goethite is not present and that another phase, similarly more reflective than hematite in the region 350–550 nm, is present and being masked by hematite.

**References:** [1] Morris et al. (1993) *GCA*, 57, 4597. [2] Morris et al. (1989) *JGR*, 94, 2760. [3] Morris et al. (1997) *JGR*, in press. [4] Bell et al. (1990) *JGR*, 95, 14447. [5] Murchie et al. (1993) *Icarus*, 105, 454. [6] Bishop and Murad (1996) *Min. Spec.: Trib. R. Burns, Geochem. Soc.*, 377. [7] Morris et al. (1996) *Min. Spec.: Trib. R. Burns, Geochem. Soc.*, 327. [8] Morris et al. (1985) *JGR*, 90, 3126. [9] Mustard and Bell (1994) *GRL*, 21, 3353.

**MÖSSBAUER MINERALOGY ON MARS.** R. V. Morris<sup>1</sup> and G. Klingelhöfer<sup>2</sup>, <sup>1</sup>Mail Code SN3, NASA Johnson Space Center, Houston TX 77058, USA (richard.v.morris@jsc.nasa.gov), <sup>2</sup>TH Darmstadt, Institut für Nuclear Physics, 64289 Darmstadt, Germany.

**Introduction:** Iron Mössbauer spectroscopy makes use of the resonance absorption of gamma rays (the Mössbauer effect) by <sup>57</sup>Fe (2.2% natural abundance) in a solid material to investigate the splitting of nuclear levels that is produced by interactions with the surrounding electronic environment. A backscatter Mössbauer spectrometer on the martian surface can be used without sample preparation to identify Fe-bearing mineralogies (e.g., olivine, pyroxene, hematite, magnetite, jarosite, and siderite) and quantitatively measure the relative abundance of Fe according to both oxidation state (2+ and 3+ for Mars) and mineralogy. Collectively, we refer to this information as "Mössbauer mineralogy." Flight prototype backscatter Mössbauer spectrometers are under development at TH-Darmstadt (Germany) [1] and at the NASA Johnson Space Center [2]. Using Mars analog samples, we show here representative Mössbauer spectra and derived data that might be obtained from a backscatter Mössbauer spectrometer on the surface of Mars.

**Results and Discussion:** We obtained Mössbauer spectra on three kinds of samples: (1) Zagami, a martian (SNC) meteorite; (2) impact melt rocks (e.g., MAN-74-342A) from Manicouagan crater (Canada); (3) palagonitic (HWMK600) and jarositic (HWMK24) tephra from Mauna Kea volcano (Hawai'i); (4) an Fe ore that contains Fe-bearing carbonate (BCS-301); and (5) an amygdaloidal basalt (Michigan). Arguments can be made for the presence of all of these materials on the martian surface.

The ability of Mössbauer spectroscopy to determine relative abundances of oxidation states of Fe is illustrated for 16 samples of impact melt rock from Manicouagan crater in Fig. 1 [from 3]. The agreement between the values of  $\text{Fe}^{3+}/\text{Fe}^{\text{total}}$  determined chemically and by Mössbauer spectroscopy is very good. Backscatter Mössbauer spectra from a prototype flight unit of the Darmstadt instrument MIMOS II [1] (except for Zagami, which is an inverted transmission spectrum) are shown in Fig. 2. It is evident even by simple inspection that the Fe mineralogy of the samples is quite different. The major Fe-bearing phases identified in the spectra are given on the

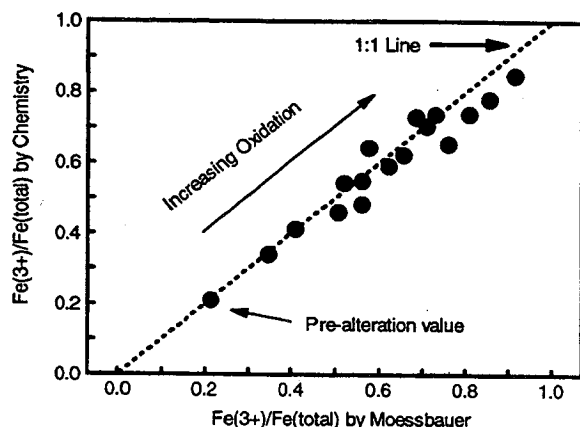


Fig. 1. Comparison of  $\text{Fe}^{3+}/\text{Fe}^{\text{total}}$  determined by chemical analysis and by Mössbauer spectroscopy [from 3].

figure. Several observations can be made: (1) the unweathered sample (Zagami) is clearly distinguishable from the other samples, which are all oxidized; (2) the sulfate-bearing (HWMK24) and carbonate-bearing (BCS-301) samples are distinguishable from each other and from the other samples; (3) magnetite can be identified and distinguished from hematite; and (4) samples oxidatively weathered at relatively low temperatures (HWMK600) and relatively high temperatures (AKB-1 and MAN-74-342A) can be distinguished by the relative proportions of the doublet from nanophase ferric oxide (np-Ox) and the sextet from well-crystalline hematite.

It is evident from Figs. 1 and 2 that a Mössbauer spectrometer will meet science objectives of lander missions to Mars by providing a mineralogical characterization of martian rocks and soils, by identification of rock types (e.g., igneous vs. impact melt rocks), by measurement of Fe oxidation state, and by providing ground-truth for remote sensing measurements, especially at visible and near-IR

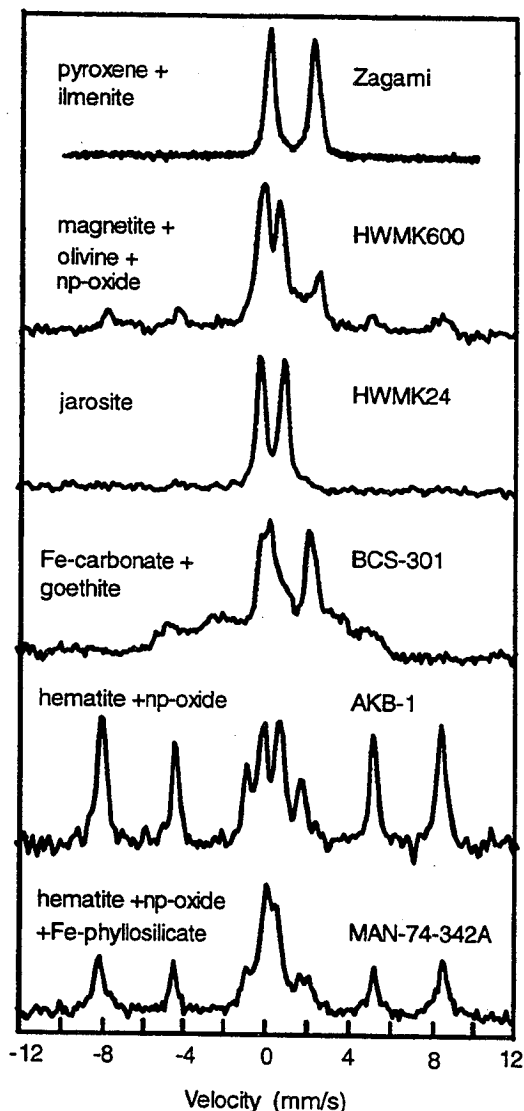


Fig. 2. Backscatter Mössbauer spectra for a martian meteorite (Zagami) and five analogs of weathered ( $\text{Fe}^{3+}$ -rich) martian surface materials.

wavelengths. These data provide information about the nature and extent of atmosphere-surface chemical and physical weathering processes, and are directly relevant to studying the evolution of volatiles and climate over time on Mars.

**Acknowledgments:** G. K. acknowledges the support and cooperation in the MIMOS project by E. Kankleit, P. Held, J. Foh, B. Fegley Jr., E. Evlanov, B. Zubkov, and O. Priloutsii. R.V.M. acknowledges the support and cooperation in the BaMS project by T. Shelfer, T. Nguyen, and D. Agresti. This work is supported by the German Space Agency DARA (G.K.) and the NASA Planetary Instrument Definition and Development Program (R.V.M.).

**References:** [1] Klingelhöfer et al. (1996) *Planet. Space Sci.*, 44, 1277. [2] Shelfer et al. (1996) *LPS XXVII*, 1185. [3] Morris et al. (1995) *JGR*, 100, 5319.

**CHEMICAL AND MINERALOGIC PROCESSES IN MARTIAN SOIL.** J. F. Mustard, Department of Geological Science, Box 1846, Brown University, Providence RI 02912, USA (John\_Mustard@brown.edu).

**Introduction:** The chemical and physical pathways of alteration on Mars are important for understanding the current state of the surface mineralogy, but are also important for considering past conditions. The conditions that existed during chemical alteration are in essence recorded in the mineralogy and the composition of the minerals. Although research has been done on the chemical alteration pathways that may exist from thermodynamics, under hydrothermal conditions, subaerial aqueous deposition, or through the acid weathering of basalts and sulfide deposits, less attention has been paid to soils and the processes that may occur in martian soils. The purpose of this work is to assess the mineralogy of martian soils and the implications for chemical and mineralogical processes.

**Martian Soils and Duricrust:** The fine-grained mobile dust on Mars is widely regarded to consist primarily of smectite clays and nanophase hematite. Duricrust refers to the case-hardened crusts observed at both Viking landing sites [1], which were observed to have several physical forms in the high-resolution images. At the Mutch Memorial Station (MMS), a thick crust with fractures and planar features was exposed by the erosion of the engine exhaust of the lander during landing. Thin and apparently weak surface crusts were also observed. For example, a small slump in a dune of drift material was observed at the MMS station that appeared to be due to failure in a weakly cemented surface layer, and at VL 2, one of the rocks displaced by the sampling arm had a thin layer of weakly cemented soil that adhered to the rock and apparently had formed at the interface between the soil and the atmosphere.

Chemical analyses of crust and clods taken at the MMS showed them to be almost identical in composition to drift material, except for an enrichment in S and Cl [2]. This enrichment, plus the increase in cohesion relative to drift material and layered form are all evidence that the crusts are fine-grained dust cemented to a variable extent by Mg sulfates and perhaps chloride salts [2]. The very thin, low-cohesion crust that formed at the soil-atmosphere interface implies that this is an active process. However, the thicker, buried crusts at MMS also show that these crusts can become quite well developed, either over time or as a function of burial.

Remote sensing observations indicate that regionally extensive deposits of duricrusted soils occur over many regions of Mars, with

important concentrations in Lunae Planum and Oxia Palus [3–5]. Duricrusted regions have moderate thermal inertia (3.5–7.7) and albedo (0.15–0.25) and show a correlation between density (from radar) and thermal conductivity [6]. These units are clearly immobile, and on the basis of Viking Orbiter and lander color observations, [3] proposed that the dark red soils in Oxia Palus and Lunae Planum are an indurated mixture of bright red dust and dark gray, unaltered lithic sands. This view has become widely accepted for the composition of dark red, duricrusted soils on Mars.

**An Alternative Hypothesis:** The problem with this model for dark red soils is that the spectral properties as observed by ISM are not consistent with a simple mixture between dark gray and bright red materials. Not only are mafic mineral absorption features expected from such a mixture not observed [7,8], but the character of the absorption near 0.9  $\mu\text{m}$  is inconsistent with the classic absorption properties of nanophase hematite observed in the laboratory and in spectra of broad regions of Mars [9,10]. The shape and position of this feature cannot be accommodated with simple mixtures of nanophase hematite and mafic minerals without the appearance of associated features in other wavelength regions that are also not observed. These spectral properties are, however, consistent with several types of very fine-grained ferric oxyhydroxides such as ferrihydrite and goethite. Although it is not possible to discriminate which oxides are present solely on the basis of the ISM data, it is possible to infer likely phases on the basis of conditions and mechanisms of formation.

On Earth, water, either as groundwater or as adsorbed water, is considered a requirement for the formation of near-surface and surface crusts in arid regions. Although liquid water is unstable in the near-surface environment of Mars, adsorbed water is stable [11]. Models that describe the exchange of water between volatile reservoirs, including adsorbed water in soils, show that significant fluxes of water in and out of surface soils are expected ( $\text{mg} \times \text{H}_2\text{O}/\text{cm}^3/\text{day}$ ) and these operate on diurnal, seasonal, and millennial timescales [12,13]. Observations from the dry valleys of Antarctica have shown that adsorbed water is capable of transporting significant amounts of dissolved ions through a soil and depositing them near and at the surface [14].

Since water is the principal medium for transport and precipitation of cementing agents, then ferric oxyhydroxides are expected in duricrusts. Hematite is the favored form of ferric oxide based on the thermodynamics of gas-solid reactions, and nanophase hematite has been unambiguously identified in reflectance spectra of Mars [10]. However, in natural environments on Earth where water is present, ferrihydrite is a necessary precursor to the formation of hematite [15]. Ferrihydrite undergoes a low-temperature dehydration-rearrangement reaction to form hematite, whereas the transformation of other ferric oxyhydroxides, such as goethite, to hematite under natural conditions requires either heat (200°–400°C) [16] or a microbial catalyst to form the ferrihydrite precursor [15].

Under current martian surface conditions, ferrihydrite is thermodynamically unstable relative to hematite and thus is expected to undergo the dehydration rearrangement reaction to form hematite when exposed. However, thermodynamic stability does not necessarily lead to this reaction, unless the kinetics of the reaction are also optimum [16]. A simple first-order hypothesis for the existence of immature ferric oxides in duricrusted soils is that the physical properties of the crusts, and associations with other phases (smectite, sulphates, etc.), promote a kinetic stability over the thermodynamic

stability. If the duricrust were disaggregated and the physical and chemical barriers to the reaction were lowered, then this transformation may be kinetically favored as well.

Is there any evidence for the dehydration-rearrangement reaction on Mars? Type II dark streaks in the dark red duricrusted soils of Oxia Palus may, in fact, be examples of regions where duricrust is being actively destabilized and allowing the dehydration-rearrangement reaction to proceed. Type II dark streaks are characterized by dark sands that apparently emanate from splotches in crater floors or depressions, and have bright red deposits on the upwind and downwind sides as well as distinctive narrow deposits of bright red material along their margins [17]. These features have been interpreted as erosional blow-outs through the dark red soils to a low-albedo substrate [18] and also as deposits of dark gray sands on the dark red soils [19]. [3] developed this view further and proposed that the bright red rims of the streaks were the results of winnowing of dust, which was deposited during global dust storms, by the action of the dark sands, and trapping of the dust in the aerodynamically rougher dark red soils at the streak margins.

An alternative hypothesis is proposed here that integrates the concepts developed above through surface processes. The sand-sized dark material of the crater floors and streaks are transported by eolian processes across the surface to form the streaks. The force of the sand grains transported across the surface is sufficient to break up the loosely indurated duricrusted soils [20]. This increases the surface-to-volume ratio in the soils, and lowers the kinetic barriers to predicted phase changes. The immature compounds of the dark red soils then mature to the typical assemblage of bright red regions.

**Implications for Processes and Environments on Mars:** This view, if correct, has important implications for a range of processes and pathways on Mars. There have been several proposed mechanisms for the ubiquitous presence of ferric oxide on Mars, including hydrothermal alteration [21,22], palagonitization of volcanic glass [23], and acid weathering of Fe-rich basalts [24]. However, low-temperature dissolution and precipitation of ferric oxides in soils, stimulated by surface-atmosphere exchange of volatiles, may be an extremely important mechanism because of the long timescales and global nature of the process. In fact, it is quite possible that much of the dust on Mars has passed through a duricrust phase, which may have significantly contributed to the apparent homogeneity of soil compositions.

Though there are a number of uncertainties regarding this hypothesis (e.g., kinetics of dissolution-precipitation and dehydration-rearrangement reactions), it is worthwhile considering some of the implications for aqueous environments on Mars. The fact that surface crusts form today under very dry conditions implies that in the past the rates of formation would have been substantially higher, due to either favorable orbital configurations or a warmer, thicker atmosphere. The presence of water is a requirement to support life, and terrestrial crusts have associated ecologies. The hypothesis presented here considers the surface-atmosphere exchange of water only, yet broad-scale evaporation of groundwater through soils could form substantial crusts. Such areas could be important targets to consider for future missions. Crusts formed under different conditions (temperature, humidity, pH) would have different mineralogy and high spatial- and spectral-resolution orbital spectroscopy could identify these materials if exposed by craters or in canyon/valley walls.

**References:** [1] Mutch T. A. et al. (1977) *JGR*, 82, 4452–4467. [2] Clark B. C. et al. (1982) *JGR*, 87, 10059–10067. [3] Arvidson R. et al. (1989) *JGR*, 94, 1573–1587. [4] Christensen P. R. and Moore H. J. (1992) in *Mars* (H. H. Kieffer et al., eds.), pp. 686–729, Univ. of Arizona, Tucson. [5] Jakosky B. M. and Christensen P. R. (1986) *JGR*, 91, 3547–3559. [6] Jakosky B. M. and Muhleman D. O. (1981) *Icarus*, 72, 528–534. [7] Mustard J. F. (1994) *Eos Trans. AGU*, 75, 407. [8] Mustard J. F. (1995) *LPS XXVI*, 1021–1022. [9] Morris R. V. et al. (1989) *JGR*, 94, 2760–2778. [10] Bell J. et al. (1990) *JGR*, 95, 14447–14463. [11] Fanale F. P. and Cannon W. A. (1974) *JGR*, 79, 3397–3402. [12] Zent A. P. et al. (1993) *JGR*, 98, 3319–3338. [13] Mellon M. T. and Jakosky B. M. (1996) *JGR*, 101. [14] Ugolini F. C. and Anderson D. M. (1973) *Soil Sci.*, 115, 461–470. [15] Schwertmann U. (1988) *Iron in Soils and Clay Minerals* (J. W. Stucki et al., eds.), pp. 267–308, NATO ASI Series C, Mathematical and Physical Sciences, Vol. 217. [16] Schwertmann U. and Cornell R. M. (1991) *Iron Oxides in the Laboratory*, VCH Publications, Weinheim, Germany, 191 pp. [17] Thomas P. C. et al. (1981) *Icarus*, 45, 124–153. [18] Kieffer H. H. et al. (1981) *Proc. LPS 12B*, pp. 1395–1417. [19] Thomas P. C. (1984) *Icarus*, 57, 205–227. [20] Greeley R. et al. (1982) *JGR*, 87, 10000–10024. [21] Allen C. C. et al. (1982) *JGR*, 87, 10083–10101. [22] Newsom H. E. (1980) *Icarus*, 44, 207–216. [23] Soderblom L. A. and Wenner D. B. (1978) *Icarus*, 34, 622–637. [24] Burns R. G. and Fisher D. S. (1993) *JGR*, 98, 3365–3372.

**HYDROTHERMAL ENVIRONMENTS AND CHEMICAL TRANSPORT ON MARS.** H. E. Newsom, Institute of Meteoritics, Department of Earth and Planetary Sciences, University of New Mexico, Albuquerque NM 87131, USA (newsom@unm.edu).

**Introduction:** The discovery of a carbonate-rich SNC (martian) meteorite, ALH 84001, is a demonstration that aqueous processes and volatile-element transport were important on Mars. The origin and temperature of the aqueous solutions that deposited the carbonate in the ALH 84001 meteorite are still uncertain; however, the possible discovery of evidence for life in this meteorite [1] emphasizes the importance of understanding the role of hydrothermal processes and chemical transport on Mars. Remote sensing studies have also indicated that weathering products and evidence for hydrothermal alteration may be widespread on Mars [2,3]. Hydrothermal in the strict sense refers to “hot water,” but in the case of Mars any water above the ambient temperature can be loosely considered “hot.” In addition, terrestrial experience has led to the suggestion that exothermic alteration reactions can maintain water at slightly above ambient temperatures for a long time, resulting in significant alteration and chemical transport effects [4]. Hydrothermal systems on Mars were probably also important in the isotopic exchange between the atmosphere and the surface [5], may be connected with the formation of the martian soil [6], and may have enriched the surface materials in mobile elements that could represent a toxic hazard to future human exploration of Mars [7].

**Chemical and Remote Sensing Evidence for Hydrothermal Activity and Chemical Transport on Mars:** Chemical information about the martian soil is very limited. The Viking landers analyzed the soil with an X-ray fluorescence spectrometer in two widely separated locations. The results were nearly identical sug-

gesting a globally mixed eolian deposit enriched in S, Cl, and Br, compared to the SNC meteorites [8]. A gamma-ray detector on the Russian Phobos-2 spacecraft in orbit about Mars [9] obtained data that are thought to characterize primarily the martian soil; estimates of the minor-element composition from this experiment range from 0.2 to 0.4 wt% K, and 1.9–3.1 ppm Th. Both the K and Th concentrations are substantially enriched compared to SNC meteorites. In addition to the evidence from ALH 84001, the other SNC meteorites also contain alteration phases and evidence of chemical transport [e.g., 10]. For example, Lindstrom et al. [11] have found enrichments of Hg in weathering products in the Lafayette martian meteorite.

Substantial amounts of information about the mineralogy of the soil and airborne dust have been obtained from other Viking experiments and remote sensing from ground and spacecraft. In general, the spectral data from infrared through ultraviolet and photopolarimetry and radiometry are consistent with the nanocrystalline structure of palagonite, an alteration product of glass [12–14], while some dark areas seem to be covered with grains coated by dark titanomagnetite [14]. The results of the Viking biology experiments were successfully simulated with montmorillonite clay containing adsorbed Fe, suggesting that alteration products are an important component of the soil. The Viking magnetic experiment suggested the presence of an iron oxide [8]. Sulfates have been detected spectroscopically on the surface or in atmospheric dust [15], consistent with the Viking inorganic analysis results.

The detection of carbonates in the martian soil is more controversial. Wagner and Schade [16] have reviewed the observations and based on laboratory experiments suggest that as much as 7–20 wt% of anhydrous carbonates could be present without detection. However, the thermal emission spectrometer on the Mars Global Surveyor now on its way to Mars will have a good chance of detecting very small amounts of carbonates.

**Shallow Hydrothermal Systems, Volcanic and Impact Related:** The supply of water for hydrothermal alteration and chemical transport involves two separate environments, shallow interactions of water with surficial hot rock from impacts and volcanic flows, and deep systems created by volcanic intrusions or conduits, and by impact melt sheets in large craters and basins, and their associated central uplifts.

Hydrothermal systems involving distal volcanic flows, and distal impact melt (away from the crater), require a shallow source of water, either groundwater or ground ice. Fanale et al. [17] showed that ground ice is stable near the surface of Mars, except in an equatorial zone that has grown throughout Mars history. At present, ice is only stable at latitudes above about 35°. There is still the problem of conducting heat downward to melt ice or to access an aquifer. This may occur locally, however, due to topographic variations, or in the case of impact cratering, the effects of large secondaries, which might expose water-bearing deposits. A major question for large impacts and basins is the amount and distribution of impact melt outside the crater.

**Deep Volcanic Hydrothermal Systems:** The second environment consists of the vicinity of volcanic conduits that can tap deep water or ice at depths of several kilometers. For this case, the water availability has not changed much through time. Based on Clifford's model [18], the water table may be within a few kilometers of the surface over much of Mars even today. In the case of a large volcanic center, Gulick [19] has shown that large hydrother-

mal systems can result that can even supply water to springs high on the sides of large volcanic constructs. Such hydrothermal systems could also be connected with the formation of the large outflow channels.

**Impact-related Hydrothermal Systems and Lakes:** The formation of large impact craters (>50 km diameter) creates depressions several kilometers deep, which can easily access deep aquifers. The influx of water can produce impact-crater lakes. Newsom et al. [20] showed that the thermal energy in buried impact melt and the geothermal energy in the uplifted central peaks can keep the lakes from completely freezing for thousands of years under a thick sheet of ice, even under current climatic conditions.

**Alteration and Chemical Transport:** The chemical alteration processes affecting minerals and glasses produced by volcanism and large impacts not only provide clays that contribute to the bulk material in martian soils, but also release fluid-mobile elements that can be transported and deposited in the subsurface [21] in hot springs and fumarole deposits, and concentrated them in local sinks, such as impact and volcanic crater lakes. Global sinks may include the Hellas Basin and the other lowland areas at the end of the large outflow channels. Chemical transport involving removal of soluble material from the soil by leaching may have also occurred during the early history of Mars.

The enrichments of S, Cl, K, Br, and Th in the soil could be contributed from three possible sources [7]. A fumarolic component resulting from high-temperature degassing of magma and impact melt, which displays a volatility-controlled signature. A hydrothermal component that represents the elements released by volcanic and impact-driven hydrothermal alteration of minerals and glass controlled by low-temperature solubility. A chondritic component is important because of the slow pace of geologic activity on Mars. This chondritic component will be enriched in siderophile and chalcophile elements compared to material derived from the martian mantle, which was depleted in siderophile elements due to core formation. Boslough and Cygan [22] showed that shock-activated minerals are more easily altered, enhancing the effects related to impacts. We have evaluated the possible signatures for these three components and have identified their characteristic elements as discussed in a companion abstract [7].

**Sampling of Hydrothermal Deposits:** A critical question for future Mars exploration is to design a strategy that will successfully allow study and recovery of samples of fossil hydrothermal deposits [23]. Yellowstone-type hydrothermal areas are an obvious target, and such deposits may occur in channels adjacent to impact melt sheets and on the flanks of volcanos. Other targets that may be important include the central uplifts and walls of large impact craters and the floors of calderas. Shallow hydrothermal systems produced by distal impact melt and lava flows may also be accessible at the surface in fretted terrains. The erosional effects of the large outflow channels provide the possibility of sampling buried evidence of hydrothermal activity. Such features include buried shallow impact melt or lava flow systems and ancient soil horizons. Impact-crater lake deposits may also be exposed in dissected craters. Impact craters are of special interest because most of the large ones formed during the early history of Mars when water was probably more available near the surface.

**Conclusions:** The existence of hydrothermal systems on Mars has been well established. Such systems have probably played an important role in the formation of the martian soil, the formation of



the outflow channels and small valley networks, and perhaps in the origin of life [24]. The process of chemical transport by hydrothermal systems on Mars has probably enriched the surface materials in fluid-mobile elements such as Cl and S. Hydrothermal systems could have also played a role in biological transport, for example spreading possible life forms in the subsurface, and carrying them into crater lakes, outflow channels, and small valleys.

**References:** [1] McKay D. S. et al. (1996) *Science*, 273, 924. [2] Calvin et al. (1994) *JGR*, 99, 14659. [3] Geissler et al. (1994) *Icarus*, 106, 380. [4] Newsom et al. (1986) *Proc. LPSC 17th*, in *JGR*, 91, E239. [5] Jakosky and Jones (1994) *Nature*, 370, 328. [6] Gooding et al. (1992) in *Mars* (Kieffer et al., eds.), p. 626, Univ. of Arizona, Tucson. [7] Newsom and Hagerty, this volume. [8] Banin et al. (1992) in *Mars* (Kieffer et al., eds.), p. 594, Univ. of Arizona, Tucson. [9] Trombka et al. (1992) *Proc. LPS*, Vol. 22, p. 23. [10] Stoker et al. (1993) in *Resources of Near-Earth Space* (Lewis et al., eds.), p. 659, Univ. of Arizona, Tucson. [11] Lindstrom et al. (1996) *LPI Tech. Rpt. 96-01*, p. 31. [12] Singer (1992) *JGR*, 87, 10159. [13] Clancy et al. (1995) *JGR Planets*, 100, 5251. [14] Dollfus et al. (1993) *JGR Planets*, 98, 3413. [15] Blaney and McCord (1995) *JGR Planets*, 100, 14433. [16] Wagner and Schade (1996) *Icarus*, 106, 256. [17] Fanale et al. (1986) *Icarus*, 106, 1-18. [18] Clifford (1993) *JGR*, 98, 10973. [19] Gulick (1995) *Eos Trans. AGU*, 76, F330. [20] Newsom et al. (1996) *JGR*, 101, 14951. [21] Griffith and Shock (1995) *Nature*, 377, 406. [22] Boslough and Cygan (1988) *Proc. LPSC 18th*, p. 443. [23] Farmer (1996) *Ciba Found. Symp.*, 202, 273. [24] McKay C. P. et al. (1992) in *Mars* (Kieffer et al., eds.), p. 1234, Univ. of Arizona, Tucson.

**COMPOSITION OF THE MARTIAN SOIL.** H. E. Newsom and J. J. Hagerty, Institute of Meteoritics, Department of Earth and Planetary Sciences, University of New Mexico, Albuquerque NM 87131, USA (newsom@unm.edu).

**Introduction:** The composition of the fine-grained soil on Mars contains important clues to the past climates and geological history of Mars. The soil probably consists of rock material and additional components added by geochemical transport mechanisms. Removal of soluble material from the soil by leaching may have also occurred during the early history of Mars. Compared to the composition of igneous Mars rocks (SNC meteorites), the Viking and Soviet Phobos mission measurements suggest that the martian soil is enriched in S, Cl, K, and probably Br [1,2]. In addition to the rock composition, three additional sources of material could represent components of the soil. A fumarolic component resulting from high-temperature degassing of magma and impact melt displays a volatility-controlled signature. A hydrothermal component represents the elements released by volcanic and impact-driven hydrothermal alteration of minerals and glass, controlled by low-temperature solubility (Fig. 1). A chondritic component will be enriched in siderophile and chalcophile elements compared to material derived from the martian mantle, which was depleted in siderophile elements due to core formation. We have evaluated the possible signatures for these three components (Fig. 2) and have identified characteristic elements.

**Degassing and Volatile-Element Emissions:** High-temperature degassing and fumarole emissions from volcanos and lava flows are well known on the Earth [e.g., 3], and are thought to represent the degassing of magmas. The existence of degassing pipes in suevite at the Ries Crater [4] suggests similar effects can occur during impact crater formation. Estimating the composition of such emissions can be roughly approximated by examining the emissions from terrestrial volcanos. Clark and Baird [1] suggested that martian soils may have high concentrations of Pb, Br, Sb, Hg, and As, based directly on the composition of Hawaiian fumarole deposits. We have utilized data from a number of additional sources to establish the range of possible enrichments [e.g., 4]. We have also corrected the terrestrial compositions for the difference between the composition of the terrestrial mantle and the martian mantle. Compared to SNC meteorites, the martian soil contains substantial enrichments of S, Cl, and K, which we use to constrain the possible contributions from the normalized flux of volcanic emissions as summarized in the conclusions.

**Hydrothermal Alteration and Palagonitization:** The chemical alteration processes affecting minerals and glasses produced by volcanism and large impacts not only provide clays that contribute to the bulk material in martian soils, but also release fluid-mobile elements that can be transported and deposited at the surface in hot springs and fumarole deposits. Boslough and Cygan [5] showed that shock-activated minerals are more easily altered enhancing the effects related to impacts. Two types of data are used to define the possible composition of this component of the martian soil, studies of altered basaltic and impact materials (Fig. 1), and the composition of thermal hot spring waters. A correction for the Mars/Earth compositional difference has also been made.

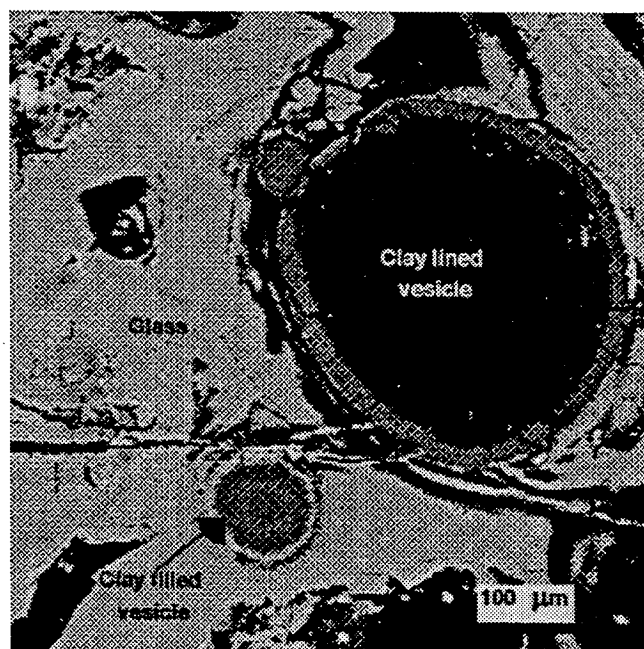


Fig. 1. Backscattered electron image of impact melt glass from Otting at the Ries Crater, Germany.



**Chondrite Additions:** The rain of chondritic debris including organic matter [6] on Mars is more intense than at the Earth because of the proximity of the asteroid belt. Clark and Baird [7] suggested that a CI component could have been added to the martian soil. The chondrites are highly enriched in siderophile elements compared to martian samples because of core formation in Mars. Martian impact melts may contain up to 40% projectile material because of the low impact velocities [8]. Alteration of impact deposits early in Mars history may have preferentially contributed to the martian soil [9]. In contrast, the incorporation of achondrite material into the martian soil would not be easily detected, since core formation and degassing also fractionated siderophile and volatile elements in most of the achondrites.

**Conclusions:** The martian soil contains trace-element clues to its origin and age. The most characteristic element for the hydrothermal fluid component is Li, which would be enriched relative to the other components (SNC composition, the CI component, and the fumarolic component). For the chondritic component, Co and Ni may be enriched relative to the other components. For the fumarolic component, the elements Mo, Cd, Ba, and W may be enriched relative to the other components. The elements Cu, Zn, and Bi, will be enriched by both the CI chondrite and fumarolic component relative to SNC compositions. Similarly Se is enriched in the fumarolic and CI chondrite components, but its hydrothermal signature is unknown. The elements Rb, Cs, and F would be enriched in the fumarolic and hydrothermal component. Enrichments of Cl and Br above the possible CI level would also indicate enrichments from

the fumarolic and hydrothermal components. Several elements, including Cl, P, S, Sb, Ag, Hg, Au, and Pb, can be enriched relative to the SNC composition by all three components. Finally, the enrichment of the soil in S, Cl, and possibly metals, such as Cd, As, and Pb has implications for the origin of life, and represents a possible hazard to future human exploration.

During the early part of martian history water was more available, leading to giant outflow episodes. Within the outflow channels, excavated outcrops of ancient buried soils may occur. The brief nature of the outflow episodes may have prevented significant leaching of exposed soils except in lakes [10]. During the later history of Mars, volcanism and the deposition of cosmic dust may have been more important as the amount of impact activity waned. Although the surficial soils analyzed by the two Viking landers suggest a globally mixed eolian deposit, significant differences may exist between soil deposits in the ancient cratered highlands of Mars, and the younger volcanic terrains of the other hemisphere. Thus the nature of soils formed at different times and places in Mars history may record different trace-element signatures.

**References:** [1] Clark and Baird (1979) *GRL*, 6, 811. [2] Trombka et al. (1992) *Proc. LPS*, Vol. 22, pp. 23-29. [3] Symonds et al. (1987) *GCA*, 51, 2083. [4] Newsom et al. (1986) *Proc. LPSC 17th*, in *JGR*, 91, E239. [5] Boslough and Cygan (1988) *Proc. LPSC 18th*, p. 443. [6] Flynn (1996) *Earth, Moon, Planets*, 72, 469. [7] Clark and Baird (1979) *JGR*, 84, 8395. [8] Boslough (1991) *Annu. Rev. Earth Planet. Sci.*, 19, 101. [9] Newsom (1980) *Icarus*, 44, 207. [10] Newsom et al. (1996) *JGR*, 101, 14951.

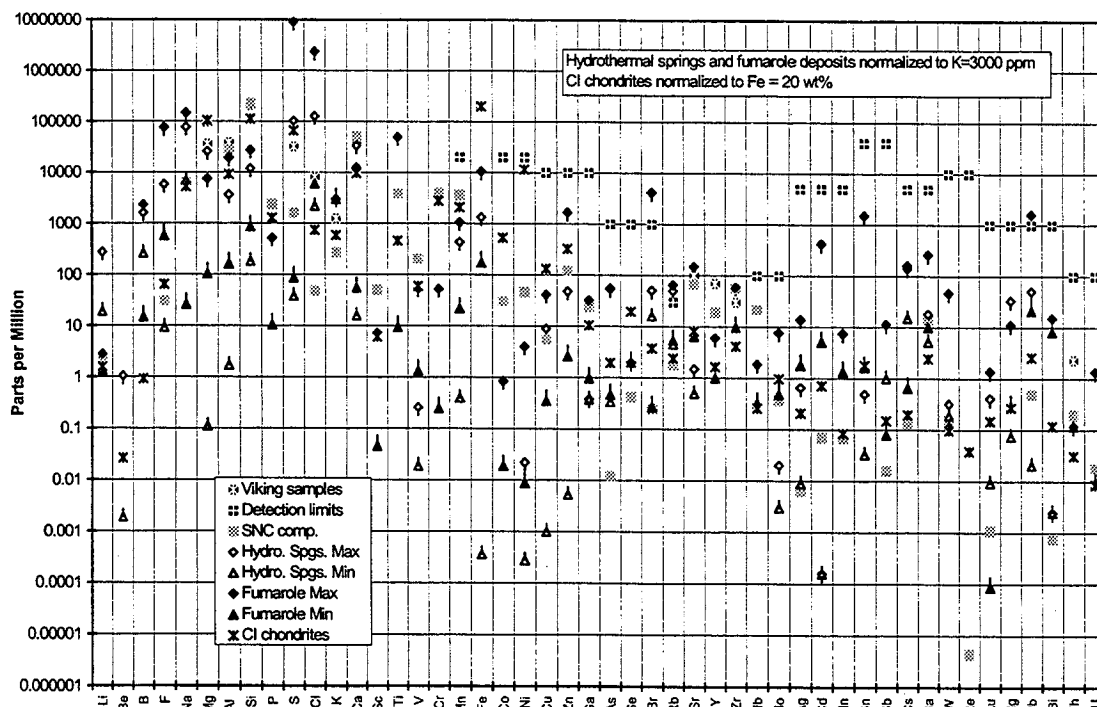


Fig. 2. Compositions of possible components of the martian soil compared to SNC meteorite compositions, and measured abundances and detection limits.

**THE SHERGOTTITE AGE PARADOX.** L. E. Nyquist<sup>1</sup>, L. E. Borg<sup>2</sup>, and C.-Y. Shih<sup>3</sup>, <sup>1</sup>Mail Code SN41, NASA Johnson Space Center, Houston TX 77058, USA (nyquist@snmail.jsc.nasa.gov), <sup>2</sup>National Research Council, Mail Code SN41, NASA Johnson Space Center, Houston TX 77058, USA, <sup>3</sup>Lockheed Martin Engineering and Sciences Company, 2400 NASA Road 1, Houston TX 77258, USA.

The radiometric ages of martian meteorites present a paradox because martian surface units are predominantly old whereas the martian meteorites, particularly the shergottites, are predominantly young ( $\leq 1.3$  Ga). Figure 1 compares the number of samplings of martian surface units as inferred from martian meteorites to the percentage of the martian surface of various ages as determined from crater counts [1]. Here, meteorites with the same values of exposure and crystallization ages are grouped together to represent single events, using exposure ages from [2]. The three nakhlites and Chassigny probably were ejected  $\sim 10$  m.y. ago by a single impact into 1.3-Ga terrain, and are represented by a single symbol in Fig. 1, whereas a separate impact  $\sim 15$  m.y. ago into much older,  $\sim 4.5$ -Ga terrain [3,4], is shown for orthopyroxenite ALH 84001. For the young basaltic and lherzolitic shergottites with ages  $< 0.33$  Ga, we have further subdivided the three ejection events suggested by [2] to account for the older crystallization age of QUE 94201 relative to the other basaltic shergottites [5]. Alternatively, if all the shergottites were ejected in the three impact events identified by [2], the  $\sim 2.6$ -Ma event must have ejected material with a range of crystallization ages from  $\sim 165$  Ma to  $\sim 330$  Ma.

The above assignment of exposure ages to martian surface impacts suggests that at least three of five, and possibly four of six, meteorite-yielding impacts occurred on young terrain. Gladman et al. [6], who compared measured exposure ages to expected transit times from Mars, preferred a model in which all martian meteorites were ejected independently, in which case 6 of 11 meteorites would be derived from terrain  $< 330$  m.y. old. However, Mouginiis-Mark et al. [7], who considered possible source craters for SNC meteorites exclusive of ALH 84001, argued for a single impact, positing that the entire exposure age spectrum resulted from secondary break-up in space. Bogard [8] did not distinguish between the exposure ages

of lherzolitic and most basaltic shergottites, and suggested that the exposure age data allowed simultaneous ejection of the nakhlites/Chassigny and ALH 84001, i.e., three events if basaltic shergottite EETA79001 was ejected separately, or only two if secondary break-up in space was responsible for the young exposure age of EETA79001. For those models exclusive of the single-impact model,  $\sim 33$ – $66\%$  of the meteorite-yielding martian impacts occurred on terrain  $\leq 330$  m.y. old; the single-impact model requires that impact be on young terrain also. Young volcanic terrain is rare on Mars, comprising  $\sim 2\%$  of the surface area (Fig. 1). Thus, young shergottites appear to be overrepresented by a factor of  $\sim 15$ – $30$ . A possible explanation is that shergottite basalts actually are present within a larger surface area, but are not recognized from orbital photography. Indeed, spectral reflectance data suggest that basaltic shergottites may be common lava types on the martian surface [9].

How might young basaltic shergottites be hiding within older, compositionally similar, terrain? One possibility is that most meteoritic shergottites derive from an impact melt [4,10] produced by cratering in old "shergottite" terrain. Isotopic evidence for mixing of crustal- and mantle-derived components, and Sr-isotopic heterogeneities on a centimeter scale within EETA79001 and Zagami are consistent with this hypothesis, as well as other possible explanations. Figures 2 and 3 show internal Rb-Sr isochrons for these shergottites [5,11], whereas Fig. 4 shows comparable data for a monzonite from the upper melt zone of the 65-km-diameter Manicouagan crater [12]. Rocks in this zone have a hypidiomorphic granular texture, mineral grain sizes  $\geq 1$  mm, and clast contents of  $< 2\%$  [13]. The analogy between the Rb-Sr isotopic data for this impact melt rock and that of the basaltic shergottites Zagami and EETA79001 is striking. The Sr-isotopic heterogeneity among the Manicouagan melt rocks (#117, #241, #417, and #408, Fig. 4) is consistent with remelting of the target rocks [12]. The isotopic analogy also extends to the K-Ar system. Potassium-argon ages of shock-metamorphosed Manicouagan anorthosites are  $\sim 70$ – $90$  m.y. older than the  $\sim 214$ -Ma Rb-Sr (or K-Ar) ages of the monzonite [14];  $^{39}\text{Ar}$ - $^{40}\text{Ar}$  ages of shergottites exceed the Rb-Sr ages as is well known [15].

Lest sampling preexisting impact melt by a second impact be considered an ad hoc suggestion, we note just this possibility for

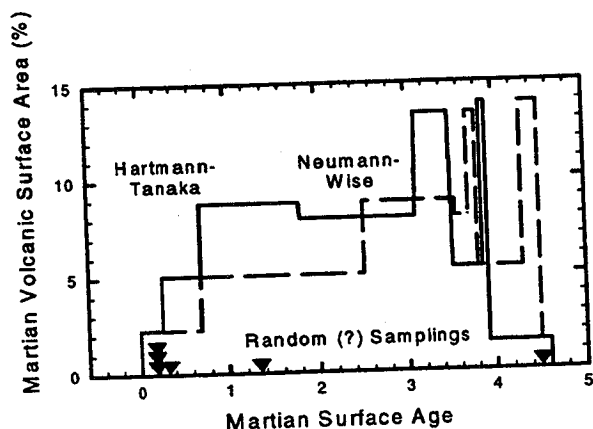


Fig. 1. Comparison of apparent time of sampling the martian surface to the relative area of martian stratigraphic units. Martian surface ages from [1].

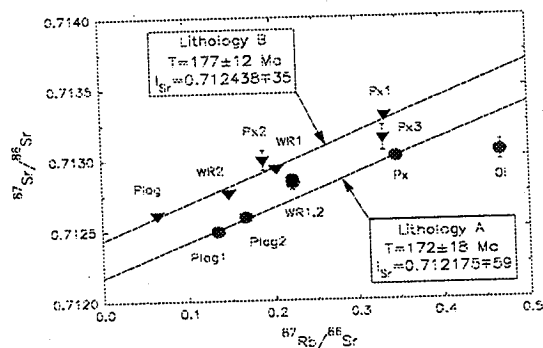


Fig. 2. Rb-Sr isochrons for EETA79001 lithologies A and B.

Crater 3 of Mougini-Mark et al. [7], located near the summit caldera of Olympus Mons. This crater is on some of the youngest terrain in the Tharsis region, considered the likely source region of the SNCs by [7]. Crater 5, preferred as "the" source crater for SNCs [7,16] is on older terrain, leading to the speculation that Crater 3 might be the source of shergottites and Crater 5 the source of nakhlites/Chassigny.

In spite of similarities between the Sr isotopic systematics of the shergottites and the Manicouagan impact melt rocks, other explanations of the shergottite data may nevertheless be possible. Mineralogical-petrographical studies of the shergottites have led to suggestions that their petrogenesis involved multiple magma pulses and/or chambers [17,18]. Strontium isotopic evidence of magma recharge of a crustally contaminated magma, as in the case of the shergottites, has been presented [16]. The presence of shallow-level "shergottite" intrusions periodically recharged from below, and occasionally excavated from above, may account for isotopic heterogeneities in the shergottites and present an alternative explanation of the shergottite age paradox. Lack of geologic control leaves open basic questions about the martian meteorites, underscoring the need for spacecraft return of documented martian samples. Such samples would permit absolute age dating of martian surface units as well as many other types of studies.

**References:** [1] Tanaka K. L. et al. (1992) in *Mars*, pp. 345–382. [2] Eugster O. et al. (1996) *LPS XXVII*, 345–346. [3] Jagoutz E. et al. (1994) *Meteoritics*, 29, 478–479. [4] Nyquist L. E. et al. (1995) *LPS XXVI*, 1065–1066. [5] Borg L. et al. (1997) *LPS XXVIII*.

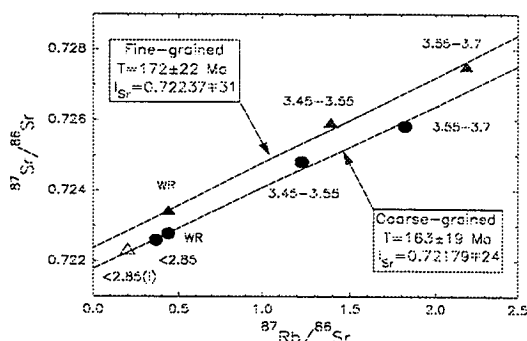


Fig. 3. Rb-Sr isochrons for Zagami coarse- and fine-grained samples.

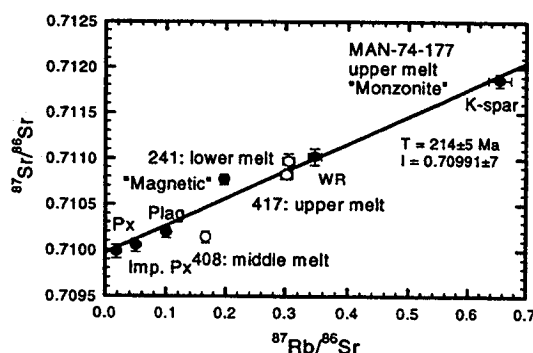


Fig. 4. Internal Rb-Sr isochron for a melt rock from the upper melt zone of the Manicouagan melt sheet.

[6] Gladman B. J. et al. (1996) *Science*, 271, 1387–1392. [7] Mougini-Mark P. J. et al. (1992) *JGR*, 97, 10213–10225. [8] Bogard D. D. (1995) *LPS XXVI*, 143–144. [9] McSween H. Y. (1994) *Meteoritics*, 29, 757–779. [10] Mittlefehldt D. W. et al. (1997) *LPS XXVIII*. [11] Nyquist L. E. et al. (1986) *LPS XVII*, 624–625. [12] Jahn B.-M. et al. (1978) *JGR*, 83, 2799–2803. [13] Floran R. J. et al. (1978) *JGR*, 83, 2737–2759. [14] Wolfe S. H. (1971) *JGR*, 76, 5424–5448. [15] Shih C.-Y. et al. (1982) *GCA*, 46, 2323–2344. [16] Nyquist L. E. (1983) *Proc. LPSC 13th*, in *JGR*, 88, A785–A798. [17] McCoy T. et al. (1992) *GCA*, 56, 3571–3582. [18] McSween H. Y. and Jarosewich E. (1983) *GCA*, 47, 1501–1513. [19] Davidson J. P. and Tepley F. J. (1997) *Science*, 275, 826–829.

## FLUVIAL AND LACUSTRINE DEGRADATION OF LARGE MARTIAN BASINS DURING THE NOACHIAN.

T. J. Parker, Mail Stop 183-501, Jet Propulsion Laboratory, California Institute of Technology, 4800 Oak Grove Drive, Pasadena CA 91109, USA (timothy.j.parker@jpl.nasa.gov).

**Introduction:** Studies of potential sites of martian paleolakes have taken two approaches. One group of investigators has focused on the planet's heavily cratered, relatively ancient southern highlands as the most likely place to preserve evidence of a former wet climate. This is because the valley networks, while they may not always indicate atmospheric precipitation, nevertheless require significant discharges for sustained periods of time. The other group of investigators has focused on the northern lowlands as a likely site for paleolakes or even a paleo-ocean. The primary sources of influx into this basin are the circum-Chryse outflow channels and several smaller outflow channels and valley networks west and south of the Elysium volcanic complex. These channels are large enough to have formed large lakes, or even oceans, in the northern plains.

**Early Noachian Basin Origins:** Tectonism is probably the most important process on Earth for producing closed depressions on the continents, and is clearly responsible for maintenance of the ocean basins through geologic time. On Mars, however, tectonism appears limited to relatively small amounts of regional extension, compression, and is dominated by vertical motion largely due to crustal loading of the two major volcanic provinces—Tharsis and Elysium [1–4].

Impact craters and large impact basins, and broad topographic depressions between them, are clearly more important sites for potential lake basins on Mars, though they were probably more important on Earth as well prior to 3.5 Ga. The global topographic dichotomy separating the heavily cratered southern highlands from the sparsely cratered northern lowland plains is an ancient feature, due either to tectonism or to the formation of a single, or several, overlapping giant impact basins in the northern plains [5–7].

**Highland Basins:** In the southern highlands, several basins on the order of several tens to a few hundred kilometers across and parts of Valles Marineris have been found to contain remnants of former alluvial or lacustrine sedimentary deposits. Many of these basins were simply in the paths of short-term catastrophic floods, and thus may not have contained lakes for very long [8]. The thick Valles Marineris layered deposits occupy deep graben and collapse depressions in the martian crust, and appear to have been fed by groundwater rather than overland flow [9,10]. The deposits are on

the order of kilometers thick and appear finely laminated in high-resolution Viking Orbiter images, and so probably indicate the presence of lakes for long periods of geologic time. These layered deposits and two notable examples of highland basin have been the focus, for a number of years, of investigations of future lander missions to Mars that might search for evidence of fossil organic materials [e.g., 11]. The first of these, the 135-km crater Gusev (15°S latitude, 184° longitude), lies at the mouth of the large, tributary-fed channel Ma'adim Vallis and contains the remnants of deltaic or alluvial fan deposits and possible lake sediments [12]. The other site is an unnamed, 200-km-diameter depression along the Parana-Loire valley system in Margaritifer Sinus (23°S latitude, 13° longitude). This basin contains a peculiar, hummocky deposit that has been interpreted by Goldspiel and Squyres [13] as the eroded remnants of lake sediments. More recently, Argyre Planitia and Schiaparelli B Crater have been added to the list of basins being studied as possible landing sites for their exobiology potential (by this author and by K. Edgett respectively).

"Perched" chaos deposits, similar to those in Gusev and Margaritifer Sinus, can be seen in other large, shallow basins in the Phaethontis region of Mars at 35°S latitude, 177° longitude (Atlantis Chaos) and nearby at 30°S latitude, 170° longitude (Gorgonum Chaos), and in the very degraded Schiaparelli B Basin at 4°S latitude, 358° longitude. On Earth, eroded lake deposits are among the more common host terranes for badlands topography, which bears some resemblance to the martian deposits, though fluvial dissection is more pronounced.

The largest highland basins, Argyre (900 km interior diameter) and Hellas (1500 km interior diameter) appear to contain massive accumulations of layered sediments that are now being exposed through eolian deflation. Those in Argyre may be on the order of hundreds of meters or more thick [14], whereas those in Hellas appear to have been as much as a few kilometers thick [15]. Both basins received discharges from radial valley networks and outflow channels. Cassini Crater (24°N latitude, 328° longitude) appears to contain similar, though less extensive, layered deposits [e.g., 16]. Oddly, however, it lacks large inward-draining channels, so influx of water could only have been through the subsurface or through precipitation over the large catchment area within the basin's rim. This basin exhibits well-developed terraces that may be paleo-shorelines that are cut into older layered mesas, crater rims, and fluidized ejecta ramps.

**Basin Degradation:** The degree of degradation of large highland basins appears to be directly related to the size of the basin and the lay of valley networks relative to the basin and regional topography. Cassini (and other, similar-sized basins) retains its ancient rim morphology, but shows moderate erosion of interior structures and deposits of extensive flat-lying, layered sediments. The rim of Argyre was found to include many mountains that are flat-topped erosional remnants of the surrounding Noachian highlands surface [17]. Scattered knobby remnants of a very degraded outer rim to Argyre have now been identified several hundred kilometers south-east and north-west of Charitum Montes. Prior to late Noachian, Argyre may have been similar to the nearby, but very degraded Ladon Basin. The modern, "fresh" appearance of Argyre is due primarily to erosional "enhancement" of the basin rim. Hellas' rim is similarly eroded. The observation is made that the rims of these two highland basins are analogous to the extensive fretted terrains along the lowland/upland boundary. It is proposed that these basin

margins developed in the same way, through basin broadening by lakeshore erosion during the late Noachian and early Hesperian epochs [18].

**Conclusions:** The following scenario for Mars' climate history, originally proposed to explain Argyre's morphology, is being further developed to explain the apparently direct correlation between the state of basin degradation and basin size.

1. The early Noachian was warm and wet, with atmospheric precipitation and surface run-off responsible for the early, nearly complete destruction of the rims of large impact (and tectonic) basins.

2. The late Noachian saw a change from this warm/wet climate to a drier climate that allowed surface water, in the form of channels and lakes, but in which atmospheric precipitation was very limited (so truly advanced dendritic valley networks could no longer form).

3. Lakes may have existed intermittently in the largest highland basins from the Noachian through the early Amazonian, a span of more than two billion years. For smaller basins, this period would have ended earlier, before the rims could be eroded to the extent that occurred in Argyre, Hellas, and the fretted terrains.

4. During the Amazonian, the planet's atmospheric pressure declined, and the climate changed gradually to its modern very cold, very dry condition. Eolian deflation of the Argyre and Hellas interior sediments was probably initially intense during the early Amazonian, but fell with the steady drop in pressure and temperatures to the present day. For smaller sediment-filled basins, deflation may have nearly completely removed these deposits (as in "perched" chaotic materials above) somewhat earlier (no crater counts have been conducted to verify this as yet).

The above scenario has important implications regarding the question of exobiology on Mars, particularly since long periods of geologic time with pluvial conditions are indicated.

**References:** [1] Banerdt W. B. et al. (1982) *JGR*, 87, 9723–9733. [2] Plescia J. B. (1991) *JGR*, 96, 8883–8895. [3] Tanaka K. L. et al. (1991) *JGR*, 96, 5617–5633. [4] Watters T. R. (1993) *JGR*, 98, 17049–17060. [5] McGill G. E. and Squyres S. W. (1991) *Icarus*, 93, 386–393. [6] McGill G. E. and Dimitriou A. M. (1990) *JGR*, 95, 12595–12605. [7] Breuer D. T. et al. (1993) *Planet. Space Sci.*, 41, 269–283. [8] DeHon R. A. (1992) *Earth, Moon, Planets*, 56, 95–122. [9] Nedell S. S. (1987) *Icarus*, 70, 409–441. [10] Komatsu G. et al. (1993) *JGR*, 98, 11105–11121. [11] Landheim R. et al. (1993) *LPS XXIV*, 845–846. [12] Schneeberger D. M. (1989) *LPS XX*, 964–965. [13] Goldspiel J. M. and Squyres S. W. (1991) *Icarus*, 89, 392–410. [14] Parker T. J. and Gorsline D. S. (1993) AGU Spring Meeting, 1 p. [15] Moore J. M. and Edgett K. S. (1993) *GRL*, 20, 1599–1602. [16] Albin E. F. (1997) *LPS XXVIII*, 2 pp. [17] Parker T. J. (1996) *LPS XXVII*, 1003–1004. [18] Parker T. J. et al. (1989) *Icarus*, 82, 111–145.

**SOLAR-WIND-INDUCED EROSION OF THE MARS ATMOSPHERE.** H. Pérez-de-Tejada, Institute of Geophysics, National University of Mexico, Ensenada, Baja California, México.

Evidence from measurements obtained in the Mars plasma environment indicate that a friction layer is observed between the solar wind flow and the planetary ionosphere. The observed features represent the effects of dissipative processes associated with the

local transport of solar wind momentum to a population of planetary ions. The drag exerted by the solar wind on the Mars ionosphere occurs within a boundary layer that extends downstream from the planet. The material that the martian ionosphere may have lost in the past through solar wind erosion could account for the mass present in a 10–20-m global layer of water.

Information on the structure and composition of the martian plasma environment has been obtained with measurements conducted with the Phobos spacecraft moved across the plasma wake on March 16, 1989, are reproduced in Fig. 1 [from 1]. Most notable is a change in the composition of the particle population in the region between the bow shock (labeled BS) and the plasma wake. Solar wind protons are dominant in the outer parts of that region but strong fluxes of planetary  $O^+$  ions are detected as the spacecraft approaches and moves through the wake.

The observed changes occurred across a sharp plasma boundary (labeled ICB) that also marks a noticeable increase in the proton temperature. This later transition represents the outer extent of a boundary layer across which there is a strong decrease in the flow speed from solar wind velocities ( $\sim 400$  km/s) to very low values ( $\sim 40$  km/s) at and within the martian plasma wake [2]. The velocity boundary layer is populated by planetary ions that have been accelerated through momentum coupling and wave-particle transfer processes [3–5].

The flow properties within the boundary layer are comparable to what would be expected in a hydrodynamic friction layer where a strong amount of eroded material would be dragged away by a streaming flow. Dissipative processes associated with the transport of solar wind momentum to the planetary plasma should result in the local heating of the flow and increased plasma temperatures. A similar plasma behavior has been observed in the solar wind-Venus interaction region where a strong velocity boundary layer flanked by a sharp external plasma transition has been reported from the Pioneer Venus Orbiter measurements [6].

Calculations of the erosion that the Mars ionosphere may have experienced in the past can be conducted by assuming conditions similar to those that should have occurred with a more dense atmosphere. A useful comparison can be made with the Venus ionosphere where a similar plasma-plasma interaction takes place.

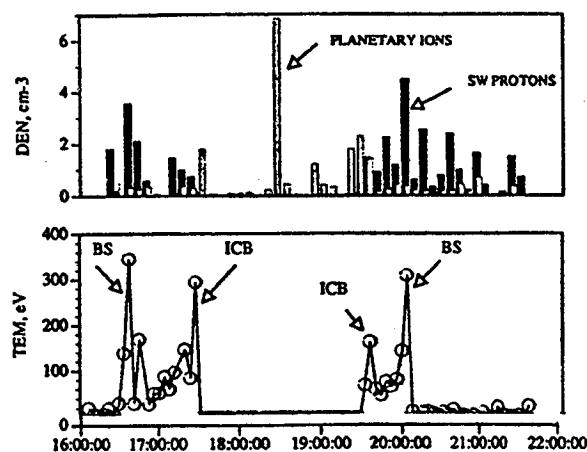


Fig. 1.

The topside ionospheric density is in the  $5 \times 10^3$ – $10^4$   $\text{cm}^{-3}$  range and can be used to calculate the ionospheric flow speed that results from the transfer of solar wind momentum. Figure 2 shows the results of that calculation based on the conservation of the solar wind momentum flux that is transferred across the boundary layer (the integrated momentum flux lost by the solar wind in the boundary layer should be delivered to the plasma within the ionosphere) [7]. The ionospheric flow speed is plotted as a function of the ratio of the boundary layer thickness  $\delta_{sw}$  to the ionospheric width  $\delta_i$  (topside densities at  $5 \times 10^3$ – $10^4$   $\text{cm}^{-3}$  correspond to curves a and b) and may become larger than the  $\sim 5$  km/s escape speed from the martian gravitational field. This later condition results from requiring a velocity boundary layer in which  $\delta_{sw} > 2\delta_i$  so that with a 1000–1500-km ionopause altitude range at the terminator (comparable to PVO observations at Venus) we have  $\delta_{sw} @ 2000$ – $3000$  km, which is consistent with values estimated from the observation of the thickness of the velocity boundary layer above the Venus ionosphere.

The momentum flux of the ionospheric plasma that is eroded by the solar wind can be calculated by using the escape speed from Mars and the expected topside ionospheric densities at the terminator. Applying those values to a 1000–1500-km ionospheric shell

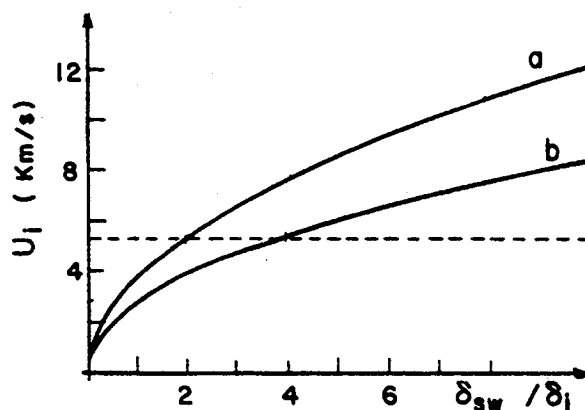
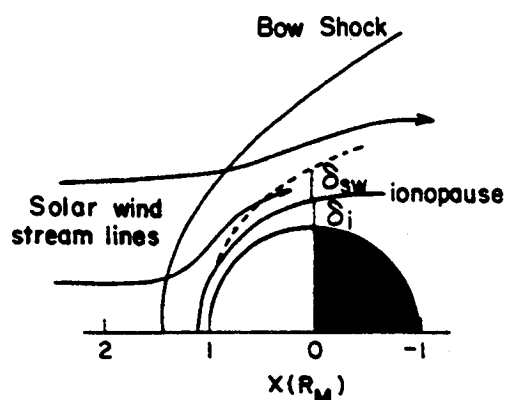


Fig. 2.

around the planetary terminator it is possible to predict that a planetary flux  $2-5 \times 10^9$  ions/cm<sup>2</sup>s could have been forced away by the solar wind [8]. The numbers obtained from this calculation lead to the mass of a 3–7-m global layer of water eroded in  $10^9$  yr and thus imply an effective total layer 10–20 m during the martian past. This result suggests that even though a substantial amount of material could have been eroded by the solar wind, it is smaller than those required to account for the entire water content released through volcanic activity [9].

**References:** [1] Dubinin E. et al. (1996) *JGR*, 101, 27061. [2] Lundin R. et al. (1989) *GRL*, 18, 1059. [3] Pérez-de-Tejada H. (1991) *JGR*, 96, 11155. [4] Shapiro V. et al. (1995) *JGR*, 100, 21289. [5] Sauer K. et al. (1992) *JGR*, 97, 6227. [6] Pérez-de-Tejada H. (1995) *Space Sci. Rev.*, 72, 655. [7] Pérez-de-Tejada H. (1987) *JGR*, 92, 4713. [8] Pérez-de-Tejada H. (1992) *JGR*, 97, 3159. [9] Greeley R. (1987) *Science*, 326, 1653.

**ELYSIUM BASIN, MARS: AN INTERMITTENT OR PERENNIAL LAKE FROM NOACHIAN TO AMAZONIAN TIME.** J. W. Rice Jr., Department of Geography, Arizona State University, Box 870104, Tempe AZ 85287-0104, USA (asjwr@asuvm.inre.asu.edu).

Martian paleolake sites are extremely important because they may hold a record of the physical and chemical conditions that prevailed in the past on Mars as well as evidence of former biological activity. As Mars became progressively colder over geological time, any lakes on its surface would have become seasonally, and eventually perennially, ice-covered. Studies of polar lakes on Earth verify that ice-covered lakes can persist even when the mean annual temperature falls below freezing [1,2]. Thus, the most recent lacustrine sediments on Mars were probably deposited in ice-covered lakes. There is a general consensus among exobiologists that the search for extraterrestrial life should be based upon liquid water. Evidence that there was liquid water in the Elysium Paleolake Basin during Amazonian time [3–5], coupled with the recent discovery of possible ancient microbial life on Mars [6], obviously leads one to question if microbial life could still exist on Mars in specialized niches or oases. A lander/sample return mission to the Elysium paleolake region would aid substantially in answering this compelling philosophic and scientific question.

For this study the Elysium Basin has been chosen as a candidate landing site for a future lander/rover Surveyor Mission [4,5]. The Elysium Basin extends more than 2500 km along the equatorial lowland plains between the Elysium volcanic rise to the north and the cratered highlands to the south. The Elysium Basin is the only known depositional basin of regional extent on Mars where direct evidence of an outflow of water (Marte Vallis) from the basin has been found [3,4]. Water appears to have flowed into the Elysium Basin from many small and some moderate-sized channels (Ma'adim and Al Qahira Vallis) in the southern highlands, from the rise around Elysium Mons, and graben in Cerberus Rupes. A former water level at an elevation of about –1000 m can be seen in places where shorelines and terraces have been eroded into the relatively soft rocks of the Medusae Fossae Formation. A spillway (Marte Vallis) is located on the eastern end of the paleolake basin. This spillway is also at the –1000-m elevation.

Streamlined bars and islands located on the floor of Marte Vallis clearly indicate that water drained northeastward from the Elysium lake into the Amazonis Basin. [8] calculated the surface area ( $18 \times 10^5$  km<sup>2</sup>), depth (1 km), and volume ( $9.1 \times 10^5$  km<sup>3</sup>) of paleolake Elysium. This lake finally drained, evaporated, and or froze in the Late Amazonian.

Low crater densities within the Elysium Basin indicate that it is one of the most recent, Late Amazonian, depositional basins on Mars. However, channels ranging in age from Noachian to Amazonian surround and empty into paleolake Elysium implying that this lake was either persistent or intermittent throughout most of Mars' history. This observation has major climatic and biologic implications. The long life span of this lake system would have provided a hospitable habitat for any life forms that may have evolved on Mars.

**Science Rationale:** Investigations into identifying aqueous sedimentary deposits (lacustrine and or deltaic) as potential landing sites will be achieved by analyzing and mapping the following type of site(s): (1) Noachian-aged lacustrine deposits formed by the discharge of ancient valley networks; (2) Hesperian-aged lacustrine deposits formed by the discharge of valley networks and/or outflow channels; and (3) Amazonian-aged lacustrine deposits formed primarily by the discharge of outflow channels.

This philosophy will permit the identification of a complete suite of paleolacustrine site(s) throughout martian geologic time (Noachian to Amazonian systems). The identification of a single lacustrine basin that satisfies all three (or two) of the above criteria would be an ideal site in terms of exobiology, history, sources, and sinks of water, and climatology. This type of site would indicate a lake system that either existed perennially or intermittently through time, which would be a very significant observation in terms of the search for life (extinct or possibly even extant).

Detailed geologic mapping of the Elysium paleolake basin will be conducted in order to plan rover traverses and sample collection locales. Viking Orbiter images for select regions of this basin have resolutions as high as 13 m/p. These high-resolution images will aid greatly in selection of a landing site and in the planning of rover traverses. Key science objectives to be addressed for this site are the sampling and documentation of fluvial and lacustrine sediments of varying age and composition. Possible types of sediments and environments that may be encountered include evaporites, carbonates, and hydrothermal spring deposits from graben and volcanic constructs. Cerberus Rupes is a system of graben or fractures that in places clearly shows where water issued forth, i.e., streamlined islands and bars [5]. The paleolake basin is bounded to the north by the Elysium Mons–Albor Tholus volcanic complex and Apollinaris Patera to the south. The rim of this basin is composed of ancient Noachian crustal material (Npld, Nplh, Npl<sub>1</sub>), Hesperian plateau material (Hpl<sub>3</sub>), and the Amazonian Medusae Fossae Formation (Aml, Amm).

It is proposed that two landings take place in this region, culminating with a sample return mission. The first lander would have a rover capable of traverses from 100 to 200 km. The rover would collect various samples along the way and carry a navigation beacon that would subsequently be used to guide the sample return vehicle to the rover's final staging area. The samples would then be emplaced within the ascent vehicle for the journey to Earth. Another scenario would have one mission conduct not only rover traverses but additionally *in situ* propellant production experiments. This technology, once proven, could be used to allow the lander to hop across the

surface. *In situ* propellant production could dramatically cut the costs of future missions, especially manned missions.

Engineering challenges in terms of latitude and elevation would be minimal for Elysium Basin because the latitude for the lander/rover package would be between 0° and 10°N; and the elevation range from -1000 to -2000 m. These characteristics would enable the mission to have excellent communications and solar power properties as well as low elevations for descent systems. The primary engineering challenge would be to create a more precise, smaller landing ellipse and durable rover capable of long traverses (hundreds of kilometers) along with a sample return vehicle.

The TES, MOC, and MOLA instruments onboard Mars Global Surveyor and this proposed study will provide enough data to help further refine and define potential landing sites within this basin. The orbital mapping by these instruments, hopefully, will locate and identify key geologic materials, i.e., evaporites, carbonates, and hydrothermal deposits.

**References:** [1] Rice J. W. Jr. (1992) in *LPI Tech. Rpt. 92-08, Part 1*, pp. 23-24. [2] Wharton R. A. et al. (1995) *J. Paleolimnology*, 13, 267-283. [3] Tanaka K. L. and Scott D. H. (1986) *LPS XVII*, 865. [4] Rice J. W. Jr. (1994) *LPI Tech. Rpt. 94-04*, p. 36. [5] Edgett K. S. and Rice J. W. Jr. (1995) *LPS XXVI*, 357-358. [6] McKay D. S. et al. (1996) *Science*, 273, 924-930. [7] Scott D. H. and Chapman M. G. (1995) *U.S. Geol. Surv. Misc. Inv. Series Map I-2397*. [8] Scott D. H. et al. (1995) *U.S. Geol. Surv. Misc. Inv. Series Map I-2461*.

**GETTING THE FIRST CRACK AT NOACHIAN CLASTS AND SEDIMENTS: A PATHFINDER'S PROSPECTUS.** J. W. Rice Jr., Department of Geography, Arizona State University, Box 870104, Tempe AZ 85287-0104, USA (asjwr@asuvm.inre.asu.edu).

**Introduction:** The selection of a site at the confluence of Ares and Tiu Valles (19.5°N, 32.8°W) for the July 4, 1997, landing of Mars Pathfinder (MPF) will potentially allow the first detailed inspection of Noachian rocks and sediments. In fact, this was one of the driving forces that led to it being proposed as a landing site [1]. The Ares Vallis landing site was originally advocated by several investigators [1,2] in April 1994 at the initial Mars Pathfinder Landing Site Workshop. MPF will examine in detail the local surface geomorphology and geology with the IMP (Imager for Mars Pathfinder) and Sojourner microrover, which will be the first rover to explore the martian surface. Naturally, geologists wonder what the landing site will look like. In this brief report I will attempt to make some predictions based upon field investigations of terrestrial analogs in Antarctic ice-free regions, Icelandic sandar deposits, Ephrata Fan deposits located in the Channeled Scabland [3], and small sedimentary structures (bar sequences, ripple marks, imbrication, scour marks, microterraces, dessication features, graded bedding, cross bedding, slump features, and channel fill sequences) associated with streams, arroyos, and gullies in Arizona and the Viking 1 landing site.

**Noachian Materials for the MPF Grab Bag:** Most of the surfaces cut by Ares and Tiu Valles are Noachian in age, namely, two types of Noachian Plateau cratered material (Npl<sub>1</sub> and Npl<sub>2</sub>). These Noachian units probably include impact breccias interbedded

with lavas, pyroclasts, and eolian and lacustrine sediments. Hydrothermal minerals/rocks might be among the materials, as well as hardpan or other low-temperature diagenetic debris. The only clue we have to the composition of Noachian rocks is ALH 84001, which might be from the highlands. The Ares Vallis landing site is thought to be a "grab bag," with rocks and perhaps intact soil units that have been transported by floods possibly choked with ice [4]. Ice rafting may have transported large knobs of rock that appear in the MPF landing ellipse. However, fluvial abrasion will reduce most of the large Noachian clasts (most of the Noachian rocks are cropping out farther upstream) to much smaller size clasts in the landing site vicinity.

**Safe Bets:** A conservative estimate of what Pathfinder will see would be that it will land upon a landscape that generally resembles the Viking 1 site in terms of rock abundance and thermal inertia [5]. I agree with this interpretation but think that the landing site will have a "stronger fluvial signature" since it is only 150 km from the mouth of Ares Vallis. Conversely, the VL-1 site is 400 km from the mouth of Maja Valles.

The MPF landing site will most likely consist of rolling plains punctuated with erosional/depositional knobs and blocks. These sedimentary deposits would also have undergone impact gardening and eolian reworking. It is important to note that based upon field investigations one could actually be located on top of a fluvial/lacustrine depositional surface and not realize it. A wild card in the mix depends upon the actual location of the lander. Once again drawing on field experience, if one were located on a depositional surface and could not verify this, one could simply walk a traverse and come upon undisputable evidence, as will be discussed in the following section.

**Bold Bets:** The following topics discussed will elaborate more fully on the "stronger fluvial signature" theme that I suggest to be present at the landing site. MPF may come to rest upon a surface that is locally dissected by smaller-scale channel branches that merge to form a wide and extensive shallow channel system. Some of these small-scale channels may contain eolian drift-filled troughs. Additionally, the region could contain all or some of these features: streamlined residual hummocks, extensive streamlined remnant boulder bars, fields of streamlined remnant pendant bars attached to the downstream side of any bedrock obstacles, transverse mega-ripples, stone lags, and scattered, imbricated clasts. Cross-bedding may also be seen in some of the fines deposited as flood waters waned. These deposits would have been dissected by small run-off streams of late-stage flow regimes or wind. Ice-rafted material may also be present at the landing site.

Sandar (outwash) deposits are among the best terrestrial analogs to the martian flood deposits. Sandar are created when a number of large meltwater channels emerge from different point sources and deposit their sediment load. Sandar are found in high northern latitude locations such as Iceland, Canada, and Alaska. Individual flood channels coalesce to produce a complex network of branching or braided channels that widen and merge downstream to form a sandar fan. The high current velocities and discharges associated with sandar-forming outburst events are major factors in the nature of sediment transport along these fans. Some Icelandic sandar deposits were formed by floods with sediment concentrations ranging from 40% to 60% [6]. These surfaces are capped by smaller-scale bedform structures that appear to represent the later and more fluid stages or runout flows of the flood event. These develop when



sediment supply has become relatively depleted, when dewatering was occurring from sediments deposited further up-sandbar, and as flow depths and velocities were progressively declining. I would envision a similar process occurring with respect to the martian outflow channel floods.

**Brash Bets:** The MPF landing site region may have once contained a lake. Hence, there is a possibility of lacustrine deposits. Lacustrine sediments are typically well stratified with beds being fairly uniform in texture and thickness. Mud cracks could be found along the paleo-shorelines along with wave ripples. If the lake persisted, it may have had an ice cover. An ice-covered lake deposit would have varves, dropstones, and fine-grained sediments draping or mantling the topography. Ice-shoved ridges could be found along the shorelines [7].

**Observational Tests:** *Debris flows.* If debris flows passed through the Pathfinder landing site, IMP and rover imagery could identify the deposits. Debris flow deposits would be a coarse, poorly sorted mixture of block, gravel, and sand, with very little silt and clay. Debris flows form very thick deposits with levees along their margins.

*Ice rafting.* Ice-rafted material could also be located at the landing site. These materials often consist of piles of lithologically diverse, striated clasts, piled up on local topographic highs. Large erratics can also be deposited in unusual places. Sometimes ice rafting can transport large sections of soil and subsequently deposit it intact.

*Cross bedding.* Cross bedding records the direction as well as the nature of the currents that deposited the grains, while the thickness and textures of individual beds can shed light on the rate of sedimentation and burial. For instance, cross bedding can be either fluvial or eolian in origin. However, fluvial cross beds can be distinguished from eolian cross beds. Eolian cross bedding is marked by extreme irregularity due to the variability of wind direction and the frequent alternation of scouring and deposition [8]. Fluvial cross beds also often have interbedded gravel layers. Additionally, eolian cross beds usually are on a larger scale than aqueous ones.

*Ripple marks.* Ripple marks are formed by either water currents, wind currents, or oscillatory motion. In profile wave ripples (oscillation ripples) are symmetrical and current ripples are always asymmetrical. Wave-made ripples are common on shallow bottoms of lakes and seas. In current ripples the shorter slope of each ridge, as seen in profile, is always inclined in the direction in which the current is moving [8]. The ripple index of water-made current ripple marks is commonly smaller than it is in wind-made ripple marks. The latter have greater width in proportion to their height than do the former.

*Other characteristics.* Other diagnostic characteristics of fluvial activity would include cut and fill structures, and well-sorted, rounded particles. Fluvial deposits are stratified, but poorly, so their strata vary greatly in thickness and there is much textural variation and local unconformities are common. Lacustrine and marine sediments are typically well stratified with beds being pretty uniform in texture and thickness.

**Sublimation Till and Its Relevance to Mars:** A possible mechanism for preserving fine-scale martian fluvial sedimentary structures is the process of sublimation. This idea is based upon a unique till-forming process. The formation of sublimation till requires long-term extremes of cold and aridity. This rarest of tills is found only in Antarctica and is formed essentially by a freeze-drying

process. This freeze-drying process is very important because it preserves extremely delicate englacial depositional structures, i.e., clast orientation and dip, foliation, and fissility [9]. Sublimation tills also tend to contain more fine-grained material than other tills because of the absence of meltwater to remove the fines [10].

Therefore, fine-scale sedimentary structures may be preserved on Mars. Examples of some sedimentary structures that may be preserved at the Pathfinder landing site include planar bedding, cross bedding, ripple marks, clast imbrication, tool marks, microterraces, and mud cracks. These features, if present, would provide valuable and important paleohydrologic information.

**Conclusions:** The long-awaited return to the martian surface will no doubt be full of unanticipated surprises, for this is the very nature of exploration. However, based upon the best terrestrial analogs of the martian floods, several attempts at predictions have been made ranging from conservative to very audacious. Reality will probably lie somewhere in between.

Furthermore, Pathfinder will provide another data point of "ground truth" on Mars. This will be used to compare and contrast the three landing sites (VL-1, VL-2, MPF). Most "geomorphologic discoveries" are made by making comparative studies of landforms and processes. This should allow both a better understanding of the Pathfinder and Viking 1 and 2 landing sites.

**References:** [1] Rice J. W. Jr. (1994) *LPI Tech. Rpt. 94-04*, p. 36. [2] Kuzmin R. O. et al. (1994) *LPI Tech. Rpt. 94-04*, pp. 30-31. [3] Rice J. W. Jr. and Edgett K. S. (1997) *JGR Mars Pathfinder Special Issue*, in press. [4] Rice J. W. Jr. and Edgett K. S. (1995) *LPI Tech. Rpt. 95-01, Part 1*, pp. 25-26. [5] Edgett K. S. and Christensen P. R. (1997) *JGR Mars Pathfinder Special Issue*, in press. [6] Maizels J. K. (1991) in *Environmental Change in Iceland: Past and Present*, pp. 267-302. [7] Rice J. W. Jr. (1992) *LPI Tech. Rpt. 92-08, Part 1*, pp. 23-24. [8] Lahee F. H. (1961) *Field Geology*, 926 pp. [9] Shaw J. (1977) *Can. J. Earth Sci.*, 14, 1239-1245. [10] Shaw J. (1988) in *Genetic Classification of Glacigenic Deposits*, pp. 141-142.

**OXYGEN ISOTOPE RATIO ZONING IN ALLAN HILLS 84001 CARBONATES.** J. M. Saxton, I. C. Lyon, and G. Turner, Department of Earth Sciences, University of Manchester, Manchester, M13 9PL, UK.

Oxygen isotope ratios of ALH 84001 carbonates have been measured *in situ* and with high spatial resolution, using an Isolab 54 ion microprobe [1]. The immediate objectives of this work, which is ongoing, is to search for and map any isotopic gradients that may exist within the carbonates. We hope in doing this to address a number of questions: Is there evidence for isotopic exchange between the carbonate and surrounding pyroxene or maskelynite, such as might arise if the carbonates were deposited at high temperature? Are profiles related in a simple way to the carbonate chemistry, which would suggest that isotopic variations were a feature of the invading fluids? Alternatively, are variations between carbonate regions unrelated to chemical composition, which would suggest that oxygen isotope ratios were determined by localized interactions with the host rock? What are the implications of the variations for the temperature of deposition?



We studied a single grain mount of a sample from the "crushed zone" of ALH 84001. Most of the carbonate lies within a vein running across the sample, much of it showing the characteristic concentric zoning in back-scattered electron images. Minor pockets of carbonate are found in pyroxene. EDX analyses confirm that the carbonate in our sample belongs to the same series of compositions as reported by other workers; however, we did not observe any ankeritic dolomite, presumably because our section does not expose any of the earliest deposited material.

The techniques used here were as reported previously [1,8]: A caesium beam typically between 0.1 and 0.3 nA focused to a spot ~10  $\mu\text{m}$  in diameter was used to sputter secondary ions from the sample. These were mass analyzed and detected in the Isolab 54 ion probe using a Faraday collector for the  $^{16}\text{O}^-$  ions and a CDS detector for the  $^{18}\text{O}^-$  ions [1]. Magnesite, calcite, and siderite standards were used for calibration. We observed no significant (<1%) matrix effect between magnesite and siderite, but a large matrix effect (~18%) between siderite/magnesite and calcite. Measurements of ankerite and dolomite will be carried out to characterize the matrix effect further. All the data here have been normalized to siderite/magnesite, and for now a fixed correction of ~2% has been applied to allow for the small Ca content of the ALH 84001 carbonate. Confidence levels in the quoted absolute  $\delta^{18}\text{O}$  values are  $\pm 2\%$ .

We previously reported analyses of  $^{18}\text{O}/^{16}\text{O}$  ratios in a carbonate rosette [7] that showed an apparent gradient in  $^{18}\text{O}/^{16}\text{O}$  from 21‰ (SMOW) near the outer rim of the rosette to 17‰ (SMOW) in the interior. These data, together with two additional analyses, are shown in Fig. 1.

We have since studied a second carbonate rosette, which shows a slightly wider range of compositions in its core than that in Fig. 1; the most Fe-rich carbonate is  $\sim\text{Mg}_{44}\text{Ca}_{17}\text{Sd}_{39}$ . The O isotope analyses of this rosette are shown in Fig. 2, which is a back-scatter electron photograph onto which the positions of the ion beam burn marks and their measured  $\delta^{18}\text{O}$  values have been added schematically. The ion probe crater diameter is about 10  $\mu\text{m}$ .  $\delta^{18}\text{O}$  values range from 10‰ to 22‰, and also appear to show an isotopic gradient between the outer and inner parts of the rosette.

Previous  $^{18}\text{O}/^{16}\text{O}$  measurements have been reported using acid dissolution [4] or ion probes [8,9], but have been used to reach conflicting conclusions concerning the formation temperature and origin of the carbonates. Romanek et al. [4] measured three  $\delta^{18}\text{O}$  values using stepped acid dissolution of carbonate rosettes, from which they inferred endmember values of 13.3‰ and 22.3‰ for the inner (Ca-Fe rich) zones and outer (Mg-rich) rims respectively. Ion probe measurements have reported a somewhat larger range of values. Leshin et al. [8] reported values between 5.6‰ and 21.6‰, while Valley et al. [9] reported values ranging between 9.5‰ and 20.6‰. Leshin et al. interpret their data as being consistent with partial high-temperature equilibration with neighboring pyroxene, whereas Valley et al. interpret their data as being consistent with low-temperature deposition. In our previously reported measurements [7], we argued that the high  $\delta^{18}\text{O}$  values for the carbonate obtained by us and others could not be used to exclude a high-temperature origin of the carbonate rosettes, only that  $\text{CO}_2$  that formed the rosettes must have been in contact with water at low temperature ( $<100^\circ\text{C}$ ) *at some time* in its history, but not necessarily during formation of the rosettes.

In Fig. 3, the  $\delta^{18}\text{O}$  values for both rosettes are plotted against mole% magnesite. There appears to be a consistent trend, with low

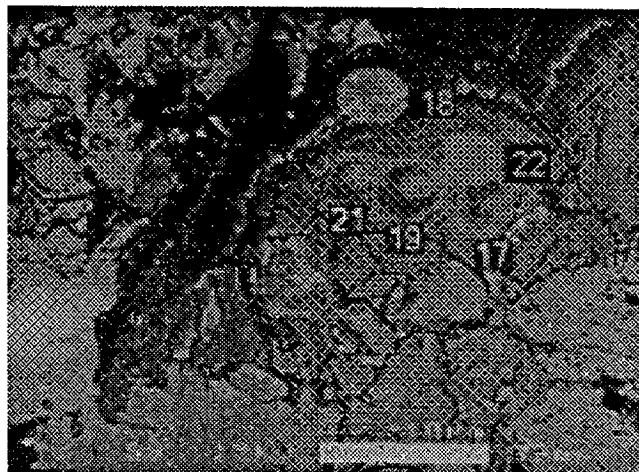


**Fig. 1.**

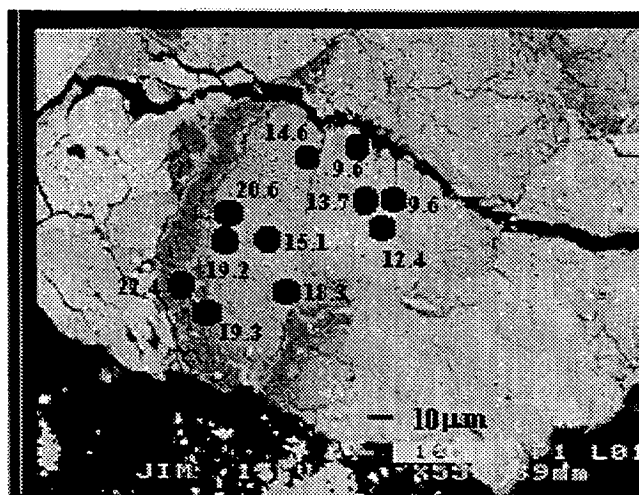


**Fig. 2.**

values, around 12‰, for the inner (early), less-Mg-rich cores and high values, around 20‰, for the (later) more-Mg-rich carbonate.

This observation is in good agreement with the data published by Romanek et al. [4], obtained by acid dissolution, and with the range of values obtained using an ion probe by Valley et al. [8], although Valley et al. reported that there was no apparent correlation between their measured  $\delta^{18}\text{O}$  values and chemical composition. Unlike Leshin et al. [9], we see no carbonate that is in equilibrium with the bulk minerals in ALH 84001. However, none of our sections so far analyzed have dolomite-rich cores [10], presumably due to polishing not having exposed the small cores. It is certainly plausible that continuation of the trend of Fig. 4 to more magnesite-poor values would be consistent with the presence of lower  $\delta^{18}\text{O}$ .

As with earlier O isotope analyses, our data are open to a number of interpretations. Nevertheless some constraints on acceptable models can be made, particularly in view of the apparent systematic variation in  $\delta^{18}\text{O}$  across the carbonate. This variation could arise as a result of a change (reduction) in the temperature of the fluid with time along the lines suggested by Romanek et al. [4]. If this is the case, the lower  $\delta^{18}\text{O}$  values observed by Leshin et al. [9] in the cores, and the trend suggested by Fig. 3, imply that the early fluids were

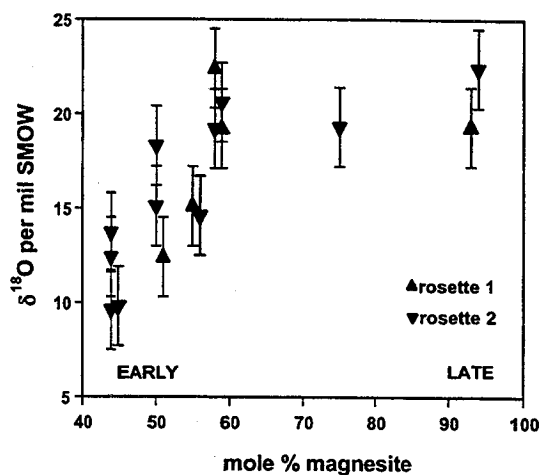


Fig. 3. ALH 84001 carbonate rosettes.

hotter than those proposed by Romanek et al. [4]. An alternative is that Fig. 3 represents a change in the isotopic and chemical composition of the fluid, rather than temperature, i.e., the changes reflect some external process. Where the isotopic exchanges took place that caused the variations in  $\delta^{18}\text{O}$  is also not clear from our data, which are currently based on just two rosettes. If Fig. 3 is representative of all the carbonates, the isotopic composition could have been acquired by exchange between fluid and rock over a wide area. If, as suggested by Valley et al. [8], there is a wide variation in  $\delta^{18}\text{O}$  between rosettes, these  $\delta^{18}\text{O}$  values must have been acquired as a result of very localized interactions.

**References:** [1] Saxton et al. (1996) *Int. J. Mass Spec. Ion Process.*, 154, 98–128. [2] Mittlefehldt (1994) *Meteoritics*, 29, 214–221. [3] Harvey and McSween (1996) *Nature*, 382, 49–51. [4] Romanek et al. (1994) *Nature*, 372, 655–657. [5] Treiman. [6] Chaco et al. [7] Gilmour et al. (1997) *LPS XXVIII*. [8] Valley et al. (1997) *LPS XXVIII*. [9] Leshin et al. (1997) *LPS XXVIII*. [10] McKay and Lofgren (1997) *LPS XXVIII*.

**IMPLICATIONS OF MARTIAN LIFE IN AN ANTARCTIC METEORITE.** W. R. Sheldon, Physics Department, University of Houston, Houston TX 77204-5506, USA (sheldon@uh.edu).

Allan Hills meteorite ALH 84001 has been identified as having a martian origin by its characteristically martian isotope ratios. A detailed investigation of this meteorite [1] has revealed the presence of polycyclic aromatic hydrocarbons and carbonate globules in fresh fracture surfaces. This evidence, along with the possible microfossil of a primitive organism obtained by electron microscopy, led to the suggestion that a biota was present on Mars some 4 b.y. ago. Although somewhat controversial, this interpretation is shown to be in good agreement with the early history of the Earth's biota and with attempts to detect intelligent life elsewhere in the universe.

According to a widely accepted scenario for the origin of the Moon, a Mars-sized planetoid collided with the primitive Earth; its Fe core coalesced with that of the Earth and a portion of the less-dense rocky debris coalesced to form the Moon. This description of

the Moon's origin is referred to as Giant Impact (GI) [2]. It seems impossible that life forms on Earth would have survived GI. At the same time GI should have vaporized the Earth's volatile material and returned it to space. Thus the origin of the Earth's biota must have occurred after GI.

Recent investigations have indicated that life was present on Earth very shortly after GI. For example, Mojzsis et al. [3] present evidence for life on Earth more than 3.8 b.y. ago. The rapid emergence of life on Earth appeared puzzling when its antiquity was established at more than 3 b.y. The realization that the terrestrial oceans needed for a biota were added to the Earth by cometary transport subsequent to GI [4] makes the situation even more puzzling. The transport of life from Mars to the Earth [1] simultaneous to the arrival of the Earth's oceans would provide a resolution to this dilemma. At the same time it would explain why the metabolic processes deduced to have occurred in ALH 84001 [1] are so similar to those of the Earth's biota.

There is another current problem that could be resolved (or, at least diminished in severity) by the transport of life from Mars to Earth: the failure to detect intelligent life elsewhere in the universe despite serious efforts to do so. If the Earth's biota is older than the time the Earth has been continuously habitable, then the calculation of the probability of finding intelligent extraterrestrial life needs to be revised downward. It is probable that Mars was habitable before the Earth; being further from the Sun, it should have accumulated water oceans earlier and there is no evidence for a cataclysm such as GI necessitating a restart of biological processes on Mars.

Following the announcement of life in a martian meteorite, there was widespread discussion of the criteria to be used to determine its validity. If it is judged on the basis of whether it makes what we think we know more or less credible, then the foregoing is supportive. However, the question of life on Mars is not likely to be resolved in the near future.

**References:** [1] McKay D. S. et al. (1996) *Science*, 273. [2] Cameron A. G. W. and Benz W. (1991) *Icarus*, 92, 204; Cameron A. G. W. (1994) *LPS XXV*, 215. [3] Mojzsis et al. (1996) *Nature*, 384, 55. [4] Delsemme A. H. (1992) *Origin of Life*, 21, 279.

**CARBONATE PRECIPITATION IN ANOXIC ENVIRONMENTS: IMPLICATIONS FOR ATMOSPHERIC  $\text{CO}_2$  REMOVAL ON EARLY MARS.** D. Y. Sumner, Geology Department, University of California, Davis CA 95616, USA (sumner@geology.ucdavis.edu).

Carbon dioxide is an important greenhouse gas on Earth and probably was on early Mars. On Earth today, it is one of the important atmospheric gases that maintains surface temperatures above the freezing point of water. Models of early Earth's atmosphere suggest that much higher  $\text{PCO}_2$  would have been necessary to maintain liquid water during early Archean time when solar luminosity was substantially lower than present. Evidence for liquid water on early Mars also implies a higher greenhouse effect than at present, which may have been due to higher  $\text{PCO}_2$  in the martian atmosphere. Higher  $\text{PCO}_2$  for both planets is consistent with models of planetary outgassing, which predict that large volumes of  $\text{CO}_2$  were released early in their histories. The volume of  $\text{CO}_2$  outgassing declined through time as the two planets cooled and volcanism

became less abundant. The decline in outgassing was particularly steep for Mars, which lacks a mechanism for recycling C back into the interior of the planet. Sinks for surface C on both Earth and Mars also changed through time. Carbonate precipitation and organic C burial are the two most important sinks for surface C on Earth. Unless Mars contained a significant biosphere early in its history, carbonate precipitation would have been the dominant sink for outgassed  $\text{CO}_2$ . Thus, the rates of carbonate precipitation may have had a substantial influence on  $\text{PCO}_2$  of both planets. In the case of Mars, understanding the rate at which  $\text{CO}_2$  was removed from the atmosphere is critical for evaluating surface temperatures and the length of time between formation and freezing of a hydrosphere.

Carbonate precipitation depends on the saturation state of carbonate, which is a function of both the cation concentration and  $[\text{CO}_3^{2-}]$ . Since  $[\text{CO}_3^{2-}]$  is a function of pH and the buffering capacity of the solution, carbonate precipitation depends on numerous chemical properties. In addition to the thermodynamic properties, carbonate precipitation often is limited kinetically under conditions characteristic of Earth's surface. For example, in the modern oceans, calcite precipitation is inhibited kinetically by various ions and molecules such as  $\text{Mg}^{2+}$ , which is one of the major kinetic inhibitors thought to maintain supersaturation of modern surface seawater. Inhibitors help maintain the supersaturation of seawater by reducing carbonate precipitation rates and thus the rate of removal of  $\text{Ca}^{2+}$  and  $\text{CO}_3^{2-}$  from seawater. The slow removal of these ions causes the saturation state of sea water to increase until the effects of the inhibitors are overcome, and the removal of  $\text{Ca}^{2+}$  and  $\text{CO}_3^{2-}$  as calcium carbonate balances the influx of these ions. Thus, by reducing precipitation rates, inhibitors kinetically maintain highly saturated solutions and provide a mechanism for sustaining supersaturated modern and ancient sea water. Also, kinetic effects can influence the mineralogy of carbonate precipitates. Two examples from modern oceans include the absence of dolomite and the presence of aragonite. Dolomite ( $\text{MgCa}(\text{CO}_3)_2$ ) is the most supersaturated carbonate in sea water, but dolomite precipitation requires ordering of Ca and Mg layers. The ordering process is so slow under ambient surface conditions that dolomite only precipitates in the subsurface. In contrast, aragonite is the high-temperature polymorph of  $\text{CaCO}_3$ . Yet calcite (the stable polymorph) is so supersaturated in modern oceans that aragonite is a common precipitate. Thus, trace-elemental chemistry and kinetics can dramatically influence both the rate and mineralogy of carbonate precipitation.

In addition to the carbonate precipitation inhibitors documented for modern oceans, experimental work has demonstrated that both  $\text{Fe}^{2+}$  and  $\text{Mn}^{2+}$  slow rates of calcite precipitation [1–3]. Both  $\text{Fe}^{2+}$  and  $\text{Mn}^{2+}$  are sensitive to the oxidation state of ambient water.  $\text{Fe}^{2+}$  rapidly oxidizes to  $\text{Fe}^{3+}$  in alkaline solutions in the presence of even very low concentrations of  $\text{O}_2$ .  $\text{Mn}^{2+}$  oxidizes much more slowly and requires higher  $[\text{O}_2]$ . Also, both can be oxidized by UV radiation. Since both elements affect calcite precipitation and are present in anoxic water, models of carbonate precipitation from low- $\text{O}_2$  environments such as on early Earth and on Mars need to include the influences of  $\text{Fe}^{2+}$  and  $\text{Mn}^{2+}$ . Potential effects include slower rates of calcite precipitation, differences in carbonate mineralogy (i.e.,  $\text{FeCO}_3$  precipitation rather than calcite precipitation), and influences on the location of precipitation.

Sumner and Grotzinger [4,5] proposed that  $\text{Fe}^{2+}$  played a substantial role in Archean carbonate deposition when surface  $[\text{O}_2]$  was

<1% of the present atmospheric level. They argue that the modes of carbonate precipitation were different in anoxic and slightly oxidizing environments. Specifically, Archean carbonates commonly contain decimeter- to meter-thick beds consisting entirely of fibrous calcite and neomorphosed fibrous aragonite that precipitated *in situ* on the sea floor. Such thick accumulations of precipitated carbonate are rare in younger marine carbonates, suggesting an important change in the modes of calcium carbonate precipitation through time. In addition, calcite textures similar to those in Archean carbonates occasionally are present in Phanerozoic carbonate build-ups associated with low  $\text{O}_2$  environments. The correlation of these textures with low  $[\text{O}_2]$  implies that carbonate deposition is affected by changes in the oxidation state of sea water. These differences may be attributable to the presence of  $\text{Fe}^{2+}$  (or  $\text{Mn}^{2+}$ ) in solution. Further field observations and experimental work are necessary to test this hypothesis, but preliminary results suggest that carbonate precipitation from anoxic water probably was substantially different texturally and dynamically than it is from oxidizing environments.

The effects proposed by Sumner and Grotzinger [4,5] have substantial implications for carbonate deposition on early Mars. If liquid and vapor water were present on Mars, the atmosphere and hydrosphere probably were anoxic. Thus,  $\text{Fe}^{2+}$  and  $\text{Mn}^{2+}$  would have been present in solutions from which calcium carbonates would be expected to precipitate. The actual concentrations and distributions of  $\text{Fe}^{2+}$  and  $\text{Mn}^{2+}$  would have been controlled by the rate of UV oxidation, sulfide precipitation, and carbonate precipitation. Unless the UV flux and sulfide deposition were high enough to remove all dissolved  $\text{Fe}^{2+}$  and  $\text{Mn}^{2+}$ , carbonate precipitation would have been heavily influenced by the distribution of  $\text{Fe}^{2+}$  and  $\text{Mn}^{2+}$  in solution. Specifically, UV oxidation would preferentially remove  $\text{Fe}^{2+}$  and  $\text{Mn}^{2+}$  from the surfaces of lakes or oceans. Thus,  $\text{CaCO}_3$  would precipitate preferentially in the shallowest water and precipitation may have been inhibited in deeper water. Restriction of calcite precipitation to shallow water would have reduced the rate of  $\text{CO}_2$  removal from the martian atmosphere. Although  $\text{FeCO}_3$  may have precipitated at depth,  $\text{FeCO}_3$  precipitation requires high  $[\text{Fe}^{2+}]$ . If  $[\text{Fe}^{2+}]$  was not high enough, all carbonate precipitation may have been excluded at depth. Thus, the rate of  $\text{CO}_2$  removal from the atmosphere through carbonate precipitation may have been substantially lowered by the presence of  $\text{Fe}^{2+}$  and/or  $\text{Mn}^{2+}$  in solution.

The high  $[\text{Fe}^{2+}]$  in carbonates from meteorite ALH 84001 supports the presence of  $\text{Fe}^{2+}$  in at least some carbonate precipitating environments. Although these carbonates may have been deposited at high temperatures, they represent the only compositionally analyzed martian carbonates. They predominantly consist of  $\text{MgCO}_3$  rather than  $\text{CaCO}_3$ . As yet, no low-temperature experimental work has been done on the effects of  $\text{Fe}^{2+}$  or  $\text{Mn}^{2+}$  on  $\text{MgCO}_3$  or aragonite precipitation. Thus, additional research on the effects of trace elements on all low-temperature carbonate minerals is necessary. Results will provide data to test the importance of low  $[\text{O}_2]$  on the dynamics of carbonate precipitation on planetary surfaces.

**References:** [1] Meyer H. J. (1984) *J. Crystal Growth*, 66, 639–646. [2] Dromgoole E. L. and Walter L. M. (1990) *Chem. Geol.*, 81, 311–336. [3] Dromgoole E. L. and Walter L. M. (1990) *GCA*, 54, 2991–3000. [4] Sumner D. Y. and Grotzinger J. P. (1996) *J. Sediment. Res.*, 66, 419–429. [5] Sumner D. Y. and Grotzinger J. P. (1996) *Geology*, 24, 119–122.

**STUDIES OF WEATHERING PRODUCTS IN THE LAFAYETTE METEORITE: IMPLICATIONS FOR THE DISTRIBUTION OF WATER ON BOTH EARLY AND RECENT MARS.** T. D. Swindle and D. A. Kring, Lunar and Planetary Laboratory, University of Arizona, Tucson AZ 85721-0092, USA.

The question of where and when there has been liquid water on Mars is one of the most fundamental problems on the red planet. Photogeological evidence suggests that there has been water flowing on the surface from time to time [1], and some interpretations suggest that there have been oceans on Mars on occasion [2]. In collaboration with D. J. Lindstrom (NASA/JSC) and A. H. Treiman (LPI), the Arizona noble gas mass spectrometry lab has been studying liquid-water-derived weathering products in the martian meteorite Lafayette in an attempt to determine absolute radiometric ages.

Those studies have (1) confirmed that the weathering products in Lafayette are martian, not terrestrial, in origin; (2) demonstrated that there has been liquid water on Mars in the last 1300 m.y., and suggested that this has occurred in the last few hundred million years; and (3) suggested that this water has been in contact with the martian atmosphere, and hence is near-surface, rather than magmatic, water. Given the fact that most photogeological evidence for liquid water on Mars suggests that it was more prevalent in the distant past, one might then expect that ancient martian meteorites would contain even more evidence for aqueous alteration. Instead, the only ancient martian meteorite known, ALH 84001, seems to have been no more altered than Lafayette. In this abstract, we will briefly describe the results of the noble gas isotopic studies, and then point out some of the puzzling implications for early Mars.

**Noble Gas Isotopic Studies of Martian Weathering Products:** Swindle et al. [3,4] studied samples of "iddingsite" from Lafayette. Iddingsite is a complicated mixture of clays, oxides and ferrihydrites that requires liquid water to form. Microstratigraphic arguments have been used to suggest that these formed on Mars [5,6]. Treiman [6] separated 16 samples that were analyzed with laser-extraction noble gas mass spectrometry.

The single largest sample (34 mg) was used for analysis of the heavy noble gases, Kr and Xe. Although the signal was only a few times the background level, the results [3] suggested that the iddingsite sample does contain trapped martian atmosphere (Fig. 1). Furthermore, both the Kr/Xe elemental ratio and the  $^{129}\text{Xe}/^{132}\text{Xe}$  isotopic ratio are consistent with the iddingsite being the primary carrier of trapped martian atmospheric noble gases in the nakhlites. On the other hand, the Kr/Xe ratio of the iddingsite (like the bulk nakhlites) is fractionated relative to the martian atmosphere. Drake et al. [7] suggested that this is the result of the iddingsite trapping martian atmosphere from water, which could fractionate Kr from Xe. This, in turn, implies that the water that formed the iddingsite was in communication with the atmosphere. This would not be expected to be true for magmatic water.

Most of the samples were used for  $^{40}\text{Ar}$ - $^{39}\text{Ar}$  [3] and K-Ar [4] studies. A range in apparent ages, from roughly 100 to 650 Ma, was observed. These demonstrate that the weathering products are not terrestrial. Since Lafayette is 1300 m.y. old, the weathering products can be no older than that. The data suggest that they might be much younger. However, it is also possible that they formed from water liberated by the magmatic episode that produced the nakhlites, but were partially degassed, to varying degrees, later.

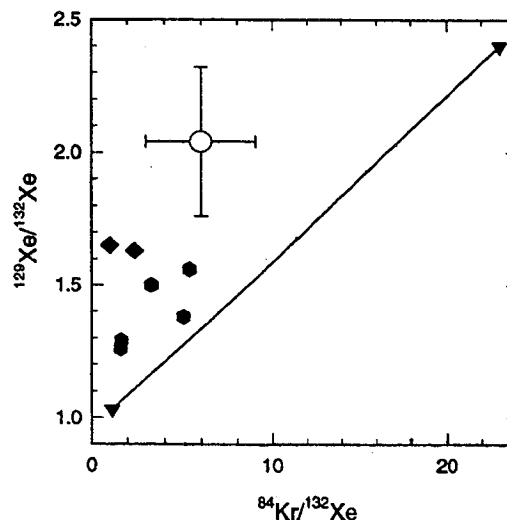


**Fig. 1.** Plot of the  $^{129}\text{Xe}/^{132}\text{Xe}$  isotopic ratio vs. the  $^{84}\text{Kr}/^{132}\text{Xe}$  elemental ratio for various martian meteorites. Most shergottites (not shown) plot along the line connecting the martian atmosphere (upper right, measurement from EETA 79001) with Chassigny (lower left, potentially a sample of volatiles from the interior of Mars). Whole-rock nakhlite meteorites (solid symbols) have elevated  $^{129}\text{Xe}/^{132}\text{Xe}$  ratios suggesting the presence of martian atmosphere, but their low Kr/Xe elemental ratios mean that if they did incorporate atmospheric gas, it was through a process that involved elemental fractionation. The iddingsite sample (open symbol) looks similar to the whole-rock nakhlites, and the absolute abundances in iddingsite are high enough to suggest that it is a major (if not the dominant) site of the atmospheric-like gases in nakhlites.

**Implications for Early Mars:** The fact that there has been liquid water flowing through martian rocks in the last 1300 m.y. has several implications for the earlier history of water on Mars. Most obviously, if such a young rock has evidence of aqueous alteration, we might (perhaps naively) expect to see much more of such alteration in a much older rock, but this is not the case for ALH 84001. There are some features that are probably the result of secondary alteration at relatively low temperatures [8], but the total abundances of these phases is comparable to that in Lafayette, no more than a few percent. In addition, the alteration seems to have involved  $\text{CO}_2$ -charged fluids, which produced carbonate, rather than the types of hydrous minerals seen in Lafayette.

In part, the relative lack of aqueous alteration features in ALH 84001 must be related to the source of the fluid. For the nakhlites, the heavy noble gas data suggest that the water is not magmatic in origin. It could come from either melted permafrost or deeper groundwater [9], released by the effects of either impacts [10] or volcanism. ALH 84001 was clearly reheated about 3.9 g.y. ago [11], but perhaps it was in a region that was exposed to neither volcanic activity nor large impacts since then.

The lack of extensive aqueous alteration in ALH 84001 is also difficult to reconcile with models of a warmer, wetter Mars that had extensive precipitation. It is clear from the shock-metamorphic cataclastic texture of ALH 84001 that by ~4.0 Ga the rock was more porous and more permeable than it was in its pristine igneous state. For the same reason, it was probably more porous and permeable than Lafayette, which has suffered very few shock-metamorphic effects. Consequently, if precipitation were widespread 4.0 g.y. ago,

it seems that it should have affected ALH 84001 at least to the extent that relatively drier conditions affected Lafayette less than 1.3 g.y. ago.

Alternatively, if precipitation and subsequent percolation of aqueous fluids have not affected ALH 84001, perhaps sapping models for the topographic degradation and valley formation seen in the highlands are more likely [12]. Assuming that a liquid water aquifer fed the sapping process, the lack of aqueous alteration in ALH 84001 suggests that the meteorite has not been within the aquifer for at least the last ~4.0 Ga. The bottom of the aquifer is defined by the level in the crust at which self-compaction eliminates porosity, estimated to be about 10 km [9]. The top of the zone in which liquid water is stable is determined by the geothermal gradient. This may have been within a few hundred meters of the surface 4.2 Ga ago [12], but would have rapidly moved deeper, except for local effects.

For meteoritic material to be launched from Mars with escape velocities, it probably has to be relatively close to the surface. At the present time, it is unclear whether or not the igneous cumulate represented by ALH 84001 was emplaced at these shallow depths, or whether it was excavated from a deeper level by an impact cratering event and emplaced as impact ejecta at a shallower depth. In either case, it has probably been at a shallow depth for the last ~4.0 g.y. Given its lack of exposure to low-temperature liquid water, this suggests that, whether precipitation or sapping caused the valley networks, there were at least regions of Mars where the near-surface region was dry by ~4.0 g.y. ago.

In summary, the 1.3-g.y.-old Lafayette is as heavily altered as the much older ALH 84001, although the alteration of Lafayette seems to have involved more water (and possible lower temperatures) than that of ALH 84001. This is hard to reconcile with models that suggest that Mars was wetter in the distant past, unless the era(s) of warm, wet climate or active sapping had largely ended by 4.0 Ga. These differences suggest that the alteration products may not be the result of global processes, but rather of localized geologic and hydrologic domains.

**References:** [1] Carr M. H. (1996) *Water on Mars*, Oxford, New York. [2] Baker V. R. et al. (1991) *Nature*, 352, 589–594. [3] Swindle T. D. et al. (1995) *LPS XXVI*, 1385–1386. [4] Swindle T. D. et al. (1997) *LPS XXVIII*. [5] Gooding J. et al. (1991) *Meteoritics*, 26, 135–143. [6] Treiman A. H. et al. (1993) *Meteoritics*, 28, 86–97. [7] Drake M. J. et al. (1994) *Meteoritics*, 29, 854–859. [8] Wentworth S. and Gooding J. (1995) *LPS XXVI*, 1489–1490. [9] Clifford S. M. (1993) *JGR*, 98, 10973–11016. [10] Newsom H. E. (1980) *Icarus*, 44, 207–216. [11] Turner G. et al. (1997) *GCA*, in press. [12] Squyres S. W. and Kasting J. F. (1994) *Science*, 265, 744–749.

**DISTRIBUTION OF CHANNELS IN THE THAUMASIA REGION INDICATES HYDROLOGIC ACTIVITY LARGELY DUE TO LOCAL HEATING DURING EARLY MARS.** K. L. Tanaka, J. M. Dohm, and T. M. Hare, U.S. Geological Survey, Flagstaff AZ 86001, USA (ktanaka@flagmail.wr.usgs.gov).

This study of channel-length densities per geologic stage for densely vs. nondensely channeled terrains provides insight into channel formation in the Thaumasia region and for Mars as a whole.

Our research indicates that during early Mars (Noachian and Early Hesperian) (1) channels formed mainly by crustal heating related to tectonism, volcanism, and impact cratering and (2) climate did not serve a primary role in channel formation.

We have carefully mapped and digitized at 1:5,000,000 scale the geology, structure, and channel features in the Thaumasia region of Mars [1]. This region is ideal for analyzing the history and genesis of ancient channel features because it comprises a wide array of Noachian and Hesperian rock materials and volcanic, tectonic, impact, and erosional terrains and features. Our stratigraphic scheme, which includes comprehensive crater counts, discriminates five stages of activity; the three earliest (involving the Noachian and Hesperian) are relevant to addressing the origin of channel formation. Each mapped erosional valley has been assigned to these stages according to the ages of the geologic units they cut. We also separated valleys into channels that have a well-developed, networking valley form from furrows that have a discontinuous, largely degraded, irregular valley or trough form. We interpret that the furrows may have formed by erosional, tectonic, and (or) volcanic processes; some appear to follow preexisting grabens.

We have compared our data (Tables 1 and 2) with that of Carr and Chuang [2], who looked at global-scale channel densities as a function of stratigraphic system based on global-scale mapping. For example, our overall stage 1 channel-only density matches their Noachian value, whereas our stage 3 density is nearly a factor of 5× higher than their Hesperian value (the values for this period probably vary widely across the planet). In addition, the heavily channeled terrains of Thaumasia are less densely channeled than values for Amazonian volcanos, which have the highest channel densities on Mars [2,3].

Our data show that only minor proportions of areas of all the material of each stage (stage 1, 17%; stage 2, 25%; and stage 3, 5%) are heavily dissected (channel-length densities ~0.01 to 0.05 km/km<sup>2</sup>). This channel activity was coeval with many volcanos (and perhaps large associated intrusive bodies), rifts, and large impacts mapped in the Thaumasia region [1] that could be responsible for local, heavy dissection. We would therefore largely attribute heavy dissection to local events of increased crustal heating. We also determined channel density relative to areas of or proximal to high relief (Table 2) and found that (1) stage 1 materials of high relief are scattered through the map area and have variable channel density, (2) stage 2 materials of high relief occur along the southern margin of the Thaumasia plateau and in the northwestern Argyre area and have greater channel density than stage 1 materials of high relief, and (3) stage 3 high-relief units are all densely channeled materials that occur in places along the lower edge of the Thaumasia plateau. In other words, heavy dissection during stages 1–3 gradually became localized, first in areas of mainly high relief (stage 2) and next

TABLE 1. Areas (10<sup>6</sup> km<sup>2</sup>) of groups of materials by stage used in this study (stage 1, Noachian; stage 2, Late Noachian and Early Hesperian; stage 3, Hesperian).

Group	Stage 1	Stage 2	Stage 3
Densely channeled materials	0.328	0.361	0.076
Less-densely channeled materials	1.649	1.060	1.515
High-relief materials	1.295	0.327	0.076
All materials	1.977	1.421	1.591

TABLE 2. Channel-length densities (km/km<sup>2</sup>) for groups of materials and erosional features.

Group	Stage 1	Stage 2	Stage 3
Densely channeled materials, channels only	0.0146	0.0320	0.0193
Densely channeled materials, channels and furrows	0.0443	0.0522	0.0366
Less-densely channeled materials, channels only	0.0012	0.0007	0.0000
Less-densely channeled materials, channels and furrows	0.0078	0.0022	0.0003
High-relief materials, channels	0.0024	0.0228	0.0193
High-relief materials, channels and furrows	0.0130	0.0304	0.0366
All materials, channels only	0.0032	0.0080	0.0019
All materials, channels and furrows	0.0134	0.0145	0.0030

in lower parts of the Thaumasia plateau margin (stage 3). A possible interpretation for this evolution is that the groundwater table lowered with time.

Other materials in the Thaumasia region are less densely channeled than the densely channeled materials by factors of six (stage 1, channels and furrows) to more than 100 (stage 3, channels and furrows). The decrease in channel features with time in these units appears to reflect a more regional, and perhaps global, effect. However, this regional effect is a minor contributor to overall channel density. Because lightly channeled Noachian rocks (stages 1 and 2) have channel densities 1–2 orders of magnitude lower than terrestrial drainage systems (which range from ~0.07 to 0.21 [2]), it appears that surface run-off caused by rainfall was not a major factor in this regional effect. Rather, higher global heat flow leading to a higher geothermal gradient and (or) impact activity more likely facilitated the modestly increased Noachian channel development.

**References:** [1] Dohm J. M. et al. (1997) *Geologic, Paleotectonic, and Paleocorrosional Maps of the Thaumasia Region, Mars; Scale 1:5,000,000*, in preparation. [2] Carr M. H. and Chuang F. C. (1997) *JGR Planets*, in press. [3] Gulick V. C. and Baker V. R. (1990) *JGR*, 95, 14325–14344.

**SEM STUDIES OF ANTARCTIC LUNAR AND SNC METEORITES WITH IMPLICATIONS FOR MARTIAN NANOFOSSILS: A PROGRESS REPORT.** A. E. Taunton, Cosmochemistry Group, Department of Chemistry and Biochemistry, University of Arkansas, Fayetteville AR 72701, USA.

Several meteorites recovered from Antarctica are believed to have a martian origin. This is evidenced by their ages, chemical compositions, morphologies, and trapped gases [1–3]. McKay et al. recently reported finding evidence of possible past life in one of the martian meteorites citing mineralogy, morphological phases, PAHs, and microfossils [4]. However, alternative explanations of the origin of the microfossils include them being laboratory artifacts or Antarctic contamination, since bacteria are known to survive in very harsh conditions including Antarctica. The purpose of this project is to examine these alternative explanations by studying several Ant-

arctic lunar and SNC meteorites. If forms are found in lunar meteorites that are similar or identical to those found in martian meteorites, then it will be hard to rule out the idea that the forms are artifacts or contamination.

The Moon is an extremely harsh environment, incapable of supporting life. The surface temperature increases approximately 260K from just before lunar dawn to lunar noon. The subsurface temperatures vary greatly from that, being about 45K higher. The Moon's atmosphere is about 14 orders of magnitude less than the Earth's. Because of this, the Moon is bombarded with radiation: solar wind, galactic cosmic rays, and solar cosmic rays [5]. Notwithstanding a recent announcement of possible ice deposits near the pole [6], the lunar surface is exceptionally dry. Thus, no type of life forms should be present in lunar meteorites.

Eight chips of lunar meteorites and three chips of martian meteorites are being studied (Table 1).

All samples, with the exception of ALH 81005, were freshly fractured. All were mounted on either a graphite disk or planchette using double-sided tape and/or carbon paint. The samples were Au-Pd sputter coated for 30–60 s at 10–12 mA and 2400 V to make them conductive for SEM study. Each sample was studied under a Philips 40XFEG scanning electron microscope. A chemical analysis of several regions in QUE 93069 was performed using energy dispersive X-ray analysis.

McKay et al. used criteria established by Folk [9]: (1) Clusters of bodies separated by large, unpopulated areas. (2) Bodies the same size as normal bacteria. Bacteria can become stressed under changing conditions and may "shrink" to nanobacteria size. However, nanobacteria have been observed in nonstressful environments, suggesting that they have no "large" size equivalent. (3) Populations the same as normal bacteria. They can be well-sorted, bimodal, or a mixture of different types of bacteria at various stages of sporulation and/or nutrition. (4) Bodies similar in shape and texture of normal bacteria: smooth to somewhat lumpy surfaces with the shapes of cocci, bacilli, ellipses, or long filaments. They can appear as chains of spheres or rods. (5) Bodies do not contain Fe, but may have Ca or Si, which are precipitates of bacteria. (6) Bodies must be distinct from minerals or artifacts. They must be observed at very high magnifications (at least 35,000×) to verify that the shapes are sphere ellipsoids or rods rather than cubes.

McKay et al. added Fe-bearing magnetotactic bacteria, bacteria that contain magnetite. Using the McKay et al. characteristics, an attempt to locate forms in the lunar and martian meteorites that could

TABLE 1. Samples studied.

Meteorite	Description [7,8]
ALH 81005*	Anorthositic regolith breccia—highland
EET 87521	Basaltic breccia—mare
MAC 88104†	Anorthositic regolith breccia—highland
MAC 88105†	Anorthositic regolith breccia—highland
QUE 93069*	Anorthositic breccia
QUE 94281	Basalt-rich breccia
EET 79001	Basaltic shergottite
ALH 77005	Lherzolithic shergottite
ALH 84001	Coarse-grained orthopyroxenite

\*Two chips were studied.

†Paired meteorites.



be possible microfossils is being made.

Approximately 235 microbiologists and SEM specialists were solicited to take part in a blind test. Out of 56 responses, 35 were positive. If attempts to locate forms in both lunar and martian meteorites are successful, then these 35 participants will be sent a plate with six unlabeled micrographs of forms in lunar meteorites mixed with six unlabeled micrographs of forms in SNC meteorites. The specialists will be asked to sort the micrographs into categories if they can, keeping in mind the characteristics used by McKay et al. They will also be asked to make any comments they wish on population distribution, size, and recognizability. A statistical analysis will be performed, and the results will be given at a later date.

With the blind test we are providing objective results to a subjective question. The microbiologists and SEM specialists were selected randomly for solicitation by collecting names and addresses of contributors in the *Journal of Microbiology*, *Scanning Electron Microscopy*, and several books on microbiology and scanning electron microscopy. A letter was sent including a return postcard indicating interest. Thus, the participants were self-selected based on their expertise in the area of SEM imaging of bacteria.

The purpose of this project is not to identify the forms found in the meteorites; it is simply to compare the forms. Regardless of what they actually are, the vital piece of information is whether or not the forms are found in both the lunar and the martian samples. If they are in both meteorites or if they are found only in lunar samples, then a martian origin can be excluded, and we have identified Antarctic contaminants, inorganic material, and/or laboratory artifacts. If found only in martian samples, then we have strengthened the case for martian microbes.

The lunar samples have presently been studied and imaged, and the SNC meteorites will be studied throughout February and March. If the project is successful, the plate of micrographs will be sent out during the first two weeks of April and statistical analysis will be completed in May.

**References:** [1] Bogard D. D. and Johnson P. (1983) *Science*, 221, 651–655. [2] Miura Y. N. et al. (1994) *LPS XXV*, 919–920. [3] Miura Y. N. et al. (1995) *GCA*, 59, 2105–2113. [4] McKay D. et al. (1996) *Science*, 273, 924–928. [5] Vaniman D. et al., eds. (1991) in *Lunar Sourcebook: A User's Guide to the Moon*, pp. 27–69, Cambridge, New York. [6] Nozette S. et al. (1996) *Science*, 274, 1495–1498. [7] Benoit P. (1996) *Meteoritics & Planet. Sci.*, in press. [8] McSween H. Y. (1994) *Meteoritics*, 29, 757–779. [9] Folk R. (1993) *J. Sediment. Petrol.*, 63, 990–993.

**WHAT IS MARS' HIGHLANDS CRUST?** A. H. Treiman, Lunar and Planetary Institute, 3600 Bay Area Boulevard, Houston TX 77058, USA (treiman@lpi.jsc.nasa.gov).

Mars' ancient highland crust formed very early in martian history, and is the backdrop for questions of water abundance and biologic activity on early Mars. The chemical and mineralogic nature of the highland crust is not known. All available data are consistent with either a basaltic or "andesitic" highlands. An anorthositic highlands seems inconsistent with the geochemistry of martian meteorites, and an undifferentiated crust seems inconsis-

tent with optical reflection spectra.

**Choices:** From knowledge of other planetary bodies, the highland crust of Mars might be undifferentiated chondritic, basaltic/pyroxenitic (Vesta), gabbroic anorthositic (lunar highlands), or "andesitic" (continents on Earth). Other types of planetary crusts in the solar system (ices, sulfur) seem unreasonable for Mars.

**Timing:** Mars' highland crust formed very early. Qualitatively, its age is apparent in its abundance of impact craters, which is comparable to that of the lunar highlands [1]. Radio-isotope data on the martian meteorites show that Mars experienced its major differentiation event, presumably including formation of the crust, by 4539 Ga [2,3], only tens of million years after solar system formation [4,5].

**Remote Sensing:** Most of the highlands is bright and orangish in color, independent of the morphology of the underlying surface. Much of the orange material is dust from global storms. Some orange material is indigenous, with variable proportions of ferric and hydrous minerals presumably reflecting alteration [6]. These orange materials retain no IR signature of their pre-alteration mineralogies.

Dark areas in the highlands show IR absorption bands of pyroxenes like those in the martian shergottite meteorites (basalts) [7,8]. A few areas have pyroxene absorptions comparable to those of the martian nakhlite meteorites (augite-olivine basalts) [9], but olivine absorptions are unknown or minor.

These data suggest that the highlands are basaltic, but this inference is not unique. Dark areas in the highlands might represent transported basaltic sands, and not indigenous bedrock. Anorthositic and "andesitic" rocks can also contain abundant pyroxenes. The absence of olivine in the highlands could argue against a chondritic crust and against a crust of alkaline basalt. But olivine alters readily to hydrous silicates and might not survive a "warm, wet" epoch.

**Samples:** At this time, we have only one rock from the martian highlands, the pyroxenite meteorite ALH 84001 [10,11]. ALH 84001 is inferred to have formed by accumulation of pyroxene crystals in a body of basalt magma, and so is not likely to be representative of Mars' highland crust. As a cumulate, it would represent only a portion of its parent magma body, which might consist mostly of gabbroic (basaltic) rocks.

**Geochemistry:** Dust is ubiquitous on Mars. As analyzed by the Viking landers, the dust is basaltic in composition and quite similar to the Shergotty martian meteorite [12]. If the dust represents a global average of fine-grained weathered rock, then the highlands are almost certainly basaltic. However, the origin of the dust is not known. It might reflect singular igneous events or singular regions of altered igneous rock, and so be irrelevant to the highlands.

The martian meteorites grudgingly yield some constraints on the composition of the highland crust. The martian meteorites are basalts, so their compositions constrain those of their source mantles and thereby the overall composition of Mars [13,14]. Differences between the mantle and planet compositions reflect material that has gone to the core, the crust, or unsampled layers of the mantle [4,13–15].

From the martian meteorites, it seems clear that the highland crust is not primarily anorthositic. None of the martian meteorites has an Eu anomaly, and all have Sr/Nd near chondritic, suggesting that their parent mantles never fractionated plagioclase [2,13]. The source mantle for the martian meteorites is, however, significantly

depleted in Al [4,13,16]. The Al could have been lost to the crust as "andesitic" magmas, or to an unsampled lower mantle as spinel or garnet. Fractionations involving garnet have been invoked to explain the strong LREE enrichments and depletions of the martian meteorite magmas [14].

There may, in fact, be more than one nonmantle composition. Both [4] and [15] were able to interpret radiogenic isotope systematics of the martian meteorites in terms of three distinct components: mantle, lithosphere, and crust. The crust was interpreted as basalt rich in incompatible elements [15], but "andesitic" rock would also fit the isotopic constraints.

**Conclusions:** The composition of Mars' highland crust remains a mystery, but one that will be solved (at least in part) when the Mars Pathfinder spacecraft successfully obtains chemical analyses of rocks on the Ares Vallis outflow plains. From the data available now, it seems unlikely that the highland crust is either anorthositic or undifferentiated. It is most likely that the highlands are made principally of basaltic rock comparable to the known martian meteorites or of andesitic-composition rock comparable to the Earth's continents.

The difference between basaltic and "andesitic" crusts, though seemingly minor, is important. When melted, a dry "chondritic" mantle would yield basaltic magma [17], but a wet "chondritic" mantle would yield andesitic or granitic magma [18]. If Mars were initially dry, it might have a basaltic crust; water in that crust would have come from outside, e.g., meteoritic infall. If Mars were initially wet, it might have an "andesitic" crust, and retain some of its initial inventory of water. Thus, the bulk composition of the highlands crust will help understand when water came to Mars, and ultimately, where it is now.

**Acknowledgments:** This work draws heavily on my earlier collaborations with M. J. Drake, and to earlier and continuing discussions with J. H. Jones. I am grateful to both.

**References:** [1] Strom et al. (1992) in *Mars*, p. 383, Univ. of Arizona, Tucson. [2] Jagoutz (1991) *Space. Sci. Rev.*, 56, 13. [3] Harper et al. (1995) *Science*, 267, 213. [4] Jones (1989) *Proc. LPSC 19th*, p. 465. [5] Musselwhite et al. (1991) *Nature*, 352, 697. [6] Murchie et al. (1993) *Icarus*, 105, 454. [7] Singer and McSween (1993) in *Resources of Near-Earth Space*, p. 709, Univ. of Arizona, Tucson. [8] Mustard and Sunshine (1995) *Science*, 267, 1623. [9] Mustard and Sunshine (1996) *LPS XXVII*, 925. [10] Mittlefehldt (1994) *Meteoritics*, 29, 214. [11] Jagoutz et al. (1994) *Meteoritics*, 29, 478; Treiman (1995) *Meteoritics*, 30, 294; Nyquist et al. (1995) *LPS XXVI*, 1065. [12] Baird and Clark (1981) *Icarus*, 45, 113. [13] Treiman et al. (1986) *GCA*, 50, 1071. [14] Longhi et al. (1992) in *Mars*, Univ. of Arizona, Tucson. [15] Jagoutz (1989) *GCA*, 53, 2429. [16] Longhi and Pan (1988) *Proc. LPSC 19th*, p. 451. [17] Jurewicz et al. (1995) *GCA*, 59, 391. [18] Campbell and Taylor (1983) *GRL*, 10, 1061.

**EFFECTS OF CRATERING ON THE EARLY HISTORY OF MARS.** A. M. Vickery, Lunar and Planetary Laboratory, The University of Arizona, Tucson AZ 85721-0092, USA.

Cratering is the most important surficial geologic process operating on the terrestrial planets, with the exception, ironically, of the Earth. I have been asked by the conveners to address a number of issues related to the effects of cratering on the early history of Mars.

There are a great number of unresolved issues, which situation I prefer to view with excitement at the number of new research avenues suggested.

The earliest history of Mars is perhaps best deciphered through its cratering record. In principle, the cratering record of a planet can tell us volumes about the history of the planet. For example, the cratering record of Venus clearly shows that it was resurfaced, in whole or piecewise, relatively recently in its history. In practice, deciphering a planet's history from its cratering record can be frustratingly complex. The only "planet" for which we have a presumably complete cratering record and some absolute ages is the Moon. The Earth's cratering record is obscured by its active geologic processes, and we have absolute ages for no other body.

Given the crater density as a function of size on the Moon and the scaling relations derived from laboratory experiments, we can calculate the flux of impactors on the Moon as a function of their size. This assumes that we know the mean velocity of impact and that this mean velocity is a fairly sharply peaked function. We also need to know reasonably accurately the relation between transient crater size, predicted by the scaling relations, and the final, observed crater size. We can thus estimate the impactor flux on the Moon as a function of time. Unfortunately, we do not know all the relevant quantities very accurately. The situation is also complicated by the fact that the oldest terrains appear to be "saturated" with craters; that is, there are craters on top of other craters to the extent that we have lost the complete record.

To apply this inferred impactor flux [1,2] to other planets, such as Mars, we need models of how the flux, in terms of both mass and mean impact velocity, varies with the target planet's position in the solar system. The best estimates, to date, predict that the martian flux is close to the lunar flux, but it may vary by a factor of 2 either way [3]. It seems clear, based on Mars' cratering record, that there was a period of late heavy bombardment, as on the Moon, followed by a period of much lower cratering flux.

The question is, how would such a cratering history have affected the evolution of Mars' surface and atmosphere? Clearly, the cratering history has modified the surface in such a way that we believe we can draw connections between the history of Mars and that of the Moon. Analyzing the atmosphere of Mars adds another degree of uncertainty to the problem of extrapolating from the Moon, since the Moon has no atmosphere nor any indication that it ever had an atmosphere. Mars is quite different; first, its current tenuous atmosphere resembles that of Earth with respect to strict atmophiles such as N and noble gases, but depleted 30–100-fold [4]. Other atmospheric components are buffered by the fact that they coexist on or within the solid surface. Second, there are geomorphic features on Mars that suggest that there once was an atmosphere dense enough to sustain at least episodes of precipitation heavy enough to have produced Earth-like valley networks of "river" beds. These two lines of evidence suggest that Mars had a much denser atmosphere early in its history.

If Mars once had a dense atmosphere, how was it lost? The most promising theory for wholesale, nonfractionating loss is atmospheric erosion due to impacts. Melosh and Vickery [1] have shown that the impact flux in the early history of the solar system was probably sufficient to have stripped Mars of most of its atmosphere during the period of Late Heavy Bombardment. Other mechanisms for atmospheric loss very early in Mars' history include hydrodynamic escape and chemical weathering. The first assumes the primordial atmo-



sphere of Mars included a significant quantity of very light gases, especially H, whose escape from a low-gravity planet under the influence of high, early solar EUV, would have carried other, heavier elements with it. These heavier elements (and their isotopes) would have been fractionated by the process [5,6]. The latter postulates chemical reactions that led to the incorporation of atmospheric components into the solid surface of the planet [7]. Other mechanisms for atmospheric loss that may have been important as the impact flux slackened are dissociative recombination and ion pick-up by the solar wind [8–10]. The relationship among these mechanisms, whether complementary or competitive, is a completely open question.

Another open question is the interaction between the dust injected into the atmosphere by frequent, early impacts and the greenhouse effect of having a relatively dense atmosphere. To my knowledge, this problem has not been addressed specifically for early Mars, but a number of studies have been done for the Earth relevant to the kill mechanism for the KT extinctions [e.g., 11,12]. Early studies suggested that sufficient dust would be entrained in the stratosphere for sufficiently long periods of time that the mean temperature of the Earth's surface would be drastically lowered and that the amount of sunlight falling on the Earth's surface would be lowered to levels that prevented photosynthesis, thus disrupting the food chain. Frequent impacts early in Mars' history might similarly have cooled the planet and prevented much sunlight from impinging on the surface. The studies for the KT case, however, are not sufficiently exhaustive to say anything definite about Mars. The residence time of dust in the atmosphere on Earth appears to be limited to 1–2 yr, depending mostly on the density of the dust (submicrometer-sized particles tend to coagulate and rain out quickly, independent of the original size of the particles). If the particles remain suspended long enough and have sufficient albedo, they may result in some cooling. The results of these calculations depend on the fact that the Earth has oceans (with high heat capacity) as well as continents. The application to early Mars is uncertain.

One thing that might add to Mars' early near-surface heat inventory is the formation of impact melt. It is most likely that the melt is almost exclusively contained in or near the crater formed by the impact. Because of Mars' lower gravity (compared to the Earth's), more melt may have been produced for a given crater size, but more of it may have been ejected from the crater. I know of no studies that have attempted to integrate the resultant heat flux over a high impact flux.

There is the related question of the thermal effects of impacts for the planet as a whole. Any shock heating due to the traverse of the impactor through the atmosphere or from the impact plume would be very transitory, lasting from minutes to perhaps days at most. Any long-lasting effects would have to be from the slow cooling of impact melt and associated, highly shocked but not melted rock. To my knowledge, there are no studies that evaluate these effects.

In summary, there are many aspects of the early history of Mars that have not been investigated in enough detail to give us any definitive answers.

**References:** [1] Melosh H. J. and Vickery A. M. (1989) *Nature*, 338, 487. [2] Chyba C. F. (1991) *Icarus*, 92, 217. [3] *Basaltic Volcanism on the Terrestrial Planets* (1981) Pergamon, New York, 1286 pp. [4] Zahnle K. J. (1993) *JGR*, 98, 10899. [5] Pepin R. O. (1991) *Icarus*, 92, 2. [6] Pepin R. O. (1994) *Icarus*, 111, 289. [7] Pollack J. B. et al. (1987) *Icarus*, 71, 203. [8] Luhmann J. G. et

al. (1992) *GRL*, 19, 2151. [9] Fox J. L. (1993) *JGR*, 98, 3297. [10] Jakosky B. M. et al. (1994) *Icarus*, 111, 271. [11] Toon O. B. et al. (1982) *Geol. Soc. Am. Spec. Pap.* 190, p. 187. [12] Toon O. B. et al. (1996) *Rev. Geophys.*

**SUBSURFACE FLUID RESERVOIRS ON MARS: A POSSIBLE EXPLANATION FOR THE FATE OF AN EARLY GREENHOUSE ATMOSPHERE.** D. Vlassopoulos, Department of Environmental Sciences, University of Virginia, Charlottesville VA 22903, and S. S. Papadopoulos and Associates, Inc., 7944 Wisconsin Avenue, Bethesda MD 20814, USA (dv3w@virginia.edu).

Mars is the only planet besides Earth to show evidence of a dynamic hydrologic cycle. Numerous geomorphic features suggest that water once flowed at the planet's surface. At present, however, the surface of Mars is too cold to support liquid water and its atmosphere is very tenuous. The implications of the existence of a significant water reservoir and the present state of the martian surface is a dilemma that has motivated research to characterize the volatile reservoirs of Mars and their evolution throughout the planet's history. One of the more popular theories contends that the climate of Mars was warmer and therefore wetter early in its history due to the existence of a dense CO<sub>2</sub> atmosphere. The existence of a CO<sub>2</sub> greenhouse in Mars' past has also been the basis for recent speculations on the development of life on Mars. Despite its acceptance by several researchers, the greenhouse hypothesis has lacked a satisfactory explanation for the fate of the large mass of CO<sub>2</sub> needed to maintain surface conditions warm enough to sustain liquid water (1–5 bar). The recent suggestion that dry ice buried in the polar ice caps may be a significant reservoir of CO<sub>2</sub> has prompted an examination of CO<sub>2</sub> and water phase equilibria and the implications for the existence of a "liquifer" zone in the martian subsurface in which liquid CO<sub>2</sub> is the saturating fluid. Model calculations suggest the existence of a CO<sub>2</sub> liquifer layer up to a few kilometers thick overlying an aqueous liquifer zone. Coupling previously made estimates of crustal porosity and the global groundwater reservoir with the estimated extent of the CO<sub>2</sub> liquifer suggests that up to 20 bar of CO<sub>2</sub> could be stored in the liquid state in the subsurface of Mars. Estimates using more conservative combinations of assumptions still allow reservoir values of several bars. Consequently, it is proposed that much of Mars' early greenhouse atmosphere may now reside in subsurface liquifers.

#### **THE CONTROVERSY OF YOUNG VS. OLD AGE OF FORMATION OF CARBONATES IN ALLAN HILLS 84001.**

M. Wadhwa<sup>1</sup> and G. W. Lugmair<sup>2</sup>, <sup>1</sup>Department of Geology, The Field Museum, Roosevelt Road at Lake Shore Drive, Chicago IL 60605, USA, <sup>2</sup>Max-Planck-Institut für Chemistry, Cosmochemistry, P.O. Box 3060, 55020 Mainz, Germany, and Scripps Institute of Oceanography, University of California–San Diego, La Jolla CA 92093, USA.

The ALH 84001 meteorite is unusual among the SNC (martian) meteorites not only because it has a significantly old crystallization age of ~4.5 Ga [1,2], but also because it contains abundant carbonates (~1 vol%) that are believed to have formed from interaction with

a CO<sub>2</sub>-rich fluid phase in a near-surface environment on Mars [3–6]. Recently it has been suggested that these carbonates may contain evidence of past biogenic activity on Mars [7]. In their study, McKay et al. [7] adopted a 3.6-Ga age for these carbonates, which was obtained by the Ar-Ar laser probe technique [8]. As indicated by [7], this relatively old age makes the interpretation of the observed microstructures within these carbonates as “nanofossils” more likely, since at that time climatic conditions on Mars may have been similar to those on the early Earth (i.e., significantly warmer and wetter than at later times in the geologic history of that planet) making it possible for primitive (bacterial?) life to thrive. However, the 3.6-Ga age for the carbonates as reported by [8] is subject to considerable uncertainties, since the K- and Ar-bearing phase that was analyzed was not the carbonate, but rather the maskelynite that is closely associated with it [9]. Therefore, the suggested 3.6-Ga age is wholly dependent on whether or not the maskelynite was completely degassed by interaction with the fluid that deposited the carbonates, further requiring that these carbonates be deposited at high temperature. However, at present, there is no consensus on the issue of the temperature of the fluid that precipitated the carbonates (see LPS XXVIII abstract volume).

Last year we reported the initial findings of our study of the Rb-Sr systematics in ALH 84001 [10]. Here we further discuss the implications for the age of carbonates based on these data. The figure shows a plot of the Sr isotopic ratios vs. the Rb/Sr ratios for the analyzed mineral separates and bulk samples of ALH 84001. It is evident from this figure that data for the bulk samples, TR1 and TR2, as well as for the pyroxene separates, Px(a) and Px(b), fall on a best-fit line corresponding to an “age” of  $3.84 \pm 0.05$  b.y., which is considerably lower than what was reported by [2]. (The reason for the severe discrepancy between the Rb-Sr age determined by us and that reported by [2] is not clear. However, it may be that the “plag” data point of [2], which, unlike most common plagioclase compositions, is the most radiogenic data point reported by these authors, may not represent a pure plagioclase separate. This is supported by *in situ* ion microprobe analyses of Rb/Sr ratios in maskelynite, indicated by the shaded zone in Fig. 1, which show a much lower Rb/Sr ratio than that reported by [2]. Our “age” recorded by the Rb-Sr system is similar to the Ar-Ar shock age reported by [11] and, therefore, most likely reflects the time of intense shock experienced by ALH 84001. It should be further noted that while TR1 was only ~3 mg, the TR2 sample was ~100 mg and, thus, is presumably representative of the true whole rock. This is important because the 4.56-b.y. reference isochron passes through the TR2 data point and this is wholly consistent with the initial formation of ALH 84001 4.56 b.y. ago with an initial  $^{87}\text{Sr}/^{86}\text{Sr} = 0.69897$ , followed by re-equilibration of the Rb-Sr system 3.84 b.y. ago, resulting in  $I(^{87}\text{Sr}/^{86}\text{Sr}) = 0.70215$  at that time.

Another feature evident in the figure is that the plagioclase data points, Pl(a) and Pl(b), as well as the carbonate data point, C(b), do not fall on the 3.84-Ga isochron defined by the bulk samples and pyroxene separates. Both plagioclase data points fall to the right, while the carbonate data point falls to the left of the 3.84-Ga isochron. It is important to note that the Rb/Sr ratio of the Pl(b) data point falls well within the range of Rb/Sr ratios measured *in situ* by ion microprobe analyses of three plagioclase grains (unpublished data) in a thin section of ALH 84001, shown by the shaded region in the figure. This indicates that the Pl(b) data point most likely represents a pure plagioclase mineral separate, while the Pl(a) separate

may have contained a small amount of a trace phase rich in Sr. Therefore, of the two plagioclase mineral separates, the Pl(b) data point most likely represents a pure plagioclase separate.

It is to be noted that chronologic information regarding carbonate formation derived from the Rb-Sr data obtained so far is dependent on the source of the Sr in the carbonates. There are three main possibilities: (1) A significant portion of the Sr is extraneously derived and has no relation to the host rock. In this case, no chronologic information can be derived from the data obtained. (2) Strontium is derived predominantly from the bulk meteorite. Assuming that TR2 is representative of the bulk sample (see above), a carbonate formation isochron can be drawn between the C(b) and TR2 data points. This would result in a carbonate formation age of  $3.69 \pm 0.06$  Ga (see Fig. 1). (3) Strontium is derived predominantly from the maskelynitized plagioclase. A carbonate isochron between the C(b) and Pl(b) data points results in a formation age of  $1.39 \pm 0.10$  Ga (see Fig. 1).

Of the above possibilities, case (1) is not favored since it requires ad hoc explanations for why TR1, TR2, Px(a), and Px(b) fall on a single Rb-Sr isochron, if the two bulk-rock fractions indeed contain variable amounts of extraneous Sr contributed by the carbonate. Case (2) is also unlikely since it cannot adequately explain why the bulk-rock and pyroxene fractions define a good isochron but the plagioclase fraction clearly lies off it. In particular, for TR1 (small bulk-rock fraction, which appears to be enriched in components that have the least radiogenic Sr, like plagioclase and carbonates) to lie on the 3.84-Ga isochron requires fortuitously correct proportions of plagioclase and carbonate. This is highly unlikely unless the plagioclase and carbonates are closely associated, as would indeed be the case if the Sr in the carbonate is largely derived from the plagioclase, i.e., case (3). Case (3) is additionally favored by (1) the close and “symmetric” (with respect to the 3.84-Ga isochron) association of the Pl(b) and C(b) data points (see Fig. 1), and (2) the predominant spatial association of the carbonates with the plagioclase, as noted by several authors [3,5,6]. Although some small carbonate grains have been found in apparent association with other phases [6], we have observed this to occur mainly in crushed domains indicating transport of these carbonates from their original site of formation.

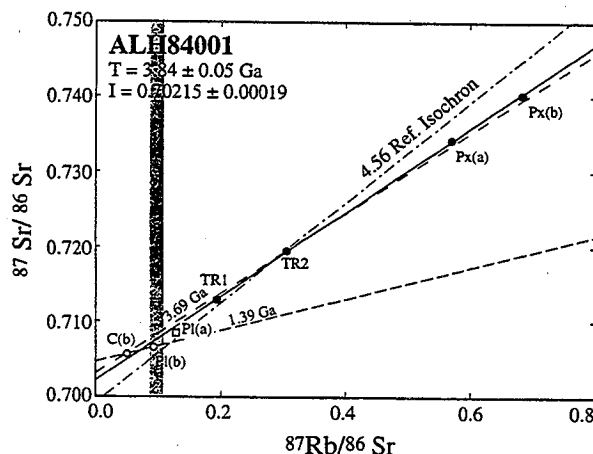


Fig. 1.

Therefore, it seems *most likely* that the formation age of the carbonates in ALH 84001 is  $1.39 \pm 0.10$  Ga. We note that if this 1.39-Ga formation age for the carbonates is indeed true, the interpretation of the microstructures observed by [7] as fossilized ancient martian nanobacteria becomes less likely since the martian climatic conditions at this more recent time may not have been conducive to life. From the above, the relatively young formation age of the carbonates is a likely possibility. However, to unequivocally confirm this finding we have begun an attempt to measure single carbonate and plagioclase grains that are found in true association with one another.

**References:** [1] Jagoutz E. et al. (1994) *Meteoritics*, 29, 478–479. [2] Nyquist L. E. et al. (1995) *LPS XXVI*, 1065–1066. [3] Mittlefehdt D. W. (1994) *Meteoritics*, 29, 214–221. [4] Romanek C. S. et al. (1994) *Nature*, 372, 655–657. [5] Treiman A. (1995) *Meteoritics*, 30, 294–302. [6] Harvey R. P. and McSween H. Y. Jr. (1996) *Nature*, 382, 49–51. [7] McKay D. S. et al. (1996) *Science*, 273, 924–930. [8] Knot S. F. et al. (1995) *LPS XXVI*, 765–766. [9] Gilmour J. D. et al. (1997) *LPS XXVIII*. [10] Wadhwa M. and Lugmair G. W. (1996) *Meteoritics & Planet. Sci.*, 31, A145. [11] Ash R. D. et al. (1996) *Nature*, 380, 57–59.

#### IDENTIFICATION OF ANCIENT CARBONACEOUS CHERTS ON MARS USING RAMAN SPECTROSCOPY.

T. J. Wdowiak<sup>1</sup>, D. G. Agresti<sup>1</sup>, S. B. Mirov<sup>1</sup>, A. B. Kudryavtsev<sup>1</sup>, L. W. Beegle<sup>1</sup>, D. J. Des Marais<sup>2</sup>, and A. F. Tharpe<sup>2</sup>, <sup>1</sup>Astro and Solar System Physics Program, Department of Physics, University of Alabama at Birmingham, Birmingham AL 35294-1700, USA, <sup>2</sup>Mail Stop 239-4, NASA Ames Research Center, Moffett Field CA 94035-1000, USA.

Increasing attention is being given to the hypothesis that Mars may have had environmental conditions in the past that were conducive to the establishment of a biosphere. This, of course, raises the issue of finding fossil evidence for life and, more specifically, the technical means for doing so. In the foreseeable future the exploration of Mars will be by robotic missions, and it is important to now identify what analytical instruments ought to be deployed for exopaleontological and even exobiological investigations. We have been examining laser Raman spectroscopy (LRS) for that purpose and have found it useful in providing a signature from Archean carbonaceous cherts found in the greenstone belt of the Barberton Mountains in Swaziland, South Africa (~3.3 Ga), an example of material of interest as a martian analog. These provide an excellent demonstration of how well silica can encapsulate the residue of bacteria for eons. This material is considered to have been the product of diagenesis of enormous bacterial meadows that existed in shallow water that flooded the flat surfaces of simatic island platforms during breaks in volcanic activity [1]. Other materials of interest are Early Proterozoic (2.09 Ga) stromatolites of the Gunflint and Biwabik Iron Formations (northern Minnesota and southwestern Ontario). Our results are presented along with recommendations pertaining to the implementation of LRS on Mars, including the need to address the problem of obtaining measurements of material interior to rocks.

Demonstrating that a terrestrial rock is an Archean fossil such as a stromatolite is a difficult task [2], and attempting to do so on Mars makes it all the more formidable. There appears to be an informal

consensus that it will be necessary to bring candidate samples to Earth or a facility in Earth orbit for detailed examination. Thus the problem of searching for evidence of past life on Mars has, as a first task, the prospecting for the small amount of most promising material that can be accommodated for transport within spacecraft constraints. In our laboratory we have been researching physical techniques, such as Mössbauer spectroscopy [3] and, more recently, laser Raman spectroscopy [4], to aid in that purpose.

The samples were investigated with HeNe 633-nm laser Raman spectroscopy. The spectrometer system assembled has characteristics similar to what might be feasible for a robotic lander spacecraft. It utilizes a small 0.15-m spectrometer and 3 mW of laser excitation power. A holographic notch filter (Kaiser Supernotch) placed at the entrance slit of the monochromator (Acton) suppresses non-Raman scattered radiation making possible the use of the small monochromator. Special care was taken to exclude noncoherent radiation from the laser plasma at wavelengths other than 633 nm from interfering with the measurements. The 3 mW of laser excitation was transmitted through a hole on the back side of a mirror onto the sample, and scattered radiation was reflected by the mirror into a collecting lens that focused it onto the slit of the monochromator after passing through the holographic notch filter. The laser spot was ~25  $\mu$ m in diameter. The spectrum is acquired by a two-dimensional CCD array, which is interfaced to a computer. No special consideration was given to processing the sample except that most measurements were made on fresh surfaces made by fracturing the rock with hammer and chisel in the laboratory. A sample having surfaces exposed over 25 yr ago was the first to be examined.

Figure 1 shows the Raman spectrum, in a Raman shift range of 200  $\text{cm}^{-1}$ –2200  $\text{cm}^{-1}$ , of the first sample we examined, from the Fig Tree Group (South Africa). It exhibits three well-defined Raman peaks superimposed on broadband laser-induced luminescence. The measured Raman shifts are 460, 1328, and 1599  $\text{cm}^{-1}$  ( $\pm 5$   $\text{cm}^{-1}$ ). These can be interpreted to be due to silica and C. The two C bands at 1328  $\text{cm}^{-1}$  and 1599  $\text{cm}^{-1}$  are of considerable interest because they represent disordered/amorphous C and graphitic C respectively. The combination of these two bands with that due to

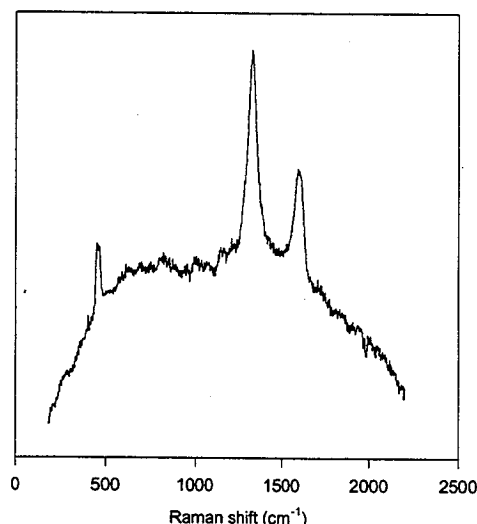


Fig. 1. Carbonaceous chert, Fig Tree Group.

quartz can be considered to be a signature of the fossil nature of the sample, where C of biological origin is encapsulated in quartz at a level of 1% or less.

The well-defined signature of C in the presence of quartz in a ~3.3-Ga-old sample whose surface had been exposed during collection over 25 yr ago stimulated examination of additional material from the Barberton Greenstone Belt, followed by samples from North American Biwabik and Gunflint Iron Formations (2.09 Ga). In all, 15 samples were studied, resulting in the conclusion that Raman spectroscopy can provide a spectral signature of C encapsulated in quartz. In some cases, laser-excited luminescence of the sample can be a source of interference; however, the spectral signature appears to be readily obtainable for most samples, provided a freshly exposed surface is interrogated. Spectra of nine black chert samples from the Barberton Greenstone Belt, ranging in age from ~3.460 Ga (top) to ~3.243 Ga (bottom), are exhibited in Fig. 2. This material was graciously contributed by D. Lowe (Stanford University). It is evident that the strengths of the C features (1328 and 1599  $\text{cm}^{-1}$ ) vary relative to that of the quartz (460  $\text{cm}^{-1}$ ).

The hematic Early Proterozoic Biwabik and Gunflint Iron Formation samples exhibiting stromatolitic structure were made available by W. Schopf (UCLA). The sample PPRG 2443 (Nolalu, Ontario) does exhibit a spectral character (Fig. 3) comparable with that of the Archean black cherts (Figs. 1 and 2). However, while the "G" band at 1599  $\text{cm}^{-1}$  is distinct, the "D" band at 1328  $\text{cm}^{-1}$  is blended with a strong Fe-associated feature that exists in the company of other features not present in the spectra of the Barberton

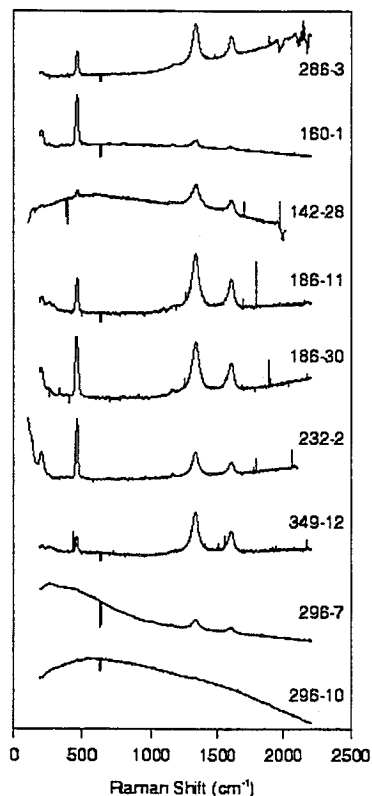


Fig. 2. Carbonaceous chert, Barberton Greenstone Belt.

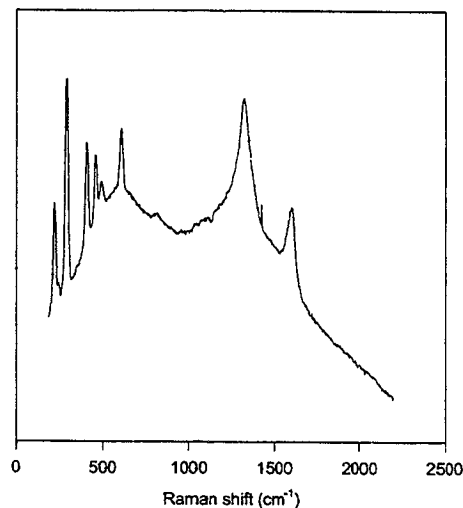


Fig. 3. Stromatolite (red area), Gunflint Iron Formation, PPRG 2443.

Greenstone Belt samples. Three of the Biwabik Iron-Formation samples (PPRG 389, 2431, and 2432) and a Gunflint Iron Formation sample (PPRG 400) did not exhibit discernible C bands. The case may be that Fe-associated bands masked the C bands. The C detected in PPRG 2243 does appear to be located in the red central portion of the stromatolitic structure.

**Acknowledgments:** This research has been supported by grants from the NASA Exobiology and PIDDP Programs.

**References:** [1] Lowe D. R. (1994) in *Early Life on Earth* (S. Bengtson, ed.), pp. 24–35, Columbia Univ., New York. [2] Walter M. R. (1994) in *Early Life on Earth* (S. Bengtson, ed.), pp. 270–286, Columbia Univ., New York. [3] Agresti D. G. et al. (1994) *Hyperfine Interactions*, 91, 523–528. [4] Wdowiak T. J. et al. (1995) *LPS XXVI*, 1473–1474.

**PROGRESS IN THE DEVELOPMENT OF A LASER RAMAN SPECTROMETER SYSTEM FOR A LANDER SPACECRAFT.** T. J. Wdowiak<sup>1</sup>, D. G. Agresti<sup>1</sup>, S. B. Mirov<sup>1</sup>, A. B. Kudryavtsev<sup>1</sup>, and T. R. Kinney<sup>2</sup>, <sup>1</sup>Astro and Solar System Physics Program, Department of Physics, University of Alabama at Birmingham, Birmingham AL 35294-1700, USA, <sup>2</sup>Control Development Inc., South Bend IN 46619, USA.

The utilization of laser Raman spectroscopy for *in situ* investigation of planetary, asteroid, and cometary materials and the general design of the instrument has become a subject of discussion [1–5].

A prototype/proof-of-principle laser Raman spectrometer system is under development through sponsorship of the NASA Planetary Instrument Definition and Development Program (PIDDP). The system consists of three components: (1) exciting laser, (2) Raman probe, and (3) spectrometer, all optically coupled in a serial architecture. Because the miniaturized spectrometer component was the item considered to have received the least prior attention, we have made that aspect of the project the lead development item during the first year.

The spectrometer component product is an F/2 grating instru-

ment, having a size of two chewing gum packages ( $2.8\text{ cm} \times 2.8\text{ cm} \times 8.0\text{ cm}$ ), and is fed by an optical fiber. The spectrometer was also configured, by utilizing an appropriate blaze angle, to work with an exciting laser operating at 785 nm. The wavelength choice is a consequence of desiring to minimize laser-induced luminescence in samples that can interfere with detection of the weak Raman spectrum, and the need to retain as much of the spectral range of the Raman shifted radiation within the spectral limit of the detector, which, in this case, is a silicon-device array.

The "Mark I" engineering model incorporated a room-temperature detector array during the testing phase to demonstrate that sufficient resolution for a meaningful science yield could be obtained in such a small device. After the initial test phase, the room-temperature detector array was replaced with a thermoelectrically cooled device. There are two reasons for this: (1) to improve thermal stability by active control, allowing extension of the duration of an integration, and (2) enhanced sensitivity at lower-temperature operation. In a spacecraft instrument, the ambient temperature is expected to be considerably lower than our laboratory situation and the detector will be cooled by passive heat exchange. Thermal stability will be achieved with the combined use of a heater and a selected material having a suitable change of phase.

The "Mark I" associated electronics is a programmable logic system permitting acquisition and storage of up to eight spectra of 40-s integration duration. The data are then transferred to the external computer, or the external computer can perform this signal averaging apart from the instrument's onboard capability.

The spectrometer system components are linked together in the architecture by optical fibers. A suitable laser, which must be narrow in bandwidth and with minimal wide-band plateau, has been identified and is a second-year-emphasis item, along with the fabrication of a laser Raman head incorporating the necessary options including a "notch" filter. The laser package will be approximately the same size as the spectrometer, and the Raman optical head about half that size. Other aspects of the project include a design for a dust exclusion device for the Raman optical head/probe and a small self-contained, multishot, and contamination-free tool for exposing fresh

rock surfaces.

Currently, the spectrometer system is being operated with computer-controlled fiber optic switching capability. This experience will be transferred into the architecture of the final prototype device. The second phase of the first-year task includes the pushing of sensitivity and detectability to the highest possible limits. Current experience has stimulated the engineering of a second spectrometer with sufficient differences to label it "Mark II," and its fabrication

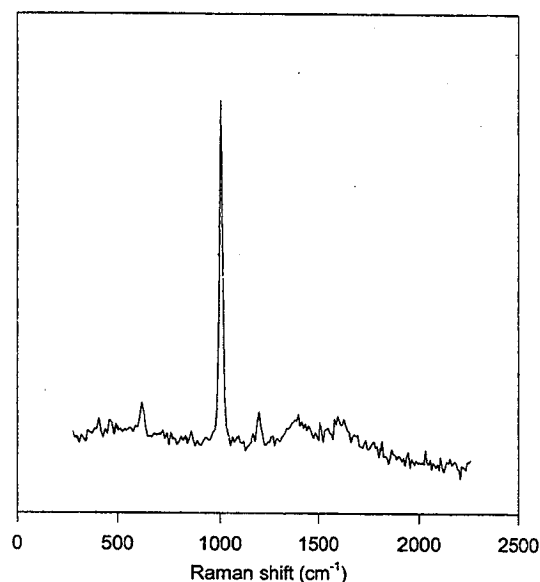


Fig. 2. Resolution test spectrum (unprocessed data) of benzene obtained with the device exhibited in Fig. 1 and a room-temperature detector array using 785-nm laser excitation.

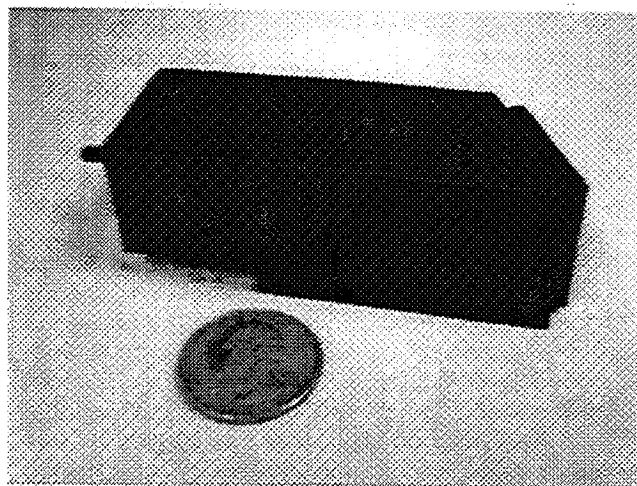


Fig. 1. Size of the spectrometer component relative to a quarter (U.S. 25-cent coin).

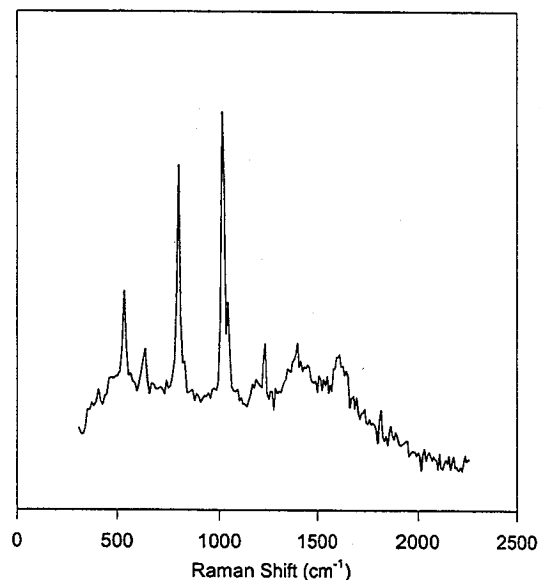


Fig. 3. Resolution test spectrum (unprocessed data) of toluene obtained with the device exhibited in Fig. 1 and a room-temperature detector array using 785-nm laser excitation.

will overlap into the beginning of year two of the project. Because both cooled "Mark I" and "Mark II" have different advantages, we considered this to be a dual-path approach. An aspect in which one device may have advantage is in reduced sensitivity to cosmic radiation. This will be tested, including at an accelerator.

Figure 1 shows the basic spectrometer component in the company of a U.S. quarter coin. Figures 2 and 3 show Raman spectra obtained during the initial (first-light) tests for performance in the area of spectral resolution, using the room-temperature detector and the aromatic hydrocarbons benzene and toluene. These spectra represent unprocessed data. The level of resolution is expressed not only in the narrow nature of individual bands, but also in the ability to discern the 1/3-strength band component of the band pair for toluene at  $\sim 1000\text{ cm}^{-1}$ . A commercial laser Raman head was utilized for these measurements, and it should be noted that this particular head, used only in testing, exhibited some spectral artifacts in the  $1400\text{--}1600\text{ cm}^{-1}$  spectral region, which should not be considered in terms of the spectrometer performance.

**Acknowledgments:** This research has been supported by grants from the NASA PIDD and Exobiology Programs.

**References:** [1] Wdowiak T. J. et al. (1995) in *LPS XXVI*, 1473–1474. [2] Treiman A. H. (1995) in *LPI Tech. Rpt. 95-05*, pp. 65–84. [3] Wdowiak T. J. (1995) in *LPI Tech. Rpt. 95-05*, pp. 65–84. [4] Wang A. et al. (1995) *JGR Planets*, 100, 21189–21199. [5] Wdowiak T. J. (1995) in *Point Clear Exobiology Instrumentation Workshop*, p. 69, on the Web at <http://www.phy.uab.edu/exobiology/>.

**THE NATURE OF FOSSIL BACTERIA.** F. Westall, DIPROVAL, University of Bologna, via S. Giacomo 7, 40126 Bologna, Italy (frances@geomin.unibo.it).

The similarity of the early environments of Mars and the Earth [1] suggests that life could have developed on Mars in the same way as on Earth. On Earth there are already indirect indications of bacterial life by 3.8 Ga [2], and the first direct evidence of life, in the form of mineral and carbonaceous microfossils, comes from 3.3–3.5-Ga Early Archean rocks from South Africa (Barberton Greenstone Belt, BGB) and Australia (Pilbara Craton) [3–6]. We have no idea what morphological form life may have taken on Mars (although fossil nanobacteria have been claimed in meteorite ALH 84001 [7]), just as we do not know what morphological form the bacterial ancestors had [8]. However, it is generally believed that the latter must have been a simple anaerobic heterotroph [9]. On Earth, the simplest self-replicating form of life presently known is the bacterium, which is the oldest form of fossil life known to date. Knowledge of the nature of bacteria and fossil bacteria can aid the search for fossil forms of life, as we presently understand the term "life," in the rocks of Mars.

The critical characteristics of bacteria that can be preserved as fossils are morphology (size and shape), constancy of morphology (i.e., extremely limited variations in size and shape for each species of bacteria), and colonial association [6,8,10]. Modern bacteria are generally small, averaging  $1\text{--}2\text{ }\mu\text{m}$  in size. Extremes include the coccoid forms of some wall-less mycoplasmas and starvation-dwarfed nanobacteria that can be as small as  $0.1\text{--}0.2\text{ }\mu\text{m}$  [11,12], cyanobacteria reaching  $10\text{ }\mu\text{m}$  in diameter, and some spirochetes that can be up to  $500\text{ }\mu\text{m}$  in length [13]. Most modern bacteria would therefore

be below the limit of resolution of the petrological microscope traditionally used in examinations of thin sections of the Early Archean rocks. The sizes of the Early Archean fossil bacteria range from  $0.6\text{--}4.3\text{ }\mu\text{m}$  for the mineral forms (imaged with the scanning electron microscope) found in the BGB and the Pilbara Craton ([6], and Westall unpublished data), and up to tens of micrometers in length for filamentous carbonaceous fossils (viewed in thin section) from the same formations [3–5]. Modern bacteria display morphologies ranging from spherical (coccoid), rod-shaped (bacillus), curved (vibrioid), to spiral (spirochete or spirilli). Of the many spherical and filamentous structures described from the Early Archean, those of assured biogenicity have a filamentous or rod-shaped morphology. The biogenicity of the carbonaceous Australian forms is based on their similarity of size and shape, and the structural complexity of the apparently septate division of the filaments, to modern cyanobacteria [5]. Similarly, the carbonaceous filamentous structures in the Early Archean rocks from South Africa have been compared to filamentous bacteria [3,4]. The smaller mineral microfossils, on the other hand, display rod-shaped morphologies of different length/width ratios. They can be distinguished from crystals by their rounded morphology (although some authigenic overgrowth can occur if the fossil-bearing formations have been subjected to metamorphism), their small size, their limited variation in size and shape, and their colonial association [6]. Unfortunately, organic coccoid morphologies can also be produced abiogenically [14]. It is therefore more difficult to confidently identify coccoid structures as fossil bacteria, and, in fact, none of the carbonaceous spheroids described has yet been classed as being of assured biogenic origin. Vibrioid and spiral morphologies have not yet been seen in fossil form in nature.

The organic and/or mineral composition of the fossil depends on many factors and is still a matter of debate. Schopf and Walter [10] noted that, although the Early Archean microfossils described are carbonaceous, fossil bacteria could also be mineral, whereas Buick [8] discounts the acceptability of mineral microfossils. The fossiliferous Early Archean rocks do contain organic C (up to 14 wt% [16]), and it has been identified in thin section by its brown color in transmitted light and low reflectance in reflected light microscopy [3]. On the other hand, recent experiments to simulate the fossilization of noncyanobacteria show that these organisms are preserved as minerals and that the organic matter is replaced, with the organic walls, as such, not being preserved [15]. However, it is possible that some of the degraded organic molecules may become trapped in the interstices of the replacement mineral. The fossilization of cyanobacteria may be different. They are a particular group of aerobic photosynthetic bacteria, some of which are characterized by a tough and more degradation-resistant outer sheath, and may therefore be more easily preserved by permineralization [17].

Buick [8] stipulated a hollow structure for true fossil bacteria, but many casts (i.e., filled structures) have been observed, not only experimentally [15] but also in nature [18,19]. In fact, a number of mineral fossil bacteria occurrences are known from the Phanerozoic, and SEM studies of these bacteria can also be used in understanding the nature of fossil bacteria: 0.7-Ma calcified bacilli [20] and 10–15-Ma silicified bacilli [21] from deep-sea Antarctic sediments; phosphatized bacilli and cocci from Early Eocene volcanic lake sediments from Southern Germany [22] and from the U. Cretaceous Santana Formation of [18].

In conclusion, in the search for fossilized life forms on Mars, the following should be taken into account: The potential fossil will

probably have a mineral composition, although the presence of associated organic matter cannot be discounted, especially if it was an organism with a tough organic sheath like that of some cyanobacteria; it will be greater than 0.1  $\mu\text{m}$  in size (the minimum size for a viable, self-replicating organism); it may be coccoid or rod-shaped; it will probably be associated with other very similarly sized and shaped structures (colony); and, finally, it may have either a hollow or a cast structure.

**Acknowledgments:** J. Hoegbom is warmly thanked for his moral and financial support, and we thank M. J. de Wit and J. Dann for the BGB samples and helpful discussions.

**References:** [1] Davies W. L. and McKay C. P. (1996) *Origins of Life and Evolution of the Biosphere*, 26, 61. [2] Mojzses S. J. et al. (1996) *Nature*, 384, 55. [3] Walsh M. M. (1992) *Precambrian Res.*, 54, 271. [4] Schopf J. W., in *The Proterozoic Biosphere* (J. W. Schopf and C. Klein, eds.), p. 25, Cambridge Univ. [5] Schopf J. W. (1993) *Science*, 260, 640. [6] Westall F. et al., *Science*, submitted. [7] McKay D. S. et al. (1996) *Science*, 273, 924. [8] Buick R. (1990) *Palaios*, 5, 441. [9] Lazcano et al. (1983) *Precambrian Res.*, 20, 259. [10] Schopf J. W. and Walter M. R. (1983) in *Earth's Earliest Biosphere* (J. W. Schopf, ed.), p. 214, Princeton Univ. [11] Brock T. D. and Madigan M. T. (1991) *The Biology of the Microorganisms*, Prentice Hall. [12] Morita R. Y. (1988) *Can. J. Microbiology*, 34, 436. [13] Prescott L. M. et al. (1993) *Microbiology*, Wm. C. Brown Communications. [14] Fox S. W. et al. (1983) *Precambrian Res.*, 23, 1. [15] Westall F. et al. (1995) *Palaeontology*, 38, 495. [16] de Ronde and Ebbesen T. W. (1996) *Geology*, 24, 791. [17] Francis S. et al. (1978) *Precambrian Res.*, 6, 65. [18] Martill D. and Wilby P. R. (1994) *Kaupia, Darmstaedter Beitr. z. Naturgeschichte*, 4, 71. [19] Liebig K. et al. (1966) *N. Jb. Geol. Palaeont. Mh.*, 4, 218. [20] Barbieri R. et al., *Paleo.*, 3, submitted. [21] Monty C. L. V. et al. (1991) *Proc. ODP Sc. Rept. 114*, 685. [22] Wuttke M. (1983) *Senckenberg. leth.*, 65, 509.

**MARS GEOTHERMAL AND VOLCANIC EVOLUTION: VOLCANIC INTRUSIONS AS HEAT SOURCES TO MAINTAIN VIABLE ECOSYSTEMS?** L. Wilson<sup>1</sup> and J. W. Head II<sup>2</sup>, <sup>1</sup>Planetary Science Group, Institute of Environmental and Biological Sciences, Lancaster University, Lancaster UK, <sup>2</sup>Department of Geological Sciences, Brown University, Providence RI 02912, USA.

**Introduction:** Geothermal systems originating from magmatic intrusion are potential sources of environments that could favor the development and sustenance of life on Mars. General thermal evolution models predict that crustal formation and evolution will favor more extensive magmatism early in the history of Mars. In this contribution, we assess the environments that might favor systematic dike intrusion at sufficiently high rates that water would persist as a liquid in the shallow subsurface for periods of tens to perhaps hundreds of millions of years.

**Structure of Volcanos:** Centers of basaltic activity located over mantle hot-spots on both Earth and Mars produce the same basic pattern of a shallow magma reservoir (commonly marked by a collapse crater or caldera) located beneath the summit of a shield volcano [1]. Near-vertically oriented dikes (pressurized magma-filled cracks) propagate mainly laterally away from the reservoir whenever it becomes excessively overpressured by the arrival of

batches of magma from the mantle beneath. These dikes either stall within the body of the volcano as intrusions or, if they grow vertically by a great enough distance, erupt at the surface to feed lava flows or explosive eruptions. The growth of many shield volcanos is influenced by preexisting regional stresses in such a way as to concentrate dike injection into relatively narrow zones—rift zones—oriented radial to the summit. Intrusions outnumber surface eruptions by a factor of several to one.

The main difference between terrestrial and martian volcanos is caused by the lower acceleration due to gravity on Mars [2,3]. The interplay between stresses arising due to gravity and stresses linked to the elastic properties of rocks causes all martian magma reservoirs to be centered at greater depths and to be larger in both horizontal and vertical dimensions [4,5]. The greater magma volumes housed by these reservoirs cause laterally propagating rift-zone dikes to be both horizontally and vertically more extensive and also wider (i.e., thicker) than those on Earth. Table 1 shows typical values of vertical height and width.

Any shield volcano grows as a stack of interleaved, subhorizontal layers of volcanic ash from explosive eruptions and vesicular lava from effusive eruptions cut, at any given level within the pile, by the near-vertical dikes feeding later eruptions. Once the products of any one eruption have cooled, the pore spaces between ash particles and the vesicles within lava flows form natural locations for the near-surface accumulation of water ice and solid  $\text{CO}_2$ . The very low atmospheric pressure on Mars causes more exsolution of magmatic volatiles (mainly  $\text{H}_2\text{O}$  and  $\text{CO}_2$ ) than on Earth; this means that explosive eruptions were more common on Mars than Earth [6] and that lava flows were more vesicular, both factors enhancing the trapping of volatiles from the atmosphere.

**Thermal Consequences of Dike Injection:** There are several ways in which the intrusion of new dikes influences the thermal structure of the old eruptives into which they are intruded and thus the state (solid or liquid) of the  $\text{H}_2\text{O}$  trapped in these rocks. If a dike is intruded into a region that has seen no activity for a long time, then close to the new dike the heat pulse will raise the temperature first above the melting point of  $\text{H}_2\text{O}$  and then above the boiling point; further away only the melting point will be exceeded. The timescale  $t_1$  over which such a heating event lasts is of order  $5(w^2/\kappa)$  where  $w$  is the dike width and  $\kappa$  is the thermal diffusivity of the magma; for  $w = 5$  m and  $\kappa = 10^{-6} \text{ m}^2 \text{ s}^{-1}$ ,  $t_1 = 4$  yr. The lateral width of the region affected is  $\sim 6w = 30$  m.

Where successive dikes are intruded near to one another in a rift zone, part of the region between any two dikes can stay at a temperature such that  $\text{H}_2\text{O}$  is a liquid for a much longer time provided that new dikes arrive on a timescale comparable with  $t_1$ . We can estimate

TABLE 1. Widths ( $w$ ) and vertical heights ( $h$ ) of dikes centered at neutral buoyancy levels in the rift zones of volcanos on Earth and Mars for a range of plausible driving pressures,  $P_0$ , defined as the amounts by which the pressure in the dike at its midpoint exceeds the external compressive stress.

$P_0/\text{MPa}$	Earth		Mars	
	$h/\text{km}$	$w/\text{m}$	$h/\text{km}$	$w/\text{m}$
5	0.95	0.45	4.8	1.4
10	4.7	2.3	12.9	5.7
20	9.7	8.7	28.0	22.6



the time interval between intrusions by noting that to assemble the typical volume of a large martian volcano ( $\sim 10^6 \text{ km}^3$  for the Tharsis shields) in 1 Ga (i.e.,  $3 \times 10^{16} \text{ s}$ ) by randomly intruding dikes 50 km in horizontal extent, 13 km in vertical extent, and 6 m thick (cf. Table 1) implies that the time between events is  $\sim 4000 \text{ yr}$ . However, if these dikes are confined to a rift zone, the time interval between events is less. The Hawaiian shield volcanos on Earth have active rift zones that at any one time are only a few hundred meters wide and occupy only about 1/200 of the horizontal cross-sectional area of the volcano. Preliminary estimates from Viking Orbiter images suggest that the ratio is similar for Mars, reducing the mean interval between nearby intrusions to  $4000/200 = 20 \text{ yr}$ . This value is close enough to the 4 yr found earlier to suggest that significant local "warm zones" can exist down to depths of several kilometers in volcanic rift zones.

**Regional Heat Flow Effects:** An alternative assessment takes account of the fact that, over the whole extent of a rift zone, the net effect of the intrusions is to increase the regional heat flow and locally raise the geotherm toward the surface on the timescale over which the rift zone remains the preferred site of activity. The total amount of heat,  $H$ , available from cooling the magma required to build a shield volcano of volume  $V$  is  $H = (V \rho S \Delta\theta)$  where  $\rho$  is the mean density of the edifice,  $S$  is the specific heat of the magma, and  $\Delta\theta$  is the temperature interval through which the magma cools. Substituting typical values of  $V \sim 10^6 \text{ km}^3$ ,  $\rho \sim 3000 \text{ kg/m}^3$ ,  $S \sim 1000 \text{ J kg}^{-1} \text{ K}^{-1}$ , and  $\Delta\theta \sim 1000 \text{ K}$ , we find  $H \sim 3 \times 10^{24} \text{ J}$ . The timescale for release of this heat is, as before,  $\sim 1 \text{ Ga} = 3 \times 10^{16} \text{ s}$  and the total surface area of the volcano with diameter 500 km is  $\sim 8 \times 10^{11} \text{ m}^2$ , implying a mean heat flux  $Q_v$  of  $\sim 1.3 \times 10^{-4} \text{ W m}^{-2}$ . If the fractional area of rift zones at any one time is again taken as 1/200 of the surface area of the volcano, the local heat flux is more like  $Q_v = 2.5 \times 10^{-2} \text{ W m}^{-2}$ . This is comparable to the present-day planetary average geothermal heat flux  $Q_g$  estimated at between  $3$  and  $4 \times 10^{-2} \text{ W m}^{-2}$  [7].

We are mainly concerned with the influence of volcanic heat sources at some time part-way through martian geological history when the geothermal heat flux was higher than the current value by a factor of, say, 2 or 3, i.e.,  $\sim 8 \times 10^{-2} \text{ W m}^{-2}$ ; the volcanic flux would then have represented a 30% increase in the heat flow. Estimates of the depth to the base of the cryosphere based on the current geothermal heat flow range from about 2 km near the equator to about 5 km near the poles. With the higher earlier flux these depths would have been  $\sim 800 \text{ m}$  and  $\sim 2000 \text{ m}$  respectively, and the 30% increase in heat flow would have changed them to  $\sim 615$  and  $\sim 1540 \text{ m}$  respectively. Thus, the vertical extent of the zone within which  $\text{H}_2\text{O}$  could be present as liquid water could have been extended by at least 200–400 m, depending on the latitude.

**Summary:** The above calculations suggest that the local volcanic heat sources inevitably present in the rift zones on the flanks of large martian volcanos could have very significantly extended the sizes of regions within which water could persist as a liquid for periods of at least tens and probably hundreds of millions of years, the latter intervals being long enough, by analogy with what happened on the Earth, for significant biological development [8]. It is possible that the ultimate limitation on the lifetime of such favored regions is not so much the availability of heat but rather the need to prevent water from leaving the regions too rapidly as a result of the imposed thermal gradient [9] or to resupply water from deeper levels in the hydrothermal system of the volcano to compensate for

that loss. We are presently investigating geological environments on Mars where such conditions might have persisted.

**References:** [1] Mouginiis-Mark P. J. et al. (1992) in *Mars* (H. H. Kieffer et al., eds.), pp. 424–452, Univ. of Arizona, Tucson. [2] Wilson L. and Parfitt E. A. (1990) *LPS XXV*, 1345–1346. [3] Wilson L. and Head J. W. (1994) *Rev. Geophys.*, 32, 221–264. [4] Parfitt E. A. et al. (1993) *J. Volcanol. Geotherm. Res.*, 55, 1–14. [5] Head J. W. and Wilson L. (1994) *LPS XXV*, 527–528. [6] Wilson L. and Head J. W. (1983) *Nature*, 302, 663–669. [7] Squyres S. W. et al. (1992) in *Mars* (H. H. Kieffer et al., eds.), pp. 523–554, Univ. of Arizona, Tucson. [8] McKay C. P. and Stoker C. R. (1989) *Rev. Geophys. Space Phys.*, 27, 189–214. [9] McKay C. P. et al. (1992) in *Mars* (H. H. Kieffer et al., eds.), pp. 1234–1245, Univ. of Arizona, Tucson.

#### FURTHER INVESTIGATION OF ISOTOPICALLY LIGHT CARBON IN ALLAN HILLS 84001.

I. P. Wright<sup>1</sup>, S. Assanov<sup>1</sup>, A. B. Verchovsky<sup>1</sup>, I. A. Franchi<sup>1</sup>, M. M. Grady<sup>1,2</sup>, and C. T. Pillinger<sup>1</sup>, <sup>1</sup>Planetary Sciences Research Institute, Open University, Walton Hall, Milton Keynes MK7 6AA, UK (i.p.wright@open.ac.uk), <sup>2</sup>Natural History Museum, Cromwell Road, London SW7 5BD, UK (m.grady@nhm.ac.uk).

Attempts to comprehend the C chemistry and stable isotopic composition of components in ALH 84001 (hereafter A84) have involved use of stepped combustion to determine the overall C inventory [1–3] acid-dissolution techniques to analyze for carbonates [4,5], organic analyses for selective determination of individual classes of compounds [6,7], and, latterly, ion probe and STXM measurements to investigate small-scale detail [8,9]. It is clear that a completely coherent picture, within which the results from all investigations of C are understood, remains to be obtained. In order to provide additional constraints, we have conducted a series of stepped pyrolysis experiments on bulk samples of A84. In many ways pyrolysis experiments give results that are inferior compared to equivalent stepped combustions. However, one of the reasons for the present effort was to try and clarify the situation regarding isotopically light C in A84 [10]. The rationale here is that organic compounds will pyrolyze to give species such as  $\text{CO}$ ,  $\text{CO}_2$ , and  $\text{CH}_4$ , whereas a contaminant such as Teflon, would not.

Samples of A84 have been pyrolyzed in a stepwise manner (from room temperature to  $1200^\circ\text{C}$ ) in three different extraction systems. The first allows qualitative (and semiquantitative) analyses of all gas species — i.e., a conventional evolved gas analysis. The second system is the one more usually used for our high-sensitivity stepped combustion analyses [11], suitably modified to allow pyrolysis; from this experiment we measured  $\delta^{13}\text{C}$  values of the sum of evolved  $\text{CO}$  and  $\text{CO}_2$ . In the third device we measured the isotopic composition of evolved methane [12]. Note that all three extraction systems and associated instruments are optimized to work with small samples — in consequence the total amount of A84 used for the three separate analyses was less than 12 mg.

Strictly speaking it is unlikely that results from one experiment can be compared with another (because of subtle differences in each extraction procedure). However, in general terms it is apparent that most of the C in A84 is liberated as  $\text{CO}$  and  $\text{CO}_2$ , with only a minor contribution from  $\text{CH}_4$ . On the basis of the evolved gas analysis, the



CO<sub>2</sub> release is seen to occur over the same temperature range as CO (with the ratio of [C] as CO<sub>2</sub>/CO being between 3 and 6 for different steps, across the major release). The major release of CO<sub>2</sub> arises from carbonate breakdown, while CO is probably the result of the interaction of [C] with O from silicates, carbonates, or other minerals (the [C] is assumed to be organic in nature). The overlapping of the releases of CO<sub>2</sub> and CO results in a maximum  $\delta^{13}\text{C}$  value for CO<sub>2</sub> + CO of 32.3‰, as opposed to about 40‰, which would have been expected for pure carbonates. This effect is not unexpected and indeed is one of the reasons why combustions are often preferred. The rest of the C isotopic data from the CO<sub>2</sub> + CO experiment are fairly well understood within the framework of what is already known. However, we draw attention to one step (200°–300°C), which gave a large release of gas (i.e., 12.2% of the total C) and which had a  $\delta^{13}\text{C}$  value of –37.7‰. It is difficult to judge the significance of this result. While it is clearly very different from the rest of the noncarbonate C (having  $\delta^{13}\text{C}$  of around –25‰), it may be an artifact of the experiment (kinetic isotope fractionation resulting from pyrolysis at low temperature?). We have to learn more about the performance of our system with respect to pyrolysis before we can be sure of the relevance of this result.

Turning to methane, both of the experiments that were capable of recording this species showed that the gas is released at 400°–600°C. The amount of methane released is extremely small, amounting to less than 1 ppm ([C] as CH<sub>4</sub>). Isotopically we are only able to measure a parameter we call  $\delta^{17}\text{M}$  [12]—unfortunately, we cannot yet distinguish between  $\delta^{13}\text{C}$  and  $\delta\text{D}$ . However, if an assumption is made about one of the isotopic systems, the other can be calculated. Now, from previous work [13] it is known that in kerogenlike organic materials from carbonaceous chondrites there is a C isotopic fractionation between evolved CH<sub>4</sub> and CO/CO<sub>2</sub> of about 10‰. Thus, if we assume  $\delta^{13}\text{C}$  of –25‰ for gaseous CO/CO<sub>2</sub> it would be anticipated that  $\delta^{13}\text{C}$  of CH<sub>4</sub> would be –35‰. On this basis,  $\delta\text{D}$  values of CH<sub>4</sub> would have to be in the range –200 to –700‰ (i.e., for the various steps of the experiment), with the average being about –300‰. Intuitively these values of  $\delta\text{D}$  seem unlikely. Consider that  $\delta\text{D}$  of water released by pyrolysis of A84 ranges from –50‰ to about 800‰ [14]; note that the relatively low  $\delta\text{D}$  values are obtained at low temperatures, at which no methane was observed to be released. Thus, just considering the temperature interval where methane is released, we would expect  $\delta\text{D}$  values of water to be at

least 500‰. If the H in the methane had become isotopically equilibrated with the H in the water (either during the laboratory extraction, or by some fundamental process within the meteorite) we would expect  $\delta\text{D}$  of the methane to be about 500‰. And in which case,  $\delta^{13}\text{C}$  of the methane (calculated as above) would have to be less than –60‰ for all steps. Even assuming a  $\delta\text{D}$  of 200‰, and taking the average value of  $\delta^{17}\text{M}$ , we still derive a  $\delta^{13}\text{C}$  value of –60‰.

At this point it is necessary to inject some caution since the quantities of methane released from A84 were very small. Indeed, the amounts were only a factor of 2 greater than system blanks; furthermore, the isotopic composition of the system blank is not yet understood. It appears that the methane blank arises from two components, namely organic compounds and C within quartz. Attempts are currently being made to constrain the characteristics of the blank so that a satisfactory correction can be applied to the sample data.

Most of the organic compounds in A84 have  $\delta^{13}\text{C}$  values that, at around –25‰, are not distinctive from similar or equivalent terrestrial materials. In other words, interpretation of the C isotope data from A84 is always going to be hampered by their ambiguous nature. However, it seems at least possible that within the organic complex there might be minor components that can be distinguished by extreme C isotopic compositions (as first suggested by Wright et al. [10]). In light of the potential importance of establishing the presence, or otherwise, of isotopically light C, it is appropriate to continue searching for evidence of such components in A84. These measurements may help to constrain the life on Mars debate.

**References:** [1] Grady M. M. et al. (1994) *Meteoritics*, 29, 469. [2] Wright I. P. et al. (1997) *LPS XXVIII*. [3] Wright I. P. et al. (1997) *LPS XXVIII*. [4] Romanek C. S. et al. (1994) *Nature*, 372, 655–657. [5] Jull A. J. T. et al. (1995) *Meteoritics*, 30, 311–318. [6] McDonald G. D. and Bada J. L. (1995) *GCA*, 59, 1179–1184. [7] Becker L. et al. (1997) *GCA*, 61, 475–481. [8] Valley J. W. et al. (1997) *LPS XXVIII*. [9] Flynn G. J. et al. (1997) *LPS XXVIII*. [10] Wright I. P. et al. (1997) *LPS XXVIII*. [11] Yates P. D. et al. (1992) *Chem. Geol. (Isotope Geosci.)*, 101, 81–91. [12] Morse A. D. et al. (1996) *Rapid Comm. Mass Spec.*, 10, 1743–1746. [13] Kerridge J. F. et al. (1987) *GCA*, 51, 2527–2540. [14] Leshin L. A. et al. (1996) *GCA*, 60, 2635–2650.

